MADCAM-1 EXPRESSION AND FUNCTION IN HUMAN LIVER

by

EVAGGELIA LIASKOU

A Thesis submitted to
The University of Birmingham
For the degree of
DOCTOR OF PHILOSOPHY

Centre for Liver Research
School of Immunity and Infection
College of Medical Sciences
The University of Birmingham
January, 2010

ABSTRACT

Mucosal addressin cell adhesion molecule-1 (MAdCAM-1) is a tissue–specific protein that promotes α4β7+ lymphocyte recruitment on gut mucosal endothelium, playing an important role in the development of inflammatory bowel disease (IBD). Recent studies have reported its expression in liver diseases such as primary sclerosing cholangitis (PSC) and autoimmune hepatitis (AIH) that complicate IBD, therefore understanding the factors that drive hepatic expression of MAdCAM-1 might elucidate the pathogenesis of these diseases. *In vitro* stimulation of HSEC with tumor necrosis factor-α (TNFα) and methylamine, the physiological substrate of vascular adhesion protein-1 (VAP-1), as well as with the end products of methylamine deamination by VAP-1, resulted in increased levels of secreted and cell surface MAdCAM-1 protein that was able to support binding of α4β7+ lymphocytes under flow conditions. *In vivo* stimulation of mice that expressed hVAP-1 as a transgene, with methylamine, induced expression of MAdCAM-1 in Peyer's patches and mesenteric lymph nodes, validating the effect of VAP-1 enzyme activity. In conclusion, we report for the first time that MAdCAM-1 is normally present in human liver and is further induced upon TNFα and methylamine stimulation resulting in the recruitment of mucosal cells to the liver, thus sustaining a destructive inflammatoty influx responsible for the establishment of chronic inflammation.

PUBLICATIONS

I. Miles, A., **Liaskou, E.,** Eksteen, B., Lalor, P.F., Adams, D. H., CCL25 and CCL28 promote alpha4 beta7-integrin-dependent adhesion of lymphocytes to MAdCAM-1 under shear flow. *Am J Physiol Gastrointest Liver Physiol* **294** (5), G1257 (2008).

II. Eksteen, B., **Liaskou, E.,** and Adams, D. H., Lymphocyte homing and its role in the pathogenesis of IBD. *Inflamm Bowel Dis* (2008).

III. Aspinall, A., Curbishley, S., Weston, C., Blahova, M., **Liaskou, E.,** Adams, R., Holt, A., Lalor, P.F., Adams, D.H., CX3CR1 and vascular adhesion protein-1 dependent recruitment of CD16+ monocytes across human liver sinusoidal endothelium. *Hepatology* (2010).

To be published:

IV. **Liaskou, E.,** Weston, C., Lalor, P.F., Jalkanen, S., Adams, D.H., Regulation of MAdCAM-1 expression on human liver tissue by amine oxidase activity (2010).

V. **Liaskou, E.,** Karikoski, M., Lalor, P.F., Adams, D.H., Jalkanen, S., Role of VAP-1/SSAO in induction of MAdCAM-1 expression in mucosal tissues (2010).

PRESENTATIONS & PUBLIC APPEARANCES

I. **Hepatic Inflammation and Immunity Conference,** Galveston Texas, January 25-27, 2008 (poster presentation).

II. **BSG The immune basis of liver disease,** Birmingham, June 9-10, 2008 (poster presentation).

III. **4th IBR Symposium,** Birmingham, July 9, 2008 (poster presentation).

IV. **American Association for the Study of liver diseases, AASLD conference,** San Francisco, California, October 31- November 4, 2008 (poster presentation).

V. **19th UK Adhesion Society Meeting,** Birmingham, April 15, 2009 (poster presentation).

"As you set out for Ithaca

hope your road is a long one,

full of adventure, full of discovery.

Laistrygonians, Cyclops,

angry Poseidon–don't be afraid of them:

you ' ll never find things like that on your way

as long as you keep your thoughts raised high,

as long as a rare excitement

stirs your spirit and your body.

Laistrygonians, Cyclops,

wild Poseidon–you won't encounter them

unless you bring them along inside your soul,

unless your soul sets them up in front of you.

Hope your road is a long one.

....

Arriving there is what you're destined for.

But don't hurry the journey at all.

Better if it lasts for years,

so you're old by the time you reach the island

wealthy with all you've gained on the way,

not expecting Ithaca to make you rich.

Ithaca gave you the marvelous journey.

Without her you wouldn't have set out.

She has nothing left to give you now.

And if you find her poor, Ithaca won't have fooled you.

Wise as you will have become, so full of experience,

You'll have understood by then what those Ithacas mean."

Ithaca of C.P Cavafy

doing a PhD is a "marvelous journey" with many difficulties but when you reach the end you have become rich ... in experience

ACKNOWLEDGMENTS

I would like to thank Prof. J. Lord for giving me the opportunity to study in the University of Birmingham, and I am heartily thankful to my supervisors Prof. D.H. Adams and Dr. P.F. Lalor for their excellent and constant guidance, and for enabling me to develop a scientific thinking. I would also like to show my gratitude to Prof. S. Jalkanen and Dr. M. Salmi, who supervised me during my six-month practice in the MediCity Laboratory in Turku, Finland.

I offer my regards and blessings to all the people in the Liver Labs who supported me in any respect during the completion of my project. I am really grateful to Dr. C.Weston who has made available his support in a number of ways, and to all post docs for their great scientific expertise provided during "Friday Tea/Coffee Mornings" that made all the troubleshooting enjoyable.

Lastly, I am indebted to my friends, my family and mainly to my parents, Sofia and Anestis Liaskos who kindly accepted my decision to come and study abroad, and with their love they gave me strength and courage to continue. Finally, I owe my deepest gratitude to my beloved Dimitris Papagiannopoulos for all his love and support, but mostly for his incredible patience to stand my weirdness during moments of despair, and being on my side all the good and bad moments.

TABLE OF CONTENTS

LIST OF FIGURES

LIST OF TABLES

List Of Abbreviations

aa	Amino acid
Ab	Antibody
AIH	Autoimmune hepatitis
ALD	Alcoholic liver diseases
APC	Antigen presenting cell
AP–1	Activator protein-1
Arg	Arginine
ASC	Antibody secreting cells
Asp	Aspartate
BCR	B cell receptor
BEA	Bromoethylamine
BFA	Brefeldin A
BLC	B lymphocyte chemokine
BM	Basement membrane
BSA	Bovine serum albumin
CCL	CC-chemokine ligand
CCR	CC-chemokine receptor
CD	Cluster of differentiation
C/EBP	CCAAT–enhancer–binding proteins
CHC	Chronic hepatitis C
CHO	Chinese hamster ovary
CLA	Cutaneous lymphocyte antigen
CLEVER-1	Common lymphatic endothelial and vascular endothelial receptor-1
CNS	Central nervous system
ConA	Concavalin A
CrD	Crohn's disease
CTLA-4	Cytotoxic T lymphocyte antigen-4
CXCL	CXC-chemokine ligand
CXCR	CXC-chemokine receptor

DC	Dendritic cell
DMSO	Dimethyl sulfoxide
EAE	Experimental allergic encephalomyelitis
ECAMs	Endothelial cell adhesion molecules
ECs	Endothelial cells
EDTA	Ethylediaminetetraacetic acid
EGF	Epidermal growth factor
ELR	Glutamic acid (E)–leucine (L)–arginine (R)
ENA-78	Epithelial cell–derived neutrophil–activating protein 78
Ets	E–twenty six transcription factor family
ESAM	Endothelial cell selective adhesion molecule
ESL-1	E-selectin ligand–1
FACS	Fluorescence–activated cell sorter
FAE	Follicle associated epithelium
FASL	Fas–ligand
FCS	Foetal calf serum
FL–MAdCAM-1	Full–length MAdCAM-1
GALT	Gut associated lymphoid tissue
GCP-2	Granulocyte chemotactic protein-2
GI	Gastrointestinal tract
GlyCAM-1	Glycosylation–dependent cell adhesion molecule-1
GRO	Growth related oncogene
HCHO	Formaldehyde
HEA-125	Human epithelial antigen-125
HEC	Hepatic endothelial cells
HEV	High endothelial venules
HGF	Hepatic growth factor
HIHS	Heat inactivated human serum

HIMEC	Human intestinal microvascular endothelial cells
hMAdCAM-1	Human MAdCAM-1
HRP	Horseradish peroxidase
HSC	Hepatic stellate cells
HSEC	Hepatic sinusoidal endothelial cells
HUVEC	Human umbilical vein endothelial cells
hVAP-1	Human VAP-1
hVCAM-1	Human VCAM-1
H_2O_2	Hydrogen peroxide
IBD	Inflammatory bowel disease
ICAM -1,-2,-3	Intracellular cell adhesion molecule -1,-2,-3
IDDM	Insulin dependent diabetes mellitus
IELs	Intraepithelial lymphocytes
IFNγ	Interferon gamma
Ig	Immunoglobulin
IL	Interleukin
*i*NKT	Invariant natural killer T cell
IP	Immunoprecipitation
IP-10	Interferon gamma–inducible protein 10
ITAC	Interferon inducible T cell alpha chemoattractant
JAM	Junctional adhesion molecule
KOTG	Knock out transgenic animal
LAK	Lymphokine activated killer cell
LBRC	Later border recycling compartment
LERs	Low expression regions
LFA-1	Lymphocyte function associated antigen-1
LGL	Large granular lymphocyte
LILs	Liver infiltrating lymphocytes

LPAM-1	Lymphocyte Peyer's patches adhesion molecule-1
LPL	Lamina propria lymphocytes
LPS	Lipopolysaccharide
LSP-1	Leukocyte specific protein -1
LYVE-1	Lymphatic vessel endothelial receptor -1
MA	Methylamine
Mac-1	Macrophage antigen-1
MAdCAM-1	Mucosal addressin cell adhesion molecule-1
MALT	Mucosa associated lymphoid tissue
MAO -A, -B	Monoamine oxidase -A, -B
MAPK	Mitogen activated protein kinase
MCF	Median channel fluorescence
MCP-1	Monocytes chemoattractant protein-1
MHC	Major histocompatibility complex
MIG	Monokine induced by interferon gamma
MIP	Macrophage inflammatory protein
MLCK	Myosin light chain kinase
MLN	Mesenteric lymph nodes
MMPs	Metalloproteinases
MOI	Multiplicity of infection
MtI	Methylation Index
MS	Marginal sinus
NAP-2	Neutrophil–activating peptide-2
NF-κB	Nuclear factor kappa-B
NH_3	Ammonia
NK	Natural killer cell
NKT	Natural killer T cell
NL	Normal liver
Nod	Nucleotide–binding oligomerisation domain

NOD	Non–obese diabetic mice
PAMPs	Pathogen associated molecular patterns
PBC	Primary biliary cirrhosis
PBL	Peripheral blood lymphocytes
PBS	Phosphatase buffer saline
PCR	Polymerase chain reaction
PECAM-1	Platelet endothelial cell adhesion molecule-1
PDTC	Pyrollidine dithiocarbamate
PG–PS	Peptidoglycan–polysaccharide
PI3K	Phosphoinositide 3–kinase
PKC	Protein kinase C
PLN	Peripheral lymph node
PNAd	Peripheral node addressin
PPs	Peyer's patches
PRRs	Pattern recognition receptor
PSC	Primary sclerosing cholangitis
PSG	Penicillin streptomycin glutamine
PSGL-1	P–selectin glycoprotein ligand-1
RANTES	Regulated activation normal T–cell expressed and secreted
RA	Retinoic acid
RHO	Ras homologue
ROR	Retinoic acid related orphan receptor
SAMP1/Yit	Senescence accelerated mice
SCID	Severe combined immunodeficiency
SFM	Serum free media
SCR	Short consensus repeat units
SDF-1	Stromal cell–derived factor-1
SLC	Secondary lymphoid tissue chemokine
SLO	Secondary lymphoid organ

sMAdCAM-1	Soluble MAdCAM-1
sVAP-1	Soluble VAP-1
SSAO	Semicarbazide sensitive amine oxidase
TACE	Tumor necrosis factor alpha–converting enzyme
TBS	Tris–buffered saline
TCR	T cell receptor
Tfh	T follicular helper cell
TGF	Transforming growth factor
Th1	T helper 1 cell
Th2	T helper 2 cell
TLRs	Toll like receptors
TNFα	Tumour necrosis factor alpha
Treg	T regulatory cell
UC	Ulcerative colitis
VAP-1	Vascular adhesion protein-1
VAP-1 EA	VAP-1 enzymatically active
VAP-1 EI	VAP-1 enzymatically inactive
VAP-1 KO	VAP-1 knock out
VCAM-1	Vascular cell adhesion molecule-1
VE-cadherin	Vascular–endothelial cadherin
VEGF	Vascular endothelial growth factor
VLA	Very late antigen
VVOs	Vesico vacuolar organelles
WT	Wild–type

CHAPTER 1

General Introduction

1.1 OVERVIEW

The immune system is one of nature's most fascinating developments. It protects against the billions of infectious viruses, bacteria and other parasites that humans are exposed to daily. However, although for the most part the immune system is beneficial, it can also have detrimental effects. During inflammation in response to an invading pathogen, healthy tissue can be damaged by the immune system itself in what is called collateral or bystander damage. Additionally, in some cases the immune system can be directed toward self–antigens resulting in autoimmune diseases. Autoimmune and chronic inflammatory liver disease is characterised by continuous and uncontrolled leukocyte infiltration of the liver. The molecular basis of leukocyte recruitment has gained much attention over recent years because it has been recognised as a critical process in the development of inflammation. MAdCAM-1 is an endothelial cell addressin that was initially recognised to be key player in gut inflammation and especially in inflammatory bowel disease (IBD). The importance of MAdCAM-1 in IBD has been validated by the efficacy of antibodies directed against either MAdCAM-1 or its counterligand α4β7 integrin to ameliorate disease effects in animal models, as well as from the positive clinical outcomes of pharmaceutical inhibitors (MLN02, humanised anti–α4β7 antibody for the treatment of IBD). Thereafter, its expression in different tissues under inflammatory conditions has been documented and there is evidence that it has a role in the recruitment of lymphocytes to extra–intestinal tissues under certain conditions. A few years ago MAdCAM-1 was detected in the liver in inflammatory liver diseases (PSC, AIH), which often occur as extra–intestinal complications of IBD. My thesis aims to identify the factors that are responsible for the hepatic expression of MAdCAM-1, thereby elucidating the molecular pathogenesis of extra–intestinal hepatic inflammation.

1.2 IMMUNE SYSTEM

The immune system is made up of a network of cells, tissues and organs, coordinated in order to recognise and destroy invading organisms, tumour and substances that may cause tissue damage. The immune system is classified as central and peripheral lymphoid tissues, and the different components of the immune system produced from the above tissues are then able to respond to pathogens in two ways, either natural (innate immunity) or more specific (adaptive immunity) (Goldsby, 2002).

1.2.1 Central and Peripheral Lymphoid Tissues

The bone marrow and thymus constitute the central or primary lymphoid organs. The peripheral lymphoid tissues are composed of secondary organs at or near possible portals of entry for pathogens. These are exemplified by the lymph nodes, spleen and mucosa–associated lymphoid tissues (*e.g.* Peyer's patches). Bone marrow is located in the hollow centre of the bones and is the site where erythroid (erythrocytes, platelets), myeloid [neutrophils, monocytes/macrophages, basophils, eosinophils, dendritic cells (DCs)] and lymphoid cells [natural killer (NK) cells, B– and T–lymphocytes and lymphoid dendritic cells] are produced in a process named haematopoiesis. Of note, during foetal development, haematopoiesis takes place initially in the yolk sac, which is then shifted to the fetal liver and finally to the bone marrow and spleen.

The thymus, is located above the heart behind the breastbone, and is the location where education and maturation of T lymphoid cells, prior to release into the circulation, occurs. Precursor T cells migrate to the thymus where they differentiate into two distinct types: the

CD4+ T helper and the CD8+ pre–cytotoxic T cells. In addition, in the thymus, T cells become educated and undergo two selection processes, an initial positive selection, in which the T cells that are capable of responding to MHC proteins complexed with foreign peptides are selected for survival, and a negative selection, in which T cells whose receptors bind strongly to the complex of self–peptides and self–MHC proteins are eliminated by apoptosis (Alberts, 2002).

1.2.2 Innate and Adaptive Immunity

Innate immunity (or natural immunity) is the first line of defence during the first critical hours and days of exposure to a new invading organism. Through anatomical barriers (skin and internal epithelial surfaces), secretory substances (lysozyme and phospholipase in tears, saliva and nasal secretions, defensins in gastrointestinal tract and lungs, acidic pH secretions) and cellular components, the natural immune system provides physical barriers between the inside of the body and the outside world. The innate immune response depends upon a group of proteins (complement system, coagulation system, lactoferins and transferins, interferons, lysozyme and interleukin-1) and phagocytic cells [neutrophils, macrophages, eosinophils, natural killer (NK) and lymphokine activated killer (LAK) cells] that possess specific receptors [pattern recognition receptors (PRRs)] in order to recognise conserved molecular patterns common to many pathogens [the pathogen associated molecular patterns (PAMPs)] but absent from the host (Gao et al., 2008).

The innate immune response thus recognises molecular motifs associated with pathogens, whereas the adaptive immune response can develop more sophisticated responses that are highly specific and which can be magnified on second or subsequent exposure, so–called

immune memory. The primary function of the adaptive immune system is to eliminate invading pathogens and any toxic substances that they produce and to develop a memory of the pathogens so that subsequent immune responses are rapid and protective. This is achieved in two ways: a humoral and a cellular immune response, carried out by divergent classes of lymphocytes, B– and T– cells, respectively. Humoral immunity is mediated by antibodies, which are secreted by activated B cells and are specific for the antigen that caused the B cell to become activated. Secreted antibodies are responsible for eliminating extracellular pathogens (*e.g.* viruses and microbial toxins) by blocking their ability to bind receptors on host cells, and also by "marking" invading pathogens for destruction, thus facilitating their recognition, destruction and ingestion by the phagocytic cells (granulocytes, macrophages, dendritic cells) of the innate immune system.

Cellular immunity is mediated by T cells, precisely by activated cytotoxic T cells (CD8+), which can kill infected target cells by several mechanisms and by helper T (CD4+) cells that secrete a variety of cytokines that can stimulate the cytotoxic T and B cells to mature and proliferate, attract neutrophils and enhance the ability of macrophages to engulf and destroy microbes (Alberts, 2002). In addition, cellular immunity involves suppressor T cells, named T regulatory cells, which are responsible for suppressing any further immune responses after the foreign pathogen is eliminated and also for maintaining immune tolerance to self (Di Nunzio et al., 2009).

In general, the hallmarks of the adaptive immune system are memory and specificity, which reside in the antigen receptors on B and T cells, the BCRs and TCRs, respectively. Moreover,

notably, the adaptive immune system "remembers" each encounter with a foreign antigen so that subsequent encounters will stimulate increasingly effective defence mechanisms.

1.2.3 Lymphocytes

There are three main types of lymphocytes, B– and T– lymphocytes (see below) and natural killer (NK) cells. NK cells are also known as large granular lymphocytes (LGL). They resemble lymphocytes in their morphology, but they are larger with numerous granules. NK cells are capable of killing virus–infected and malignant target cells, after exposure to IL-2 and IFNγ and can be identified by the presence of CD56 and CD16 cell surface markers (Trotta et al., 2005).

1.2.3.1 B and T lymphocytes

Both B and T cells originate in the bone marrow. B cells mature in the bone marrow whereas progenitor T cells migrate to the thymus to differentiate. Naïve B and T (helper and cytotoxic) lymphocytes are cells that have not encountered an antigen, and these naïve cells are small, motile and non–phagocytic with similar morphological characteristics with a lifespan of several months (von Boehmer and Hafen, 1993). Upon interaction with an antigen, lymphocytes enlarge into lymphoblasts, which then proliferate and eventually differentiate into effector or memory cells. These populations are distinguishable from naïve precursors since they express additional and different membrane molecules (Goldsby, 2002).

Apart from CD4 T helper (Th1 and Th2) cells, a few more CD4 T cell populations have been described: the T regulatory cells (Tregs), the Th17 cells, the follicular helper T cells (Tfh), the Th9 cells and the natural killer T (NKT) cells. The Tregs are currently divided into two major

subpopulations, the naturally arising thymic CD4+CD25+ Tregs, and the peripherally induced Tr1 and Th3 cells (Bluestone and Abbas, 2003)(Jonuleit and Schmitt, 2003). The natural Tregs express high levels of IL-2Rα chain (CD25) on their cell surface and the transcription factor forkhead box p3 (Foxp3). They are specific for self–antigens and can act via contact–dependent mechanisms, whereas the adaptive Tr1 and Th3 cells can act against both self and non–self antigens via cell–contact–independent inhibition by generation of IL-10 and TGF-β cytokines, respectively. Both natural and adaptive Tregs require IL-2 for their activation and function and can actively suppress the activation and expansion of self–reactive T cells (Miyara and Sakaguchi, 2007). Expression of Foxp3 has also been demonstrated in CD8+ Tregs, which also contribute to immunoregulation (Andersen et al., 2009).

Another recently identified CD4+ T helper subset, is the population of IL-17 producing Th17 cells that play critical role in autoimmunity. Th17 cells produce additional cytokines IL-21, IL-22, TNFα and IL-6, and their development is driven by TGF-β and IL-6. Of note, Th1 and Th2 related cytokines inhibit Th17 cell differentiation, but on the contrary, IL-17 cannot suppress Th1 and Th2 cells or can do so but very weakly (Bettelli et al., 2008)(Gocke et al., 2007)(X. O. Yang et al., 2008).

An effector T cell population, initially described as Th1 and/or Th2, was found to be resident at the edge of the B cell zones and follicular regions and germinal centres, thus named the follicular helper T cells (Tfh). Since these cells expressed the B–cell promoting cytokines IL-10 and IL-21, not associated with Th1 or Th2 cells, this led to the suggestion that this T cell population represents a separate effector T cell subset (Nurieva et al., 2008). Tfh cells express

high levels of CXCR5, which is the receptor for CXCL13, which is abundant in the B cell zones (Vermi et al., 2008).

A new type of helper T cell, the Th9 cell has been reported that appears to develop from Th2 cells upon stimulation with TGF-β or by antigenic stimulation of naïve T cells in the presence of TGF-β and IL-4. Th9 cells are characterised by the secretion of IL-9, they lack expression of specific transcription factors, and thus they are not recognised by any lineage specific characteristics (Dardalhon et al., 2008)(Veldhoen et al., 2008).

Finally, another subpopulation of T cells has been recognised, named natural killer T (NKT) cells, defined by co–expression of T–cell receptor (TCR) and NK1.1 expression [CD161 in humans (marker of NK cells)]. Two major subtypes of NKT cells have been identified, termed type I or *i*NKT (invariant) cells and type II NKT (non–invariant) cells. In general, NKT cells can be CD4+, CD8+ or double negative for these molecules, and recognise antigens presented by the MHC class I related antigen CD1, adapted for presentation of lipid antigens. Upon activation NKT cells are able to rapidly produce both Th1–type (IFNγ and TNFα) and Th2–type (IL-4, IL-10 and IL-13) cytokines and IL-17. Moreover, activated NKT cells are able to release cytotoxic molecules and kill other cells through FASL–mediated and perforin–dependent pathways, hence contributing to the protection of hosts from infections and tumours by regulating immunity (Godfrey et al., 2004)(Swain, 2008)(Tupin et al., 2007).

1.2.3.2 The Career of B– and T– lymphocytes

Once mature, lymphocytes leave the bone marrow or thymus and start circulating through the secondary lymphoid organs. This continuous recirculation of lymphocytes significantly enhances the chance of a successful encounter with specific antigen. Naïve antigen inexperienced cells pass directly from the blood to secondary lymphoid tissues through specialised high endothelial venules (HEVs) into the surrounding T (–rich) zones (Mackay et al., 1990). Naïve B cells follow the same route but after they have entered the T cell zone, they move further to the adjacent B (–rich) cell follicles that also contain follicular dendritic cells (Picker and Butcher, 1992). If lymphocytes do not encounter an antigen in the lymph nodes, they return back to the blood circulation via the main lymphatic vessel (the thoracic duct). This continuous circulation between the blood and lymph ends only when the lymphocyte encounters its specific antigen, along with a co–stimulatory molecule on the surface of an antigen–presenting cell (APC) in peripheral lymphoid organs.

Upon activation, lymphocytes proliferate and differentiate into effector cells. Precisely, activated B cells within the lymphoid follicles, known as follicle centre cells, undergo clonal expansion; with the most of the family clones becoming antibody–producing plasma cells. The other B cells become long–lived memory cells. Activated T cells, differentiate in either CD4 T helper cells (Th1 and Th2) or T cytotoxic cells (CD8). After several days, some of the effector cells leave the peripheral lymphoid organs via the lymph and migrate through the blood to the site of infection. This change in migration is a consequence of activation, differentiation and functional maturation of lymphocytes re–programming their expression profiles of adhesion molecules and chemokine receptors promoting their migration towards the tissue in which they

were activated (Butcher et al., 1999)(Sallusto et al., 2000)(Yoshie et al., 2001). Thus, T cells that have encountered their antigen in Peyer's patches, express the leukocyte integrin α4β7, which preferentially binds to MAdCAM-1 on gut endothelium and thereby promotes recruitment to the gut (Mackay, 1993)(Schweighoffer et al., 1993). Similar principles have been demonstrated for other anatomical sites such as the skin, where skin homing lymphocytes express high levels of cutaneous lymphocyte antigen (CLA) that binds E–selectin, and CCR4 that responds to the chemokines CCL17 and CCL22 (Eksteen et al., 2004b)(Picker and Butcher, 1992). Therefore, T cells are primed in this way in order to migrate into sites where is more likely that they will re–encounter the same activating antigen. Interestingly, the memory cells, in a second encounter with antigen, follow different recirculation pathways than naïve cells, in the sense that they can enter draining lymph nodes directly from blood by afferent lymphatics without the need to migrate through HEVs (Mackay, 1993).

1.3 Leukocyte Recruitment Cascade

Leukocytes circulate continuously from blood into tissues and secondary lymphoid organs, and then return back to the blood to patrol the body in search for antigens, thus providing an effective immune surveillance (Girard and Springer, 1995)(Warnock et al., 1998). Activation by an antigen confers the T cell with the ability to home to non–lymphoid tissues, preferentially to those that are connected to the secondary lymphoid organs where antigen was first encountered (D. J. Campbell and Butcher, 2002)(Masopust et al., 2001). Therefore, in order to complete all these tasks, leukocytes must be capable of crossing multiple vascular barriers and in all cases the key interaction is between leukocyte and endothelial cells lining the vessels (Springer, 1995).

Leukocytes leave the bloodstream through the specialised postcapillary vascular sites, named high endothelial venules (HEV), which are present in all secondary lymphoid organs (with exception of spleen, where lymphocyte migration occurs via the blood sinusoids in the marginal zone), and through microvascular endothelium within tissue. HEV–like vessels are also observed in chronically inflamed non–lymphoid tissues thus supporting unremitting leukocyte recruitment to these sites (Girard and Springer, 1995)(Grant et al., 2002a). The initial interactions between endothelium and leukocytes induce tethering or rolling of the latter on the endothelial surface (Lalor et al., 1997)(Tedder et al., 1995a). Because blood flow generates shear forces, leukocytes have to resist these significant forces whilst interacting with the endothelium (Sackstein, 2005). This first contact allows leukocytes to sample the endothelial microenvironment for chemokines, which are immobilised by glycosaminoglycans on the endothelial luminal surface (Adams and Lloyd, 1997)(Tanaka et al., 1993). The appropriate pairing of chemokine/chemokine receptor induces intracellular signals that trigger activation of the leukocyte integrins, which in turn are able to bind to their ligands, members of the immunoglobulin superfamily expressed on the endothelial surface, hence becoming firmly arrested on the endothelium. In the final step, leukocytes pass through the endothelial monolayer in a process named transendothelial migration or diapedesis, mediated by poorly understood mechanisms, and then follow directional cues to the site of infection or tissue injury (Figure 1.1) (Muller, 2003).

Different classes of adhesion and activation molecules mediate each step of the recruitment cascade, all of which are critical for an efficient extravasation process, since the presence of the appropriate pair in one step is needed for the next step to occur. Adhesion molecules and

chemokines are induced with inflammation allowing peripheral tissues to readily recruit effector cells. In addition, effector cells generated in the different lymphoid organs undergo a re–programming process to express tissue specific adhesion molecules resulting in tissue selective homing. This latter process controls the extent and scope of immune responses, and accounts for the regional compartmentalisation of immune system (Butcher and Picker, 1996).

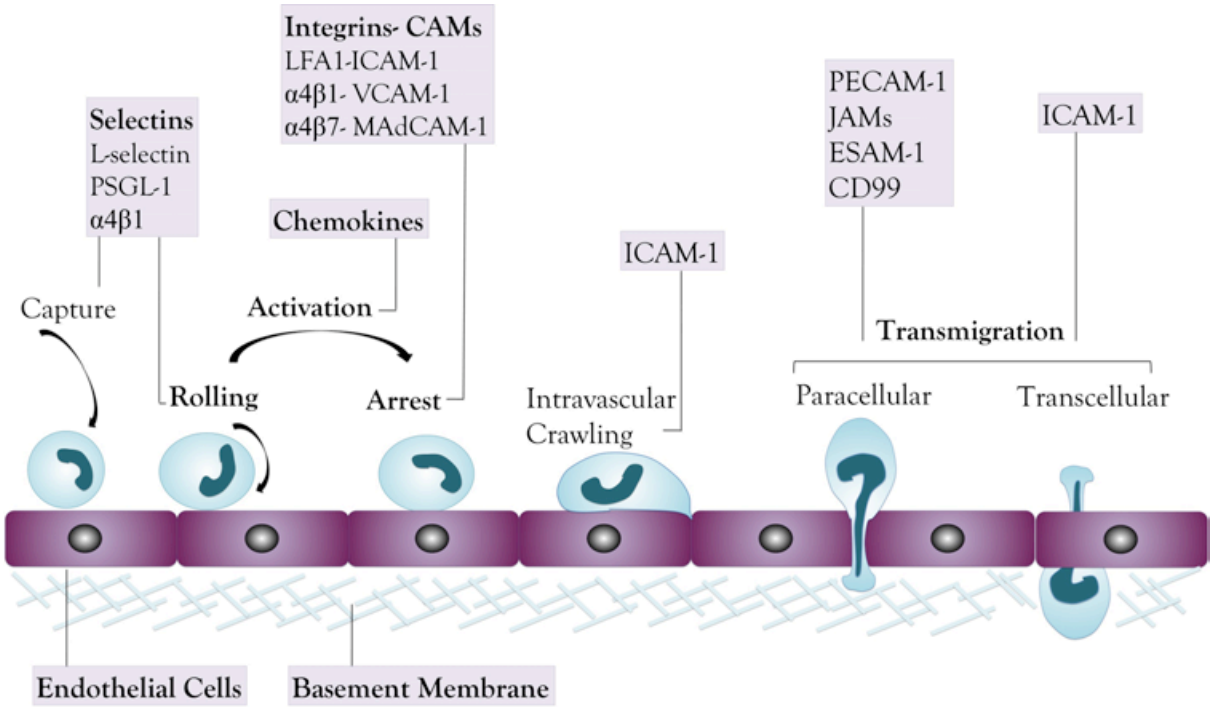

Figure 1.1 The leukocyte recruitment cascade. The initial capture of leukocyte is followed by rolling on the endothelial surface, mediated by members of the selectin family and some integrins. The cell starts moving along the endothelial lining at reduced velocity, sampling the endothelial microenvironment for appropriate chemotactic signals (chemokines), either soluble or immobilised by glycosaminoglycans on the endothelial surface. Binding of chemokines to their cognate chemokine receptors on the leukocyte surface, leads to rapid G-protein coupled signalling pathways, which finally trigger cytoskeletal rearrangement and integrin activation. Then, activated integrins are able to bind with high affinity and avidity to their ligands, members of the immunoglobulin superfamily (CAMs), promote firm adhesion and allow the leukocyte to crawl on the endothelial surface towards the endothelial borders searching for signals in order to transmigrate. Thereafter, the leukocyte can pass to the basement membrane following either the "legal" way through the endothelial junctions (paracellular) or the peculiar way through the endothelial body (transcellular). The latter route is accepted, although it is still unknown what makes leukocyte decide which route to follow. Some of the molecules taking part in the leukocyte process are demonstrated in boxes. PSGL-1, P-selectin glycoprotein ligand-1; ICAM-1, intracellular cell adhesion molecule-1; VCAM-1, vascular cell adhesion molecule-1; MAdCAM-1, mucosal addressin cell adhesion molecule-1; LFA-1, lymphocyte function-associated antigen 1 (also known as αLβ2- integrin); JAM, junctional adhesion molecule; PECAM-1, platelet endothelial cell adhesion molecule -1; ESAM-1, endothelial cell selective adhesion molecule (Ley et al., 2007).

1.3.1 Rolling

The rolling step has been described as an inherently unstable transition state, poised between firm adhesion and lack of adhesion (Hammer and Apte, 1992). The adhesion molecules that classically mediate this rolling step are members of the selectin family and their carbohydrate ligands on the vascular endothelium surface (Tedder et al., 1995a). The driving force for rolling is the hydrodynamic force of the bloodstream (Alon et al., 1995a). Although the wall shear stress in postcapillary venules varies widely within tissues as well as under inflammation or exercise, the velocity of rolling cells both *in vitro* and *in vivo* appears more stable, suggesting the importance of the rolling step as a checkpoint in the leukocyte recruitment process, especially in inflammation (Lawrence and Springer, 1991).

During rolling, selectin–ligand bonds are clustered and thus can resist to force collectively rather than individually (Chen and Springer, 1999). Furthermore, as shear stress increases, the number of selectin–ligand bonds between the flowing cell and the substrate increases at the front edge of the cell, hence counterbalancing the elevated rate of pre–existing bond dissociation at the rear edge (Yago et al., 2007). In addition, the increased shear stress, prolongs the selectin–ligand bond lifetimes, meaning that each bond is strengthened and the molecules lock more tightly, in a phenomenon named "catch–bond" (Marshall et al., 2003). Of note, the velocity of a rolling cell will determine the time duration of exposure of the leukocyte to activating stimuli on the vessel wall, and thus is important in determining whether activation will occur or not. In the absence of appropriate stimuli, leukocytes might roll through a postcapillary venule without undergoing firm adhesion or transmigration (Chen and Springer, 1999).

Of note, although integrins are critical players in the following firm adhesion step of the extravasation cascade, it has been reported that α4 and β2 integrins can also support rolling. The α4β1 integrin can support rolling on VCAM-1 that lacks a mucin domain (Alon et al., 1995b), however the α4β7 integrin can support more efficient rolling when binding to its ligand MAdCAM-1 that contains a mucin–domain (Berlin et al., 1995). The β2 integrins, αLβ2 (LFA-1) and αMβ2 (Mac-1; macrophage antigen-1) have also been suggested to mediate rolling when binding to ICAM-1 and ICAM-2 (Dunne et al., 2002).

1.3.1.1 Selectins

The selectin family consists of three closely related cell–surface molecules: L–selectin (CD62L), E–selectin (CD62E) and P–selectin (CD62P), which are named after the cells in which they are expressed (Bevilacqua and Nelson, 1993)(McEver, 2001)(Vestweber and Blanks, 1999).

L–selectin is expressed on hematopoietic cells, with most classes of leukocytes constitutively expressing this molecule. The majority of B and naïve T cells, as well as circulating neutrophils, monocytes and eosinophils express L–selectin, whereas only a subpopulation of memory T cells and NK cells are L–selectin positive. Moreover, early myeloid progenitor cells express L–selectin, although mature erythrocytes are L–selectin negative. The broad expression of L–selectin explains its critical role in the trafficking of all leukocyte lineages into secondary lymphoid tissues and peripheral sites of injury and inflammation (Gallatin et al., 1983)(Tedder et al., 1990).

P–selectin is produced and stored in the α granules of platelets and in the Weibel–Palade bodies of endothelial cells. After stimulation with pro–inflammatory factors (oxygen–derived free radicals, complement fragments and cytokines) and thrombogenic mediators (thrombin, histamine), P–selectin is rapidly released and immobilised to the cell surface (Hsu-Lin et al., 1984)(McEver et al., 1989). Moreover, P–selectin is constitutively expressed on the endothelium of lung and choroid plexus microvessels (Kivisakk et al., 2003) and is induced on endothelial cells under several inflammatory diseases, including atherosclerosis (Kansas, 1996)(Ley, 2003).

E–selectin is *de novo* expressed on endothelial cells upon cytokine stimulation (*e.g.* by TNFα, LPS and IL-1) in most organs. E–selectin is only constitutively expressed in skin microvessels allowing it to recruit skin homing memory T cells that express the E–selectin ligand cutaneous lymphocyte antigen (CLA) (Vestweber and Blanks, 1999).

All selectins are type I membrane proteins (transmembrane proteins having their N–terminus exposed to the extracellular or luminal space), composed of five domains, which are starting from the N–terminal end: a calcium (Ca^{2+}) dependent lectin domain, an epidermal growth factor (EGF)–like domain, two to nine short consensus repeat (SCR) units, a transmembrane domain and a cytoplasmic tail (Kansas, 1996)(Vestweber and Blanks, 1999). The long extracellular molecular structure of E– and P– selectin renders them the most suitable for the rolling step, since the well extended structure above the surrounding glycocalyx allows them to capture flowing leukocytes that express the appropriate receptors (Lasky, 1992). L–selectin, possesses only two SCRs, but since it is localised to leukocyte microvilli extending from the

leukocyte body, is able to support optimal leukocyte–endothelial cell interactions (Erlandsen et al., 1993).

Selectins recognise sialyl Lewis X and related carbohydrate ligands, presented on specialised glycoprotein scaffolds (Ley and Kansas, 2004)(McEver, 2002). The ligands for selectins are various glycoproteins, including P–selectin glycoprotein–1 (PSGL-1), E–selectin ligand–1 (ESL-1) (Steegmaier et al., 1995) and CD44 (Hidalgo et al., 2007), both ligands for E–selectin, glycoslylation–dependent cell adhesion molecule–1 (GlyCAM-1) and CD34, both members of the peripheral node addressin family (PNAd) that serve as ligands for L–selectin (Puri et al., 1995)(Rosen, 2004). Another adhesion molecule, mucosal addressin cell adhesion molecule–1 (MAdCAM-1), a member of the immunoglobulin superfamily, can also serve as ligand for L–selectin, when it is properly glycosylated (M. J. Briskin et al., 1993)(Streeter et al., 1988). PSGL-1 can bind to all three selectins when properly glycosylated (Moore, 1998). Very interestingly, the binding of PSGL-1 to L–selectin (both expressed on leukocytes) can mediate a secondary tethering process, so that leukocytes expressing PSGL-1 can adhere to leukocytes already rolling on L–selectin. Moreover, through this secondary tethering process, leukocytes that do not express ligands for E–selectin or P–selectin can still reach sites of inflammation (Ley et al., 2007).

1.3.2 Activation and Arrest

During leukocyte rolling, the cells bind endothelium via fast acting molecular bonds, which are unable to arrest the leukocytes firmly. The movement in the vicinity of endothelial cells enables

the leukocytes to sample the endothelial microenvironment for chemoattractant cytokines, named chemokines, which are needed for integrin activation and subsequent firm arrest.

1.3.2.1 Chemokines

Chemokines are a group of small, closely–related chemotactic cytokine proteins that play important roles in both innate and adaptive immunity (Baggiolini et al., 1997). The chemokine family is rapidly increasing and to date there are more than 50 human members identified (Cyster, 1999)(Kim and Broxmeyer, 1999), which have been classified into four major families on the basis of the number and spacing of conserved cysteines in the NH_2–terminus (Rossi and Zlotnik, 2000). These are termed the CXC, CC, C and CX_3C chemokine families. The CXC chemokines are further subdivided into two subclasses based on the presence or absence of the ELR amino acid motif (glutamic acid [E]–leucine [L]–arginine [R]) at the N–terminus. The ELR chemokines include CXCL1/GROα, CXCL5/ENA-78, CXCL6/GCP-2, CXCL7/NAP-2 and CXCL8/IL-8, which are strong neutrophil chemoattractants and exert angiogenic effects. The non–ELR chemokines consist of CXCL9/MIG, CXCL10/IP-10, CXCL11/-TAC, CXCL12/SDF-1a and CXCL13/BLC, which recruit mainly lymphocytes and exert angiostatic effects (Koch et al., 1992).

The CC group includes the chemokines CCL5/RANTES, CCL3/MIP-1α and CCL4/MIP-1β, CCL2/MCP-1, CCL11/eotaxin, CCL21/6ckine, CCL20/MIP-3α and CCL19/MIP-3β, which exert their effects on monocytes, lymphocytes, eosinophils and basophils but not neutrophils (Baggiolini et al., 1997)(Luster, 1998)(Rollins, 1997). In the C chemokine group, lymphotactin attracts lymphocytes and natural killer (NK) cells but not monocytes (Kelner et al., 1994)

(Kennedy et al., 1995). The chemokine fractalkine defines the CX_3C group. CX_3CL1 (fractalkine) along with CXCL16 of the CXC group are expressed as transmembrane molecules, which possess an N–terminal chemokine domain, a mucin–like stalk, a transmembrane domain and a short cytoplasmic tail. Both CX_3CL1 and CXCL16 also exist in soluble forms after proteolysis at the cell surface (Bazan et al., 1997)(Schulte et al., 2007). The current chemokine nomenclature is based on the chemokine receptor nomenclature, which uses CXC, CC, C or CX_3C followed by R (receptor) and then a number. The new nomenclature replaces R with L (ligand) to designate the ligands (Table 1.3) (Zlotnik and Yoshie, 2000).

Chemokines can be divided into homeostatic and inflammatory types based on their functional properties. Homeostatic chemokines are constitutively expressed at high levels in lymphoid organs as well as in non–lymphoid tissues such as skin and mucosa (Oo and Adams, 2009) where they mediate the naïve and memory lymphocyte trafficking to lymphoid and effector tissues, as well as their guidance to the correct microenvironment within the tissue (Olson and Ley, 2002). Among this group CCL19 (Yoshida et al., 1997) and CCL21 (SLC; secondary lymphoid organ chemokine) (Nagira et al., 1997) are ligands for CCR7, and their importance is highlighted in mice deficient in CCR7 or CCL21, which show defective recruitment of naïve T cells to secondary lymphoid organs (Forster et al., 1999)(Gunn et al., 1999). On the other hand, inflammatory chemokines are up–regulated by inflammatory stimuli in inflamed tissues by resident and infiltrating immune cells, and mainly regulate the recruitment of neutrophils, monocytes, NK cells and effector lymphocytes into effector sites (Olson and Ley, 2002)(Oo and Adams, 2009).

Activated endothelial cells, epithelial cells and leukocytes produce chemokines, but virtually any cell is capable of chemokine generation upon stimulation with lipopolysaccharides or inflammatory cytokines (Kim and Broxmeyer, 1999). After secretion chemokines can bind to heparin–like glycosaminoglycans on the cell surface and in the extracellular matrix, which helps leukocytes to track down these immobilised chemokines in a process named haptotaxis (Cyster, 1999)(S. Jung and Littman, 1999). The binding of chemokines to glycosaminoglycans not only prevents them from being washed away, but also maintains them in mono/dimeric forms, which increases their affinity for their chemokine receptors (Baltus et al., 2003). Additionally, the immobilised chemokines can persist at high concentrations in tissues for longer than freely diffusible chemokines (von Andrian and Mackay, 2000). Thereafter, chemokines can elicit their effects during leukocyte recruitment through interactions with their receptors, members of the seven–transmembrane, rhodopsin–like G protein–coupled receptors (Yoshie et al., 2001). Some chemokines recognise multiple receptors whereas others only have one receptor and similarly some receptors bind only one chemokine whereas others are highly promiscuous and bind multiple chemokines (Zlotnik and Yoshie, 2000).

	Chemokine Receptor	Chemokine Ligands	Target Cells
Subfamily XC			
	XCR1	XCL1, XCL2	T cells and Natural Killer cells
Subfamily CC			
	CCR1	CCL3, CCL5, CCL7, CCL14	T cells, monocytes, basophils and eosinophils
	CCR2	CCL2, CCL7, CCL8, CCL13, CCL16	Memory T cells, monocytes and DCs
	CCR3	CCL5, CCL7, CCL8, CCL11, CCL13	Eosinophils, basophils, mast cellsm Th2 cells and platelets
	CCR4	CCL17, CCL22	Th2 cells, DCs, basophils, macrophages and plateletes
	CCR5	CCL3, CCL4, CCL5, CCL11, CCL14, CCL16	T cells, monocytes
	CCR6	CCL20	T cells, B cells and DCs
	CCR7	CCL19, CCL21	T cells and DCs
	CCR9	CCL25	T cells and plasma cells
	CCR10	CCL27, CCL28	T cells
Subfamily CXC			
	CXCR1	CXCL6, CXCL8	Neutrophils and monocytes
	CXCR2	CXCL1, CXCL2, CXCL3, CXCL5, CXCL6, CXCL8	Neutrophils, monocytes and vascular endothelial cells
	CXCR3-A	CXCL9, CXCL10, CXCL11	Th1 cells, mast cells and mesangial cells
	CXCR3-B	CXCL4, CXCL9, CXCL10, CXCL11	Neoplastic cells and vascular endothelial cells
	CXCR4	CXCL12	Multiple cells
	CXCR5	CXCL13	B cells and T helper cells
	CXCR6	CXCL16	CD8+T cells, NK cells and memory CD4+ T cells
Subfamily CX3C			
	CX3CR1	CX3CL1	Macrophages and smooth muscle cells

Table 1.1 Chemokines and chemokine receptors. The chemokine and chemokine receptor family have been classified into four groups dependent on the number and spacing of conserved cysteines in the NH_2-terminus. The two largest groups are the CC chemokines, where conserved cysteines lie adjacent to each other, and the CXC chemokines where the first two cysteines are separated by a non–conserved amino acid. The two minor groups include the XC chemokines, which lack two out of four canonical cysteines and the CX_3C chemokines in which three amino acids separate both cysteines.

1.3.2.2 Integrins

Integrins are a family of over 20 heterodimeric membrane–bound glycoproteins composed of one α and one β chain. In addition to their role in mediating cell adhesion and migration, they can also regulate cell growth and survival (Kummer and Ginsberg, 2006). Integrin subunits have large, structurally complex extracellular domains, which contain three to four divalent cation–binding sites that are involved in ligand binding, a single–pass transmembrane helix and cytoplasmic tails that regulate integrin function (Hynes, 2002). The two subunits are non–covalently associated; therefore α chains can associate with more than one β chains, and *vice versa*, thus creating a large molecular variety.

Integrins can be broadly grouped into further subfamilies based on the β subunit. The most essential integrin subfamilies for the leukocytes are the β1, β2 and β7 integrins. The β1 integrins (also known as VLA proteins) share a common β chain (CD29) paired with different α subunits (CD49a- CD49f), and mainly bind with the extracellular matrix components such as fibronectin, laminin and collagen. The β2 integrins have a common β chain CD18 paired with the α chains CD11a (LFA-1), CD11b (Mac-1) or CD11c (p150, 95), and they are expressed on lymphocytes (CD11a), neutrophils and monocytes (CD11a and CD11b) and dendritic cells (CD11a and CD11c), and bind to ICAM-1 and ICAM-2 on other cells including endothelial cells (Adams and Shaw, 1994)(Diamond et al., 1990)(Makgoba et al., 1988)(Sadhu et al., 2007). The α4β7 integrin belongs in the β7 integrin group and is expressed on leukocytes where it mediates binding to fibronectin, VCAM-1 (Postigo et al., 1993) and more efficiently to MAdCAM-1. The αEβ7 integrin, which is constitutively expressed by intestinal intraepithelial lymphocytes, mediates binding to E–cadherin (Berlin et al., 1993)(Cepek et al., 1994). The

most important integrins on leukocytes responsible for mediating adhesion to endothelial targets are members of the β2 integrins, LFA-1 (CD11a/CD18 or αLβ2) and Mac-1 (CD11b/CD18 or αMβ2), the β1 integrin α4β1 (VLA-4) and the β7 integrin α4β7 (Hynes, 2002).

Integrins function as bi–directional signalling molecules and their ability to bind to their ligands is dynamically regulated by conformational changes (Schwartz et al., 1995). In particular, in resting cells, integrins exist predominantly in a non–adhesive state and change into an adhesive state only upon cellular stimulation (Carman and Springer, 2003). The binding of chemokines to their receptors is one signal that results in integrin activation via phosphorylation of carboxyl–terminal serine/threonine residues, dissociation of heterotrimeric G proteins, generation of inositol triphosphate, intracellular calcium release and activation of protein kinase C (PKC) (Luster, 1998). With additional activation of the Ras and Rho families of guanosine triphosphate (GTP)–binding proteins, chemokine receptors mediate multiple signalling pathways that regulate integrin activation. The activation of the G–protein coupled receptor leads to the binding of intracellular proteins (such as talin–1, an actin–binding protein) to the integrin cytoplasmic domains, thereby triggering conformational signal transmission to the extracellular domains (Kinashi, 2005). Thereafter, the integrin extracellular domains undergo structural changes that result in conformations competent for ligand binding. Interestingly, this dynamic regulation of integrin adhesiveness, termed "inside–out" signalling (Carman and Springer, 2003), induces integrins to undergo a dramatic transition from a bent low–affinity conformation to an extended intermediate and high–affinity conformation, which in turn leads to an opening of the ligand–binding "pocket" (Arnaout et al., 2005). Divalent

cations such as Mg^{2}+ and Mn^{2}+ are also able to modulate integrin affinity (Stewart and Hogg, 1996). This "inside–out" signalling along with the shear forces exerted on the arrested leukocyte, are thought to play a critical role in the process of leukocyte recruitment, in which the appropriate balance between up–regulation of ligand binding at the leading edge and down–regulation at the trailing edge maintains the forward locomotion of leukocytes (Alon and Ley, 2008)(Kinashi, 2005)(Sanchez-Madrid and del Pozo, 1999).

Moreover, binding of integrins to their ligands, induces signalling pathways from the extracellular domain to the cytoplasm in the classical outside–in direction ("outside–in" signalling), regulating various cellular functions, including cell motility, proliferation and apoptosis (Giagulli et al., 2006)(Shattil, 2005). During the leukocyte recruitment process, the overall strength of cellular adhesiveness, named avidity, is governed by two parameters; the intrinsic affinity of the individual receptor–ligand bonds and the number of the bonds formed, which is dependent on the ability of integrins to move in the plasma membrane and cluster together into the zone of cell adhesion (Carman and Springer, 2003).

1.3.3 Transmigration

After adhesion and crawling, leukocytes move towards the endothelial cell borders looking for signals in order to complete transendothelial migration, or diapedesis. Of note, while the preceding steps of tethering, rolling and firm adhesion are reversible, diapedesis is arguably the "point of no return" for the leukocyte (Gunn et al., 1998). In depth investigations of this process however have revealed that after diapedesis leukocytes might reverse transmigrate, although this has phenotypic and functional consequences (Buckley et al., 2006)(Muller, 2009).

Slow progress has been made in understanding leukocyte transmigration due to the complex nature of the vessel wall, which is difficult to accurately model and study *in vitro* (Voisin et al., 2009). Particularly, venular walls have two cellular components, the endothelial cells, which are the primary barrier for emigrating leukocytes, and the pericytes that are long cells forming a discontinuous, subendothelial layer. Both appear to contribute to the generation of the non–cellular specialised matrix or basement membrane (BM) that surrounds blood vessels (Hirschi and D'Amore, 1996). The vascular BM consists of two independent protein networks formed by laminin-8 and laminin-10, and collagen type IV, all largely interconnected with other components of the BM such as nidogen-2 and perlecan (Timpl, 1996).

The well–accepted dogma is that leukocytes transmigrate through endothelial cell junctions (the paracellular route) although studies have reported an additional route, through the body of an endothelial cell (transcellular route) which has been observed in the central nervous system and in various inflammatory scenarios (Engelhardt and Wolburg, 2004)(D. Feng et al., 1998). Although contradictory opinions have been presented over the years, it has become clear that lymphocytes can migrate both in a "paracellular" and "transcellular" way although the precise contribution of each mechanism is poorly understood in most circumstances (Phillipson et al., 2006).

In general, luminal chemoattractants in combination with hydrodynamic shear forces can induce transendothelial cell migration (Cinamon et al., 2001b)(Cinamon et al., 2004). Initially, the interaction of an already firmly arrested leukocyte integrin, αLβ2 (LFA-1) with its counter–receptor on endothelial cells, ICAM-1, induces the clustering of ICAM-1 as the leukocyte

approaches the endothelial cell border (Barreiro et al., 2002), which in turn stimulates the phosphorylation of contractin that leads in actin polymerization and recruitment of more ICAM-1 around the tightly adherent leukocytes (Durieu-Trautmann et al., 1994). If endothelial cells express VCAM-1 and leukocytes α4β1, their interaction also induces VCAM-1 clustering around the leukocytes, into endothelial projections termed "transmigratory cups" (Carman and Springer, 2004).

The multimerisation of ICAM-1 and VCAM-1 on the endothelial cell surface transmits a variety of signals to the cell. The most important of those is the increased intracellular $Ca^{2}+$ which leads to endothelial cell contraction and loosening of endothelial cell junctions, therefore facilitating the movement of leukocyte through the endothelial barrier (Huang et al., 1993). Additionally, the loosening of the endothelial junctions by ICAM-1 and VCAM-1 signalling pathways is mediated by their effects on VE–cadherin phosphorylation, a molecule that is a prerequisite for adherens junction disassembly (Turowski et al., 2008). While the leukocyte is transmigrating there is a continuous recycling of membrane from the later border recycling compartment (LBRC) to the position where the leukocyte is migrating, providing increased surface area and un–ligated molecules for leukocytes to interact with before passing through the endothelial layer (Muller, 2009). In the intracellular pathway of migration, ligation of ICAM-1 by leukocyte integrin leads to translocation of ICAM-1 to actin and caveolae–rich regions. The caveolae (typical recycling endosomes) that contain ICAM-1 are linked together forming vesico–vacuolar organelles (VVOs) that create an intracellular channel through which the leukocyte can migrate (Ley et al., 2007).

After leukocytes have migrated through the endothelial cell barrier, they need to migrate through the endothelial basement membrane as well. The existence of regions of low matrix protein deposition, named "low expression regions" or LERs, has been previously reported in the vascular basement membrane (BM) of the postcapillary venules. Interestingly, these LERs seem to be aligned with the gaps between adjacent pericytes, thus acting as "gates" for infiltrating neutrophils and monocytes (Voisin et al., 2009). Additionally, it has been proposed that leukocytes possess a variety of proteases that they use in order to degrade matrix components, thus facilitating their transmigration through the BM (S. Wang et al., 2006).

1.3.3.1 Junctional Adhesion Molecules

Several junctional adhesion molecules have been implicated in transendothelial migration of leukocytes (Muller, 2003). These molecules include immunoglobulin superfamily members such as PECAM-1, ICAM-1, ICAM-2, VCAM-1, JAM-A, JAM-B, JAM-C (Barreiro et al., 2002)(Woodfin et al., 2007), the endothelial cell selective adhesion molecule (ESAM) and the non–immunoglobulin molecule CD99 (Vestweber, 2002). Of note, apart from ICAM-1 and VCAM-1, a characteristic of all the molecules involved in transmigration is that they are concentrated at cell junctions where they appear to play an important role in the steps just before diapedesis. Notably, during transmigration both ICAM-1 and VCAM-1 are also translocated to cell borders (Muller, 2009).

Although all the preceding steps of the cascade (tethering, rolling, adhesion) are based on heterophilic interactions between one class of molecule on the leukocyte surface and another class of molecule on the endothelial cell, transmigration proceeds by both heterophilic

(LFA1/JAM-A, Mac-1/JAM-C and α4β1/JAM-B) and homophilic interactions between lymphocyte and endothelial PECAM-1, CD99, JAM-A and JAM-C (Muller, 2003). In addition, these adhesion molecules appear to mediate leukocyte transmigration in either leukocyte–specific or stimulus–specific manner. For example, PECAM-1, ICAM-2 and JAM-A mediate leukocyte transmigration in response to IL-1β but not TNFα (Nourshargh et al., 2006) whereas, ESAM appears to mediate the migration of neutrophils rather than T cells, without showing any stimulus–specific role (Wegmann et al., 2006).

1.4 MAdCAM-1: An Endothelial Cell Adhesion Molecule

MAdCAM-1 or "mucosal addressin cell adhesion molecule–1" is an endothelial cell adhesion molecule significant for directing leukocytes into mucosal and inflamed tissues, via interactions with the leukocyte alpha4 beta7 integrin (LPAM-1), L–selectin and alpha4 beta1 integrin (VLA-4) (Girard and Springer, 1995). MAdCAM-1 belongs to the immunoglobulin (Ig) superfamily and shows many common characteristics with the other two members of the family, ICAM-1 (intercellular cell adhesion molecule–1) and VCAM-1 (vascular cell adhesion molecule–1). Additional members of the immunoglobulin superfamily are ICAM-2 and ICAM-3.

1.4.1 Genomic Organisation of MAdCAM-1

MAdCAM-1 protein is encoded by a gene, located at p13.3 on chromosome 19, in close proximity to the ICAM-1 and ICAM-3 genes (19p13.2–p13.3), raising the possibility that these molecules are clustered together in the short arm of chromosome 19. The coding sequence of human MAdCAM-1 is contained in 5 exons, under the control of a 717bp 5' flanking promoter region. The signal peptide, the two Ig domains and the mucin domain (major and

minor) are each encoded by separate exons, whereas the transmembrane domain, the cytoplasmic tail and the 3' untranslated region are encoded on exon 5. Several potential transcriptional regulatory elements, including NF-κB, SP1, AP2, PEA3, NF-E1, Adh1, MyoD, E2A, ENKCRE, IRS sites and a GC box, have been indentified in the promoter region of the gene. Notably, only two NF-κB sites, one SP1 and a potential TATA box are also present in the mouse MAdCAM-1 gene promoter region and are conserved in position (Leung et al., 1997).

1.4.2 MAdCAM-1 Protein Structure

The encoded MAdCAM-1 protein is a 40kDa (406aa) protein that is extensively post–translationally modified *in vivo,* through O–linked glycosylation leading to the formation of a 60kDa mature glycoprotein. Structurally MAdCAM-1 comprises two N–terminal Ig domains of 52 and 71 amino acids (aa) respectively, each possessing the invariant cysteine residue responsible for stabilisation of the Ig loop, with the first domain having doublet cysteines (Leung et al., 1996), and both Ig domains being separated from the cell surface by a 117aa mucin like region. Human MAdCAM-1 also comprises a transmembrane domain of 20 hydrophobic residues and a 43aa cytoplasmic tail, which is longer than the murine homologue (Shyjan et al., 1996). The extracellular domain of murine MAdCAM-1 contains an additional Ig domain, adjacent to the transmembrane segment that displays high homology to the Ca2 domain of IgA1 (33%) (M. J. Briskin et al., 1993) and is separated from the second Ig domain by a mucin–like region. An additional Ig domain has also been observed in rodents, dogs, pig and ruminant homologues (Tachedjian et al., 2006). In rats, the last immunoglobulin–like domain shows homology to the a3 domain of the rat MHC class I molecule, but not to the Ca2 region of IgA1 (Rada et al., 1990). Studies have shown that the two N–terminal Ig domains of

MAdCAM-1 are sufficient for activation–independent adhesion to α4β7 (M. J. Briskin et al., 1996) and a number of structural elements such as the cysteine residues that stabilise the Ig loops are conserved in those two Ig domains across many species (rodents, dogs, ruminants, pigs) (Tachedjian et al., 2006), supporting their role in α4β7 integrin binding.

The human MAdCAM-1 mucin domain is rich in proline/serine/threonine (P/S/T) residues (58%) and this motif is repeated 8 times, whereas in mice this mucin–like region is also rich in P/S/T (51%), but only found once probably because this region is shorter (37aa). The suggested primary function of the MAdCAM-1 mucin–like region is to provide a framework for decoration with carbohydrate moieties allowing MAdCAM-1 to serve as a vascular ligand for the L–selectin (Berg et al., 1993). Indeed, human MAdCAM-1 has 19 potential sites for O–linked glycosylation, and one N–linked glycosylation site within the first Ig domain, which is conserved in all MAdCAM-1 homologues except those from the mouse and rat. Of note, site–directed mutagenesis to remove the N–linked glycosylation site in human MAdCAM-1 has revealed that it is not essential for activity (Tan et al., 1998). Intriguingly, human MAdCAM-1 has compensated for a lack of the third Ig domain (present in the murine and other species homologues) by extending its mucin domain as two separate regions (major and minor domain) in order to hold the two N–terminal ligand–binding domains above the glycocalyx for presentation to α4β7 integrin. The fact that the repeats apparent in the mucin domain are highly similar to one another (75–100%) suggests that they arose by duplication. Another possibility is that the repeats in the major domain may have been inserted possibly by a gene conversion event that involves a mucin gene, resulting in enrichment of Ser–Thr–Pro residues

(40% in the major domain) and thus enabling better presentation to L–selectin (Leung et al., 1996).

Two general functions have been proposed for the mucin–like domains. The primary general function, based on the extended structure of the mucins would be to hold the distal Ig domains further above the glycocalyx, thus allowing more efficient interactions between the N–terminal domains and ligand. Secondly, the mucin domain could facilitate the physical presentation *in vivo* of the N–terminal domains under flow conditions, where the hemodynamic parameters do not favour close physical contact between cells (Jentoft, 1990). Hence, similar functions might apply for MAdCAM-1 mucin domain for α4β7 integrin recognition.

Of note, the overall nucleotide and protein identity between human and murine MAdCAM-1 is poor (42% and 39% respectively), although the two first Ig domains are highly conserved (59% and 65% respectively). Additional phylogenetic analysis of domains I and II have shown that there is a relatively close evolutionary relationship amongst ruminant, pig, dog and primate MAdCAM-1 whereas the rodent counterparts seem to be more distantly related (Tachedjian et al., 2006). The transmembrane domain is 55% identical between human and murine MAdCAM-1, and the short cytoplasmic regions share only 35% identity (Leung et al., 1996). Homology searches of multiple databases have shown that human MAdCAM-1 only has significant homology to ICAM-1 and VCAM-1, as has been reported for murine MAdCAM-1. Specifically, the first Ig domain of murine MAdCAM-1 displays homology to the first domain of ICAM-1 (32%) and VCAM-1 (28%), and the second MAdCAM-1 Ig domain shows homology with the fifth domain of VCAM-1 (30%) (Sampaio et al., 1995).

1.4.3 Alternative Splice Variants of MAdCAM-1

At least seven alternatively spliced transcripts encoding different human MAdCAM-1 protein isoforms have been identified, but the full–length nature of some variants has not been determined. In particular, the splice variants identified include: one that lacks three mucin repeats, several other that lack almost all of the second Ig domain and the major mucin domain, and two others that have lost half of Ig domain II and 2–3 mucin repeats. An additional isoform of human MAdCAM-1 has been recognised that lacks exon 4, which encodes for the whole mucin domain, therefore this shorter MAdCAM-1 would be unable to accept and present specialised carbohydrate modifications and as a result would have a reduced capacity to support lymphocyte adhesion through binding to L–selectin (Figure 1.2) (Leung et al., 1996). In mouse too, an alternative splicing that results in deletion of exon 4, which in this case encodes for the mucin–like and IgA domains has been also recognised (Sampaio et al., 1995). Different MAdCAM-1 protein isoforms have been also detected in the pig.

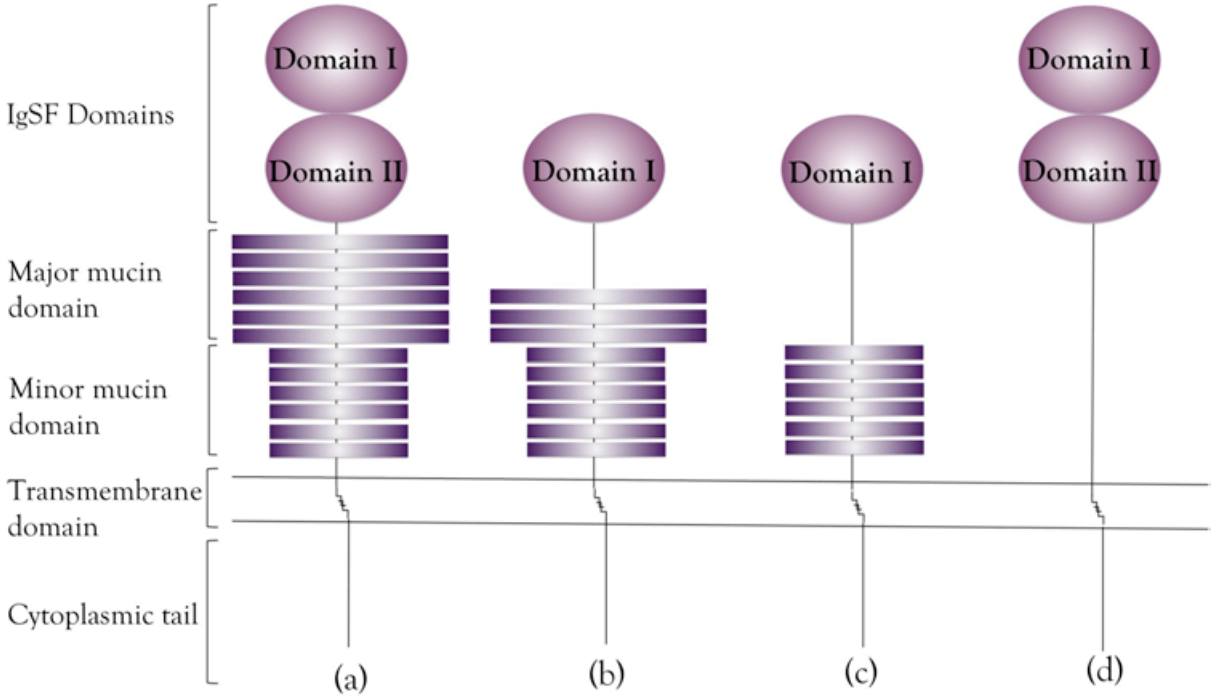

Figure 1.2 Proposed structures of MAdCAM-1 splice variants. Several alternatively spliced variants of human MAdCAM-1 gene have been identified that encode different protein isoforms. (a) The full–length MAdCAM-1 protein consisted of two Ig domains (domain I and II), a major and minor mucin domain, a transmembrane region and a cytoplasmic tail. Splice variant (b) lacking the second Ig domain (domain II) and some of the major mucin repeats, (c) lacking the domain II and the entire major mucin domain and (d) lacking both major and minor mucin domains (Leung et al., 1996).

1.4.4 MAdCAM-1 Motifs for α4β7 Integrin Recognition and Binding

The study of the crystal structure of the N–terminal fragment of human MAdCAM-1, which contains the two Ig domains, has revealed unique characteristics among the Ig integrin ligands regarding specificity for the α4β7 integrin interaction. The presence of an aspartate residue, Asp42, located in the CD loop of the N–terminal domain (domain I) of MAdCAM-1 has been shown to be of key importance for integrin binding (M. J. Briskin et al., 1996)(Shyjan et al., 1996)(Viney et al., 1996). The C and D strands form an "edge" of the domain, and as a result the side chain of Asp42 points up allowing it to be free for integrin recognition. The critical nature of the Asp42 has been substantiated by its conservation amongst mammalian MAdCAM-1 species (Tachedjian et al., 2006). In the case of VCAM-1, the critical integrin–binding residue is also an aspartate (Asp40), located in the CD loop of domain I (Jones et al., 1995). However, there is a key distinction between these two integrin recognition motifs in MAdCAM-1 and VCAM-1. In the overall superposition of domain I of MAdCAM-1 and VCAM-1, Asp42 in MAdCAM-1 and Asp40 in VCAM-1 lie 8Å apart (Tan et al., 1998), although in a new overlaying model for hMAdCAM-1 and hVCAM-1, the positions of the two aspartate residues are found to be only 2Å apart, probably accounting for the differences in binding α4β7 and α4β1 integrins, respectively (Dando et al., 2002).

Interestingly, in previous studies involving domain–swapping experiments, it was found that the first domain alone is not sufficient to support efficient integrin binding and sequences from the second domain are also required. Thus a construct containing Ig domain I of MAdCAM-1 in place of domain I of ICAM-1, resulted in a poor α4β7 interaction (M. J. Briskin et al., 1996). In addition, a fragment containing a single Ig domain of VCAM-1 was inefficient at supporting

adhesion to α4β1 (Pepinsky et al., 1992) and even when domain II of VCAM-1 was replaced with the corresponding domain of ICAM-1, a diminished binding to α4β1 was detected, implying that stabilisation of the N–terminal domain by a similar structure (domain II) is not sufficient to support integrin interaction (Osborn et al., 1992).

In MAdCAM-1, the most striking structural feature identified in domain II, is a negatively charged β ribbon that extends from the D and E strands. This region contains a very high proportion of negatively charged residues, with seven of the eleven residues being glutamate or aspartate (149–159). The importance of these residues has been highlighted by the substitution of six of the nine acidic residues with alanine, which resulted in a significant loss of α4β7 binding (Green et al., 1999). Moreover, the residues in this loop have very high temperature factors, indicating high motility, a fact that led Tan and coworkers to suggest that this negatively charged loop might function as an antenna, electrostatically orientating the MAdCAM-1 integrin binding face above the cell membrane (Tan et al., 1998). Interestingly, both the CD loop in domain I and the DE loop in domain II occupy the same face of the hMAdCAM-1 molecule, providing further evidence that these loops are involved in ligand binding (Figure 1.3) (Green et al., 1999). In domain II of hVCAM-1 an equivalent negatively charged loop, the C'E loop, which is shorter and less negatively charged than hMAdCAM-1, but is still important for integrin binding, has also been identified (Jones et al., 1995). Another essential characteristic of domain II of hMAdCAM-1 is its unusually high proline content (12.3% compared to 5.1% for average proteins) (McCaldon and Argos, 1988), concentrated on the bottom of domain II near to the boundary with the mucin–like domain, and this is suggested to

add rigidity and support the bottom of domain II against the forces exerted during adhesion to integrins (Tan et al., 1998).

Mutational studies have revealed another critical arginine residue for ligand binding (Arg70) (Green et al., 1999) fully buried in the domain I surrounded by seven hydrophobic residues with no negatively charged residues in the vicinity to neutralise the strong positive charge (Tan et al, 1998). Of note, although buried un–neutralised arginines are rare, they have structural roles by forming multiple hydrogen bonds to backbone carbonyl oxygens (Borders et al., 1994). In the new model presented by Dando *et al.*, however, the guanidium group Arg70 rather than being buried and supporting the structure of the loop through hydrogen bonds, was found located at the base of a surface cleft. In the monomeric form of MAdCAM-1, this leaves the arginine surface accessible and potentially free to interact with ligand (Dando et al., 2002).

Overall, the critical elements for α4β7 integrin recognition and binding by hMAdCAM-1 are: an aspartate residue (Asp42) in the CD loop of domain I, a negatively charged β ribbon on the DE loop of domain II that stretches out far from the body of domain II, and thus optimally orienting domains I and II for recognition of integrin, and an arginine (Arg)70 in domain II, important for formation of a MAdCAM-1 dimeric form (see section 1.4.5).

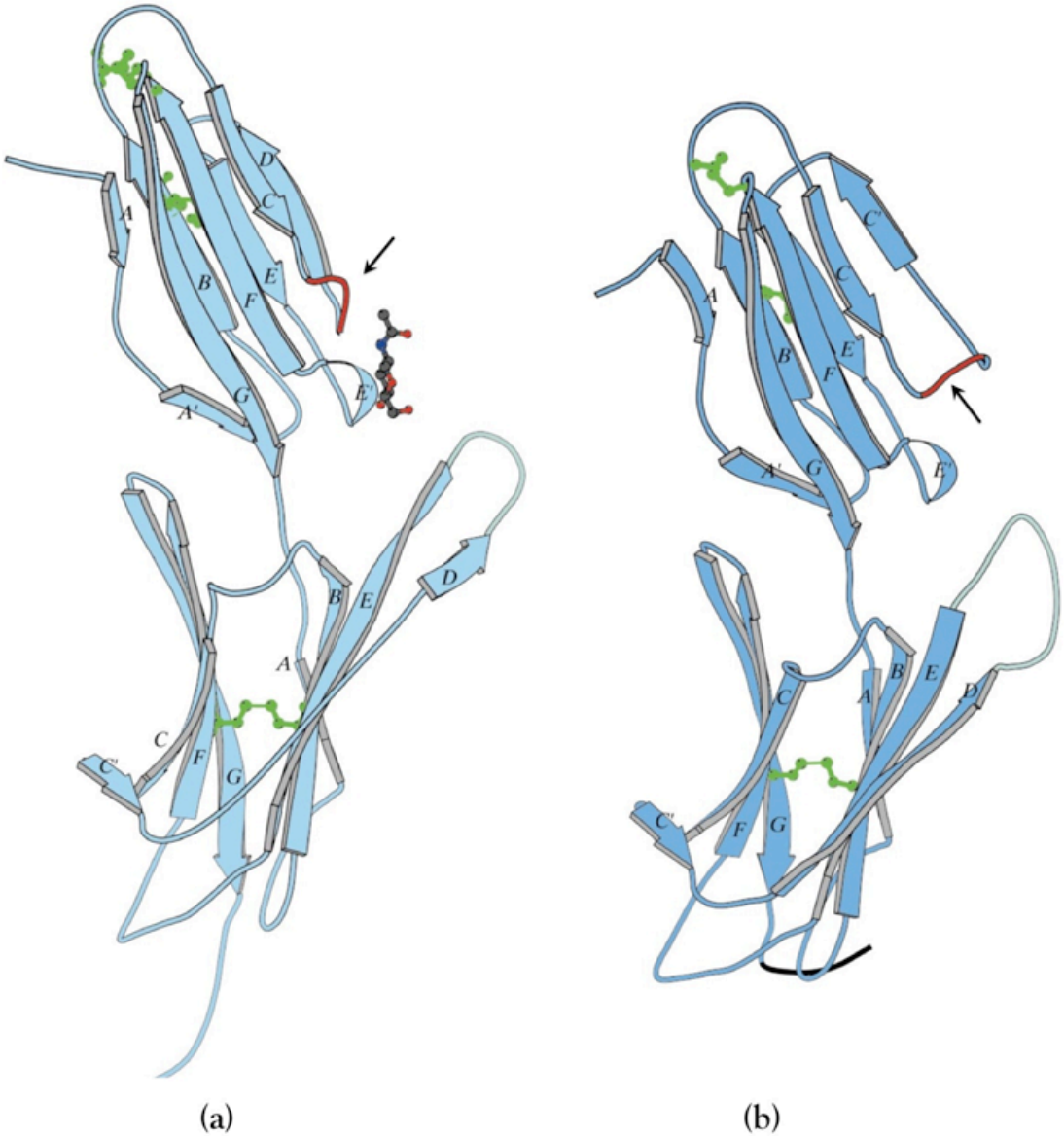

Figure 1.3 Structure of the N-terminal domains of human MAdCAM-1. (a) Ribbon drawing showing the N–terminal two–domain structure of human MAdCAM-1 as described by Tan *et al.* and (b) as described by Dando *et al.* Residues, amongst which the Asp42, in the C/D (a) or C/C' (b) loop of domain I are shown in red. (Figure was taken from the publication of Dando *et al.*, 2002).

1.4.5 MAdCAM-1 Oligomerisation: Dimeric Form

In the study of Dando *et al.,* a dimeric form of MAdCAM-1 was observed created by two symmetry–related full–length molecules within the crystal lattice, through an extensive interface formed by residues from the edge of a β–sandwich in domain I (Dando et al., 2002). Such edge–to–edge dimerisation of Ig domains has also been reported for human ICAM-1 (Casasnovas et al., 1998)(Reilly et al., 1995). In addition, the fact that the two Ig domains of MAdCAM-1 project approximately 22nm away from the cell surface by an extended mucin domain (Shyjan et al., 1996), indicates that there are no steric restrictions for the formation of a dimer. Moreover, the previously identified arginine (Arg)70 residue important for integrin recognition also contributes to the formation of the MAdCAM-1 dimer, via formation of bifurcated charged hydrogen bonds across the dimer interface. The previous mutational analysis experiments that identified the significance of Arg70 in integrin binding (Green et al., 1999) might suggest that the diminished integrin binding of the mutants could be a consequence of dimeric structure disruption, thus suggesting that the arrangement of MAdCAM-1 in a dimeric form is essential for activity. Interestingly, in the dimer form, the two loops that are important for integrin binding are brought closer together than in the monomer, with the CD loop in domain I and the DE loop in domain II being 15Å apart on the dimer surface (Figure 1.4) (Dando et al., 2002).

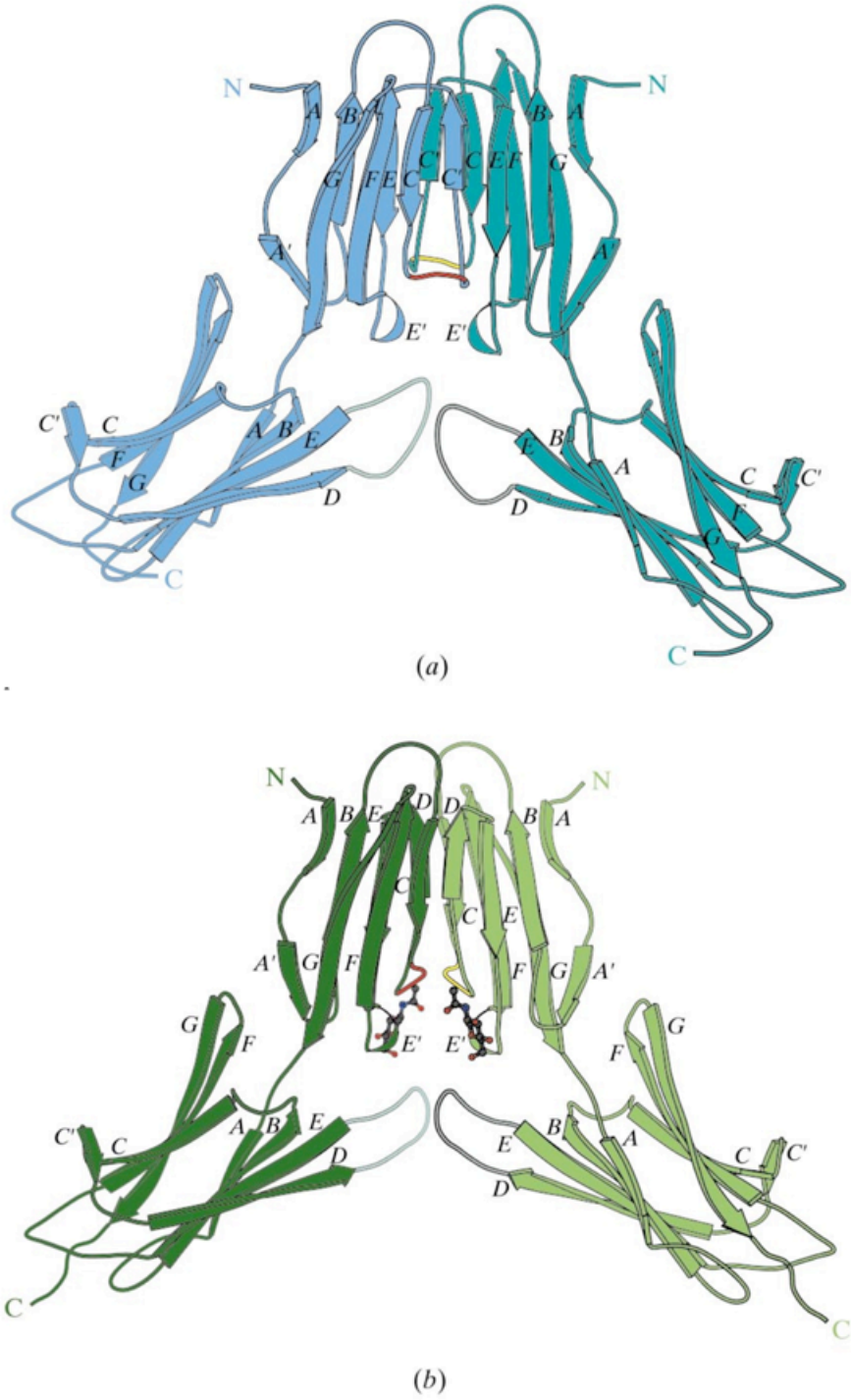

Figure 1.4 MAdCAM-1 dimer structure. Ribbon diagrams showing the crystal packing of MAdCAM-1 monomers described by (a) Dando *et al.* (2002) and (b) Tan *et al.* (1998). Individual monomers within each dimer are represented by dark and light shading (of blue and green respectively). Residues in the C/C' (a) or C/D (b) loop of domain I are shown in red and yellow and residues in the D/E loop of domain II are shown in cyan and grey. (Figure was taken from the publication of Dando *et al.*, 2002).

1.4.6 Soluble MAdCAM-1

Elevated levels of circulating soluble adhesion molecules have been suggested to be essential for understanding the prognosis and pathology of certain diseases. In support of this, reports have shown that soluble forms of ICAM-1 and VCAM-1 are elevated in inflammatory, infectious and malignant diseases (Gearing and Newman, 1993) and are correlated with disease activity. Leung *et al.* revealed for the first time that human MAdCAM-1 can be secreted as a soluble molecule into serum, urine and probably other biological fluids. In particular, the average levels of MAdCAM-1 detected in the serum were 237ng/ml (range 180–315ng/ml), levels most similar to those of ICAM-1 in serum and the levels of sMAdCAM-1 in urine ranged from 20–123ng/ml. Therefore, increased levels of circulating MAdCAM-1 could be a marker for the presence or progression of a chronic inflammatory disease (Leung et al., 2004).

1.4.7 Sites of MAdCAM-1 Expression

MAdCAM-1 is expressed on the high endothelial venules of the organised lymphoid tissues of Peyer's patches (PPs) and mesenteric lymph nodes (MLN) as well as in the flat–walled vessels of the non–lymphoid tissues of lamina propria in both human and mice (M. J. Briskin et al., 1993)(Shyjan et al., 1996). To a lesser extent, MAdCAM-1 is expressed in the spleen, pancreas and colon and expression at these sites increases under inflammation. In normal colon, human MAdCAM-1 is constitutively expressed on venular endothelium of the lamina propria and submucosa (M. Briskin et al., 1997), whereas in murine experimental colitis models MAdCAM-1 expression is induced on colonic vascular endothelium and on the vessels within the muscularis propria and serosa when compared to control animals (Viney et al., 1996). In the inflamed pancreas of non–obese diabetic mice, elevated levels of MAdCAM-1 in HEV–like

vessels of Langerhans islets is also observed (Hanninen et al., 1993). In addition, murine MAdCAM-1 has been detected in the lactating mammary glands (Nishimura, 2003) and there are rare reports of human MAdCAM-1 on the venular endothelium of tonsils (M. Briskin et al., 1997). MAdCAM-1 has been reported to be absent in the thymus, heart, lung, placenta, brain, liver, skeletal muscle, kidney, prostate, ovaries, testis and peripheral blood leukocytes, as well as on arterial endothelium (Viney et al., 1996).

In foetal and neonatal mice, MAdCAM-1 is expressed both in peripheral lymph nodes (PLN) and mesenteric lymph nodes (MLN) at high levels. After the fourth week of postnatal life, MAdCAM-1 expression on PLN HEV declines until it is almost absent, and remains expressed only in MLN HEV (Mebius et al., 1996)(Salmi et al., 2001a). In murine adult PLN rare high endothelial venule cells expressing MAdCAM-1 have also been observed (Mebius et al., 1996). In addition to vascular and lymphatic endothelium, MAdCAM-1 has been also detected on follicular dendritic cells throughout B cell follicles, as well as in dendritic cells in the Peyer's dome of normal and inflamed mice, in DCs of chronically inflamed spleen (M. Briskin et al., 1997)(Szabo et al., 1997), and in lymphoid aggregates of several human liver diseases (Grant et al., 2001). In addition, fibroblasts with an unusual phenotype located in the perifollicular zone, the outer marginal zone, and the T cell zone of the splenic white pulp, as well as fibroblasts from murine tails, are also MAdCAM-1 positive (Steiniger et al., 2001). In addition, MAdCAM-1 expression has been reported in astrocytes surrounding blood vessels in lesions from animals displaying chronic relapsing experimental autoimmune encephalomyelitis (Cannella et al., 1991).

Interestingly, although for many years MAdCAM-1 was thought to belong to the few truly tissue–specific adhesion molecules (M. Briskin et al., 1997), in 1999 Hillan *et al.* demonstrated MAdCAM-1 expression in adult liver in association with portal tract inflammation in chronic diseases (Hillan et al., 1999). In agreement Grant *et al.*, subsequently demonstrated expression of MAdCAM-1 on portal tract vessels and sinusoidal endothelium during liver inflammation (Grant et al., 2001).

1.4.8 The Role of MAdCAM-1 in Leukocyte Recruitment

1.4.8.1 MAdCAM-1 during homeostasis

Lymphocytes continuously circulate through the blood and lymphoid tissues as part of a process of immune surveillance that allows the immune system to respond appropriately to antigen wherever it enters the body. MAdCAM-1 plays an essential role in lymphocyte contact and rolling (L–selectin and α4β7–dependent rolling) as well as in strengthening adhesion and arrest (α4β7–mediated activation–dependent adhesion) (Berlin et al., 1995) as part of the multistep process that regulates lymphocyte homing into mucosal tissues associated with the gastrointestinal tract (Nakache et al., 1989)(Schweighoffer et al., 1993). The important role of the MAdCAM-1/α4β7 interaction has been highlighted by studies using monoclonal antibodies directed against either MAdCAM-1 or α4β7 integrin, which show diminished lymphocyte recruitment to the intestine (Hamann et al., 1994). Moreover, the essential role of the α4β7/MAdCAM-1 interaction for formation of gut–associated lymphoid tissue has been revealed in β7–integrin deficient mice, which show hypocellular Peyer's patches as well as loss of lymphocytes in the lamina propria (Wagner et al., 1996). In contrast, in L–selectin–deficient mice, the cellularity of Peyer's patches is unaffected but they show reduced numbers of

lymphocytes within peripheral lymph nodes (PLN) (Tedder et al., 1995b). Of note, simultaneous loss of both β7 and L–selectin (both ligands of MAdCAM-1) results in a significant decrease in the size and cellularity of Peyer's patches (Wagner et al., 1998).

Moreover, the interaction of MAdCAM-1 with α4β7 is a prerequisite for B cell localisation to Peyer's patches, a process that cannot be compensated for by the interaction of L–selectin with MAdCAM-1 or of α4β7 with VCAM-1 (Schippers et al., 2009). Studies in MAdCAM-1 deficient mice have also revealed that MAdCAM-1 is important for migration of IgA–secreting plasma cells to the intestinal lamina propria. This is a very important role since secretoty IgA protects the host from invading pathogens, facilitating antigen capture by M cells within the follicle associated epithelium (see section 1.6.3) and is needed for preserving the homeostasis of the gut with the commensal microflora (Macpherson et al., 2008).

MAdCAM-1 has been reported to serve functions additional to those in leukocyte recruitment. Specifically, in spleen MAdCAM-1 plays a role in the organisation of the marginal sinus around the splenic white pulp nodules. Moreover, it has been demonstrated that recombinant MAdCAM-1 can enhance MLN T lymphocyte activation (Viney et al., 1996), similar to VCAM-1 (Lukacs et al., 1994). In addition, human peripheral blood T cells can be co–stimulated with antibodies to the α4β7 integrin (Teague et al., 1994).

1.4.8.2 MAdCAM-1 under inflammation

Although the expression of MAdCAM-1 has been tightly linked with a physiological role in normal immune surveillance in the gut, in conditions of chronic gastrointestinal tract

inflammation, MAdCAM-1 facilitates increased lymphocyte extravasation thereby contributing to mucosal damage. During mucosa–associated inflammatory events, constitutively expressed MAdCAM-1 in gut associated lymphoid tissue, is greatly amplified (Connor et al., 1999). Most notably, such over–expression has been linked with inflammatory bowel disease (IBD), an idiopathic disorder of chronic inflammation of the gastrointestinal tract, which has been traditionally classified into two subtypes, Crohn's disease (CrD) and ulcerative colitis (UC), based on histological appearance and anatomical distribution. In particular, UC is characterised by mucosal inflammation and extensive formation of ulcers, usually confined to the submucosa, whereas CrD is characterised by non–caseating granulomas, lymphoid aggregates and extension of inflammation through all layers of bowel wall (Arihiro et al., 2002). Interestingly, divergent distribution of MAdCAM-1 is observed in these two diseases. Precisely, more prominent expression of MAdCAM-1 is detected in the ulcer base and lymphoid aggregates, formed in the deeper layer of the intestinal wall in CrD. In addition, the occurrence of MAdCAM-1^{+} venules is higher in the submucosal lymphoid aggregates than in subserosa, suggesting that MAdCAM-1 expression is induced by enhanced entry of dietary antigens or various bacteria into the intestinal tissue (Arihiro et al., 2002).

Up–regulation of MAdCAM-1 during gut inflammation has been suggested to be responsible for the sustained recruitment of α4β7 expressing lymphocytes and the establishment of chronic inflammation (Eksteen et al., 2004b). The functional significance of MAdCAM-1 in IBD has been highlighted by several studies where immunoneutralisation of either MAdCAM-1 or α4β7 integrin, attenuate inflammation in animal models as well as in patients with colitis (Feagan et al., 2005)(Hamann et al., 1994) and Crohn's disease (Feagan et al., 2008)(Guagnozzi and

Caprilli, 2008). Notably, several studies have also reported the efficacy of monoclonal antibodies directed against other endothelial cell adhesion molecules (CAMs), especially VCAM-1, to abolish recruitment and reduce disease severity in colitis models (Burns et al., 2001), suggesting that a combination of adhesion molecule/ligand interactions take part in the destructive inflammatory influx that characterises IBD.

Numerous animal models of colitis have been used in order to study the hidden mechanisms responsible for the development of chronic bowel inflammation. In the SAMP1/Yit mouse strain, which develops spontaneous ileal inflammation and shares histological features with human ileal Crohn's disease, MAdCAM-1 was found to be significantly increased with worsening of disease from 4 to 40 weeks of age (Burns et al., 2001). Interestingly, the inhibition of MAdCAM-1 alone during established inflammation was less effective than the combined blockade of MAdCAM-1 and VCAM-1, which is also strongly expressed in the SAMP1/Yit mice with spontaneous ileitis. Therefore, since the simultaneous blockade of both CAMs significantly attenuated T–lymphocyte binding to microvessels in the ileal mucosa, it is suggested that pathways independent of the α4β7/MAdCAM-1 can also mediate trafficking to inflamed intestine (Kosiewicz et al., 2001)(Matsuzaki et al., 2005). Furthermore, the prophylactic Ab blockade of MAdCAM-1 prevented the development of ileitis, whereas the early administration of VCAM-1 Ab had no effect, indicating that the contribution of MAdCAM-1 is probably most pronounced during the early phases of the disease. Therefore, it is likely that MAdCAM-1 affects ileal inflammation locally not only in the mucosa but also in the MLN, as significant amelioration of acute and chronic inflammatory infiltrates has been observed when both MAdCAM-1 and L–selectin were blocked (Rivera-Nieves et al., 2005).

Additional studies have shown that administration of anti–β7 integrin and anti–MAdCAM-1 Abs to SCID mice significantly reduced the number of leukocytes infiltrating the lamina propria and mesenteric lymph nodes of inflamed colons (Picarella et al., 1997). Moreover, using antisense MAdCAM-1 oligonucleotides in mice suffering from trinitrobenzene sulfonate–induced colitis, significant suppression of the disease was reported (Goto et al., 2006). The interaction of α4β7 integrin with MAdCAM-1 in the intestine is mainly dependent on the CCL25/CCR9 interaction. Interestingly, therapeutic studies in the SAMP/Yit mice, where targeting CCL25 or CCR9, have shown that this receptor/ligand pair is important during the early stages of induction of spontaneous chronic murine ileitis, but not in late disease, suggesting that in the late stages the recruitment process is less dependent on this chemokine/receptor pair (Rivera-Nieves et al., 2006). To that effect, TRAFICET–EN, an orally active pharmaceutical CCR9 inhibitor is currently being assessed for the treatment of CrD and might be more effective early in disease.

Increased expression of MAdCAM-1 has been observed in other animal models such as the dextran sulphate sodium (DSS)–induced colitis, SCID mice with $CD45RA^{high}$ CD4+ T cells, IL-10 deficient mice, and in the granulomatous colitis induced by peptidoglycan–polysaccharide (PG–PS), where expression of MAdCAM-1 was elevated on the vessels in the lamina propria and the submucosal layer, thus providing further evidence for the role of MAdCAM-1 in the development of ileitis (Matsuzaki et al., 2005). Moreover, elevated levels of MAdCAM-1 have been observed in animal models that are not associated with inflammatory bowel disease, such as in the non–obese diabetic (NOD) mice (Faveeuw et al., 1994)(Hanninen et al., 1993) and in the central nervous system in chronic relapsing experimental encephalomyelitis (Kanwar et al.,

2000). In NOD mice, which spontaneously develop an autoimmune syndrome similar to human insulin dependent diabetes mellitus (IDDM) (Atkinson and Maclaren, 1994), MAdCAM-1 has been reported to be strongly induced on islet vessels playing a major role in the recruitment of lymphocytes from blood into the inflamed pancreas (Faveeuw et al., 1994)(Hanninen et al., 1993)(X. D. Yang et al., 1994). This role of MAdCAM-1 has been further validated by function blocking antibodies specific for L–selectin and α4 integrins, which resulted in inhibition of insulitis and prevention of autoimmune diabetes. MAdCAM-1 is also induced on brain endothelial cells during chronic relapsing experimental allergic encephalomyelitis (EAE), where functional blockade of MAdCAM-1 has been shown to effectively prevent the development of a progressive, non–remitting form of EAE. Of note, combinational treatment with anti–MAdCAM-1, anti–VCAM-1 and anti–ICAM-1 antibodies induced a more rapid remission than the anti–MAdCAM-1 treatment alone (Kanwar et al., 2000).

In humans, enhanced expression of MAdCAM-1 has also been reported in the gastric mucosa of patients with nodular gastritis (Ohara et al., 2003), and in malignant pancreatic tissues where MAdCAM-1 protein levels were significantly elevated and were able to recruit CD62L+ β7+ Tregs both *in vitro* and *in vivo*. Interestingly, blocking antibodies directed against MAdCAM-1 or its ligands CD62L and β7–integrin, strongly reduced the Treg transmigration, with the anti–β7 integrin blockade having the highest effect in abolishment of Treg transmigration through the tumour endothelium (approximately 50%) (Nummer et al., 2007). Furthermore, aberrant expression of MAdCAM-1 has been detected on inflamed portal vein and sinusoidal endothelium of patients with autoimmune liver diseases, PSC and AIH, where it supports the

adhesion of α4β7+ lymphocytes from patients with IBD and PSC, an effect that could be abolished by anti–MAdCAM-1 and anti–α4β7 antibodies (Grant et al., 2001).

1.4.8.3 Therapies directed against the MAdCAM-1/α4β7interaction

The important role of the MAdCAM-1/α4β7 interaction in leukocyte recruitment under inflammatory conditions and its consequent role in establishment of chronic inflammation in both gut (IBD) and liver (PSC, AIH) has led pharmaceutical companies to develop humanised blocking monoclonal antibody–based therapies aimed at selectively inhibiting the pathways associated with these two molecules. For example MLN02, from Millenium Pharmaceuticals, is a humanised monoclonal antibody that inhibits adhesion and migration of leukocytes into the gastrointestinal tract by binding to the α4β7 integrin, and thus reducing inflammation. Currently, MLN02 has shown promising results in patients with active ulcerative colitis (Behm and Bickston, 2009). Another humanised monoclonal antibody, vedolizumab, which represents an enhanced form of MLN02, has been developed that targets α4β7 integrin exclusively, but not α4β1 or αEβ7, therefore inhibiting only the adhesion of α4β7 expressing cells to MAdCAM-1, without inducing the systemic immunosuppression that characterises anti–α4 chain monoclonal antibodies (Soler et al., 2009).

Natalizumab (Biogen Idec), is another humanised (95% human–derived) monoclonal antibody, directed against human α4 integrins, which inhibits leukocyte adhesion by blocking both VCAM-1/α4β1 and MAdCAM-1/α4β7 pathways (Stefanelli et al., 2008). It was initially approved in 2004, for induction and maintenance of moderate to severe Crohn's disease, but later on it was withdrawn from the market after 3 patients developed progressive multifocal

leukoencephalopathy (Targan et al., 2007)(Van Assche et al., 2005). This is a consequence of defective immune surveillance of the central nervous system (CNS) because α4β1 is required for T cell trafficking to the CNS. Natalizumab is back on the market in US where it is used for the treatment of patients with Crohn's disease.

Very recently, the first human blocking anti–MAdCAM-1 mAb from Pfizer, PF00547659 has been described, which selectively binds to MAdCAM-1 and reduces homing of specific lineages of leukocytes to the gastrointestinal tract without impairing normal CNS immune surveillance. Thus this reagent is suggested to represent a better therapeutic approach for treatment of IBD than other available antibodies (Pullen et al., 2009).

1.5 HUMAN LIVER

The adult human liver is the largest internal organ in the human body, normally weighing 1.2–1.5kg. It is located below the diaphragm in the thoracic region of the abdomen, to the right of the stomach overlying the gallbladder and possesses a unique location between the gastrointestinal tract and peripheral lymphoid organs. One of the most interesting characteristics of the liver is its capacity for natural regeneration, a feature recognised since the earliest times, which features in ancient Greek mythology. Prometheus, a Titan who stole fire from Zeus and gave it to mortals, was punished by Zeus, by being bound to a rock and his liver was eaten by a great eagle every day only to "regenerate" in the night and be eaten again the next day. Of note, as little as 25% remaining liver can generate into a whole liver again, which has the ability to adjust in size in order to match its host in cases of transplantation.

1.5.1 Architecture of The Liver

The liver has been subdivided on the basis of both its external aspect and its internal architecture. Based on external appearance, traditional gross anatomy has divided the liver into four anatomical lobes. Observing the liver from the anterior side, a left and a larger right lobe are distinguished, being divided by the falciform ligament, whereas from behind, two additional minor lobes exist between the right and the left lobes, the caudate lobe (the more superior) and the quadrate lobe (the lower one) (Figure 1.5).

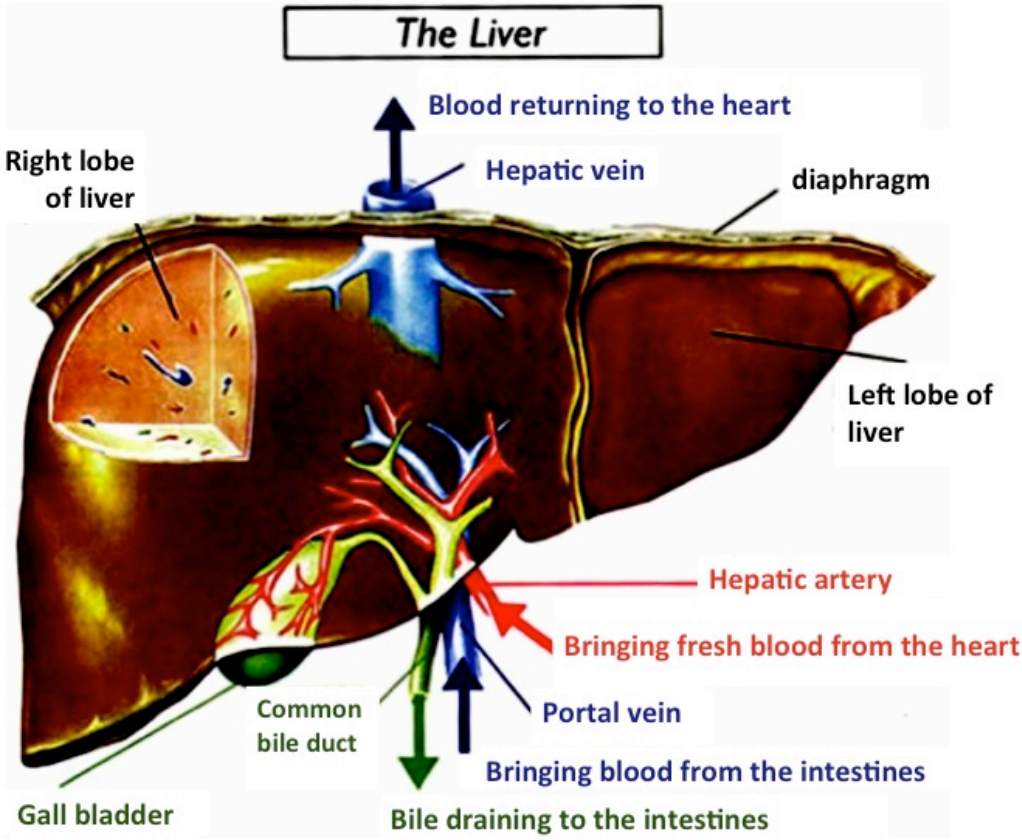

Figure 1.5 Structure and morphology of human liver. The liver is divided into four anatomical lobes. In the figure are shown the bigger right and the smaller left lobe, whereas two more minor lobes exist in the posterior side (not shown). The liver is supplied with blood from the portal vein that transfers deoxygenated but nutrient–rich blood from the intestines, and with blood from the hepatic artery that supplies liver with oxygenated blood from the heart. Hepatocytes secrete bile, which is stored in the gall bladder and is transferred through the common bile duct into the duodenum (upper part of the intestine) to facilitate digestion (Liver Cirrhosis Case Study, 2008).

Investigation of the liver's internal anatomy has revealed that its structural unit is the lobule. The lobule is a polyhedral prism (0.7 x 2mm), the boundaries of which are limited by four to five portal triads prolonged by connective tissue septa. One portal triad contains three structures, one bile duct and two blood vessels, which are branches of the hepatic artery and the hepatic portal vein. Within each lobule, epithelial cells called hepatocytes are arranged in layers that radiate out from a central vein, and between the group of hepatocyte layers lay the hepatic sinusoids (Figure 1.6) (Malarkey et al., 2005).

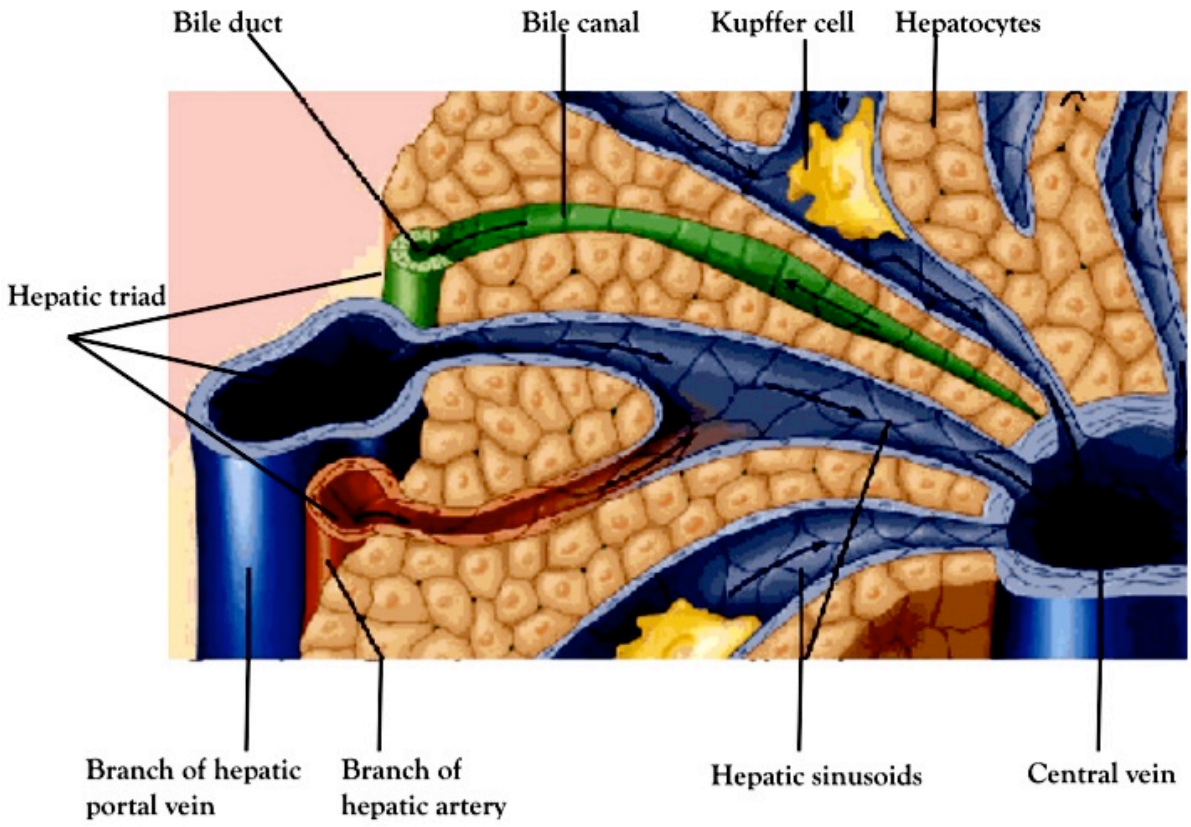

Figure 1.6 The hepatic triad. A hepatic triad consists of three vessels, one branch of the hepatic portal vein, one branch of the hepatic artery and one bile duct. Hepatic triads are located at the corners of the polyhedral (usually hexagonal) lobules. Arterial and portal venous blood percolate through the hepatic sinusoids into the central veins that coalesce into hepatic veins and finally drain into the inferior vena cava (The Internet Encyclopedia of science, Anatomy & Physiology, Liver).

1.5.1.1 Liver blood supply

The liver has a dual blood supply. In particular, the hepatic artery supplies the liver with oxygenated blood from the heart (20%), and the hepatic portal vein with deoxygenated but nutrient–rich blood from the gastrointestinal tract (80%). Arterial and portal–venous blood percolate through the hepatic sinusoids generating a mixed arterial–venous perfusion collected in the central vein (Figure 1.6). Finally, the central veins of all the lobules coalesce into hepatic veins, draining into the inferior vena cava, therefore sending de–oxygenated blood from the lower half of the body into the right atrium of the heart (Lalor and Adams, 2002).

1.5.1.2 Liver cell populations

The liver is composed from many different cell types. Up to 80% of the liver cell population consists of hepatocytes, large polyhedral epithelial cells that are highly metabolically active. Hepatocytes are arranged into cell plates separated by hepatic sinusoids lined with endothelial cells. The lumen of the sinusoids is narrow and is penetrated by Kupffer cells and Pit cells (Enomoto et al., 2004). Kupffer cells are the resident macrophages that "guard" the entrance of sinusoids and they are predominantly located in the peripheral region of the liver lobule and to a lesser extent in the midzonal and central areas (Nemeth et al., 2009). Their strategic position allows them to phagocytose and eliminate antigens or pathogens that enter the liver with portal venous blood (Knolle and Gerken, 2000). Pit cells are large granular lymphocytes resident in the sinusoids providing protection against viral infections and tumour cells (Lalor et al., 2002b).

Between hepatocytes and sinusoidal endothelial cells lies the space of Disse, which is characterised by extracellular matrix, including different types of collagen (mainly type III but

also type I and IV), proteoglycans and fibronectin. The role of the extracellular matrix is complex as it serves to anchor cells, allowing intercellular communication and affecting cellular differentiation. Hepatic stellate cells (HSC) are located in the space of Disse. These perisinusoidal mesenchymal cells belong to the myofibroblast family. Under normal conditions they store vitamin A, which they lose on activation when they produce collagen, and assume features of fibrogenic, contractile myofibroblasts (Senoo et al., 1998). In addition HSC can mediate the inflammatory response by the production of several cytokines and chemokines (Pinzani and Marra, 2001). Of note, activated HSC have been reported to control sinusoidal blood flow by contraction, thus leading to reduction of the sinusoidal diameter (Figure 1.7) (Reynaert et al., 2002).

Another type of cell, the cholangiocyte resides in the biliary tract and represents the first line of defence against pathogens that invade the bile ducts, through their ability to express pattern recognition receptors (PRRs), and to produce adhesion molecules, cytokines, chemokines and antimicrobial peptides (Nemeth et al., 2009).

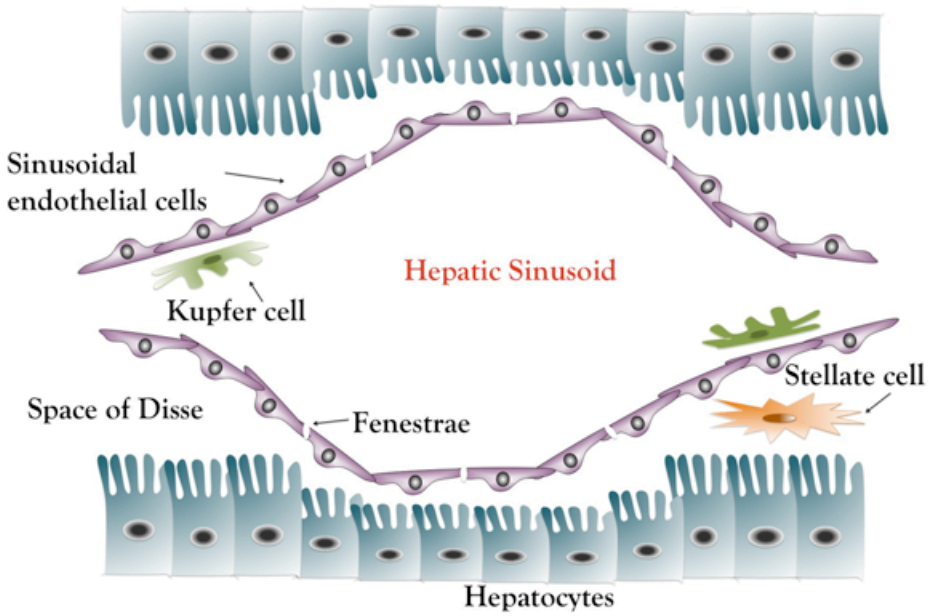

Figure 1.7 Hepatic sinusoids. The hepatocyte population of the liver is separated by the hepatic sinusoids lined by specialised endothelial cells, that lack underlying basement membrane thus forming a discontinuous cell lining with fenestrae. The lumen of the sinusoids is narrow and penetrated by Kupffer cells, mainly located in the peripheral region. Between hepatocytes and endothelial cells lies the space of Disse in which stellate cells are located.

1.5.1.3 Liver hepatic sinusoidal endothelial cells

Hepatic sinusoidal endothelial cells (HSEC) form a highly specialised layer of cells that line the sinusoids (Enomoto et al., 2004), physically separating leukocytes passing through liver within the bloodstream from hepatocytes. It is estimated that 20% of the cells in liver are HSEC, making the second most frequent cell type after hepatocytes. HSEC have some characteristics, which distinguish them from the endothelial cells of the microvasculature of most other organs and from large liver blood vessels. Liver sinusoidal endothelia are very thin, lack an underlying basement membrane and tight junctions and form a discontinuous cell lining, thus creating a vascular bed with fenestrae (pores), with a mean diameter of 100 to 150nm (Braet and Wisse, 2002). This characteristic morphology of HSEC makes them act as a "sieve" allowing the

passage of molecules of smaller diameters and excluding the passage of macromolecules to the space of Disse and thereafter to hepatocytes (Wisse et al., 1985). Of note, upon contact with substances like alcohol or nicotine, the diameter of these fenestrae can dynamically change (Braet and Wisse, 2002).

Moreover, HSEC are scavenger cells equipped with surface C–type lectins and mannose receptors that allow them to scavenge the sinusoidal blood for pathogens and macromolecules. HSEC take up such macromolecules, internalise and efficiently endocytose them through their numerous specialised pinocytic vesicles. After endocytosis they deliver the degradation products to the space of Disse, where hepatic microvilli take them up either for destruction and elimination via the bile or for further metabolism (Knolle and Limmer, 2003)(Smedsrod, 2004). HSEC also express molecules that are relevant to antigen presentation, MHC class I and class II molecules, CD40, CD80, CD86 and CD54 allowing them to act as antigen–presenting cells (Knolle et al., 1999)(Limmer et al., 2000). Interestingly, HSEC can perform all the functions of an APC (uptake, processing and presentation of an antigen), however, without the requirement for maturation, thus ensuring that antigen presentation of blood–borne antigens by HSEC occurs within a short time (Knolle and Gerken, 2000). It is believed that activation of lymphocytes in the liver by resident APCs, HSEC and hepatocytes, usually results in tolerance rather than immunity (Adams et al., 2008).

Finally, HSEC play an important role in immunity and inflammation since they can facilitate leukocyte extravasation (Knolle and Limmer, 2003). The strategic position of HSEC in the hepatic sinusoid as well as the small diameter of the hepatic sinusoid (7–12μm) and the slow

and peculiar blood flow supports the establishment of interactions with leukocytes in the blood flowing through the liver.

1.5.1.4 Liver leukocyte populations

The uninfected normal liver contains about 10^9 to 10^{10} resident lymphocytes, and this lymphocyte population in the liver differs considerably from that of the blood and other organs. It includes liver–resident subpopulations of the innate (NK and NKT cells) and adaptive (T– and B– lymphocytes) immune response (Doherty and O'Farrelly, 2000).

NK cells are present at a high frequency (about 30%) among liver–resident lymphocytes and this percentage is further enhanced under inflammatory conditions (Doherty and O'Farrelly, 2000)(Emoto et al., 2000). NK cells mediate antiviral and cytotoxic effector functions and can regulate innate and adaptive immune responses by secreting IFNγ and chemokines including CCL3 (MIP-1α) and CCL4 (MIP-1β), that subsequently lead to T cell recruitment to the liver (Itoh et al., 2001).

NKT cells constitute a divergent population of T cells that express MHC class I, CD3 and the NK cell markers CD56, CD161 and CD94 on their surface (Kronenberg and Gapin, 2002)(MacDonald, 1995). In the liver, both classical (CD4+ or CD4/CD8 double negative) and non–classical NKT cells (TCRαβ and TCRγδ T cells) are present and constitute up to 30% of the intrahepatic lymphocyte pool. Intrahepatic NKT cells are more activated than peripheral blood NKT cells. Upon TCR induced activation, NKT cells release substantial amounts of Th1 (IFNγ and TNFα) and Th2 (IL-1, IL-10 and IL-13) cytokines (Swain, 2008), which in turn

contribute to activation of other innate (NK cells, monocytes) and adaptive (CD4+ and CD8+ T cell) immune cells or to suppression of tissue destruction/allograft tolerance respectively (Godfrey and Kronenberg, 2004). In liver diseases, NKT cells are implicated in immune responses to bacterial, viral and parasitic infections and to tumours (Notas et al., 2009).

The intrahepatic T cell population includes the conventional CD8+ and CD4+ T cells that display a diverse TCRαβ repertoire and recognise antigens in the context of MHC class I and II molecules, respectively. In peripheral blood, the ratio of CD4:CD8 T cells is about 2:1, whereas this ratio is reversed in normal liver (1:2.5). Apart from the conventional lymphocyte populations in the liver a large population of unconventional lymphocytes such as CD4/CD8 "double negative" T cells, CD4/CD8 "double positive" T cells and γδ T cells is also present (Doherty and O'Farrelly, 2000)(Adams et al., 2008).

Intrahepatic B cells comprise less than 10% of the total intrahepatic population. They are characterised by the expression of CD5 and they can be activated in a T–cell independent way producing low affinity autoreactive IgM antibodies. Of note, they have been suggested to be equivalent of γδTCR+ cells, thus bridging the innate and adaptive immune system (Nemeth et al., 2009).

The liver contains natural CD4+CD25+Foxp3+ Tregs at much lower frequencies than lymph nodes but with increased numbers when peripherally activated CD8+ T cells are present. The total number of liver Tregs seems to be negatively correlated with disease activity (Nemeth et al., 2009).

Several types of hepatic DCs have been identified in mice: lymphoid (CD8α+ B220–CD11b–), myeloid (CD8α– B220– CD11b+), plasmacytoid (CD8α– B220+), a mixture of myeloid and lymphoid DCs (B220– CD11b–) and natural killer DCs (B220– $CD11c_{int}$ CD69+ 2B4+ DC5+) (Nemeth et al., 2009). In humans, plasmacytoid and myeloid DCs have been described in the liver. DCs reside as "immature" APCs, expressing low levels of MHC and co–stimulatory molecules such as CD40, CD80 and CD86, all necessary for T cell activation. They are mainly located within portal tracts and around central veins, and together with Kupffer cells they scavenge pathogenic agents from portal venous blood (Thomson et al., 1999). Upon activation, DCs migrate from the parenchyma via the space of Disse to portal area carrying the ingested antigenic particles in order to interact with lymphocytes and initiate an effective immune response (Adams et al., 2008). Of note, hepatic DCs have been suggested to be the key players in maintaining the balance between liver tolerance and immunity (Nemeth et al., 2009).

1.5.2 Function of The Human Liver

The liver performs multiple vital functions. The hepatocyte cellular machinery is responsible for numerous metabolic functions, including synthesis of plasma proteins, complement components, growth factors, cytokines and blood clotting factors, synthesis of lipids and bile. Bile consists of bile salts, bilirubin, phospholipids (including lecithin), cholesterol and various ions. It is secreted into the duodenum where it is responsible for emulsification of fats. Another important function of the liver is the metabolism of amino acids and carbohydrates, plasma proteins and vitamins, as well as the regulation of glucose levels in the blood, by two processes: glycogenesis (conversion of glucose to glycogen and storage of the latter when the levels of glucose in blood are high) and glycogenolysis (break down of glycogen into glucose and release

into the blood). In addition, the liver acts as a storage site of vitamins (A, D and B_{12}) and minerals. The liver is also responsible for xenobiotic detoxification, by cytochrome P450 enzymes that are involved in hepatic phase I drug metabolism (Pearson and Roberts, 1984). In order for all these functions to be efficiently served, hepatocytes must extract nutrients, as well as waste and toxic products from the blood circulating through the liver via the sinusoids (Knolle and Gerken, 2000).

1.5.3 Lymphocyte Recruitment in Human Liver During Homeostasis and Inflammation

The liver has a large population of resident leukocytes that provide ongoing immune surveillance. However, in response to an infection or injury, these cell populations are rapidly expanded and additional lymphocytes are recruited and infiltrate the liver, following the process of leukocyte recruitment described above (see section 1.3) (Lalor and Adams, 1999). Interestingly, the liver has a unique feature in the sense that it has several anatomical compartments for leukocyte recruitment including via endothelial cells lining hepatic sinusoids, as well as through those lining the portal and terminal hepatic veins (Edwards et al., 2005).

1.5.3.1 Lymphocyte recruitment in hepatic sinusoids

HSEC fail to express high levels of the selectin family of adhesion receptors. E–selectin and P–selectin are absent from resting sinusoidal endothelium, and the non–expression of the latter is consistent with the lack of Weibel–Palade bodies in HSEC (G. Steinhoff et al., 1993). Further studies in animals deficient in both E–selectin and P–selectin demonstrate only minimal alteration in leukocyte adhesion, suggesting a negligible role of selectins in the capturing and tethering of leukocytes within the sinusoids (Adams et al., 1996)(Wong et al., 1997). However,

this could be explained by the narrow diameter (7–12μm) of the sinusoids in combination with the low velocity of blood flow (25μm/min to 250μM/min) which probably promote the contact of passaging leukocytes with the sinusoidal endothelial cells in the absence of selectins.

In the absence of selectins, other tethering molecules might be responsible for the initial capture of flowing leukocytes on hepatic endothelium. Under basal conditions, VCAM-1 is expressed at low levels and favoured by the low shear stress forces in the sinusoids (Lalor et al., 1997) it can directly capture lymphocytes by supporting rolling adhesion (Alon et al., 1995b)(Lalor and Adams, 1999). Another candidate for mediating rolling in the absence of selectins has been VAP-1. In the absence of inflammation the endothelial expression of VAP-1 is largely confined to hepatic vessels (McNab et al., 1996). The function of VAP-1 as a rolling receptor has been suggested by *in vitro* and *in vivo* studies. VAP-1 can support sialic acid dependent adhesion to hepatic endothelium both in tissue binding assays and in primary cultured HSEC under shear stress (Lalor et al., 2002a) and *in vivo* VAP-1 supports rolling on mesenteric vessels (McNab et al., 1996)(Tohka et al., 2001). Firm adhesion of arrested lymphocytes in the sinusoidal endothelium is mediated by ICAM-1 and ICAM-2, which are both expressed constitutively under normal conditions, and the low levels of VCAM-1 (Iigo et al., 1997). Functional studies have suggested the important role of ICAM-1 in recruitment via the sinusoids (Yoong et al., 1998) and additional blocking assays in *in vitro* studies have supported the role of both ICAM-1 and VCAM-1 in lymphocyte binding to primary cultured sinusoidal endothelium (Edwards et al., 2005). Stabilin-2 is another molecule constitutively expressed in hepatic sinusoidal endothelium where it supports αMβ2 mediated adhesion of lymphocytes, and its' functional importance has been shown by blocking antibodies against

stabilin-2 that significantly abolish lymphocyte binding to hepatic sinusoidal endothelial cells under both static and flow conditions (M. Y. Jung et al., 2007).

Thereafter, arrested lymphocytes undergo transendothelial migration. Interestingly, hepatic sinusoidal cells express low levels of the junctional adhesion molecules PECAM-1 and JAMs (Scoazec and Feldmann, 1994), which might be explained by the lack of tightly regulated cell junctions in HSEC, but other molecules such as ICAM-1 and VAP-1 have been reported to be important for diapedesis through hepatic sinusoids (Lalor et al., 2002a)(Yoong et al., 1998). CLEVER-1, a member of the scavenger receptor family, has also been reported as a potential molecule involved in lymphocyte transmigration since it is widely expressed in both vascular and lymphatic endothelium and has been demonstrated to mediate transmigration through both distinct types of endothelial cells both *in vitro* and *in vivo* (Salmi et al., 2004).

Under normal conditions low levels of chemokines are detected in hepatic sinusoids. However, upon inflammation increased levels of both adhesion molecules and chemokines have been observed. Particularly, ICAM-1 and stabilin-2 expression are considerably increased, and VCAM-1 and PECAM-1 expression is induced (Adams et al., 1994)(Adams et al., 1991)(Lalor et al., 2002a)(Yachida et al., 1998). Moreover, upon inflammation the CXC chemokines, CXCL9, CXCL10, CXCL11 all of which bind to CXCR3 and CXCL16 that binds to CXCR6 are up–regulated on sinusoidal endothelium (Figure 1.8) (Table 1.2) (Heydtmann and Adams, 2009). Further evidence supporting the preferential expression of these chemokines by sinusoidal endothelium comes by the high levels of the CXCR3 receptor detected on liver infiltrating lymphocytes in chronic inflammation (>80%) (Curbishley et al., 2005).

1.5.3.2 Lymphocyte recruitment in portal vessels

Under normal conditions, portal vessel endothelium expresses VAP-1, ICAM-1 and ICAM-2 and low levels of several chemokines including CCL3, CCL4 and CCL5, which lead to the recruitment of $CCR5^{high}$ T cells to portal cells in the normal liver during immune surveillance (Lalor and Adams, 1999). However, in inflammatory conditions, portal vessels induce the expression of P–selectin, E–selectin and VCAM-1 and up–regulate ICAM-1 levels (Ward et al., 1998) as well as strongly express the chemokines CCL3, CCL4 and CCL5. Therefore, it seems that the inflamed portal vessels use the induced selectins to promote primary tethering and rolling with subsequent firm adhesion via LFA-1 and α4β1 integrins, which are elevated on liver infiltrating lymphocytes, and bind to their receptors ICAM-1 and VCAM-1, respectively (Yoong et al., 1998). The expression of VAP-1 is also maintained on inflamed portal endothelium where it supports lymphocyte binding (Figure 1.8) (Table 1.2).

Interestingly, in certain inflammatory diseases that complicate IBD, such as PSC and AIH, elevated levels of the gut specific molecules MAdCAM-1 and CCL25, have been observed mainly in portal vessels promoting the recruitment of α4β7+CCR9+ gut derived lymphocytes to the liver (Eksteen et al., 2004a). Moreover, CCL28 has been detected in inflamed endothelium, in cholangiocytes and hepatocytes in a variety of liver diseases (Eksteen et al., 2006) (Figure 1.8). Finally, another chemokine CCL21, which is predominantly expressed in lymphoid tissues has been detected in small vessels and occasional cells with the morphology of CD11c+ dendritic cells in portal associated tertiary lymphoid follicles in chronic inflammatory liver diseases, mainly in PSC and PBC, two diseases associated with portal tract infiltration and formation of neolymphoid aggregates (Grant et al., 2002b) (Figure 1.8) (Table 1.2).

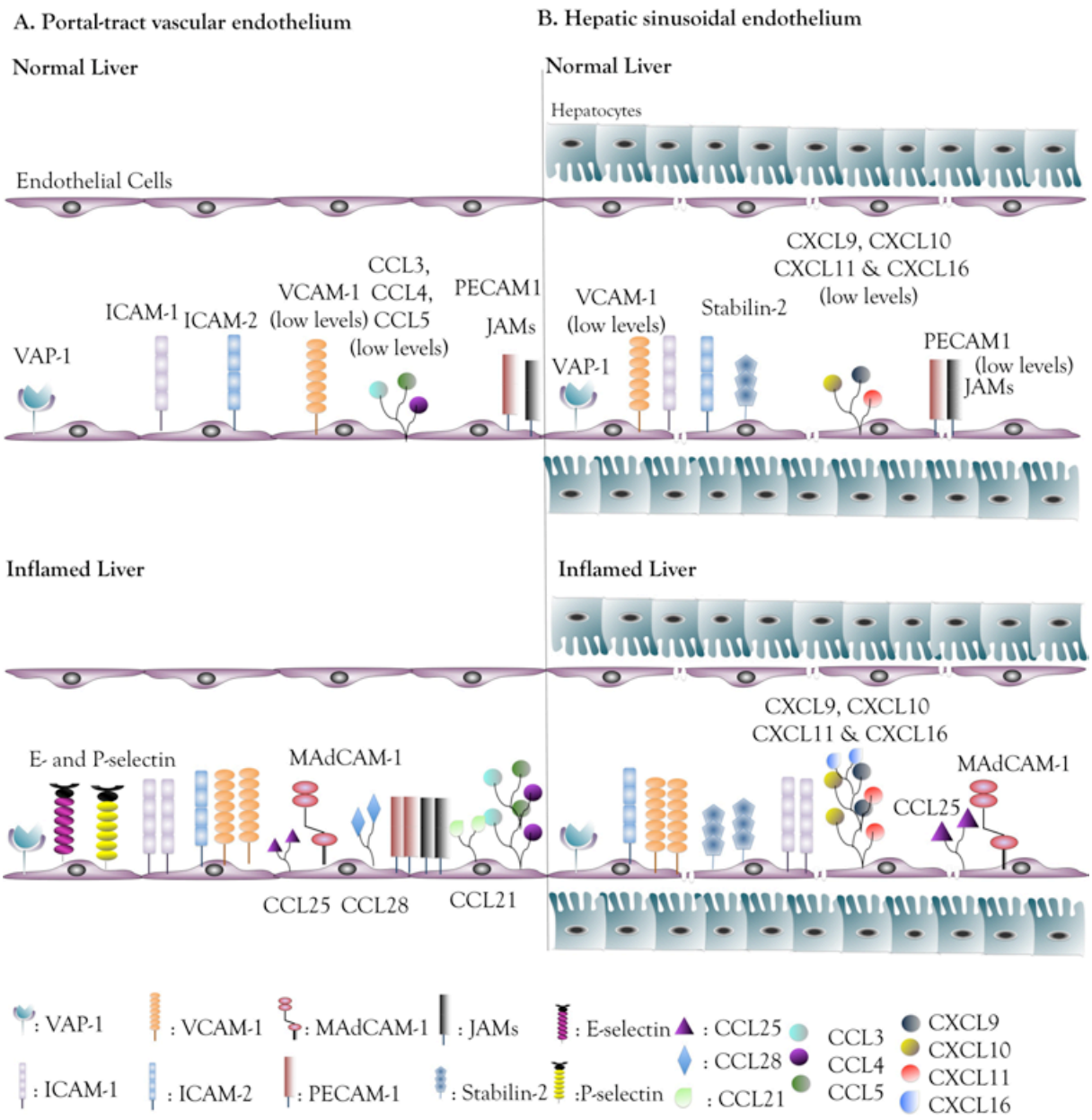

Figure 1.8 Lymphocyte recruitment to the liver. Adhesion molecules and chemokines being reported to mediate lymphocyte recruitment in the liver via (A) the portal tract endothelium and (B) the hepatic sinusoidal endothelium under normal and inflammatory conditions (Adams et al., 2006).

Molecules Implicated In Lymphocyte Recruitment Within The Different Hepatic Anatomical Compartments			
Hepatic Sinusoids		Portal Vessels	
Normal Liver	**Inflamed Liver**	**Normal Liver**	**Inflamed Liver**
VAP-1	VAP-1	VAP-1	VAP-1
VCAM-1 (low levels)	VCAM-1	VCAM-1 (low levels)	VCAM-1
ICAM-1, -2	ICAM-1, -2	ICAM-1, -2	E-selectin
Stabilin-2	Stabilin-2	PECAM-1	P-selectin
CLEVER-1	MAdCAM-1	JAMs	ICAM-1, -2
PECAM-1 (low levels)	CLEVER-1	CCL3, -4, -5 (low levels)	MAdCAM-1
JAMs (low levels)	PECAM-1		PECAM-1
CXCL9, -10,-11	CXCL9, -10, -11		JAMs
CXCL16	CXCL16		CCL3, -4, -5
	CCL25		CCL25, CCL28, CCL21

Table 1.2 Molecules involved in recruitment of lymphocytes to the different hepatic anatomical compartments. Adhesion molecules and chemokines implicated in lymphocyte recruitment via hepatic sinusoids and portal vessels under normal and inflamed conditions.

1.6 Anatomy & Function of The Gut

1.6.1 Overview of The Digestive System

The human digestive system consists of linked organs and glands responsible for food processing, digestion and absorption of nutrients. Two basic divisions of the digestive system have been recognised: the gastrointestinal (GI) tract (also known as the alimentary canal), a continuous tube consisting of the mouth, pharynx, esophagus, stomach, small and large intestine, through the walls of which the nutrients are absorbed prior to entering the blood or lymphatic vessels. The accessory organs are the second part of the digestive system and include the teeth and tongue, salivary glands, liver, gallbladder and pancreas, which are responsible for producing and storing digestive chemicals.

1.6.2 Anatomy and Function of The Gut

The digestive tract from mouth to anus is characterised by a wall of four layers: the mucosa, submucosa, the muscularis externa and the serosa (Figure 1.9).

The mucosa is a mucous membrane lining the inside of the digestive tract, which protects the GI tract wall by secretion of substances and absorption of the end products of digestion. Three more layers define the mucosa: the epithelium, composed of columnar or stratified squamous epithelium, goblet cells that secrete mucus therefore protecting the epithelium from digestion, and endocrine cells that secrete hormones into the blood. The second layer, the lamina propria, lies outside the epithelium. Blood and lymphatic vessels are present in the lamina propria and provide nutrients for the epithelial layer, distribute the hormones that are produced in the epithelium and absorb the end products of digestion from the lumen. In addition, the lamina

propria contains the mucosa–associated lymphoid tissue (MALT) and the nodules of lymphatic tissue bearing lymphocytes and macrophages that protect the GI tract wall from bacteria and other pathogens that might be mixed with the food. The third layer, the muscularis mucosae, is the outer layer of the mucosa, consisting of a thin layer of smooth muscle responsible for the generation of local movements. In particular, in the stomach and small intestine, the smooth muscle generates folds that increase the absorptive surface area of the mucosa. The surface of the mucosa is covered by villi, fingerlike projections that increase the surface area over which absorption and digestion occurs and additional microscopic extensions, the microvilli, are also present in the outer surface of the absorptive cells present in each villus.

The submucosa underlies the mucosa and contains blood vessels, lymphatic vessels and nerves. The small intestine submucosa has the following distinct characteristics: Brunner's glands, which are found only in the submucosa of the duodenum and secrete an alkaline mucus that neutralises the gastric acid in the incoming chyme, and Peyer's patches, aggregated lymphatic nodules, that provide a defensive barrier against bacteria.

The muscularis externa is a layer of muscle that in the mouth and pharynx consists of skeletal muscle to aid swallowing, and in the rest of the GI tract consists of smooth muscle and associated nerve fibers. The smooth muscle is responsible for the movement of food by peristalsis and mechanical digestion by segmentation.

Finally, the serosa is a serous membrane that lines outside the GI tract, and different serosae are associated with the different parts of the digestive tract.

Overall, the digestive system can serve the following main functions: mechanical and chemical digestion of food with the aid of secreted digestive enzymes, absorption of the digested end products and transfer into the blood and lymphatic vessels.

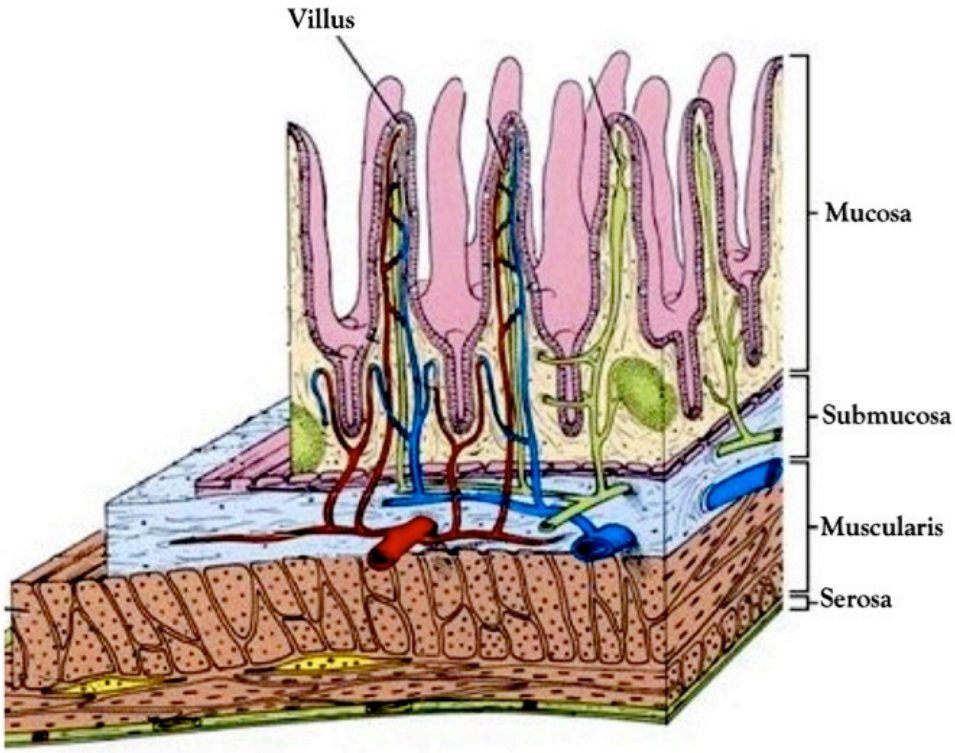

Figure 1.9 Structure of the digestive tract. Representative image showing the four layers consisting the internal wall of the digestive tract: mucosa, submucosa, muscularis externa and serosa (Tortora and Grabowski, 1996).

1.6.3 Intestinal Immune System

The gastrointestinal mucosal surfaces are the physical interfaces of the immune system with the outside world and, in addition to nutrient absorption the GI tract must also provide defence against exogenous pathogens. The gut harbors an abundant number of microbes, named commensal bacteria, which shape the normal functioning of the mucosal immune system (Hooper and Gordon, 2001). The gut is susceptible to inflammation and even under normal conditions there is a baseline degree of "physiological inflammation" in the mucosa, caused by tightly controlled immune responses directed against the wide array of local dietary and microbial antigens (Danese and Fiocchi, 2006).

The intestinal immune system maintains immunologic homeostasis in response to self and foreign antigens through specific compartments that respond to invading pathogens and through a complex network of lymphoid and non–lymphoid cell populations and humoral factors. The first line of protection is provided by the intestinal epithelium, a polarised single layer covered by mucus that forms a primary cell barrier rich in antibacterial substances such as defensins and secreted IgA antibodies (Ayabe et al., 2000)(Macpherson et al., 2000) (McCracken and Lorenz, 2001). Each epithelial cell maintains tight contacts with its neighbours, thus creating tight junctions that prevent bacterial translocation (Madara, 1998) (Macdonald and Monteleone, 2005). Moreover, intestinal epithelium constitutively expresses evolutionary conserved and structurally related receptors, named pattern recognition receptors (PRRs), as well as Toll–like receptors (TLRs) TLR1 and TLR9 and the nucleotide–binding oligomerisation domain (Nod) molecules Nod1 and Nod2 (also present in NK cells) (Strober et al., 2006)(Takeda and Akira, 2004)

In addition, gut epithelium contains abundant intraepithelial lymphocytes (IEL), mainly CD8α+ T cells, divided into two major groups and a low percentage of CD4+ T cells. The first group of CD8α+ cells consists of the conventional CD8αβ+TCRαβ+ IELs, the majority of which enter the epithelium after being activated in secondary lymphoid organs (SLOs). Of note, this group represents the predominant lymphocyte population in the human intestinal epithelium (Jabri and Ebert, 2007). The second group comprises CD8β– CD8αα+ IELs that express either TCRαβ+ or TCRγδ+ (Lambolez et al., 2007). IELs express CCR9 and are thus attracted by epithelial CCL25 to the intraepithelial compartment (Ericsson et al., 2004).

The second immune compartment in the gut is the lamina propria, which is filled with numerous CD4+TCRαβ+ or CD8αβ+TCRαβ+ T cells displaying a previously activated or memory phenotype, that have entered the intestinal mucosa subsequent to their priming and activation in SLOs (Macdonald and Monteleone, 2005). IgA–producing plasma cells, macrophages, dendritic cells (DCs), and eosinophils are also present. Moreover, in the intestinal lamina propria and its associated lymphoid follicles, Foxp3+ regulatory T cells, IL-10 expressing Tr1, TGFβ–producing Th3 cells and invariant NKT cells are resident, to help maintain tolerance to food antigens (Eksteen et al., 2008).

Peyer's patches present in the sub–epithelial compartment are lymphoid aggregates covered by a specialised follicle–associated epithelium (FAE). The FAE is composed of specialised epithelial cells, named M cells, which serve as a means to transport luminal antigens to antigen presenting cells (DCs) in the dome of the follicle (Neutra et al., 2001). M cells are able to sample the gut lumen for antigens and transport bacteria to professional antigen–presenting cells (DCs) on

their basolateral surface. Most of the bacteria are killed rapidly by macrophages, but those transferred by M cells to DCs can survive several days. Moreover, DCs can open the tight junctions between the epithelial cells and through their dendrites extend beyond the epithelium to directly sample luminal contents. DCs that take up antigens in the lamina propria migrate either to local mesenteric lymph nodes (MLN) or to Peyer's patches, where they interact with naïve lymphocytes to generate primed, effector lymphocytes that leave the MLN through the efferent lymph, enter the bloodstream at the thoracic duct and home back to the intestinal mucosa (Macpherson and Harris, 2004)(Niess and Reinecker, 2006). After the antigen is cleared, most effector cells die, leaving a cohort of long–lived memory cells that can rapidly augment immunity on re–encounter with their cognate antigen (Hendriks et al., 2000).

DCs in the gut are key players in controlling immunity against pathogens and tolerance towards commensals. They can distinguish between commensals and pathogens using pattern recognition receptors and co–stimulatory molecules (TLRs and Nods) and consequently can either activate or silence T cell responses (Iwasaki and Medzhitov, 2004)(Baumgart and Carding, 2007). In healthy individuals, an orchestrated system regulates intestinal T cells to sequester commensal microbiota within the intestinal lumen, in order to prevent their contact with innate and adaptive immune cells, thus restricting the production of pro–inflammatory cytokines and the induction of effector immune responses (Maynard and Weaver, 2009). Hence, even upon antigen encounter via DCs, balanced differentiation of naïve T cells to effector CD4+ T cells (Th1, Th2, Th17) and regulatory T cells (Tr1, Th3) is sufficient to maintain tolerance towards commensal organisms (Banchereau and Steinman, 1998). On the other hand, dysregulated effector T cell responses to commensal flora in genetically susceptible

individuals can cause spontaneous inflammation as happens with IBD (Maynard and Weaver, 2009).

1.6.4 Leukocyte Recruitment in Normal and Inflamed Gut

1.6.4.1 Leukocyte recruitment during homeostasis

P–selectin and its counter–receptor P–selectin glycoprotein ligand–1 (PSGL-1) mediate leukocyte tethering and rolling on mucosal vessels, a role supported by experimental evidence from mice that lack P–selectin and show aberrations in their intestinal T–cell numbers (U. Steinhoff et al., 1998). In order to firmly adhere to the mucosal vessels appropriate signals from chemokines are required.

In the small bowel, the chemokine CCL25 is secreted by epithelial cells. In humans, CCL25 is localised in the crypts of Lieberkun in the small intestine, whereas in mice CCL25 is more widely expressed in villous epithelial cells and within the villi of the small intestine (Papadakis et al., 2000). In addition to epithelial cells, CCL25 has been detected on the venular endothelium, however since no message is present it seems that CCL25 expressed by epithelial cells is transported and presented by endothelial cells (Hieshima et al., 2004). This is a property of endothelial cells to take up, transcytose and finally present on their apical surface chemokines produced by surrounding cells (Schrage et al., 2008). Binding of CCL25 to its receptor CCR9, which is restricted to GALT lymphocytes (Kunkel et al., 2000), leads to activation of $\alpha 4\beta 7$ integrin and subsequent binding to its ligand, MAdCAM-1, firmly arresting lymphocytes. Interaction between the leukocyte function–associated molecule-1 (LFA-1) and its

ligand ICAM-1 further promotes firm attachment and transmigration to mucosa associated lymphoid tissue (Schuermann et al., 1993).

The homing of IgA–producing plasma B cells is also dependent on CCR9/CCL25 interactions (N. Feng et al., 2006). CCR9–deficient mice show reduced numbers of IgA+ plasma cells in the lamina propria of the small intestine and in addition CCR9–deficient IgA+ plasma cells show impaired migration into the small intestine when compared to wild–type controls (Pabst et al., 2004). Moreover, compared to resting cells, activated B cells express different carbohydrate epitopes, which serve as ligands for selectins such as E– and P–selectin (Sinha et al., 2006).

CCL28 is another epithelial chemokine highly expressed in the small intestine, and is responsible for attracting IgA–producing B cells, which bear its receptor CCR10 (Kunkel and Butcher, 2003). CCL28 is also expressed on epithelium in the colon, lung, liver and exocrine glands, suggesting that it acts as a common mucosal chemokine (Wilson and Butcher, 2004). In addition, the chemokine CXCL12 is found on high endothelial venules of Peyer's patches (Okada et al., 2002) and promotes the homing of CXCR4 expressing cells to the small and large intestine. Functional studies using blocking antibodies against CXCL12 or its receptor CXCR4 have shown significant inhibition of leukocyte adhesion to ileal and colonic microvessels under both normal and inflammatory conditions (Oyama et al., 2007).

The chemokines CCL6, CXCL16 and CX_3CL1 are expressed throughout the non–inflamed intestine. Other chemokines showing a more restricted expression profile are CCL5 being

predominantly expressed in the small intestine (as is CCL25) and CCL19, CCL21 and CXCL5 being expressed in the large intestine (Shang et al., 2009).

1.6.4.2 Leukocyte recruitment under inflammation

Under inflammation, the mucosal vasculature undergoes changes, and the haemodynamics and permeability of the vessels are altered, leading to activation of the local microvascular endothelial cells (Nathan, 2002). The expression of the adhesion molecules, MAdCAM-1 (M. Briskin et al., 1997), ICAM-1 and P–selectin is enhanced whereas further adhesion molecules, E–selectin, VCAM-1 and VAP-1 are induced on the endothelium of mucosal vessels, thereby promoting continuous leukocyte adhesion and extravasation into tissue (Salmi et al., 1993)(Butcher et al., 1999)(Mori et al., 1999)(Sans et al., 1999). Moreover, in addition to adhesion molecules, the chemokine expression pattern, along with chemokine receptor profiles, is also altered in inflammation. In IBD, elevated levels of CCL2 and CCL5 chemokines have been observed, and knockout animals lacking the receptors for these chemokines show resistance to IBD–like inflammation (Papadakis, 2004). In addition, increased levels of CCL25, CCL28 and CCL20 along with their receptors CCR9, CCR10 and CCR6, respectively, are involved in the pathogenesis of IBD. In inflamed colonic lamina propria of UC patients, increased levels of CXCL10 the ligand for CXCR3 have been also observed (Uguccioni et al., 1999). Finally, CX_3CL1 chemokine is increased in IBD patients, which is consistent with the increased expression of its receptor CX_3CR1 on patient CD4+ T cells (Kobayashi et al., 2007).

1.7 LINKS BETWEEN THE LIVER AND THE GUT

Inflammatory bowel disease (IBD) is an idiopathic disorder of the gastrointestinal tract, characterised by several intestinal inflammatory features, ranging from granulomatous, transmural inflammation (in Crohn's disease) to crypt abscesses, restricted to the colon (in ulcerative colitis) (Adams and Eksteen, 2006). It is well known that patients with IBD are susceptible to develop inflammation at extra–intestinal sites, either in parallel with gut inflammation (such as pyoderma gangrenosum, erythema nodosum and anterior uveitis) or independently of the course of IBD [such as autoimmune hepatitis, primary sclerosing cholangitis (PSC) and ankylosing spondylitis]. In the latter case, the association of PSC and IBD is of particular interest, since patients can develop PSC *de novo* many years after total colectomy for fulminant colitis and, colonic inflammation can occur for the first time in patients after many years of liver transplantation for PSC (Adams and Eksteen, 2006). The association between IBD and liver diseases may be partly explained by observations that show ectopic expression in the liver of what were previously thought to be "gut–specific" addressins. Thus, in the extra–intestinal complications of IBD in the liver, PSC and AIH, aberrant expression of MAdCAM-1 has been detected (Hillan et al., 1999)(Grant et al., 2001), which supports α4β7–integrin mediated lymphocyte adhesion to hepatic endothelium. Moreover, CCL25 which was thought to have a restricted expression in the gut and the thymus (Kunkel et al., 2000) was also detected in inflamed PSC tissues, where it could support recruitment of α4β7+CCR9+ lymphocytes to MAdCAM-1 expressing inflamed hepatic endothelium (Eksteen et al., 2004a). Furthermore, the ectopic expression of VAP-1, which is up–regulated on mucosal endothelium upon inflammation (Salmi et al., 1993), supports the existence of an "entero–hepatic" circulation where long–lived memory T cells are able to migrate to both gut and liver, thus

providing immune surveillance against gut–derived pathogens entering the liver via the hepatic portal tract circulation (Grant et al, 2001) (Figure 1.10).

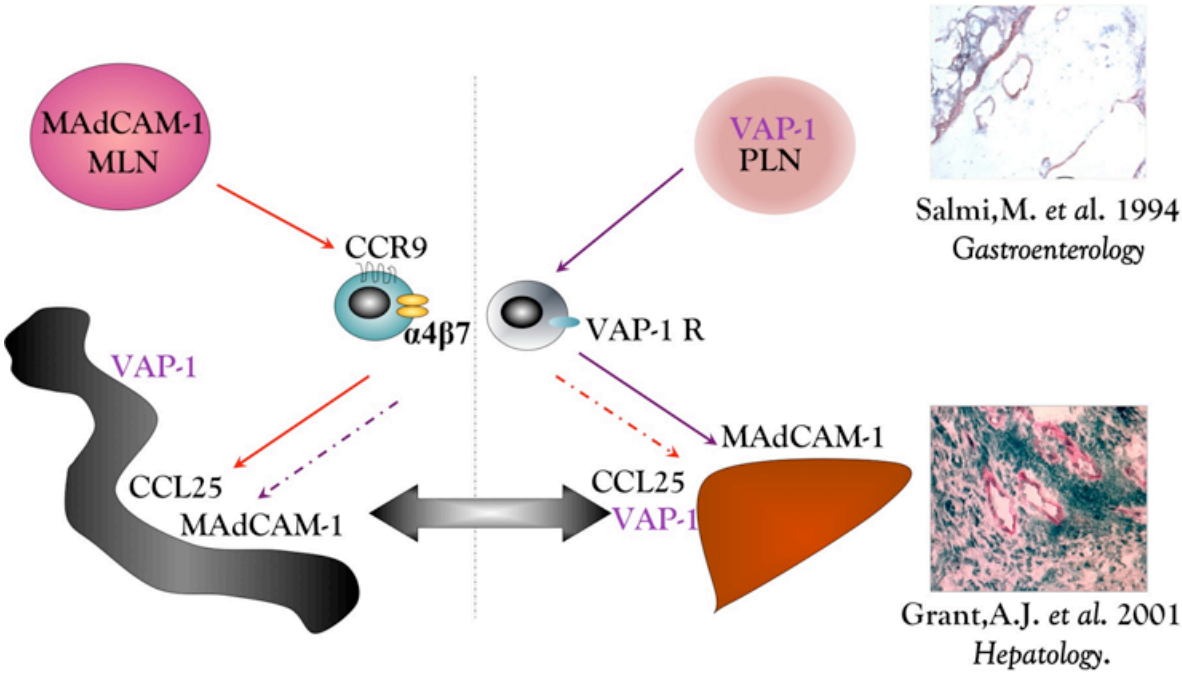

Figure 1.10 Overlapping expression of adhesion molecules in gut and liver. MAdCAM-1 is normally expressed in gut mucosa associated lymphoid tissues where it recruits α4β7+ lymphocytes initially activated in mesenteric lymph nodes (MLN). Similarly, the constitutively expressed in the liver VAP-1 attracts lymphocytes primarily activated in peripheral lymph nodes (PLN). However, during inflammation, MAdCAM-1 is induced in the liver and VAP-1 in the gut, leading both to aberrant recruitment of gut–and liver– derived lymphocytes to the liver and gut respectively.

1.8 AIMS OF THE THESIS

The broad aim of this thesis was to investigate the mechanisms that regulate the expression of MAdCAM-1 in human liver under certain chronic inflammatory conditions, and to evaluate its function, in order to understand the pathogenesis of these disorders. More precisely the specific aims were:

I. To investigate the presence of MAdCAM-1 and CCL25 in a variety of diseased human liver tissues.

II. To use primary cultures of human hepatic and human umbilical vein endothelial cells to investigate the role of specific factors in the regulation of MAdCAM-1 expression.

III. To study the role of VAP-1/SSAO enzyme activity in MAdCAM-1 expression both *in vitro* and *in vivo* using animal models.

IV. To develop a flow–based adhesion using primary cell cultures in order to determine the function of MAdCAM-1 in the liver and the role of different chemokines in lymphocyte adhesion to MAdCAM-1.

CHAPTER 2

Materials & Methods

2.1 HUMAN TISSUE

Human liver tissue was obtained from explanted diseased livers that were removed after transplantation, or from normal tissue surplus to transplantation requirements or from excised tumour margin tissue collected after resection of tumours at the Queen Elizabeth Hospital, Birmingham, UK. Human umbilical cords were collected from the Women's Hospital, Birmingham, UK. Whole blood was obtained from healthy volunteers, and for purposes of specific experiments, peripheral blood was obtained from patients with inflammatory bowel disease (IBD). All human tissue and blood samples were collected with local research ethics committee approval and patient consent.

2.2 CELL CULTURE

2.2.1 Solutions Used for Cell Culture

Human AB serum purchased from HD Supplies, Bucks, UK and Fetal Calf Serum (FCS) purchased from Invitrogen were both heat inactivated at 56°C for 20min prior to use. Penicillin, Streptomycin and Glutamine (PSG) were purchased from Sigma-Aldrich. TrypLE™ Express (1x) stable Trypsin-like enzyme with Phenol Red and Trypsin 0.5% (10x) with EDTA 4Na (used in the MediCity laboratory, Turku) were both purchased from Invitrogen. Phosphate buffered saline (PBS) was prepared from tablets (Oxoid, UK) according to manufacturer's instructions. All non–sterile solutions and glassware were autoclaved prior to use for cell culture.

2.2.2 Tissue Culture Plastics

Sterile 5,10 and 20ml pipettes, 25 and 75 cm^2 culture flasks, sterile 6–well and 24–well plates, sterile 15ml and 50ml tubes and sterile cryovials were all purchased from Corning Costar Incorporated, Bucks, UK. Sterile flat–bottomed 96–well plates were purchased from Becton Dickinson Labware. Tissue culture cell scrapers 25cm were purchased from Starstedt Ltd. 20ml plastic tubes and 5ml bijous were acquired from Ramboldi. Sterile plastic gloves used daily were from Premier Nitric. All tissue culture was carried out in a class II microflow safety cabinet. At all times aseptic technique was followed by swabbing the cabinets with industrial methylated spirit (IMS; Adams Healthcare, Leeds, UK) before and after use.

2.2.3 Cell Culture and Passage

All cells were cultured on tissue culture plastic in appropriate media (as indicated in the following sections) and maintained at 37°C in a humidified 5% CO_2 incubator. Cell viability and growth were monitored using an inverted phase contrast microscope (Olympus IX50) where live cells appeared phase bright. Adherent cells formed projections and became flattened when attached to the growth surface and cells in suspension typically remained rounded and symmetrical. All cultures were examined daily by observing the morphology of cells, the colour of the medium and the density of cells.

Adherent cells were passaged using an appropriate volume of the proteolytic enzymes TrypLE or trypsin (i.e 3–5ml in a 75cm^2 flask, enough to cover the cell monolayer). Initially, used media was discarded, and cells were washed with PBS, TrypLE or Trypsin was then added and the flask was agitated gently to help detachment of cells. Occasionally, the cell monolayers were

incubated at 37°C until cells had loosened. Once detachment was complete, PBS was added to the cell suspension and the cells were collected by centrifugation at 550g for 5min. The cell pellet was re–suspended in appropriate media and re–seeded in new culture flasks for further culture.

Non–adherent cells were passaged without trypsinization by centrifugation of the suspension at 550g for 5min. The cell pellet was re–suspended in appropriate media and cells were re–seeded in new culture flasks. Dependent on experimental requirements, the viability of cells was assessed using trypan–blue, and cells were counted using a haematocytometer (CAMLAB, Cambridge, UK) and finally re–seeded.

2.2.4 Maintenance of Cells by Freezing and Storing

For long–term storage, cells were cryopreserved in liquid nitrogen. After detachment and pelleting, cells were re–suspended in chilled freezing media consisting of 95% FCS+5% DMSO (Sigma-Aldrich). Cells were aliquoted into cryovials and placed into a Mr Frosty™ freezing container (Wessington Cryogenics, Tyne & Wear, UK), which was transferred to –80°C to permit gradual cooling at a rate of 1°C per minute, thus preventing ice crystal formation in cell cytoplasm. Once the container had reached –80°C (after 4 hours or more conveniently overnight), the vials of cells were immediately placed into liquid nitrogen storage. When required, cells were taken out of liquid nitrogen on ice, thawed as quickly as possible by washing in PBS and centrifuged in order to remove any cell debris. Cells were counted and viability was assessed with trypan–blue exclusion before re–suspension and culture in the appropriate media.

2.3 Isolation And Culture of Primary Endothelial Cells

2.3.1 Preparation of Rat tail Collagen

Collagen for cell attachment was prepared in house from rat tails. Frozen rat–tails were thawed in sterile PBS and the outer skin was cut using pliers. After twisting the tail a string of collagen became visible, which was carefully collected and dropped into sterile PBS. Finally, the accumulated collagen from the whole tail was collected using forceps, drained of excess of PBS and weighed. The collagen was transferred into 70% ethanol for about 10min and then into an appropriate volume of 4% acetic acid (1gr of wet collagen to 100ml of 4% acetic acid). The collagen was covered with foil and left at 4°C to stir for 2days. Finally, the solution was transferred to bottles and centrifuged at 4°C for 30min at 550g. The collagen solution was sieved through fine mesh, aliquoted and stored at 4°C. Occasionally, the rat–tail collagen that was used was purchased from Sigma.

2.3.2 Endothelial Cell Media

Both HSEC (Hepatic Sinusoidal Endothelial Cells) and HUVEC (Human Umbilical Vein Endothelial Cells) were cultured in complete human endothelial basal growth medium (Gibgo, Invitrogen, UK) supplemented with 60μg/ml benzylpenicillin, 100μg/ml streptomycin, 2mM L–glutamine plus 10% heat inactivated human AB serum. Furthermore, HSEC media was supplemented with 10ng/ml hepatocyte growth factor (HGF) and 10ng/ml vascular endothelial growth factor (VEGF) (both from PeproTech, UK). The HUVEC media contained in addition 10ng/ml epidermal growth factor (EGF) (R & D Systems, UK) and 10μg/ml hydrocortisone (Sigma-Aldrich, UK).

2.3.3 Isolation of Human Hepatic Sinusoidal Endothelial Cells

HSEC were isolated from human liver tissue according to a previously described protocol (Lalor et al., 2002a). Briefly, approximately 150gr of tissue was finely chopped and enzymatically digested at 37°C using 0.2% collagenase Type 1A (Sigma-Aldrich, UK) for 20–40 min, depending on the texture of the liver. Once the liver was digested it was filtered in an excess of sterile PBS. The cell suspension was further washed in PBS (approximately x4) and purified via density gradient centrifugation over 33/77% Percoll™ (Amersham Bioscience, UK) at 550g for 30min. The layer of cells at the interface between the different solutions of Percoll™ was collected and washed in PBS. HSEC were extracted from the mixed non–parenchymal population firstly via negative magnetic selection to remove biliary epithelial cells and secondly via positive selection for endothelial cells. Specifically, the cell suspension was incubated initially with mouse anti–HEA–125 antibody (Progen Biotechnic, Germany; 50μg/ml), for 30min at 37°C. After that, cells were incubated with a secondary antibody conjugated to magnetic beads (10μl per prep of sheep anti–mouse Dynabeads®, Dynal, Wirral, UK) for 30min at 4°C. HEA–125 labeled cells were removed by magnetic selection and the remaining cells were incubated with anti–CD31 antibody conjugated to dynabeads (Dynal, Liverpool, UK; 10μg/ml) for 30min at 4°C. CD31 positive cells were extracted from the heterogeneous cell mixture by magnetic selection, re–suspended in complete HSEC media and cultured in rat–tail collagen coated flasks.

2.3.4 Isolation of Human Umbilical Vein Endothelial Cells

HUVEC were isolated from approximately 15cm of fresh umbilical cord according to an isolation procedure previously published (Jaffe et al., 1973). Firstly, the cords were rinsed

thoroughly with 70% (v/v) IMS to avoid any contamination and one end of vein was cannulated. PBS was flushed through the vein until the solution ran clear. Once washed, the other end of the cord was cannulated and sealed to permit infusion of 1mg/ml solution of collagenase Type–1A (Sigma-Aldrich, UK). Both ends of vein were clamped and the cord was incubated for 15 min at 37°C. Cells were then collected by gently massaging the cord, flushing through the vein with PBS and centrifugation for 5min at 550g. Pelleted cells were re–suspended in complete HUVEC media and cultured in 1% gelatin coated flasks.

2.4 Culture Of Cell Lines

Chinese Hamster Ovary (CHO) cells, transfected with a full–length (FL)–MAdCAM-1 construct were used as a positive control in almost all experimental procedures. Parental CHO cells containing no MAdCAM-1 construct were used as negative controls. CHO cells were grown in nutrient F-12 Ham (Sigma-Aldrich, UK) medium supplemented with 20mM HEPES and 10% (v/v) FCS. For reselection of cells that expressed MAdCAM-1, hygromycin B (350μg/ml; Sigma) was added to their media. The JY cell line, a b–lymphoblastoid cell line which expresses α4β7 integrin, was also used. JY cells were grown in RPMI (Invitrogen) containing L–glutamine and supplemented with 10% (v/v) FCS. All cell lines were available in house. Cells were maintained in a humidified atmosphere with 5% CO_2 at 37°C.

2.5 WESTERN BLOTTING

2.5.1 Total Protein Lysates

2.5.1.1 Preparation of total protein lysates

Confluent cultures of HSEC and HUVEC, stimulated for 2 hours with TNFα (20ng/ml; Peprotech, UK) and methylamine (50 μM; Sigma-Aldrich) alone or in combination, were washed in ice cold PBS and harvested in RIPA buffer (table 2.7) or CelLytic™ MT lysis buffer (Sigma), containing protease inhibitor cocktail (Sigma-Aldrich). The cell lysates were incubated at 4°C under constant agitation for about 2 hours and then stored at –20°C in small aliquots for further use. Protein lysates were also obtained from pelleted CHO and JY cells using the above method.

Human liver tissue blocks and tissue blocks (liver, kidney, spleen, mesenteric lymph nodes and Peyer's patches) harvested from mice, were homogenised in lysis buffer and maintained under continuous stirring at 4°C overnight. The following day, the mixture of protein lysate and tissue was centrifuged at 700g for 20min at 4°C, and the supernatant was aspirated and placed in a clean tube. Protein concentration was measured (see section 2.5.1.3) and aliquots were prepared and stored at –20°C.

2.5.1.2 Extraction of subcellular fractions from adherent cells

In order to determine the exact location of MAdCAM-1 protein in hepatic sinusoidal endothelial cells, cytosolic, membrane, nuclear and cytoskeletal fractions were prepared. Buffers for cytosolic (buffer I), membrane (buffer II), nuclear (buffer III) and cytoskeletal (buffer IV) fragments were prepared (see tables 2.1–2.5), according to the ProteoExtract® Subcellular

Proteome Extraction Kit. HSEC were stimulated as previously and after the 2 hour incubation period, they were washed by carefully overlaying the cell monolayers with 2ml ice cold PBS. The cells were gently agitated for 5min at 4°C and the washing step was repeated until all contaminating media components were removed.

To isolate cytosolic protein fragments, 1ml of extraction buffer I and protease inhibitor cocktail (Sigma-Aldrich, used at 1:50 dilution) were mixed and added to the flask without disturbing the endothelial monolayer and ensuring all cells were covered. Cells were incubated for 10min at 4°C under gentle agitation. The supernatant was transferred into properly labelled sample tubes and kept on ice. Then, 1ml of ice cold extraction buffer II was mixed with protease inhibitor cocktail and immediately added to the flask. Cells were incubated at 4°C for 30min under gentle agitation. Supernatant containing the membrane bound fragments was then removed, transferred into sample tubes and kept on ice. Next, 500µl of ice–cold extraction buffer III with protease inhibitor cocktail and DNAase (Sigma-Aldrich) were mixed and immediately added until all cells were covered with buffer and incubated with gentle stirring for 10 min at 4°C. The supernatant containing the nuclear fragments was removed, collected and stored on ice. Finally, 500µl of extraction buffer IV and protease inhibitor cocktail were mixed, and added to the flask to cover all the cells. Remaining cell structures were detached upon treatment with buffer IV. After complete solubilisation of the residual materials, the extract containing the cytoskeletal structures was removed, placed in sample tubes and stored on ice. All samples were stored at –20°C for further analysis by western blotting.

Reagents Required	Molecular Weight (FW)	Source
PIPES	302.37	Sigma-Aldrich
$Na_2EDTA{\cdot}2H_2O$	372.2	Sigma-Aldrich
Sucrose	342.3	Sigma
NaCl	58.44	Sigma
$MgCl_2$ anhydrous	95.21	Sigma
β-mercaptoethanol	78.13	Sigma
Trisma base	121.14	Sigma
Trisma-HCl	157.6	Sigma
NP-40 (Igepal CA-630)	-	Sigma-Aldrich
Triton X-100	-	Sigma-Aldrich
Sodium deoxycholate	414.55	Sigma-Aldrich
Tween20	-	Sigma

Table 2.1 Source and molecular weight of all reagents required for preparation of extraction buffers I – IV

Extraction Buffer I- Cytosolic Fragments- pH 6.8	
Reagents	Final Concentration
PIPES	10mM
EDTA	5mM
Sucrose	300mM
NaCl	100mM
$MgCl_2$	3mM
NP-40	0.01% (v/v)

Table 2.2 Reagents and their final concentration required for preparation of extraction buffer I

EXTRACTION BUFFER II- MEMBRANE BOUND FRAGMENTS- PH 7.4	
REAGENTS	FINAL CONCENTRATION
PIPES	10mM
EDTA	3mM
Sucrose	300mM
NaCl	100mM
$MgCl_2$	3mM
Triton X-100	0.5% (v/v)

Table 2.3 Reagents and their final concentration required for preparation of extraction buffer II

EXTRACTION BUFFER III- NUCLEAR FRAGMENTS- PH 7.4	
REAGENTS	FINAL CONCENTRATION
PIPES	10mM
Sodium deoxycholate	0.5% (w/v)
$MgCl_2$	1mM
Tween20	1% (v/v)
NaCl	10mM

Table 2.4 Reagents and their final concentration required for preparation of extraction buffer III

EXTRACTION BUFFER IV- CYTOSKELETAL FRAGMENTS	
REAGENTS	FINAL CONCENTRATION
SDS	0.3% (w/v)
β-mercaptoethanol	200mM
Trisma-HCl	28mM
Trisma base	22mM

Table 2.5 Reagents and their final concentration required for preparation of extraction buffer IV

2.5.1.3 Protein concentration measurement

A Bio-Rad *DC* Protein Assay was performed according to manufacturer's instructions in order to determine the protein concentration of all samples. Dilutions of bovine serum albumin (BSA; Sigma) were used as protein standards.

2.5.2 SDS Poly Acrylamide Gel Electrophoresis (SDS-PAGE)

Protein samples were separated by electrophoresis on a 10% or 12% acrylamide gels using the BioRad Mini Trans Blot Cell System. Initially, glass plates were assembled, resolving and stacking gels were prepared (see tables 2.7-2.8), poured into the glass space and left to set. Solubilised protein samples (20–100μg/lane) were diluted in 5x laemli buffer, with or without β-mercaptoethanol and boiled either at 100°C for 10min or at 37°C for 20min dependent on the antibody used (see table 2.9) and its epitope recognition characteristics. Protein samples were centrifuged and set aside to cool before loading. In the meantime, the gel apparatus was assembled and 1x electrophoresis buffer was then poured onto the tank ensuring that the electrodes were fully covered. 30μl of each protein sample was slowly loaded into the stacking gel. Pre–stained rainbow molecular weight markers (Amersham, GE Healthcare) were used as size markers. Electrophoresis was performed at 200V for 30min until the dye front reached the bottom of the gel.

2.5.3 Western Blot Transfer

Resolved proteins were transferred onto hybond–ECL nitrocellulose membrane (Amersham Biosciences) or occasionally onto PVDF membrane (Millipore, U.S.A) using BioRad Mini-protein system. PVDF membranes were soaked in methanol for 5min before immersion in

transfer buffer whereas nitrocellulose membranes were directly immersed into transfer buffer in order to facilitate binding of proteins. Soaked membranes were placed on top of the gel, sandwiched between filter papers and sponges; which were also pre–immersed in transfer buffer and the assembly was placed into the transfer buffer apparatus which in turn was placed in the transfer tank containing an ice pack. Transfer buffer was added into the tank and a current of 100V was applied for 1hour. Efficient transfer was evident from the appearance of rainbow markers on the membrane. Moreover, after transfer the membrane was stained with Ponceau S solution [0.1% Ponceau S (w/v) in 5% acetic acid (v/v); Sigma] for 5min followed by rinsing with water to visualise successfully transferred protein.

2.5.4 Western Blot Development

After transfer, membranes were blocked for at least 2 hours in 0.1% PBS–Tween20 containing 10% (w/v) non–fat dry milk with continuous agitation. The blocking buffer was removed and membranes were probed overnight at 4°C with primary antibodies (Table 2.9). After several washes in PBS–Tween20 (x3 for 30min), membranes were incubated with peroxidase–conjugated secondary antibodies for 1 hour at room temperature. After several washes with PBS–Tween20, the blots were incubated with enhanced chemiluminescence reagents (ECL and ECLplus from Amersham Pharmacia, Biotech, UK and Immobilon Western HRP Substrate from Millipore Corporation, used in MediCity, Turku). Enhanced chemiluminescence detection film (Amersham Biosciences) was exposed to the membrane and developed using a Kodak X–Omat 1000 processor (Birmingham, UK) or a Curix 60, AGFA processor (Turku, Finland). After visualisation, bound antibodies were stripped by incubation in stripping buffer (Table 2.7) for 45min at 50°C and several washes in dH_2O. The membranes were then blocked

with 10% (w/v) non–fat milk and re–probed with anti–actin or anti β–actin. The bands were detected with ECL and the films were exposed as previously.

MAdCAM-1 and β-actin staining density was measured by staining the 120kDa and 40kDa bands respectively, and performing densitometry using ImageJ or Quantity One programs. All experiments were performed at least in triplicate. Protein lysates generated from CHO cells transfected with FL–MAdCAM-1 were used as a positive control.

REAGENTS	MOLECULAR WEIGHT (FW)	SOURCE
Trisma base	121.14	Sigma
NaCl	58.44	Sigma
Glycine	75.07	Sigma
Sodium dodecyl sulfate (SDS)	288.38	Sigma
NP-40 (Igepal CA-630)	-	Sigma-Aldrich
Sodium deoxycholate	414.55	Sigma-Aldrich
Tween20	-	Sigma
Methanol	-	Fisher Scientific
β-mercaptoethanol	78.13	Sigma
Non-fat milk	-	Marvel

Table 2.6 Molecular weight and source of reagents required for western blot buffers

BUFFERS	CONSTITUENTS
RIPA Buffer	50mM Trisma base, 150mM NaCl, 1% (v/v) NP-40, 0.25% (w/v) sodium deoxycholate, 1mM EDTA, 0.1% SDS
10x Electrophoresis Buffer	Per 1L: 30.3gr Trisma base, 144gr glycine, 10gr SDS
Transfer Buffer	Per 2L: 28.8gr glycine, 6.0gr Trisma base, 400ml MeOH, 1gr SDS
Resolving Gel Buffer	1.5M Trisma base pH 8.8 (adjust pH with HCl)
Stacking Gel Buffer	1.0M Trisma base pH6.8 (adjust pH with HCl)
Stripping Buffer	Per 100ml: 20.0ml 10% SDS, 12.5ml 0.5M Trisma base pH 6.8, 67.5ml dH_2O, 0.8 β-mercaptoethanol
Blocking Buffer	PBS + 0.1% (v/v) Tween20, 10% (w/v) non-fat milk (25ml per membrane)

Table 2.7 Buffers used in SDS-PAGE

	STACKING GEL (5%)	RESOLVING GEL (10%)	RESOLVING GEL (12%)
ddH_2O	6.8ml	4.0ml	3.3ml
30% Acrylamide mix (BioRad)	1.7ml	3.3ml	4.0ml
Stacking Gel Buffer	1.25ml	-	-
Resolving Gel Buffer	-	2.5ml	2.5ml
10% (w/v) SDS	0.1ml	0.1ml	0.1ml
10% (w/v) ammonium persulfate (APS) (Sigma-Aldrich) *	0.1ml	0.1ml	0.1ml
N,N,N',N'-tetramethylethylenediamine (TEMED) (Sigma-Aldrich)*	40μl	40μl	40μl

Table 2.8 Components of SDS-PAGE gels. *APS and TEMED were added just prior to pouring of gels into the glass spaces, as the oxygen free radicals released from the reaction between APS and the tertiary amine TEMED are responsible for the polymerisation of bis-acrylamide.

ANTIBODIES	CLONE	FINAL CONCENTRATION	SOURCE
*MAdCAM-1[1]	CA102.2C1	4μg/ml	Serotec
*MAdCAM-1[2]	MECA367	10μg/ml	Kind gift from E.Butcher, Stanford University
*MAdCAM-1 (H-116)[1] (polyclonal)	sc-28645	1μg/ml	Santa Cruz Biotechnology
*MAdCAM-1[1]	P1	4μg/ml	Pfizer
**VAP-1[1]	TK8-14	5μg/ml	MediCity, Turku
**Anti- chicken T cell protein (negative control)	FU7-3G6	5μg/ml	Microbiol V. Vainio, MediCity, Turku
*Anti-actin[1,2]	-	1μg/ml	Sigma-Aldrich
*β-actin[1]	Clone AC-15	1μg/ml	Sigma-Aldrich
Anti-mouse HRP	-	1:2000	Dako
Anti-human HRP	-	1:2000	Sigma-Aldrich
Anti-rabbit HRP	-	1:2000	Dako Cytomation
Anti-rat HRP	-	1:2000	Dako Cytomation

Table 2.9 Concentrations, clone names and sources of all antibodies used for western blotting and immunoprecipitation. [1]Monoclonal anti-human antibodies, [2]monoclonal anti-mouse antibodies. *Antibodies recognising reduced and denatured protein. **Antibodies recognising protein in its native and non-denatured form.

2.6 IMMUNOPRECIPITATION

2.6.1 Immunoprecipitation using Protein G Sepharose Beads

The presence of MAdCAM-1 in human liver and umbilical vein endothelial cells was verified by immunoprecipitation. Protein lysates prepared from treated HSEC and HUVEC, were incubated with anti–MAdCAM-1 Ab (Clone CA102.2C1; 10μg/ml) prior to addition of protein G beads (Sigma-Aldrich). Any MAdCAM-1 protein present bound to the antibody, was then immobilised on the protein G sepharose beads. Following initial capture of the protein, the solid support was washed several times with RIPA buffer for removal of any non–specific proteins. Finally the washed precipitated protein was eluted and analysed by western blotting using a different antibody specific for MAdCAM-1 (humanised anti–human P1; 4μg/ml from Pfizer, UK).

2.6.2 Immunoprecipitation using DYNABEAD-Protein G from Culture Supernatants

HSEC were treated as previously described with TNFα and methylamine alone or in combination. After 2 hours stimulation the supernatant–media was removed and collected in 15ml tubes in order to test for the presence of soluble MAdCAM-1 by immunoprecipitation with Dynabead–protein G (Invitrogen, Dynal, UK). Firstly, the dynabeads were completely re–suspended by constant rotation on a roller for 5min and then 50μl of beads per reaction were transferred to separate 1.5 ml eppendorf tubes for removal of diluent using a magnet. Then 10μg of MAdCAM-1 polyclonal antibody H–116 was diluted in 200μl PBS plus 0.02% Tween20 and mixed with the cleaned beads. The mixture was incubated with rotation for 10min at room temperature and then the beads–Ab complex was washed in PBS plus 0.02% Tween20 and finally re–suspended in 50μl of PBS. Next, the cleaned beads–Ab complex was

pipetted into the tubes containing the culture supernatant and incubated with constant rotation for 30min at room temperature to allow the antigen to bind to the complex. The complex of dynabeads–Ab –Ag was washed in PBS and re–suspended in 50µl 5x laemli buffer. The mixture was either stored at –20°C for further western blot analysis or heated for 10min at 70°C, prior to removal of supernatant with the aid of a magnet to collect the Ab–Ag complex. Samples were loaded in SDS–PAGE gels for detection of sMAdCAM-1 using the monoclonal mouse anti–human antibody (CA102.2C1; 4µg/ml).

BUFFERS	Phosphate Buffered Saline (PBS)
REQUIRED	Phosphate Buffered Saline (PBS) + 0.02 (v/v) Tween20

Table 2.10 Buffers required for immunoprecipitation using Dynabead-Protein G

2.7 POLYMERASE CHAIN REACTION (PCR)

2.7.1 RNA Extraction

2.7.1.1 RNA Extraction from human endothelial cells

Total RNA isolated from HSEC and HUVEC previously stimulated with TNFα (20ng/ml) or methylamine (50µM) alone or in combination for 2 hours, was extracted using the RNEasy mini kit (Qiagen, UK), according to manufacturer's instructions. DNAase treatment with RNAase free DNAase (Qiagen) was performed as part of the protocol instructions. Total RNA was also extracted from HSEC after transfection with hVAP-1 adenoviral constructs (see paragraph 2.14.2) and stimulation with TNFα or MA alone or in combination for 2 hours.

Formaldehyde, ammonia and hydrogen peroxide are produced during VAP-1 catalysed deamination of methylamine. In order to study whether these end products have a role in

induction of MAdCAM-1, non–transfected HSEC, were exposed to 1μM and 10μM hydrogen peroxide (30% H_2O_2; VWR PRoLABO BDH), ammonia (ammonia solution 32% extra pure; Merck) and formaldehyde (formaldehyde solution 37%; JT Baker) for 4 hours. Cells were also subjected to repeated dosing with H_2O_2 (8x 10μM at 30min intervals) and to a combination of all three end products (single dose). On occasion one set of HSEC was exposed to sVAP-1 (500ng/ml; Biotie Therapies, Turku, Finland) (enzymatically active) and its substrate methylamine at 1μM and 10μM. After the stimulation period, cells were processed for total RNA extraction as above.

2.7.1.2 RNA extraction from human liver tissues

Tissue blocks from normal liver (NL), and from patients with alcoholic liver disease (ALD), primary biliary cirrhosis (PBC), autoimmune hepatitis (AIH) or primary sclerosis cholangitis (PSC) were submerged into RNA later (Qiagen) for RNA preservation. About 30mg of tissue was used for RNA extraction using the RNEasy mini kit, according to manufacturer's instructions. A DNAase treatment step was included as previously.

2.7.1.3 RNA extraction from mouse tissues

Total RNA was isolated from the liver, Peyer's patches (PPs), mesenteric lymph nodes (MLN), kidney and spleen of wild-type (WT) untreated mice, and from wild-type mice, VAP-1 deficient mice (VAP-1_KO), VAP-1 deficient mice that contained enzymatically active hVAP-1 as a transgene (VAP-1_EA) and VAP-1 deficient mice that contained enzymatic inactive hVAP-1 as a transgene (VAP-1_EI) (the background of these mice is described in paragraph 2.13) treated for 14 days with methylamine. All RNA was extracted as previously using the RNAeasy mini kit

from Qiagen. Paraffin embedded liver tissue blocks from VAP-1_KO mice and VAP-1_KOTG mice expressing hVAP-1 as a transgene, which had been treated with Concavalin A (10mg/kg, *i.v*, 4 hours) to induce hepatitis, were also used for RNA isolation using the RNEasy FFPE Kit (Qiagen) according to manufacturer's instructions.

For all the above samples, concentration of eluted RNA was measured using the NanoDrop Spectrophotometer (Thermo Fisher Scientific) and RNA was stored at –80°C. Moreover, the 260/280 nm absorbance ratio was calculated in order to determine sample purity with a value of 2 being indicative of pure preps.

2.7.2 cDNA Synthesis

In all cases 50μg of the extracted total RNA were transcribed into cDNA using the iScript cDNA synthesis kit (BioRad, Hercules, CA). The concentration of cDNA was measured using the NanoDrop Spectrophotometer. An OD260/OD280 ratio value of 1.8 was representative of a pure DNA prep.

2.7.3 Conventional PCR

The presence of MAdCAM-1 mRNA in HSEC and HUVEC was confirmed by conventional PCR. Reverse transcription was carried out for both human MAdCAM-1 and β–actin, which was used as endogenous control. PCR encoded products of 357bp and 220bp for MAdCAM-1 and β-actin respectively, were visualised on a 1.5% (w/v) agarose gel (diluted in 0.5x TBE) stained with ethidium bromide. The TrackIt™ 50bp DNA ladder (Invitrogen) was used as amplicon length marker. The primers for hMAdCAM-1 and β–actin, the reagents used and

their final concentrations as well as the thermal profile of each reaction are shown in the following tables.

PRIMERS	MADCAM-1
Forward	5'- CCC CTG TGA AAG CAA AAT AGC -3'
Reverse	5'- AGG TTT ATT TGC CAA AGC CTC -3'
Amplicon Length: 357bp	
PRIMERS	**B-ACTIN**
Forward	5'- CAT CAC CAT TGG CAA TGA GC -3'
Reverse	5'- CGA TCC ACA CGG AGT ACT TG -3'
Amplicon Length: 220bp	

Table 2.11 Primer sequences and amplicon lengths of hMAdCAM-1 and human β-actin amplified products

REAGENTS	FINAL CONCENTRATION	SOURCE
5x Green GoTaq® Flexi Buffer	1x	Promega, Southampton, UK
$MgCl_2$	1mM	Promega, Southampton, UK
dNTPs	0.2mM (total)	Roche
GoTaq® DNA Polymerase	1.25U	Promega, Southampton, UK
Primers	0.25pmole/μl	Alta Bioscience
cDNA	10μg/ml	Human primary endothelial cells

Table 2.12 Components of a conventional PCR reaction mix

MAdCAM-1		
Number Of Cycles: 35	**Temperature (°C)**	**Time (min)**
	95	02:00
Denaturation	95	01:00
Annealing	60	01:00
Extension	72	01:00
	72	05:00
β-Actin		
Number Of Cycles: 29	**Temperature (°C)**	**Time (sec)**
	95	05:00
Denaturation	94	00:30
Annealing	55	00:45
Extension	72	00:45
	72	05:00

Table 2.13 Thermal profile for human MAdCAM-1 and β–actin gene amplification

10x TBE Electrophoresis Buffer			
Reagents	**Molecular Weight (FW)**	**Final Concentration**	**Source**
Trisma Base	121.14	0.89M	Sigma
Boric Acid	61.83	0.89M	Sigma
$Na_2EDTA{\cdot}2H_2O$	442.5	0.5M	Sigma-Aldrich
ddH_2O	-	Fill up to 1L	

Table 2.14 TBE buffer components for electrophoresis of PCR products

2.7.4 Quantitative PCR

For analysis of relative expression of human and murine MAdCAM-1 mRNA Taqman Fluorogenic 5' nuclease assays using gene–specific 5' FAM labelled probes run on an ABI Prism 7700 sequence detector (at MediCity, Turku, Finland) as well as on an ABI Prism 7900 sequence detector (at University of Birmingham, UK), were used. Human and murine GAPDH were used as internal control to which the threshold cycle (Ct) values of the target gene were normalised. Differential expression levels were calculated according to the $2^{-\Delta\Delta Ct}$ method.

	PRIMER/PROBE ASSAY ID	SOURCE
hMAdCAM-1	Hs00175533_ml	Applied Biosystems
hGAPDH	Hs99999905_ml	
mMAdCAM-1	Mm00522086_g1	
mGAPDH	Mm99999915_g1	
EXPENDABLES		
Taqman® Universal PCR Master Mix		
Taqman® 2x Master Mix		
MicroAmp® Optical 96-well reaction plate-0.1ml		
MicroAmp® Optical adhesive film		

Table 2.15 Primers and Taqman probe assay mixes for each gene as well as expendables used in quantitative PCR

REAGENTS	FINAL CONCENTRATION
ABI Taqman 2x Master Mix	1x
20x Assay mix	0.5x
cDNA	100-200µg/ml
RNAase free water	Up to 10µl

Table 2.16 Components of a quantitative PCR reaction mix

2.8 IMMUNOHISTOCHEMICAL STAINING

2.8.1 Preparation of Tissue Sections

For the examination of adhesion molecule expression in human liver and in murine liver, Peyer's patches, mesenteric lymph nodes and spleen, tissue sections for immunohistochemical analysis were produced in house. 1–2cm^3 blocks of tissue were snap–frozen in liquid nitrogen and stored at –80°C until required. Tissue sections 5–7μm thick were cut using a BRIGHT (model OTF) cryostat, mounted on glass microscope slides (BDH) and fixed in absolute acetone (Fisher Scientific, Loughborough, UK), before storage at –20°C. Before staining, tissue sections were warmed to room temperature, re–fixed in absolute acetone for 5min and a line around the tissue section was drawn, creating as such a small well for retaining antibody solutions, using a wax pen (The Binding Site, Birmingham, UK). Immunohistochemical staining was carried out at room temperature in a humidified chamber to prevent evaporation of antibody solutions. Details of the antibodies and buffers used are shown in tables 2.17 – 2.18.

2.8.2 AEC–based Immunohistochemical Staining

Expression of adhesion molecules in human liver tissues was examined by immunohistochemical staining using the AEC substrate kit for peroxidase (Vector Laboratories, Inc, Burlingame, CA). Sections were primarily incubated with 0.3% H_2O_2 (diluted in methanol) for 10 min in order to block endogenous peroxidase activity and then washed in TBS pH 7.4 prior to incubation with 2% horse serum for 20min. Then the tissue sections were incubated with primary antibodies and isotype–matched control antibodies for 30–40 min, washed x2 in TBS pH 7.4 and incubated with secondary antibody (ImmPress Kit) for 30 min. Two washing steps in TBS pH 7.4 were followed, and in the meantime the AEC peroxidase substrate

solution was prepared and applied according to manufacturer's instructions. Finally, sections were counterstained with Haematoxylin (Sigma) for 3 min, rinsed with distilled H_2O, mounted with glass coverslips (SurgiPath, UK) using aqueous Immunomount solution (Thermoscientific, UK) and examined for positive staining using an upright light microscope. Images were captured using a digital camera and image analysis software (Axionvision, Zeiss, Germany).

BUFFERS	CONSTITUENTS
Tris Buffered Saline (TBS) pH 7.4	0.607% (w/v) Trisma Base, 0.81% (w/v) NaCl in dH_2O, pH 7.4 with HCl (all from Sigma-Aldrich)
1x Phosphatase Buffer Saline (PBS) pH 7.4	137mM NaCl, 2.7mM KCl, 10mM phosphate buffer pH 7.4 - equals with 1 tablet (Oxoid, UK) per 100ml

Table 2.17 Buffers used in immunohistochemical staining

MONOCLONAL ANTIBODY	REFERENCE No. (CLONE)	CONCENTRATION	SOURCE
IgG1[1]	11711	20µg/ml	R & D Systems
CD31[1]	9G11	20µg/ml	R & D Systems
MAdCAM-1 (MCA2320) [1]	314G8	20µg/ml	Serotec
ImmPress secondary Ab	-	-	Vector Laboratories
MAdCAM-1[2]	MECA367	100µg/ml	Kind gift from E.Butcher, Stanford, CA
VAP-1[1]	JG2.10	20µg/ml	Kind gift from E.Butcher, Stanford, CA
HERMES-1[1]	9B5	20µg/ml	Kind gift from E.Butcher, Stanford, CA
Anti-rat IgG FITC	-	10µg/ml	Sigma
Alexa anti-fluorescein 488 conjugate	-	10µg/ml	Invitrogen

Table 2.18 Concentration and source of the primary and secondary antibodies used for immunohistochemical staining. Antibodies were used for staining of frozen human liver sections and were diluted in TBS pH 7.4 to the appropriate concentration. [1] Mouse anti-human monoclonal antibodies, [2] rat anti-mouse monoclonal antibodies.

2.8.3 DAB–based Immunohistochemical Staining

The specificity of the MAdCAM-1 antibody that was used for detection in human liver tissues was tested in lymph node sections where MAdCAM-1 is abundantly expressed. The initial steps of the procedure were the same as described in the previous section (2.8.2). During the washing steps after incubation with secondary Ab, the 3,3'-diaminobenzidine tetrahydrochloride (DAB) chromogenic substrate solution (ImmPact™ DAB Diluent, solution 2, and ImmPACT™ DAB chromogen solution 1, Vector Laboratories) was prepared according to manufacturer's instructions. Sections were incubated with the DAB solution for 3min, washed in TBS pH 7.4 x2 and counterstained with haematoxylin for 3min. Following this, sections were washed under running tap water with a final wash with ddH_2O, air dried, dehydrated in ascending ethanol series (70% for 2min, 96% for 2min, absolute ethanol for 2min), cleared in xylene (Surgipath) for 2min and finally mounted in DPX (depex mounting media, Surgipath) under a coverslip. Before viewing slides were left to dry thoroughly.

2.8.4 Immunofluorescent Staining

MAdCAM-1 expression in mouse liver, Peyer's patches, mesenteric lymph nodes and spleen was demonstrated by immunofluorescent staining. Frozen tissue sections were incubated with anti–mouse MAdCAM-1 (MECA 367), VAP-1 (JG2-10) and isotype–matched negative control (9B5) antibodies for 30–40min. Then sections were washed twice in PBS solution and then appropriate FITC–conjugated second stage anti–rat FITC antibodies diluted in 5% (v/v) mouse serum were used. For enhanced signal generation, Alexa anti fluorescein/Oregon (green goat IgG fraction, Alexa Fluor 488 conjugate, Invitrogen) was also used (Table 2.18). At the end, sections were washed in PBS and mounted using VECTASHIELD mounting media (Vector

Laboratories) to preserve fluorescence. Images were obtained using an Olympus Bx60 microscope (Olympus Optical, Hamburg, Germany) equipped with UPlanFI 20x /0.50 numeric aperture (NA) Ph1. Images were acquired using a ColorView 12 camera (Olympus Soft Imaging Solutions, Munster, Germany).

2.9 Flow Cytometry

2.9.1 Single Colour Flow Cytometry

CHO cells transfected with a FL–MAdCAM-1 construct and the CHO parental cell line that did not express MAdCAM-1, were used for validation of antibody specificity and the ability of trypsin to cleave membrane bound proteins from the cell surface. CHO cells cultured on gelatin coated flasks, were either trypsinised or detached using a non–enzymatic cell dissociation solution (Sigma-Aldrich) and pelleted after centrifugation. The pellet was re–suspended in wash buffer and mouse anti–human MAdCAM-1 Ab conjugated to FITC (CA2320F) was applied. Control samples were labelled with isotype–matched control IgG1 Ab conjugated to FITC.

For detection of intracellular versus extracellular MAdCAM-1 on adherent HSEC, the non–enzymatic dissociation solution was used. Initially, HSEC were stimulated as previously with TNFα (20ng/ml) or methylamine (50μM) alone or in combination for 2 hours (untreated samples were used as control). Cells were then washed in ice cold PBS, scraped very gently in the presence of non–enzymatic dissociation solution and centrifuged. The cell pellet was re-suspended in wash buffer [PBS containing 10% (v/v) FCS] and surface marker staining was performed using mouse anti–human MAdCAM-1 conjugated to FITC before fixation and

permeabilization of cells with fixation medium (Reagent A) and permeabilization medium (Reagent B) respectively (GAS-003, Caltag Laboratories). Surface marker staining was also carried out for CD31, as a control. Intracellular staining was performed after fixation and permeabilisation with the same Reagents A and B and the same MAdCAM-1 Ab. Control samples were labeled with matched isotype control IgG1 conjugated to FITC. All samples were run on a Cyan flow cytometer and results were analysed using Summit Software (Dako Cytomation).

Occasionally, Brefeldin A from *penicillium brefeldianum*, (≥99% Sigma) was used in order to disrupt the structure and function of the Golgi apparatus to prevent the transfer of new synthesised proteins from the cytoplasm to membrane. Cells were incubated for 2 hours in complete media supplemented with Brefeldin A (BFA at 1μg/ml) and then stimulated with TNFα or methylamine as previously. Control samples did not receive BFA treatment. Surface and internal labelling was performed as previously referred.

Single color flow cytometry was also used to detect VAP-1 in adherent HSEC that had been transfected with hVAP-1 adenoviral constructs. In this case cells were detached with enzymatic dissociation solution (TrypLE or Trypsin). Staining was performed with mouse anti–human VAP-1 antibody (TK8–14 FITC conjugated), and control samples were labeled with matched isotype control (3G6 and IgG1 FITC) conjugated antibodies.

ANTIBODY (FITC conjugated)	CLONE	CONCENTRATION	SOURCE
MAdCAM-1	314G8 (CA2320F)	10µg/ml	Serotec
IgG1	DAK-G01	10µg/ml	Dako
CD31	WM59	10µg/ml	BD Pharmingen
VAP-1	TK8-14	10µg/ml	MediCity, Turku
Anti- chicken T cell protein (negative control)	FU7-3G6	10µg/ml	Microbiol V. Vainio, MediCity, Turku

Table 2.19 Clone name, source and concentration of antibodies used for single colour flow cytometry

2.10 FLOW BASED ADHESION ASSAY

A flow based adhesion system was developed in order to assess the functional role of MAdCAM-1 under conditions comparable to those seen *in vivo*.

2.10.1 Microslide Preparation

Glass microslides obtained from Gamlab Ltd, Cambridge, UK, are 5cm long capillary tubes that have a rectangular cross section of 0.3 x 0.03cm (Figure 2.1A). They have good optical qualities and support laminar flow of perfused fluids. Before use in flow based adhesion assays, microslides were treated with 3–aminopropyltriethoxysilane (APES; Sigma-Aldrich), to aid cell attachment. Here, microslides were washed in 70% v/v nitric acid (Sigma-Aldrich) overnight and then washed with copious volumes of tap water finishing with a wash in distilled water for removing all traces of acid. Microslides were blotted dry, washed thoroughly in several changes of anhydrous acetone to remove any residual water and then submerged in APES solution [4% (v/v) in anhydrous acetone] for 10–15 min. The slides were then rinsed in 2–3 changes of anhydrous acetone with a final wash in distilled water to remove all traces of acetone. Finally,

microslides were left to dry overnight in the glass oven at 60°C. Before use, silicone adaptor tubing (Portex Ltd, Kent UK) was securely attached to one end of the microslides (Figure 2.1 B), which were then autoclaved prior to use in cell–based adhesion assays.

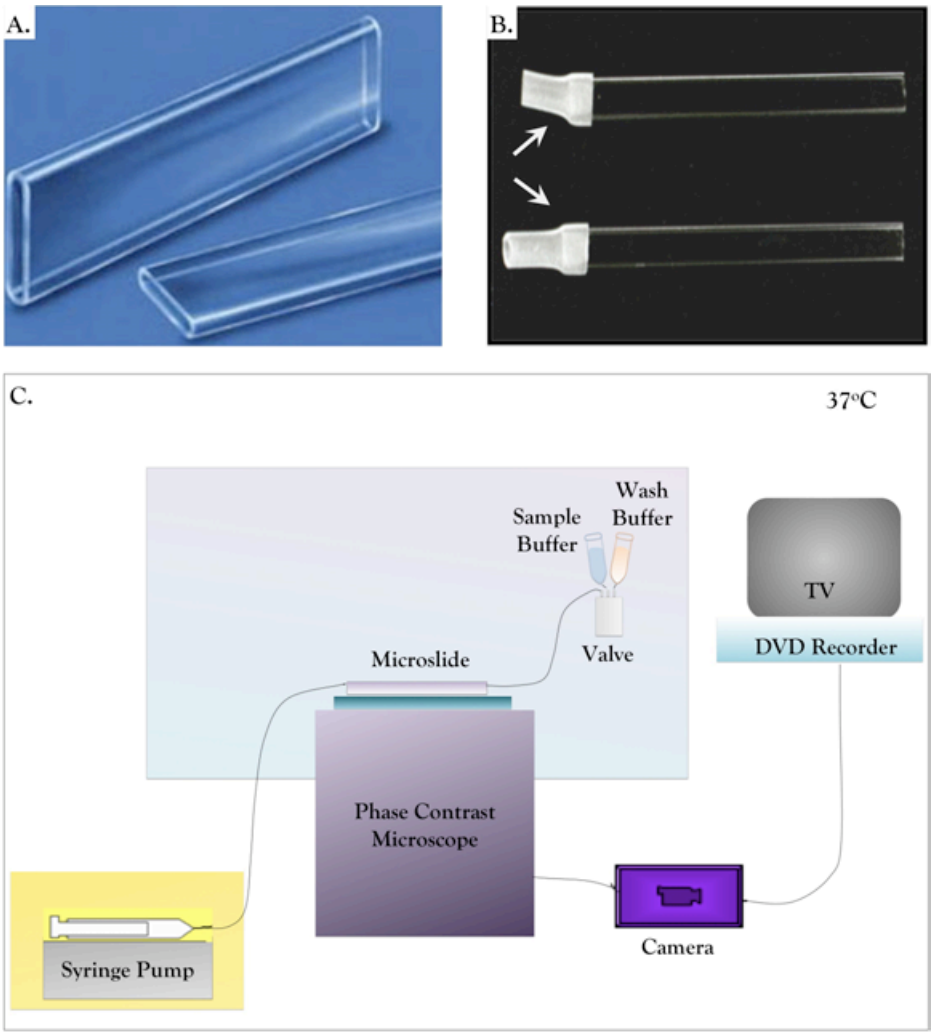

Figure 2.1 The flow based adhesion assay. (A) Glass microslides, 5cm long capillary tubes with a rectangular cross section of 0.3 x 0.03cm with good optical qualities were used for supporting laminar flow of perfused fluids. Before use, silicone adaptor tubing (B) was attached to one end to aid the uptake of fluids and connection to the culture dish. (C) For the flow based adhesion assay to occur the microslides with the treated endothelial monolayers were glued onto a glass microscope slide and placed on the stage of heated videomicroscope. One end of microslide was connected to a syringe pump and the other on an electronic switching valve allowing the flow of cells or wash buffer. Lymphocytes were perfused over the microslides at a constant shear stress of 0.05Pa. Video clips were recorded and experiments were analysed offline.

2.10.2 Preparation of Endothelial Cell Monolayers

To ensure good adhesion of endothelial cells to the slides, APES coated microslides were pre–coated with 1% gelatin (when HUVEC were seeded) or rat–tail collagen (when HSEC were seeded). Endothelial cells from one confluent T75 were trypsinised and used for seeding 6 microslides ($3x10^6$ cells per microslide). After seeding, ECs were incubated at 37°C in a humidified 5% CO_2 incubator for approximately 2–3 hours until cells had formed a confluent monolayer. Then microslides containing confluent monolayers of endothelial cells were connected to a culture dish, which was filled with 40ml of complete media. The culture dish was then connected to a pump to permit automatic changing of media in the tubes every two hours. The following day, microslides were disconnected from the dish, and the cells were treated with TNFα and methylamine for 2 hours prior to the flow based adhesion assay.

Occasionally, HSEC were seeded in microslides as previously described and the cell monolayers were infected with a viral construct containing full–length MAdCAM-1 protein (FL–MAd–GFP–Adenovirus) or empty vector, at a concentration previously determined to induce maximal gene expression and minimal cell damage (MOI of 10) (Miles et al., 2008). The transfected monolayers were then incubated for 24 hours or 48 hours prior to flow based adhesion assays to permit induction of protein expression. Occasionally, purified human recombinant chemokines (CCL25, CCL28, CCL21 and CXCL12; at 10μg/ml, PeproTech, London, UK) were immobilised on the HSEC monolayer transduced with FL–MAdCAM-1 for 30min before lymphocyte perfusion, in order to examine the effects of different chemokines on lymphocyte adhesion to MAdCAM-1.

2.10.3 Preparation of CHO Cell Monolayers in Microslides

APES coated microslides were pre–coated with fibronectin (50μg/ml; Sigma-Aldrich) for 2 hours at 37°C. Any excess of fibronectin was removed with PBS and CHO cells transfected with FL–MAdCAM-1 were seeded and incubated at 37°C in a humidified 5% CO_2 incubator for 2–3 hours until cells had formed a confluent monolayer.

2.10.4 Preparation of the JY Cell Line

The JY cell line, which expresses α4β7, was cultured in RPMI (Invitrogen) supplemented with 10% (v/v) FCS. Cells were maintained in suspension in T75 flasks. Prior to the flow based adhesion assay, JY cells were centrifuged at 550g for 5min. The pellet was resuspended in 1ml of RPMI+10% (v/v) FCS and a small aliquot was removed for cell number counting and viability assessment with trypan–blue exclusion. After counting, the remaining cells were resuspended to 10^6 cells/ml in complete basal endothelial medium (SFM; Gibco, Invitrogen) + 0.1% (v/v) BSA (Sigma).

2.10.5 Preparation of Peripheral Blood Lymphocytes (PBL)

PBL were isolated as indicated in section 2.15. Prior to the flow based adhesion assay PBL were collected, centrifuged and pelleted, had their viability confirmed, and were resuspended to 10^6 cells/ml in SFM + 0.1% (v/v) BSA as in 2.10.4.

2.10.6 The Flow-based Adhesion Assay

After the treatment of endothelial monolayers with TNFα and/or methylamine for 2 hours, microslides were glued to a glass microscope slide and placed on the stage of a thermostatically

controlled videomicroscope (Figure 2.1C). The microslides were attached via silicon rubber tubing (2mm diameter; Fisher Scientific) to a Harvard pump (Harvard Apparatus, South Natic, USA) to permit perfusion of cells or cell–free buffer (wash buffer) through the microslide at a constant flow rate of 0.05Pa. An electronic valve (Lee products, UK) allowed rapid alteration between wash buffer [SFM plus 0.1% (v/v) BSA or HAMsF10 for CHO cells], and a lymphocyte or cell line suspension. JY or PBL suspensions were perfused over the endothelial monolayers at a constant shear stress of 0.05Pa for 5min, then wash buffer was perfused over for 1min before lymphocyte adhesion was analysed. Adherent lymphocytes that were captured via molecular interactions with the functionally expressed MAdCAM1 on the stimulated HSEC, or in chemokine stimulated HSEC transduced to express MAdCAM-1, were visualised by phase contrast microscopy (x10 magnification), and video clips were recorded of a minimum of 10 fields along the length of microslide, for offline analysis. Adherent cells were classified as rolling, static and activated/migrated cells. Total cell adhesion was determined by counting all visible adherent cells in a number of fields of known dimension, then converted to give a value of adhesion/mm^2 and normalised according to the number of lymphocytes perfused. Static adhesion was either expressed as adhesion/$mm^2/10^6$ cells perfused or percentage of total adhesion, as indicated. Migration of cells was also expressed as migration/$mm^2/10^6$ cells perfused or percentage of total migration.

2.10.7 Adhesion Molecule Blockade and Pertussis Toxin Treatment

In order to confirm that lymphocyte adhesion to stimulated HSEC was MAdCAM-1 specific, endothelial monolayers were treated with a function–blocking antibody against MAdCAM-1 (humanised anti–human P1 Ab, for 30 min at 37°C) prior to perfusion of lymphocytes.

Moreover, JY cells were incubated with a blocking antibody directed against α4β7 integrin, (ACT-1). An isotype–matched antibody (IgG1) was used as negative control at equivalent concentration. In order to determine that the chemokine effects were mediated via specific G–protein mediated signalling, PBL were incubated with 200ng/ml pertussis toxin (a G_a protein inhibitor) (PTX; Sigma-Aldrich), for 30 min at 37°C, prior to perfusion over the MAdCAM-1 transduced hepatic endothelial cells.

ANTIBODY	FINAL CONCENTRATION	SOURCE
P1	10ng/ml	Pfizer
ACT-1	50ng/ml	Kind gift from M.Briskin, Millenium, USA
IgG1	10ng/ml	Dako

Table 2.20 Function-blocking antibodies used in flow based adhesion assay

2.11 CELL BASED ELISA

HSEC and HUVEC were grown to confluency on collagen coated 96–well ELISA plates (Microtest Tissue Culture Plate, BD Bioscience UK). Before ELISA development, cells were stimulated with TNFα (20ng/ml; PeproTeck, UK), rVAP-1 (100ng/ml, gift from Biotie Therapies, Turku, Finland) and the amines methylamine and benzylamine (25–200μM; both from Sigma-Aldrich) alone or in combination with TNFα or rVAP-1 for 2–48hours. After the end of the incubation period, cells were fixed with methanol. Non–specific binding of antibodies was prevented by pre–incubation of cells with 5% goat serum (Sigma) for at least 45 min. Endothelial cells were then incubated with anti–human primary antibodies (ICAM-1, VCAM-1, CD31, IgG1 or MAdCAM1) for 45min. After washing, cells were incubated either with a peroxidase conjugated goat anti–mouse secondary antibody or streptavidin conjugated

anti–mouse antibody for 45min. OPD tablets from Dako or Sigma (Sigma Fast™ OPD) were used to visualise antibody binding. The ELISA substrate was used according to manufacturer's instructions and the absorbance values were determined at 490nm and 450nm respectively. All treatments were performed in triplicate for each experiment.

ANTIBODY	FINAL CONCENTRATION	SOURCE
ICAM-1	2µg/ml	R & D Systems
VCAM-1	2µg/ml	R & D Systems
CD31	5µg/ml	BD Cytomation
MAdCAM-1	5µg/ml	Pfizer
IgG1	5µg/ml	Dako
Goat anti-mouse HRP (GAM-HRP)	1:3000	Dako
Streptavidin conjugated anti-mouse HRP	1:3000	Serotec

Table 2.21 Concentrations and sources of antibodies used for detection of adhesion molecule expression with ELISA

2.12 METHYLATION ANALYSIS

2.12.1 Overview of Methylation Analysis

DNA methylation is an epigenetic event that affects cell function by altering gene expression. The majority of DNA methylation occurs at CpG islands typically found in or near promoter regions of housekeeping genes. Many techniques have been developed for determination of DNA methylation including high–performance capillary electrophoresis (Fraga et al., 2000), and methylation–sensitive arbitrarily primed PCR (Gonzalgo and Jones, 1997). However, the most common technique used today remains the bisulfite conversion method (Frommer et al., 1992) (EZ DNA Methylation–Direct™ Kit, ZymoResearch). This method consists of treating

DNA with sodium bisulfite, which converts the unmethylated cytosine bases to uracil while the methylated cytosines remain unaffected. The bisulfite–modified DNA is then amplified by PCR and the resulting PCR products are analysed either by DNA sequencing or by restriction endonuclease digestion. In the present study, PCR products were analysed by DNA sequencing (Figure 2.2).

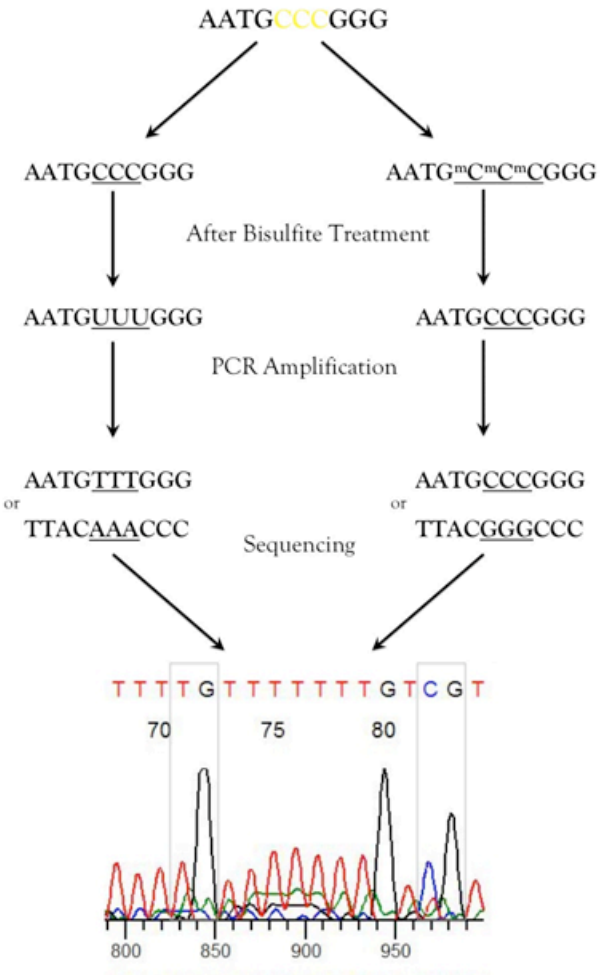

Figure 2.2 Schematic illustration of the bisulfite conversion method, a technique for determining DNA methylation. An example of DNA sequence containing CpG islands is shown (on top). After bisulfite treatment unmethylated cytosines (C) are converted into uracils (U) whereas methylated cytosines (^{m}C) remain the same. After further amplification and sequencing of bisulfite modified products all unmethylated cytosines are measured as the relative content of T at the CpG sites (or A dependent on which sequence the primer is complementary to), and all methylated cytosines, ^{m}C, are measured as the relative content of C (or G) at the CpG sites.

2.12.2 Bisulfite Treatment of DNA

HSEC and HUVEC were treated with stimulating agents as before for 2 hours. Then, cells were counted and up to $2x10^3$ cells (to ensure optimal and complete bisulfite conversion) were collected for digestion with proteinase K and release of DNA according to the EZ DNA methylation–Direct™ Kit from ZymoResearch. The released DNA was then treated with sodium bisulfite and the eluted bis–DNA was amplified with forward and reverse primers (see below) specific for not annealing to any of the CpG islands examined. Primers were designed using the MethylPrimer Express® Software, provided online from Applied Biosystems. After electrophoresis of the PCR products in a 1.5% (w/v) agarose gel the bis–DNA bands were extracted from the gel and purified according to the instructions of the QIAquick gel extraction kit (Qiagen, UK). After elution of purified bis–DNA and prior to sequencing, the purified products were electrophorised again in a 1.5% (w/v) agarose gel.

PRIMERS	MADCAM-1
methForward	5'- GTG TTT GAA TAT GAG GTT TGG A-3'
methReverse	5'- AAT CCA TAG TCA ATC CCC TCT A-3'
Amplicon Length: 258bp	

Table 2.22 Primers specifically designed to anneal with bisulfite converted DNA, amplifying MAdCAM-1 gene replacing the uracils with thymines

REAGENTS	FINAL CONCENTRATION	SOURCE
10x PCR Cold Buffer	1x	Applied Biosystems
$MgCl_2$	1.5mM	Applied Biosystems
dNTPs	0.2mM(total)	Roche
methF+R primers	0.32pmole/µl (total)	Alta Bioscience
AmpliTaq Gold Hot Start Polymerase	1.25U	Applied Biosystems
bis-DNA	2-10µl from purified bis-DNA	Human primary endothelial cells

Table 2.23 Constituents of PCR reaction mix

NUMBER OF CYCLES: 40	TEMPERATURE (°C)	TIME (sec)
	95	05:00
Denaturation	94	00:30
Annealing	55	00:45
Extension	72	00:45
	72	10:00

Table 2.24 Thermal profile for amplification of bisulfite treated DNA

2.12.3 Sequencing

In order to determine the methylation profile of the untreated versus TNFα, methylamine and TNFα plus methylamine treated cells, sequencing was carried out according to standard protocols in the Genomics Laboratory of Biosciences Department in the University of Birmingham.

SEQUENCING	
CONSTITUENTS	FINAL CONCENTRATION
Purified bis-DNA	1μg/ml
methForward primer	3.2μM
sterile ddH_2O	adjust
Total Volume	10μl

Table 2.25 Constituents of sequencing reaction

TEMPERATURE (°C)	TIME (sec)
NUMBER OF CYCLES: 25	
96	00:10
50	00:50
60	04:00

Table 2.26 Thermal profile of sequencing reaction

2.12.4 Methylation Analysis

The CpG islands that were assayed were identified by the MethylPrimer Express® Software which performs *in-silico* bisulfite conversion. After sequencing, alignment between the bisulfite converted and sequenced products and the non–methylated MAdCAM-1 sequence as given by GenBank was performed, using the Sequence Scanner software (Applied Biosystems). The average of methylated cytosines/non–methylated cytosines (^{m}C/C) ratio observed was then calculated in order to give the methylation index (MtI).

2.13 MOUSE MODELS

Wild-type mice (WT), VAP-1 deficient mice that lack mouse VAP-1 (VAP-1_KO) (C57BL background), and VAP-1 transgenic animals, specifically VAP-1 deficient mice that contain

enzymatically active hVAP-1 as a transgene (VAP-1_EA) and VAP-1 deficient mice that contain enzymatically inactive hVAP-1 as a transgene (VAP-1_EI), expressing human VAP-1 on the endothelial cells under the control of the mouse Tie-1 promoter, as previously described (Stolen et al., 2005), were used in the MediCity Laboratory in Turku for determination of the role of methylamine in MAdCAM-1 expression *in vivo*.

2.13.1 VAP-1 Dependent Signalling In Vivo

Methylamine [0.4% (w/v)], a VAP-1 substrate, was administered in the drinking water of the above animals for 14 days. After sacrifice, tissue samples from liver, kidney, spleen, mesenteric lymph nodes and Peyer's patches were excised. Parts of the same tissue were snap–frozen, lysed for extraction of protein and RNA (see sections 2.5.1, 2.7.1.3 and 2.8.4).

2.14 Adenoviral Infection of Human HSEC With VAP-1 Constructs

2.14.1 Determination of The Enzymatic Activity of VAP-1 Constructs by the AMPLEX Ultra Red Method

HSEC were seeded in a 24–well plate and cultured until confluency. Then, cells in each row were transfected with viral constructs containing hVAP-1 enzymatically active, hVAP-1 enzymatically inactive, or adenoviral constructs without any VAP-1 (LacZ only). Non–transfected cells were used as an additional control. The adenoviral transfection process is described below (paragraph 2.14.2).

The AMPLEX Red assay is based upon detection of H_2O_2 released by the enzymatic activity of VAP-1. More precisely, the reaction between VAP-1 and its substrate, *i.e.* benzylamine, results in

the production of H_2O_2, ammonia and aldehyde. Firstly, transfected and non–transfected cells were treated with a mixture of PBS plus benzylamine (2mM, Sigma), clorgyline and pargyline (both at 200μM, Sigma). Clorgyline and pargyline are inhibitors of monoamine oxidases type A and B respectively (MAO–A and MAO–B) and they are used in order to block the enzymatic activity of other amine oxidases (*i.e.* not VAP-1) that would lead to false positive results. Similarly, to ensure the specificity of the reaction, 5' bromoethylamine (specific VAP-1 inhibitor) (BEA, at 400μM) was added to some wells (with PBS plus pargyline, clorgyline and benzylamine). Next the AMPLEX Red reagent was added, which is consisted of 1/100 Amplex Red Ultra (20mM stock; Invitrogen) and 1/100 HRP (200U/ml stock, Invitrogen). In the presence of HRP, the Amplex Red reagent (10–acetyl-3, 7–dihydroxyphenoxazine) reacts with H_2O_2 with a 1:1 stoichiometry resulting in the production of a red fluorescent product, which can be detected in a fluorescent plate reader detecting for 3 hours, as it is a kinetic reaction.

2.14.2 Adenoviral Transfection of Human HSEC

Adenoviral constructs encoding wild-type hVAP-1 and enzymatically inactive hVAP-1 (Y471F) have been previously described (Koskinen et al., 2004). HSEC were plated in T25 tissue culture flasks and cultured until confluency. Before transfection, complete medium containing human serum was removed, cells were washed in PBS, to ensure complete removal of any human serum present, and fresh EBM–2 media (Clonetcis, Lonza) supplemented with 10% (v/v) FCS was added for at least one hour before adenoviral transfection. Meanwhile the number of cells per T25 flask was counted according to the mathematical formulae represented below (Table 2.27). The medium was discarded, cells were washed again and finally adenoviral transfection at a multiplicity of infection of 600 occurred for 4 hours. After the 4 hour transfection period the

adenoviral transfected cells were washed, fresh HSEC media was added (see paragraph 2.3.2) and cells were incubated overnight at 37°C in a humidified atmosphere containing 5% CO_2. The following day, transfected cells were stimulated with TNFα or methylamine as previously described for 2 hours, in SFM basal endothelial medium containing 2.5% (v/v) HIHS without any growth factors. Finally, RNA and protein lysates were extracted and single–color flow cytometry was performed for detection of hVAP-1 positivity. Table 2.28 describes the adenoviral constructs used in the experiment.

METHOD 1
N= Average Number of cells from 2 fields x 931 x 2.6 • cells were counted using a 100 squared gridlined microscope lense. • 931: multiplicity factor when cells counted at 10x magnification. • 2.6: multiplicity factor for cells cultured on a surface of T25 flask.
METHOD 2
$N = \frac{\text{Average number of cells from 2 fields x } 100\text{cm}^2 \text{ x } 25}{0.1496}$ • cells counted in a field of 0.1496mm^2 at x10 magnification.

Table 2.27 Methods used for calculation of number of cells/T25 flask. Method 1 was used in the MediCity Laboratory, in Turku and method 2 in the Centre for Liver Research, in Birmingham.

ADENOVIRAL CONSTRUCTS	CONCENTRATION (PFU/ML)	LOT NUMBER
Padre hVAP-1	1.4 x 10^{10}	842
hVAP-1_Y471F	4.8 x 10^{10}	493
hVAP-1_Y471F	2.6 x 10^{10}	1025
LacZ	4.2 x 10^{10}	950

Table 2.28 Adenoviral constructs used for HSEC transfection

2.15 Isolation and Culture of Human Peripheral Blood Lymphocytes (PBL)

Peripheral venous blood was collected into EDTA and the mononuclear fraction was isolated by density gradient centrifugation over Lymphoprep (Sigma-Aldrich) according to manufacturer's instructions. Contaminating monocytes were depleted by adhesion to tissue culture plastic for 30min, and the lymphocyte–rich supernatant was transferred to a fresh tissue culture flask containing RPMI–1640 media (Invitrogen) supplemented with streptomycin, 2mM glutamine and 10% (v/v) FCS, and rested overnight at 37°C in a humidified incubator containing 5% CO_2. The following day, cells were counted, and resuspended to a concentration of 10^6 cells/ml, in basal endothelial medium containing 0.1% (v/v) bovine serum albumin (BSA) (Sigma).

2.16 Statistical Analysis

Data were analysed using Student's *t*–test when comparing numerical variables between two groups, and one–way ANOVA analysis followed by Bonferroni's post test for between more than two groups comparisons. Statistical analysis was performed using the GraphPad Prism software. A value of $P \leq 0.05$ is considered statistically significant. Generally statistical data are expressed as follows: *≤0.05, **≤0.01, ***≤0.001.

CHAPTER 3

Expression of Madcam-1 In Human Liver Tissues

3.1 INTRODUCTION

Human MAdCAM-1 is an endothelial adhesion molecule particularly expressed in high endothelial venules of Peyer's patches, in flat–walled venules of the lamina propria and in other gut associated lymphoid tissues including appendix and mesenteric lymph nodes (Streeter et al., 1988)(M. Briskin et al., 1997). In intestinal inflammation elevated levels of MAdCAM-1 have been reported, and more particularly in the inflammatory bowel disease (IBD), Crohn's disease (CrD) and ulcerative colitis (UC), where its over–expression has been suggested to be important for the establishment of chronic bowel inflammation via the sustained recruitment of circulating α4β7+ lymphocytes (Eksteen et al., 2004b).

IBD is an idiopathic inflammatory disorder of the gastrointestinal tract, the aetiology of which still remains elusive, although both genetic and environmental factors have been linked to this disorder (Shih et al., 2008). A common characteristic of both CrD and UC is a massive influx of destructive inflammatory cells into the gut. Pro–inflammatory cytokines are highly up–regulated during IBD which lead to increased expression of vascular adhesion molecules that promote sustained leukocyte recruitment and lead to chronic inflammation and symptomatic disease (Koizumi et al., 1992). The up–regulation of MAdCAM-1 during gut inflammation has been suggested to be responsible for the sustained recruitment of circulating α4β7+ lymphocytes and as such for the establishment of bowel inflammation (Eksteen et al., 2004b).

Interestingly, Hillan *et al.* were the first to report expression of MAdCAM-1 in tissues where previously none had been detected (Hillan et al., 1999). In this study MAdCAM-1 expression was observed in adult human liver in association with portal tract inflammation in a variety of

liver diseases. Subsequently, strong expression of MAdCAM-1 protein on hepatic endothelium was demonstrated by our group, in the context of chronic inflammation. Using tissue–binding assays, it was shown that MAdCAM-1 on liver endothelium could support the adhesion of α4β7+ lymphocytes (Grant et al., 2001). This ectopic expression of a molecule previously thought to have a more restricted localisation, parallels recent observations relating to the chemokine CCL25. Expression of CCL25 was considered restricted to the small intestine and thymus (Kunkel et al., 2000)(Kunkel et al., 2003a), but expression has also been reported in the liver of patients with PSC, an autoimmune liver disease which is frequently an extra–intestinal complication of IBD (Eksteen et al., 2004a). Here CCL25 was responsible for the recruitment of mucosal lymphocytes that express α4β7 integrin and the CCL25 receptor, CCR9 (Figure 3.1). Therefore, in the current chapter, expression of MAdCAM-1 in human liver tissues at the protein and mRNA levels, as well as co–localisation of MAdCAM-1 with CCL25 in human liver, were studied.

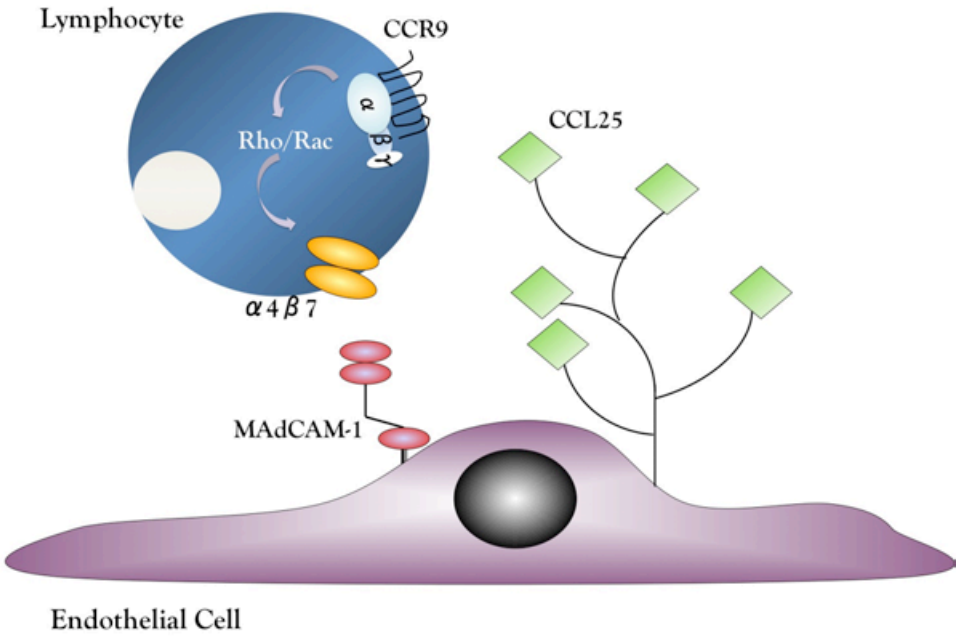

Figure 3.1 Alpha4 beta7 integrin activation by CCL25/CCR9 interaction. Recruitment of lymphocytes in the gut requires not only the MAdCAM-1/α4β7 integrin interaction but also a chemokine signal provided by CCL25. CCL25 is selectively expressed in the thymus and small intestine but not in the colon. The only known receptor for CCL25 is CCR9, which is highly expressed on developing thymocytes, small intestinal lamina propria lymphocytes and intraepithelial lymphocytes. CCL25 presented by glycosaminoglycans on the endothelial surface interacts with CCR9 on the leukocyte surface leading to activation of the Rho/Rac intracellular signalling pathways, which in turn induce conformational changes in the α4β7 integrin. The activated integrin is then able to bind to MAdCAM-1 with high affinity.

3.2 RESULTS

3.2.1 MAdCAM-1 Protein and mRNA Expression In Human Liver Tissues

The efficacy of our immunohistochemical technique and the specificity of the antibodies used were validated by staining human liver and lymph node tissues for CD31, MAdCAM-1 and LYVE-1 respectively. Figure 3.2 shows that CD31 antibody stained the endothelial cells of central veins, small vessels and hepatic sinusoidal endothelial cells in both diseased and normal livers. It was apparent that in diseased liver CD31 expression levels were higher than in normal liver where it was faintly expressed (Figure 3.2A and 3.2B). As expected, MAdCAM-1 staining of high endothelial venules in lymph nodes (Figure 3.2D) and LYVE-1 expression on lymphatic endothelial cells, was also demonstrated (Figure 3.2E).

Immunohistochemical detection of MAdCAM-1 in human liver samples, revealed an inconsistent pattern of expression. In all of the diseased livers tested (3AIH, 3ALD, 3PBC, 3PSC), MAdCAM-1 was detected on the endothelial cell lining of central veins and small vessels (Figure 3.3B–E). Of note, not all vessels in a particular tissue section stained positive, showing a patchy distribution of MAdCAM-1 protein. In only 1/3 NL samples tested there was faint staining for MAdCAM-1 in hepatic sinusoidal endothelial cells (Figure 3.3A). Occasionally, MAdCAM-1 expression was seen in structures inside the hepatocyte cytoplasm (Figure 3.4A), as well as in structures that had the morphology of dendritic cells (Figure 3.4B, 3.4D & 3.4E). Moreover, in some cases a brownish smear was stained, which could represent soluble MAdCAM-1 in the stroma matrix (Figure 3.4C). In all cases the isotype–matched control antibody used displayed no reactivity.

The presence of MAdCAM-1 protein in the same liver tissues was confirmed by immunoprecipitation, which revealed the existence of MAdCAM-1 in all of the livers tested. Weak bands were detected in three normal tissues and MAdCAM-1 levels were increased in PSC livers although variation in the levels of expression was apparent (Figure 3.5). When the order of the antibodies used for immunoprecipitation (IP) (*i.e.* using the polyclonal for IP and the monoclonal for detection) was reversed, much higher levels of MAdCAM-1 protein in the same normal livers were detected. For this reason, it was tested whether the folding of MAdCAM-1 protein in normal livers is such that the monoclonal antibody cannot easily detect its specific epitope. Western blotting of the unbound protein in the supernatant from immunoprecipitated samples with the polyclonal anti–MAdCAM-1 Ab (H–116) revealed the presence of high levels of MAdCAM-1 protein. After stripping the same membrane and re–probing with the monoclonal Ab that was used during IP, no MAdCAM-1 was detected (Figure 3.6), which confirmed that MAdCAM-1 protein in normal liver tissues may have a structural conformation that is not recognised by the monoclonal antibody.

Immunoprecipitation and western blotting of additional different liver tissues (ALD, PBC, PSC, AIH and NL livers) again confirmed MAdCAM-1 protein expression (Figure 3.7). Intriguingly, the chemokine CCL25 had previously been detected in the same samples (unpublished data from Dr. C. Weston, Centre for Liver Research). Analysis of the MAdCAM-1 mRNA in all the above liver tissues, revealed higher mRNA levels in the diseased livers relative to the normal livers (*$^{**}P<0.01$, $^{**}P<0.001$) (Figure 3.8A), with statistically significant higher expression in AIH (*$^{*}P<0.05$) and PSC (*$^{**}P<0.01$) liver tissues (Figure 3.8B). As an extra

confirmatory step we verified the identity of the bands attributed to MAdCAM-1 in the normal liver samples by sequencing (Figure3.9).

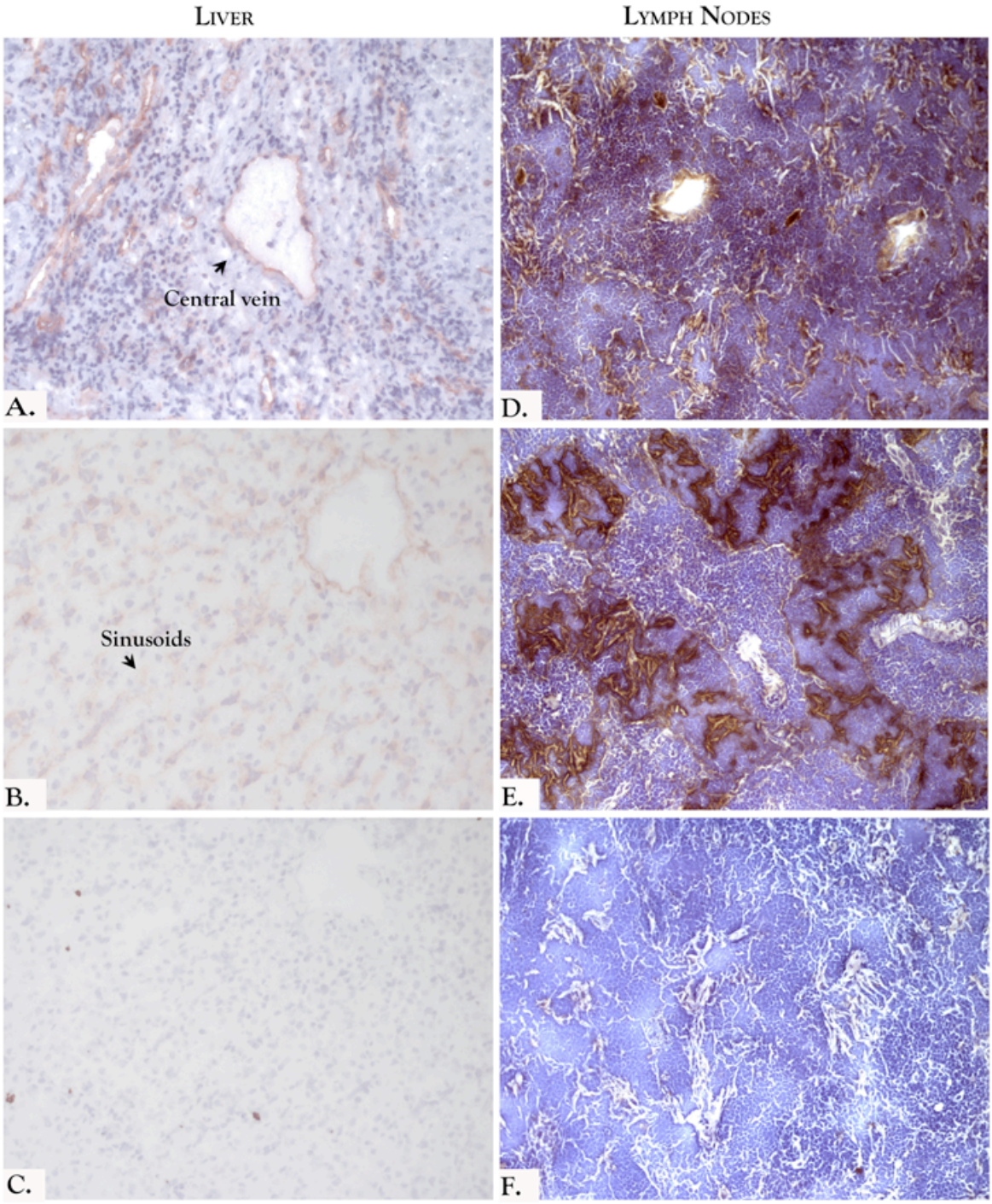

Figure 3.2 Expression of phenotypic markers in human liver and lymph nodes. Immunohistochemical staining for the CD31 endothelial marker in human (A) PBC and (B) normal liver. (D) MAdCAM-1 and (E) LYVE-1 expression in human lymph nodes. Staining with isotype–matched control antibodies is also shown (C and F). Fields were captured using 20x objectives resolution.

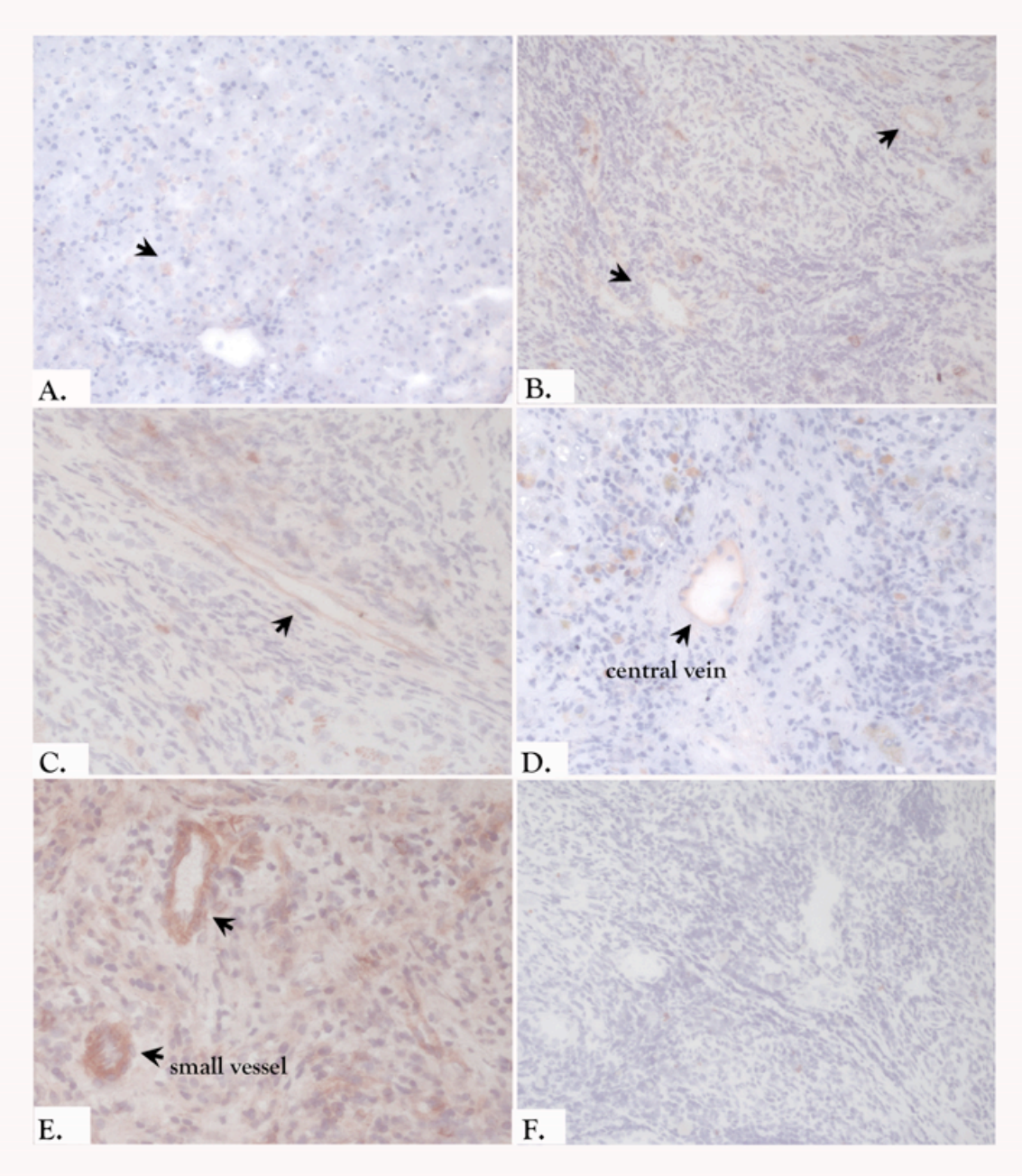

Figure 3.3 MAdCAM-1 expression in human liver tissues. Immunohistochemical staining for MAdCAM-1 in (A) sinusoidal endothelium of normal liver, (B) in small vessels of PBC, (C) and (D) in central vein of AIH and PSC respectively and in (E) central vein and small vessel in ALD. (F) Representative image of isotype–matched control stained tissue. Images are representative from staining of sections from 3 different livers of each disease/group. Fields were captured using 20x objectives resolution.

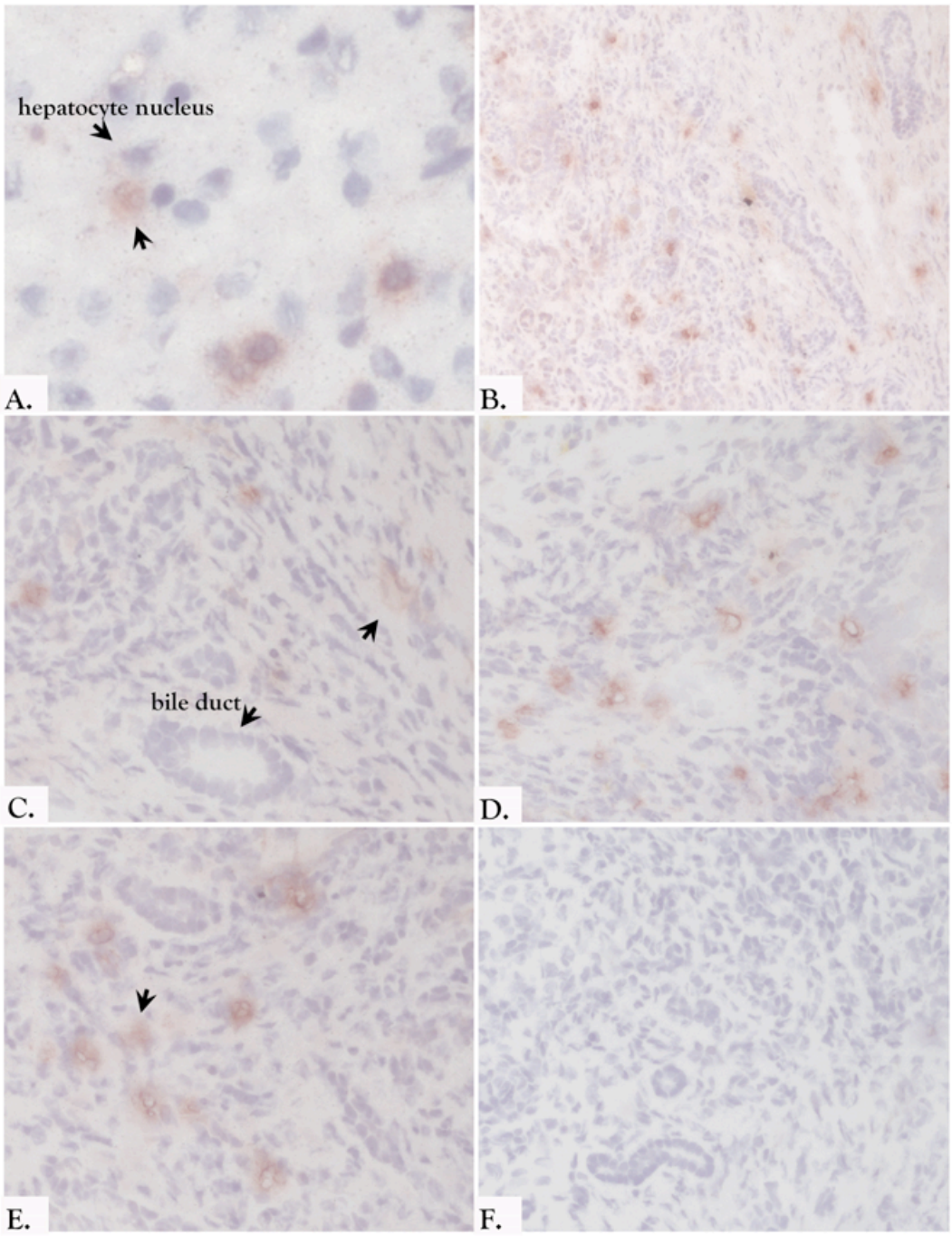

Figure 3.4 MAdCAM-1 expression in human liver tissues. Immunohistochemical staining for MAdCAM-1 protein in human (A) normal (B) PSC (C) AIH (D) PBC and (E) ALD liver tissues. (A) MAdCAM-1 staining of defined structures in the hepatocyte cytoplasm. (B), (D) and (E) MAdCAM-1 staining of immune cells and (C) a smear of staining suggests the presence of soluble MAdCAM-1. (F) Representative image of isotype–matched control stained tissue. The specificity of MAdCAM-1 staining is indicated by the fact that bile ducts (in B and C) were not stained. Fields were captured using 20x objectives resolution.

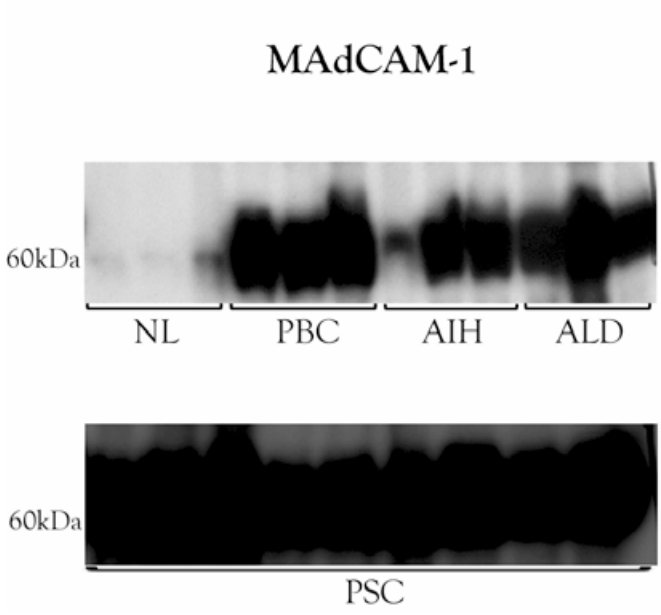

Figure 3.5 MAdCAM-1 protein expression in human liver tissues. MAdCAM-1 protein was detected in immunoprecipitated protein lysates from 3 different NL, PBC, AIH, ALD and 9 different PSC liver tissues. During immunoprecipitation MAdCAM-1 protein was pulled out by monoclonal antibody (CA102.2C1) and then a 60kDa molecular weight protein was detected by western blot using a polyclonal antibody (H-116).

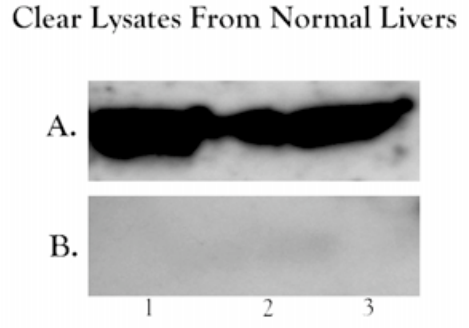

Figure 3.6 MAdCAM-1 protein folds differently in normal livers. (A) MAdCAM-1 protein was detected in the non–beaded samples of 3 normal liver tissues after immunoprecipitation with the monoclonal antibody and detection with the polyclonal Ab. In (B) MAdCAM-1 could not be revealed by the monoclonal Ab after stripping and re–probing the same membrane.

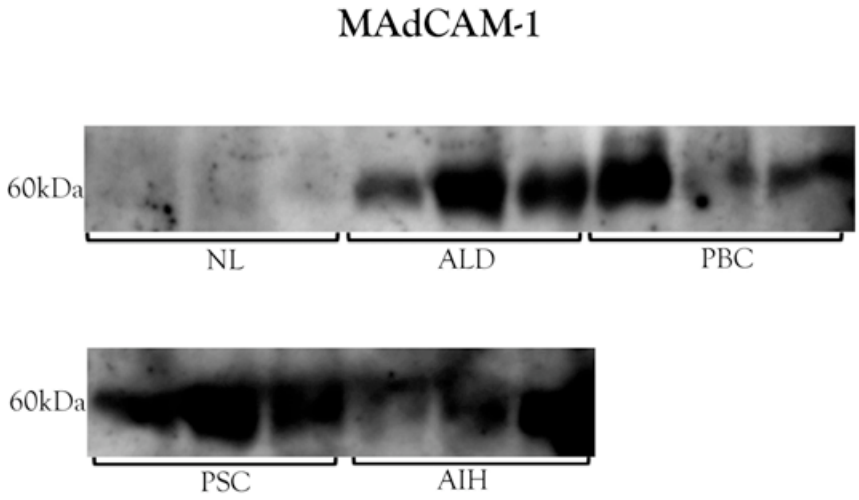

Figure 3.7 Detection of MAdCAM-1 protein in tissue lysates from samples where CCL25 is known to be expressed. Immunoprecipitation of the protein lysates where CCL25 was detected revealed also the expression of MAdCAM-1. During immunoprecipitation MAdCAM-1 was captured with the polyclonal H-116 Ab and then detected by the monoclonal CA102.2C1 Ab.

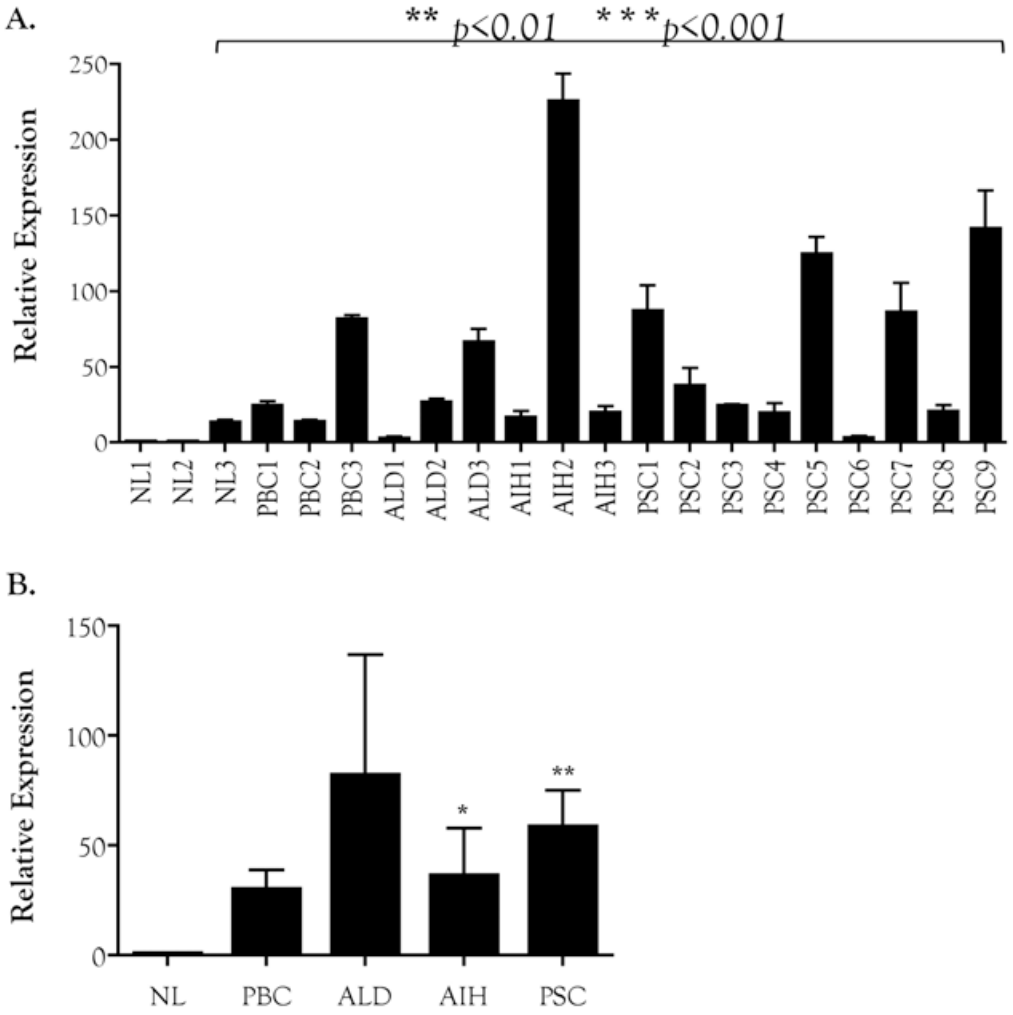

Figure 3.8 MAdCAM-1 mRNA expression in human liver tissues. RNA extracted from fresh human normal (NL), PBC, AIH, ALD and PSC liver tissues, was transcribed into cDNA and used to evaluate MAdCAM-1 transcripts by quantitative PCR. (A) Data represent relative expression levels (mean ± SD) from n=9 PSCs and n=3 of all other diseased and normal livers. The y–axis shows the N–fold change of MAdCAM-1 mRNA expression in each liver relatively to one normal liver (NL1). (B) Overall MAdCAM-1 mRNA expression in diseased livers relatively to normal liver tissues. In panel (A) statistical analysis performed by Student's t-test revealed significance in all samples (**P<0.01, ***P<0.001*) with exception of NL2, ALD1 and PSC6 samples. In panel (B) Student's t-test also revealed significance in AIH and PSC liver tissues (**P<0.05, **P<0.01*).

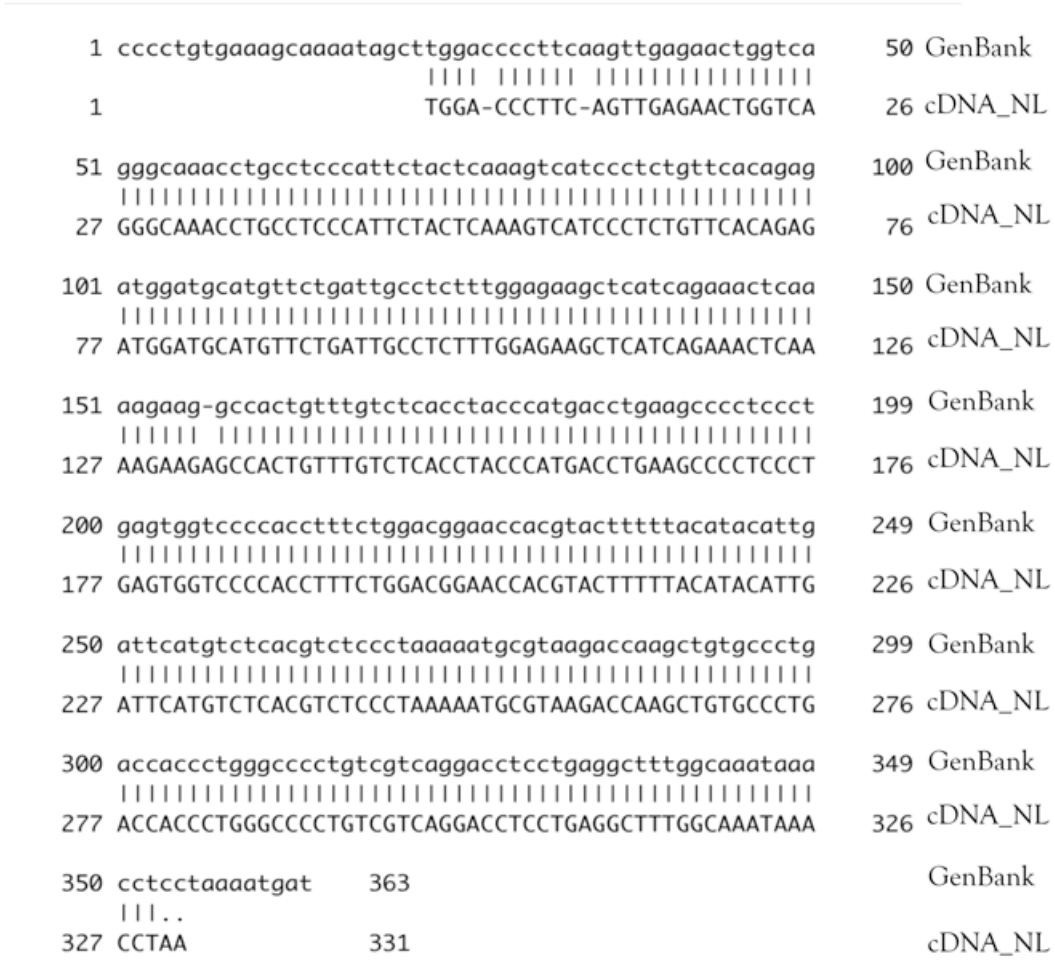

Figure 3.9 Sequencing of MAdCAM-1 mRNA extracted from a normal liver. Representative sequencing data from amplified cDNA transcribed from total RNA extracted from a normal liver, indicating consensus between sequenced material and MAdCAM-1 sequence information from GenBank.

3.3 DISCUSSION

The expression of MAdCAM-1 has previously been reported in human livers in a variety of liver diseases, most prominently in AIH and PSC, the autoimmune hepatic complications of IBD (Hillan et al., 1999)(Grant et al., 2001). Therefore, in this study, a more detailed analysis of MAdCAM-1 mRNA and protein expression in normal and diseased human liver tissues was carried out.

Immunohistochemical analysis revealed that in all the disease livers but not normal liver tissue (3AIH, 3PBC, 3PSC, 3ALD), MAdCAM-1 was detected in the endothelial cell lining of central veins and small vessels. Sinusoidal staining was mostly absent except in one normal liver, where it was faintly expressed. These results are in accordance with what was previously found by Grant *et al.,* who detected sinusoidal MAdCAM-1 in 2/10 (20%) patients with AIH and 2/11 (18%) patients with PBC (Grant et al., 2001). However, we cannot draw any absolute conclusions regarding expression of MAdCAM-1 in particular diseases, such as AIH and PSC, because the number of samples tested in the present study was small (n=3).

Interestingly, in addition to the expression of MAdCAM-1 in vascular endothelium, positive staining was also detected in structures that seemed to be inside the hepatocyte cytoplasm. There are no published studies reporting expression of MAdCAM-1 in hepatocytes, thus our data may suggest either that hepatocytes make MAdCAM-1 protein, which is unlikely given what is known about MAdCAM-1 expression, or that circulating soluble MAdCAM-1 can be taken up and transported into cytoplasmic vehicles in hepatocytes in order to be processed or degraded. A third explanation is that the staining was non–specific but this is unlikely given the

negative staining seen with an isotype–matched control antibody. Intriguingly, expression of MAdCAM-1 in epithelial type cells has been reported in choroid plexus epithelium, where MAdCAM-1 is expressed *de novo* during experimental autoimmune encephalomyelitis (EAE) and also participated in leukocyte adhesion to the epithelium (Steffen et al., 1996). Hence, our hepatic epithelial MAdCAM-1 expression may be genuine. In addition, in most cases tested, there was a smeary brownish stain of the tissue, which does not appear to be associated with specific cellular structures. It is unclear what this staining represents, it could be staining of soluble MAdCAM-1 immobilised on matrix. In all cases the isotype–matched control antibody used displayed no reactivity, suggesting that the staining with anti–MAdCAM-1 was real.

Occasionally, MAdCAM-1 staining was seen in immune cells with the morphology of dendritic cells. Previous studies (Szabo et al., 1997) have demonstrated expression of MAdCAM-1 on follicular dendritic cells, throughout the B cell zone in Peyer's patches in normal mice, as well as in the follicular dendritic cells within the germinal centres of chronically inflamed spleen. In addition, dendritic cells within some germinal centres and mantle zone in the follicular cortex of both mesenteric and peripheral lymph nodes, dendritic cells within germinal centres of Peyer's patches in humans (M. Briskin et al., 1997), and in lymphoid aggregates of several human liver diseases (Grant et al., 2001), also stain for MAdCAM-1. Recently, our laboratory (Eksteen et al., 2009) has demonstrated that the imprinting of α4β7+CCR9+ T cells requires primary activation by gut dendritic cells a process that is retinoic acid dependent, meaning that the α4β7+CCR9+ T cells that infiltrate the liver during inflammation are primed in the gut. Therefore, the expression of MAdCAM-1 by hepatic dendritic cells might serve to retain α4β7+ gut specific lymphocytes to the liver. In addition, it has been reported that isolated primary

follicular dendritic cells express VCAM-1 (Freedman et al., 1990) and ICAM-1 (Koopman et al., 1991) through which they can support the clustering with and presentation of antigen to α4β1 and LFA-1 expressing B cells, respectively, in germinal centres, thus leading to their affinity maturation and differentiation into memory cells, and a similar role might be served by MAdCAM-1. However, more extensive dual staining using cell specific markers for different dendritic cell subsets is required to define exactly where MAdCAM-1 protein is expressed. If MAdCAM-1 is expressed on DCs within the liver this would suggest it may play a broader role than just acting as an addressin in the chronic liver disease.

In accordance with the staining results, MAdCAM-1 protein was also detected by immunoprecipitation of the same liver tissue samples. Only a very faint protein band was detected in the normal liver tissue samples, whereas all the diseased livers showed strong MAdCAM-1 protein bands. When the order of antibodies used was reversed during the immunoprecipitation procedure, with the polyclonal Ab used for detection, it was noted that MAdCAM-1 protein in the normal samples appeared similar to the levels in the diseased livers. Thus, the possibility of MAdCAM-1 existing in a different conformational structure in the normal livers, which changes during inflammation, was further investigated. Surprisingly, western blotting of the non–beaded supernatant of immunoprecipitated samples with the polyclonal Ab revealed the presence of MAdCAM-1, which was not detected when probing with the monoclonal Ab. Currently, the epitope where the monoclonal Ab binds is not known, but as it acts as a function–blocking Ab it is likely that it recognises an epitope in either of the two extracellular Ig domains. Thus, it is possible that MAdCAM-1 is present in normal liver where it exists with a divergent structural folding. This divergence could also explain the low

expression levels of MAdCAM-1 detected after immunostaining of normal tissue samples with certain antibodies in other studies.

Our findings for MAdCAM-1 expression have interesting parallels with the chemokine CCL25, which also shows expression restricted to the gut (Kunkel et al., 2000)(Kunkel et al., 2003a). CCL25 is responsible for the activation of α4β7 integrin and its subsequent binding to MAdCAM-1. As with MAdCAM-1, CCL25 was found to be up–regulated in the liver during inflammatory liver diseases including PSC (Eksteen et al., 2004a). Of note, CCL25 was also found to be present in human liver tissues including normal livers (unpublished data from Dr. C. Weston, Centre for Liver Research), and we detected CCL25 in the same livers as we had observed the presence of MAdCAM-1 protein in the current study. This supports the relationship between these two molecules and their role in sustained recruitment of α4β7+CCR9+ lymphocytes both in gut and in extra–intestinal sites. A pharmaceutical inhibitor of CCR9 (the CCL25 chemokine receptor) has been developed, named TRAFICET–EN (Chemocentryx) which is currently in a Phase II/III clinical trial in moderate–to–severe Crohn's disease highlighting the potential therapeutic importance of these molecules.

To confirm the MAdCAM-1 protein results and to determine whether MAdCAM-1 is expressed in the liver, MAdCAM-1 mRNA expression was examined and was detected in both normal and diseased livers. Furthermore, sequence analysis of mRNA from a normal liver revealed complete alignment with the MAdCAM-1 gene sequence provided by GenBank validating the presence of MAdCAM-1. Additional mRNA analysis by Northern blot or *in situ* hybridization would be also useful in validating the presence of MAdCAM-1 mRNA in human liver tissue.

There was not a constant pattern of MAdCAM-1 expression between particular types of disease and some patients had higher expression than others. However, in general, statistically significant higher levels in the diseased livers of AIH and PSC were observed. This aberrant expression of MAdCAM-1 could be a factor explaining the link between liver inflammation in PSC and colitis as manifest by the findings that PSC develops in 2.4–7.5% of people with ulcerative colitis and 70–85% of people with PSC will eventually develop inflammatory bowel disease (Grant et al., 2002b). The fact that much higher percentage of people with liver disease go on to develop gut disease may suggest that there is a missing mechanistic link relating to the liver microenvironment (*e.g.* expression of divergent roles for molecules or immune priming roles) which predisposes to bowel inflammation.

In conclusion, in this chapter the presence of MAdCAM-1 protein in the human liver tissues was demonstrated, with a most prominent staining in the endothelial lining cells of the portal veins. Very faint expression was detected in normal livers, and a novel possibility that this MAdCAM-1 exists in a non–functional state is suggested. Under inflammatory conditions a conformational change and increased expression results in increased functional MAdCAM-1 that leads to the recruitment of gut–derived lymphocytes to the liver tissues. Interestingly, MAdCAM-1 protein was detected in the same liver tissues as the gut associated chemokine CCL25, which can trigger α4β7/MAdCAM-1 binding. The activation of this pathway could lead to the sustained recruitment of gut–derived lymphocytes and the establishment of chronic inflammation.

CHAPTER 4

Expression and Function of MAdCAM-1 In Human Primary Endothelial Cells

4.1 INTRODUCTION

The significant role of MAdCAM-1 in inflammatory bowel disease (IBD), as well as its aberrant expression in chronic inflammatory liver diseases complicating IBD, led to the hypothesis that an "entero–hepatic" link promotes the recirculation of long–lived memory lymphocytes originally activated in the gut, between the gut and the liver. Such cells could trigger hepatic inflammation in the presence of gut antigens that had entered the liver via the portal circulation (Grant et al., 2002b)(Eksteen et al., 2004b).

Another element supporting "entero–hepatic" lymphocyte recirculation is vascular adhesion protein–1 (VAP-1). VAP-1 has adhesive functions and is also an enzyme member of the semicarbazide–sensitive amine oxidase family (SSAO) (Smith et al., 1998). Under normal conditions VAP-1 is strongly expressed on liver endothelium but is only faintly present on mucosal vessels. However, gut expression of VAP-1 is greatly increased in IBD suggesting that liver derived lymphocytes expressing the VAP-1 ligand may be able to enter the inflamed gut (Salmi et al., 1993). Our observations of the expression pattern of VAP-1 and MAdCAM-1, suggested that there is an association between the two. Further support for this association comes from previous studies in our group (Lalor et al., 2007) reporting that binding of the amine substrate benzylamine to VAP-1 expressed on hepatic endothelial cells leads to rapid activation of NF-κB. This results in expression of pro–inflammatory proteins such as E–selectin and ICAM-1 and in the up–regulation of leukocyte adhesion. Similar mechanisms may operate in the induction of MAdCAM-1 (see below) suggesting to us that VAP-1 enzyme activity could be a factor for the aberrant expression of MAdCAM-1 in the liver.

Many studies support the role of TNFα and other stimulatory cytokines in induction of MAdCAM-1 expression *in vivo*. Induction of MAdCAM-1 expression on endothelial cells *in vitro* has been more difficult to demonstrate although some studies have reported that TNFα induces MAdCAM-1 expression in murine endothelial cells (Oshima et al., 2001a)(Oshima et al., 2001b)(Watanabe et al., 2002), including murine hepatic endothelial cells (HEC), exposed to TNFα and IL-1β (Ando et al., 2007). In addition, in an *in vivo* mouse model it has been demonstrated that intraluminal administration of butter significantly increases TNFα production by lamina propria macrophages, which leads to an increased expression of the adhesion molecules, MAdCAM-1, ICAM-1 and VCAM-1 and subsequently to increased lymphocyte adherence to intestinal microvessels (Fujiyama et al., 2007).

The ability of TNFα to induce MAdCAM-1 expression is also evident in cells that do not belong to the endothelial cell family. In NIH 3T3 fibroblasts and B16F10 melanoma cells it was shown that TNFα induced MAdCAM-1 expression and also that the induced MAdCAM-1 protein in NIH 3T3 was biologically active as it could support adhesion of TK–1 cells in an α4β7–dependent manner (Leung et al., 2003).

Moreover, in cultured human stomach explants, increased expression of MAdCAM-1 following TNFα and IFNγ stimulation of endothelial cells has been reported (Lindholm et al., 2004). More recent studies using primary cultures of human gut–derived microvascular endothelial cells (HIMEC) have shown that MAdCAM-1 expression is strongly induced by TNFα, LPS and IL-1β by distinct signalling mechanisms involving both NF-κB and PI3-k/Akt (Ogawa et al.,

2005). All these studies support a role for TNFα in the expression of MAdCAM-1 in gut endothelial cells, non–gut endothelium and even in non–endothelial cells.

Both the human and murine MAdCAM-1 genes share common characteristics as indicated by their genomic organisations. They are both encoded by 5 exons located on chromosomes 19p13.3 and chromosome 10, respectively (Figure 4.1A), and the sequences of their N–terminal Ig–like domains show homology (59%–65%). The DNA sequence of the 5' flanking promoter region of the human MAdCAM-1 gene contains potential transcription factor binding sites (Figure 4.1B), many of which are conserved in the mouse homologue MAdCAM-1 gene (Leung et al., 1997). These transcription factor–binding sites (Figure 4.1C) include sites for NF-κB docking which may explain the inducibility of MAdCAM-1 following stimulation with cytokines such as TNFα, which activate NF-κB. Although cytokines are clearly important for the regulation of expression of many pro–inflammatory genes including MAdCAM-1, additional complexity can be provided by epigenetic events such as promoter methylation.

DNA methylation occurs naturally in both prokaryotic and eukaryotic organisms. In higher eukaryotes, DNA methylation has been proven to play a central role in a number of biological processes such as X chromosome gene silencing, embryonic development, gene imprinting and cell cycle regulation (Warnecke et al., 1997). DNA methylation usually occurs in CpG islands, which are often located around the promoters of housekeeping genes or other genes frequently expressed in a cell. Human MAdCAM-1 is encoded by a gene located on chromosome 19p13.3. Of note, chromosome 19, which contains the human MAdCAM-1 gene, has the highest gene density of all human chromosomes, and its high G + C content and density of CpG islands and

repetitive DNA sequences indicate a chromosome rich in biological and evolutionary significance (Grimwood et al., 2004). The density of CpG islands on this chromosome suggests that MAdCAM-1 gene may be a candidate for regulation by methylation.

In the current chapter, the effects of TNFα, VAP-1 and its substrates methylamine and benzylamine on the expression of MAdCAM-1 by primary human hepatic endothelial cells were studied. Furthermore, the methylation pattern of the human MAdCAM-1 promoter region was investigated in order to determine whether the ectopic expression of MAdCAM-1 was due to switching on the gene in hepatic cells. Finally, a flow based adhesion assay was developed in order to evaluate whether the induced MAdCAM-1 protein was functional.

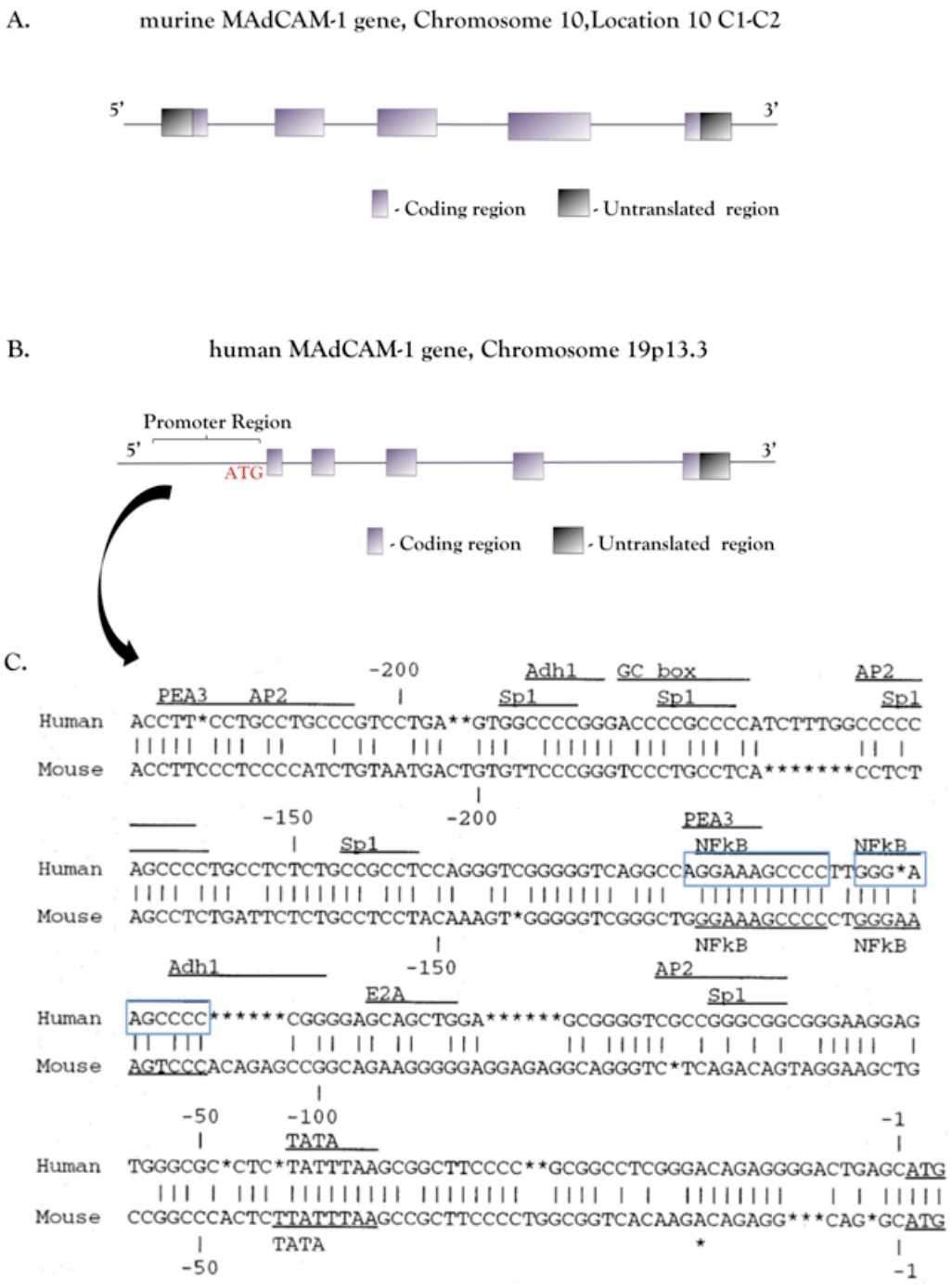

Figure 4.1 Schematic representation of the murine and human MAdCAM-1 genes. (A) The murine MAdCAM-1 gene is located on chromosome 10 and (B) the human MAdCAM-1 gene is located on chromosome 19p13.3. Both consist of five exons (in purple). (C) Representative part of the DNA sequence of the 5' flanking region of the human MAdCAM-1 gene and comparison with the mouse MAdCAM-1 promoter region. Transcriptional regulatory elements identified both in human and mice are underlined. Two tandem NF-κB sites (highlighted in blue) located 100bp upstream of the start site of transcription in the mouse promoter are conserved. Numbers refer to nucleotide positions and are all relative to the transcriptional start codon (ATG). The transcriptional start site identified in the mouse MAdCAM-1 gene is denoted by an asterisk [figure C is published by (Leung et al., 1997)].

4.2 RESULTS

4.2.1 The Induction of MAdCAM-1 Expression In HSEC and HUVEC

In order to investigate whether MAdCAM-1 expression in HSEC and HUVEC could be regulated, the effects of adding TNFα and recombinant enzymatically active VAP-1 and its substrates methylamine and benzylamine were tested. Monolayers of HSEC and HUVEC were stimulated with different combinations of TNFα (20ng/ml), rVAP-1 (100ng/ml which is equivalent to serum levels of shed VAP-1), methylamine and benzylamine (25–200μM) for 2 to 48 hours. In some experiments, the VAP-1 enzyme inhibitor 2'–bromoethylamine (BEA) was used at 0.5mM. Low levels of cell surface MAdCAM-1 protein were detected by cell–based ELISA and the combination of TNFα (20ng/ml) and methylamine (50μM or 200μM) (*P=0.01 and *P=0.04, respectively) significantly increased MAdCAM-1 expression in HSEC after 2 hours stimulation (Figure 4.2A). Similarly in HUVEC, TNFα plus methylamine (at 50μM) (Figure 4.2B) increased MAdCAM-1 expression but this did not achieve significance. The effects of the stimulants described above, were further examined by conventional and quantitative PCR and western blotting. MAdCAM-1 mRNA was detected in HSEC isolated from different liver diseases as well as in HUVEC (Figure 4.3), in both untreated (control samples) and treated samples. Quantitative PCR confirmed that stimulation of endothelial cells with TNFα alone (*P=0.02) or in combination with methylamine (*P=0.01) for 2 hours, significantly increased expression of MAdCAM-1 mRNA in HSEC (Figure 4.4A). Although, there was more expression when cells were stimulated with TNFα plus methylamine compared to TNFα alone, statistical analysis did not reveal a significant difference. In HUVEC, statistical analysis also confirmed significant differences in MAdCAM-1 mRNA expression levels relative to untreated samples under all three stimulatory conditions of TNFα (***P=0.0002),

methylamine (*$P=0.04$), and their combination (***$P=0.0001$) (Figure 4.4B). Of note, the expression levels of MAdCAM-1 in HSEC stimulated with TNFα (*$P=0.01$) and TNFα plus methylamine (**$P=0.004$) were higher than in HUVEC (Figure 4.4C). MAdCAM-1 protein was also detected in resting and stimulated HSEC and HUVEC by western blotting. In contrast to the mRNA analysis however, no differences between the divergent stimulations were observed (Figure 4.5A and 4.5B). The molecular weight of the MAdCAM-1 protein identified was 120kDa, which represents the dimer form of the glycosylated monomer (60kDa). In our positive control, CHO cells, a band of different molecular size (80kDa) was detected which probably represents the dimeric form of the unprocessed precursor.

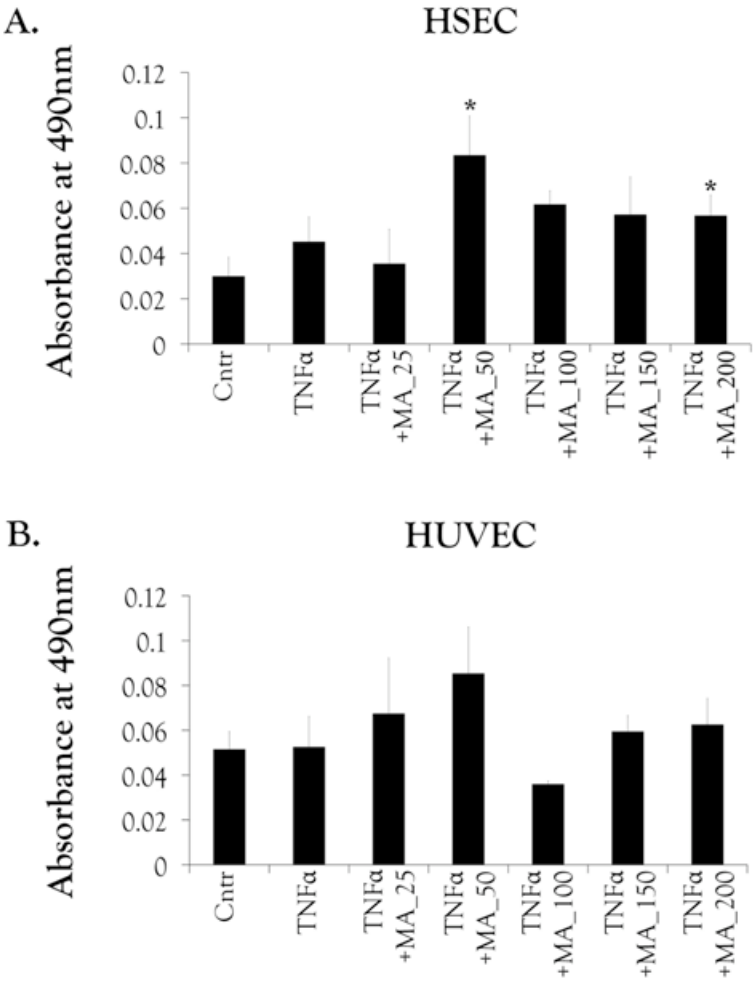

Figure 4.2 Expression of MAdCAM-1 on HSEC and HUVEC. (A) HSEC and (B) HUVEC were stimulated with TNFα (20ng/ml) and methylamine (MA; 25μM-200μM) for 2 hours. Data represent mean ± SEM of MAdCAM-1 expression minus the signal from isotype control Ab in n=4 HSEC and n=3 HUVEC. Statistical analysis performed by Student's t-test [**P=0.04*, TNFα+MA (50μM); **P=0.01*, TNFα+MA (200μM), both compared to untreated control samples].

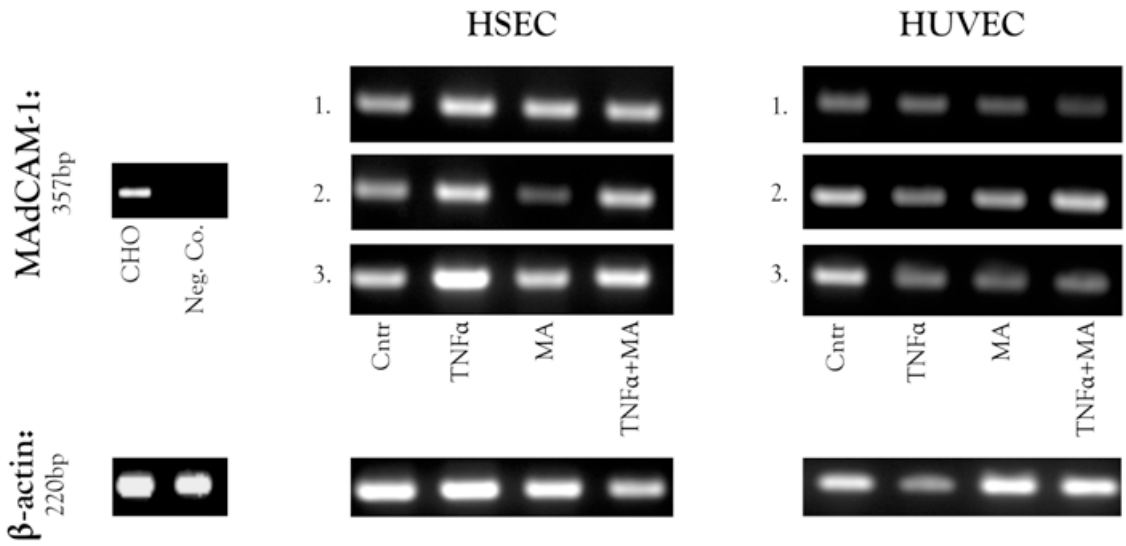

Figure 4.3 MAdCAM-1 mRNA expression in HSEC and HUVEC. Endothelial cells were stimulated with TNFα (20ng/ml), methylamine (MA; 50μM) and their combination for 2 hours, prior to extraction of RNA, cDNA synthesis and conventional PCR. MAdCAM-1 mRNA in CHO cells was used as positive control and in JY cells as a negative control (Neg.Co). Images represent PCR products from 3 different representative HSEC and HUVEC, after electrophoresis in 1.5% (w/v) agarose gels. β-actin was used as endogenous control.

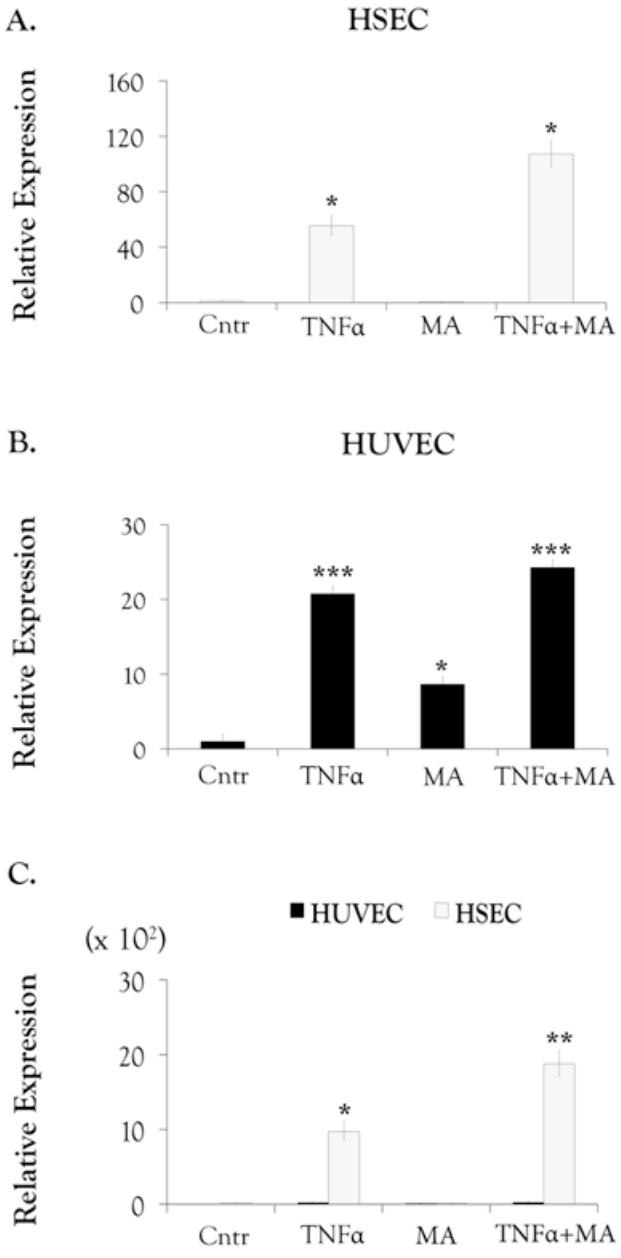

Figure 4.4 MAdCAM-1mRNA expression in HSEC and HUVEC by quantitative PCR. Endothelial monolayers were stimulated with TNFα (20ng/ml), methylamine (MA; 50μM) and their combination for 2 hours, prior to relative expression analysis by qPCR. MAdCAM-1 mRNA expression in (A) n=7 HSEC and (B) n=3 HUVEC. Data represent relative expression of treated versus non-treated endothelial cells (Cntr). (C) MAdCAM-1 mRNA expression in HSEC shown relative to HUVEC. Statistical analysis performed by Student's t-test revealed significantly elevated levels in stimulated versus untreated control samples [(A) *P=0.02, TNFα; *P=0.01, TNFα+MA (B) ***P=0.0002, TNFα; *P=0.04, MA; ***P=0.0001, TNFα+MA (C) *P=0.01, TNFα; **P=0.004, TNFα+MA].

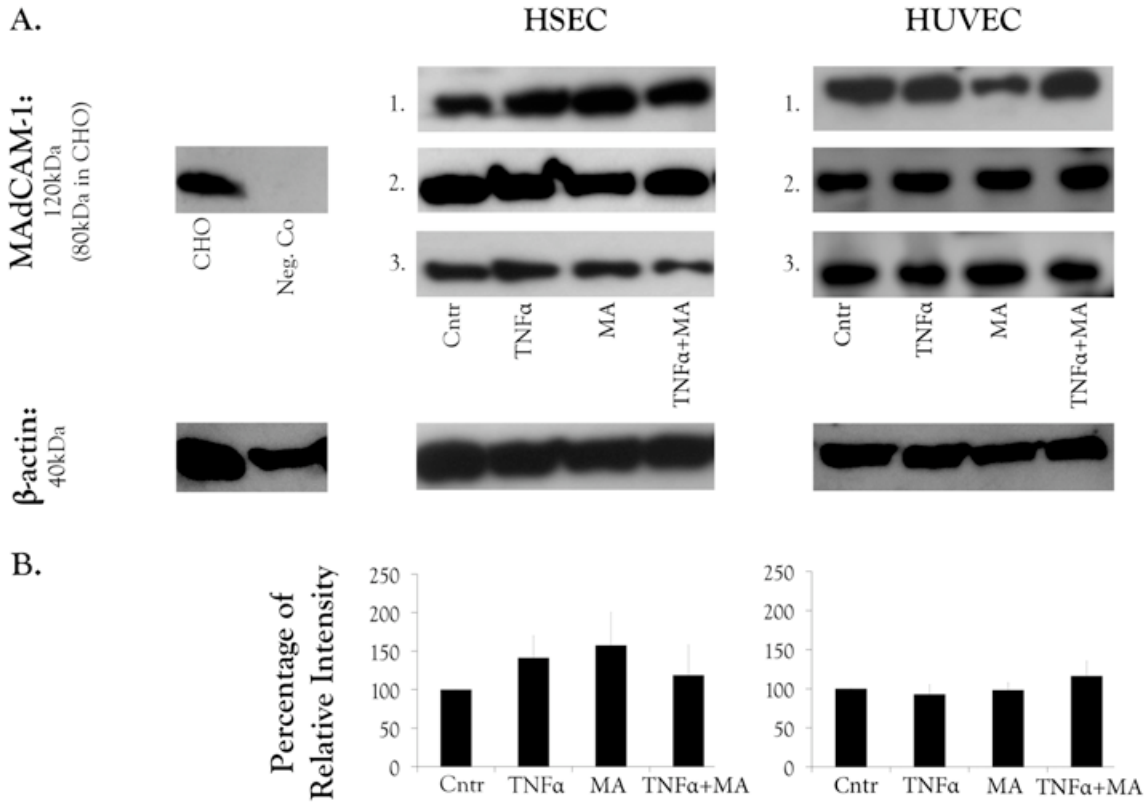

Figure 4.5 MAdCAM-1 protein expression in HSEC and HUVEC. Endothelial monolayers were stimulated with TNFα, methylamine (MA) and their combination for 2 hours as previously described, prior to lysis and western blot analysis. Protein lysates extracted from CHO cells transfected with FL-MAdCAM-1 and after hygromycin B reselection were used as positive control (CHO) and protein lysate from a JY cell line was used as negative control (Neg. Co). (A) Representative images of western blots from 3 different HSEC and HUVEC isolates. (B) Densitometric analysis of replicate blots. Data represent mean ± SEM of percentage of relative intensity [compared to expression in un–stimulated cells (set to 100%)] from n=8 different HSEC and n=3 different HUVEC.

4.2.2 Optimisation of Cytometric Analysis of MAdCAM-1 Expression

CHO cells stably transfected with a FL–MAdCAM-1 expression plasmid and untransfected parental CHO cells, were used as positive and negative control respectively, for confirmation of anti–MAdCAM-1 antibody specificity. Cytometric analysis confirmed CHO–FL–MAdCAM-1 cells stained with anti–MAdCAM-1 antibody in contrast to the parental cells (Figure 4.6). The CHO–FL–MAdCAM-1 cells were then used to test the effects of trypsin on surface expression of MAdCAM-1 prior to later experiments, which required trypsinisation of treated HSEC. Figure 4.7 confirms that MAdCAM-1 is cleaved by trypsin, since the median channel fluorescence (MCF) values for expression on trypsinised cells (Figure 4.7B and 4.7C) are lower than those on cells detached non–enzymatically (Figure 4.7A and 4.7C). The expression of CD31 was also confirmed on HSEC populations by cytometry as this marker is used to isolate hepatic endothelial cells and is a good marker of endothelial phenotype (Lalor et al., 2006). Figure 4.8 shows a representative cytometry histogram for CD31 expression in HSEC.

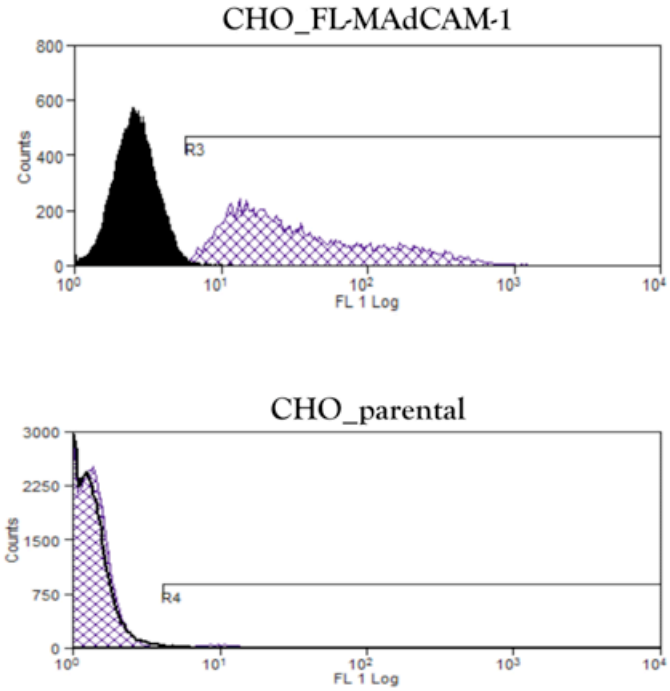

Figure 4.6 MAdCAM-1 expression in CHO cells. Expression of cell surface MAdCAM-1 protein was examined in CHO cells by flow cytometry. Representative histograms for MAdCAM-1 staining (in purple), compared to staining with isotype–matched control antibody (in black) in CHO transfected with a full length MAdCAM-1 construct (top panel) compared to the parental CHO (bottom panel).

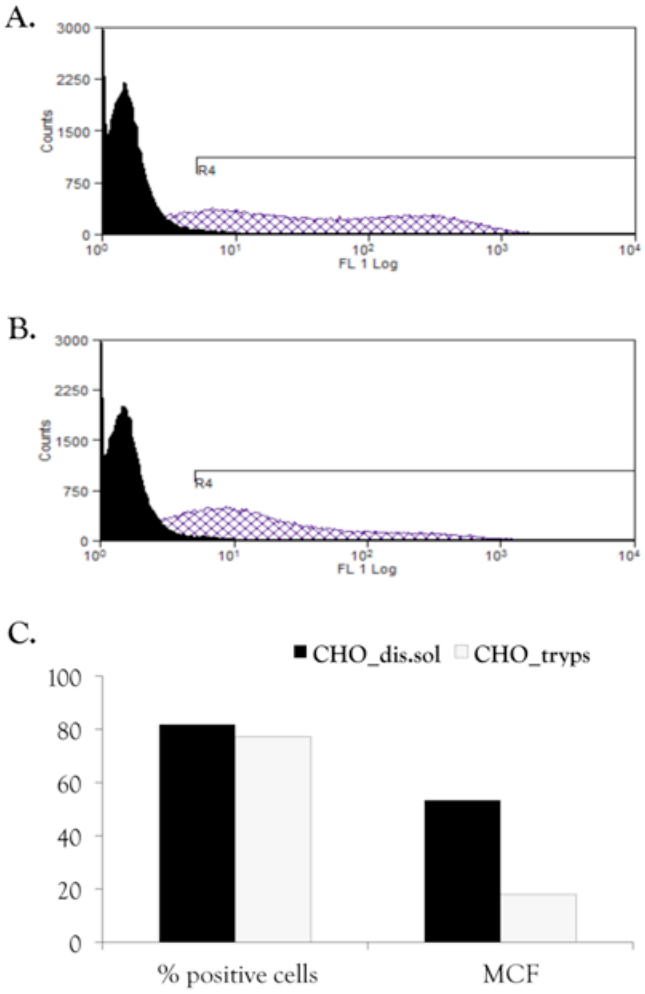

Figure 4.7 MAdCAM-1 protein is cleaved by trypsinization. Representative histograms for MAdCAM-1 expression (in purple) after detachment of CHO cells using (A) non-enzymatic dissociation solution or (B) trypsin, compared to staining with an isotype–matched control antibody (in black). (C) The percentage of positive cells and median channel fluorescence (MCF) values for a representative experiment are presented.

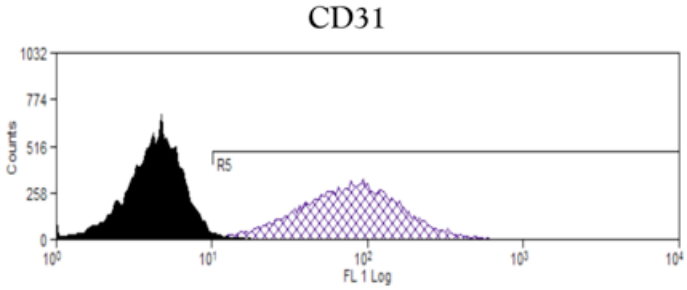

Figure 4.8 CD31 expression in hepatic endothelial cells. Representative cytometry histogram for CD31 expression (in purple) on HSEC compared to staining with an isotype–matched control antibody (in black).

4.2.3 Localisation of MAdCAM-1 Protein Expression In Hepatic Endothelial Cells

The localisation of MAdCAM-1 in hepatic endothelium following stimulation was subsequently examined. Cells isolated from different livers were labelled fresh (surface expression) or after fixing and permeabilisation (internal expression). The data confirm that MAdCAM-1 is expressed on the endothelial surface as well as in the cytoplasm of both treated and untreated samples (Figure 4.9A and 4.9B) and that levels are similar on HSEC from normal and diseased livers. Interestingly, no differences in MAdCAM-1 protein expression levels (% positive or MCF) were noted after treatment (Table 4.1).

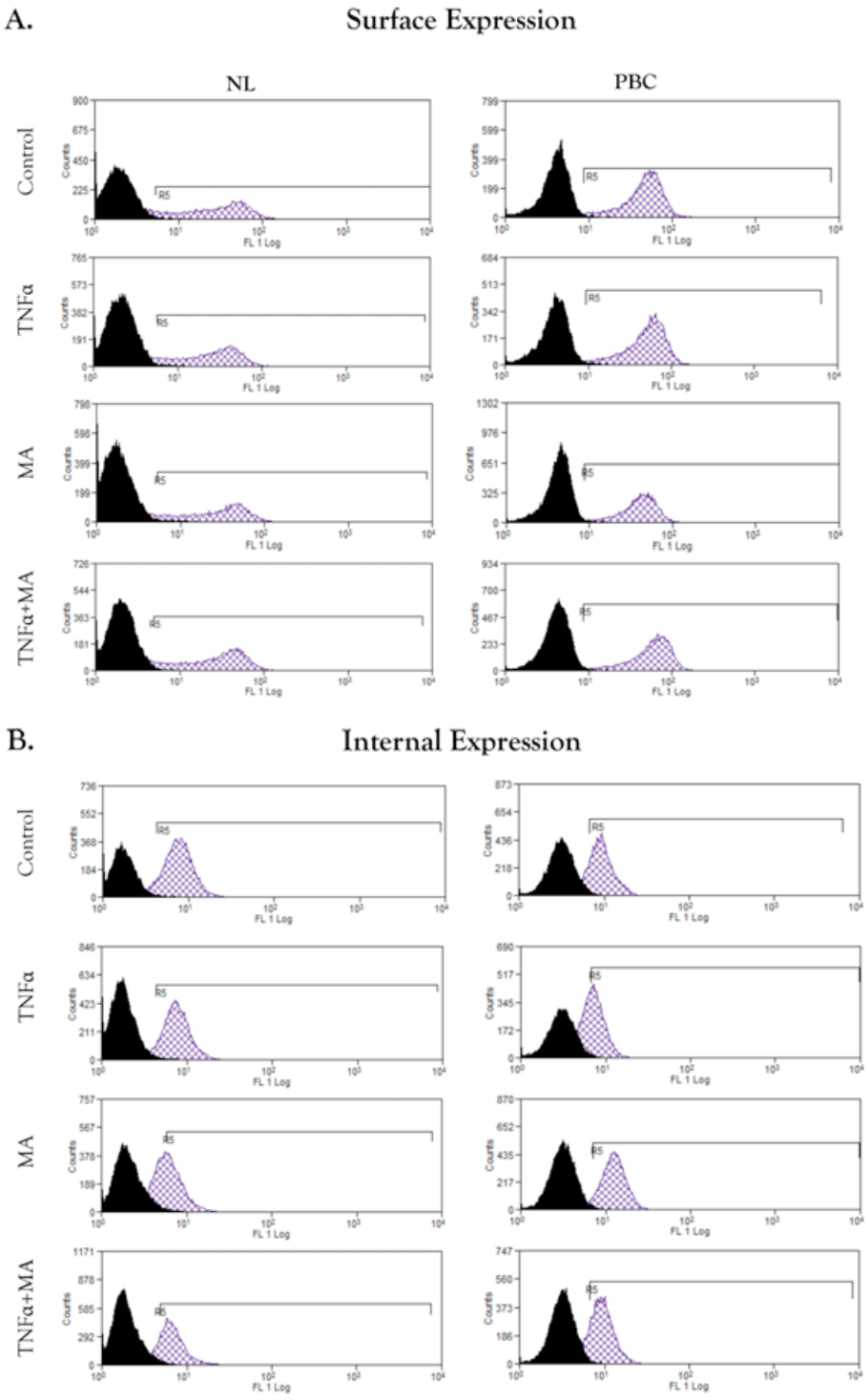

Figure 4.9 Extracellular and intracellular MAdCAM-1 protein expression. Endothelial cells were stimulated with TNFα, methylamine (MA) and their combination for 2 hours. Panels illustrate representative histograms for (A) surface and (B) internal MAdCAM-1 expression (purple) on two HSEC isolates (normal and PBC liver, respectively) compared to staining with an isotype–matched control antibody (in black).

SURFACE EXPRESSION		
MAdCAM-1	**% Positivity**	**MCF**
Control (No Treatment)	38.33 ± 12.03	22.36 ± 5.65
TNFα	37.86 ± 11.38	21.72 ± 6.45
MA	34.06 ± 11.42	20.79 ± 4.94
TNFα+MA	39.79 ± 12.00	22.31 ± 8.04
INTERNAL EXPRESSION		
MAdCAM-1	**% Positivity**	**MCF**
Control (No Treatment)	86.25 ± 5.24	11.16 ± 1.08
TNFα	80.63 ± 7.66	10.55 ± 1.03
MA	81.18 ± 7.62	10.88 ± 1.04
TNFα+MA	81.31 ± 8.33	10.34 ± 0.85

Table 4.1 Surface and internal expression of MAdCAM-1 protein is unaffected by treatment. Pooled data from 7 different HSEC isolates (2Normal, 2Resections, 2PBC, 1AIH) showing percentage of positive cells and median channel fluorescence values (MCF) for MAdCAM-1 on live cells (surface expression) and fixed and permeabilised cells (internal expression). Data represent mean±SEM and no significant differences were noted between control and stimulated cells.

4.2.4 Different Cellular Compartments Contain Distinct MAdCAM-1 Species

Endothelial cells were treated as previously, prior to extraction of protein from the cytosolic, membrane, and cytoskeletal compartments. Western blotting of these fractions revealed that MAdCAM-1 protein species of different molecular sizes were present at different densities in the different compartments (Figure 4.10A and 4.10B). The glycosylated MAdCAM-1 monomer (60kDa) was present only in the cytoplasmic fraction. The dimeric form (120kDa) was present in both the cytoplasm and membrane but much higher levels were apparent in the membrane fragments. The presence of a larger protein was also noted, possibly trimeric MAdCAM-1 (180kDa) in some cell fractions.

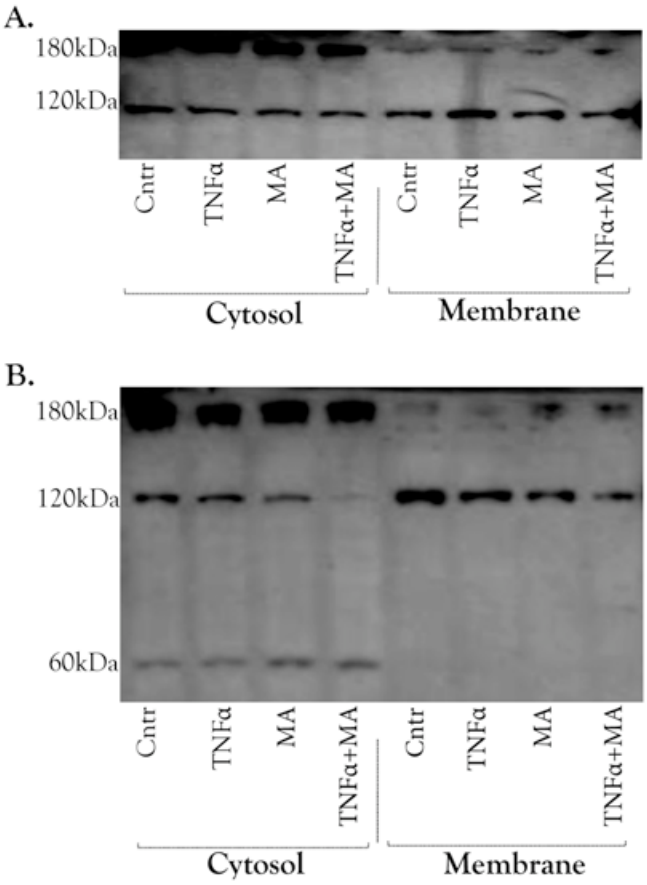

Figure 4.10 MAdCAM-1 species of different molecular weights are detected in different cell compartments. Protein lysates from the cytosolic and membrane compartments were prepared from n=3 different HSEC after stimulation with TNFα, methylamine (MA) and their combination for 2 hours. Blotted proteins were probed using the mouse anti-human MAdCAM-1 Ab (CA102.2C1; 4μg/ml). Representative images of western blot from two different HSEC isolates (A) and (B) from resected liver.

4.2.5 Soluble MAdCAM-1 Is Released From Endothelium After Stimulation

Stimulation of endothelial cells with TNFα or methylamine alone or in combination for 2 hours resulted in significantly increased levels of MAdCAM-1 mRNA. However, extracellular and intracellular protein levels remained the same. A previous study of Leung *et al.* revealed that soluble MAdCAM-1 is secreted into serum and urine of both normal individuals and chronically inflamed patients (Leung et al., 2004). Therefore, we tested whether MAdCAM-1 protein was cleaved from our cells under stimulatory conditions.

After stimulation cell supernatant was collected and examined for the presence of sMAdCAM-1 by immunoprecipitation. Figure 4.11 shows that MAdCAM-1 (60kDa) was detected in the supernatant from control and stimulated cells, and that statistically significant increased amounts were present after treatment with TNFα plus methylamine (*$P=0.017$). Moreover, under brefeldin A treatment (a chemical substance that disrupts the normal function of Golgi complex thus preventing the transport of the newly synthesised proteins to the membrane) of endothelial cells prior to stimulation with TNFα, methylamine and their combination for 2 hours, increased levels of intracellular MAdCAM-1 were detected (about 45%) after TNFα plus methylamine stimulation when compared to the TNFα plus methylamine treated HSEC that were not pre–treated with brefeldin A (Figure 4.12).

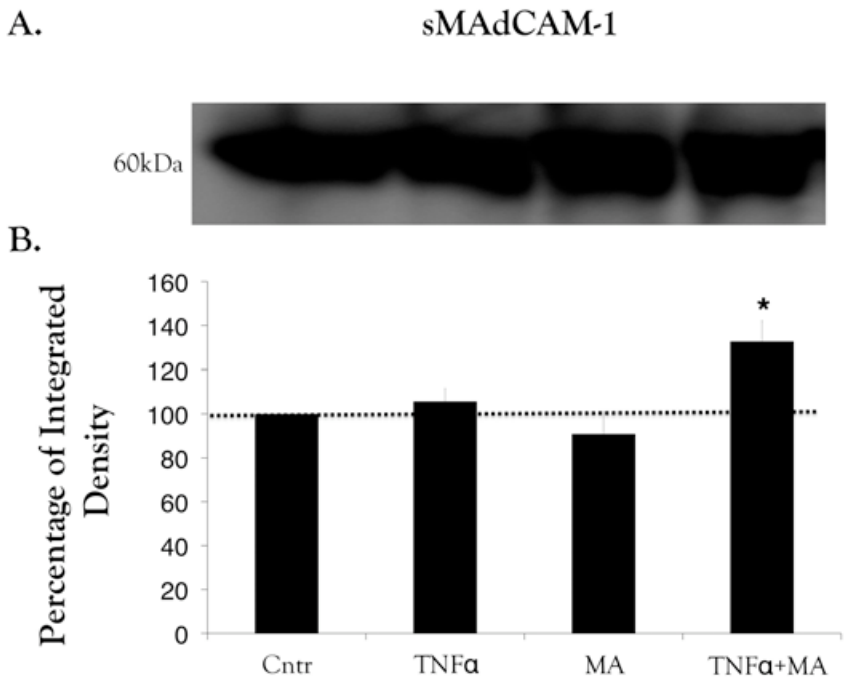

Figure 4.11 Soluble MAdCAM-1 is detected in the supernatants of HSEC after stimulation. Soluble MAdCAM-1 protein released in the culture media of HSEC after 2 hours treatment with TNFα, MA and their combination, was captured by the polyclonal Ab (H-116) and then (A) a 60kDa molecular weight band was revealed after detection with the monoclonal Ab (CA102.2C1). (B) Densitometric analysis of n=6 different HSEC isolates (2Resections, 2PBC, 1AIH, 1ALD). Data represent mean ± SEM of percentage of integrated density compared to expression in un–stimulated HSEC (Cntr; set to 100%). Statistical analysis performed by Student's *t*-test (**P=0.017*).

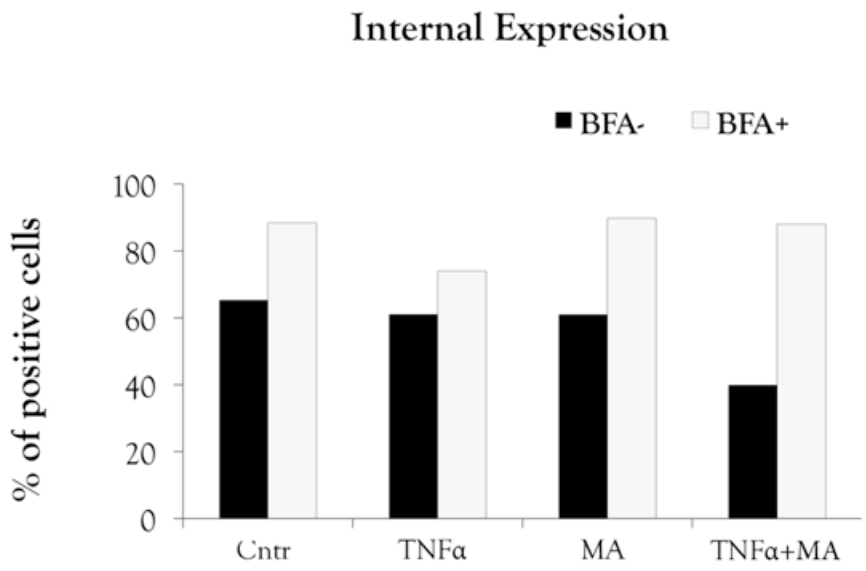

Figure 4.12 Brefeldin A prevented the transfer of newly synthesised MAdCAM-1 protein to the endothelial surface. Endothelial cells under stimulation with TNFα, methylamine and their combination synthesised new MAdCAM-1 protein whose transfer to the membrane was prevented from the disruptive Golgi apparatus caused by BFA. The percentage of positive cells under treatments with or without pre-treatment with Brefeldin A, BFA+ or BFA-, respectively, from one HSEC isolate, are presented.

4.2.6 Analysis of The Methylation Pattern of The MAdCAM-1 Promoter Region

MAdCAM-1 genomic sequence was accessible via GenBank and in order to investigate the methylation status of the MAdCAM-1 promoter region, 16 CpG islands located upstream of the transcription start site of the gene were identified by the MethylPrimer Express® Software (Applied Biosystems) and were assayed (Figure 4.13). DNA was extracted from 4 different HSEC (2PBC, 1NL and 1Resected liver) and 4 different HUVEC samples. Cells were left un–stimulated or were stimulated with TNFα and methylamine and bisulfite conversion was performed prior to methylation analysis by sequencing. In order to calculate an overall methylation figure per endothelial cell type, the methylation index (MtI) was calculated as the average of the $^{m}C/C$ ratio observed in all of the 16CpGs identified in each sample (Figure 4.14). Statistical analysis did not reveal a significant difference in the methylation status of MAdCAM-1 promoter regions before and after stimulation in both HSEC and HUVEC.

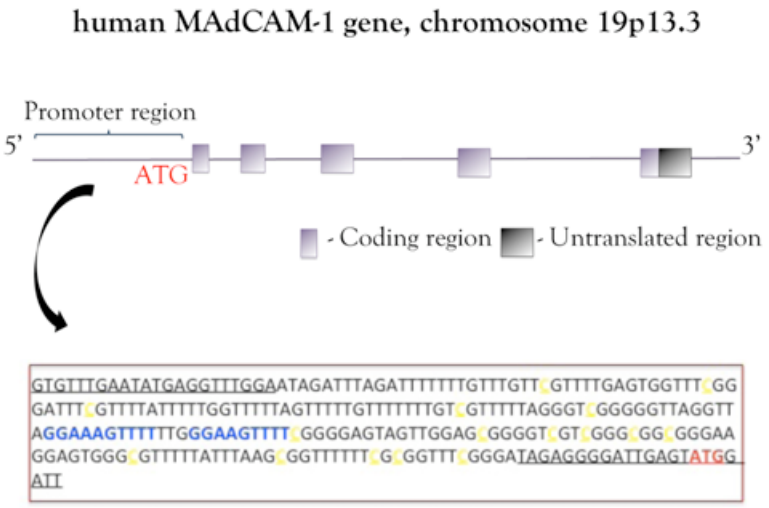

Figure 4.13 Methylation analysis of human MAdCAM-1 promoter region. The yellow highlights indicate 16CpG islands located upstream of the transcription start site (ATG highlighted in red) which were assayed. Two tandem NF-κB sites are also present (highlighted in blue).

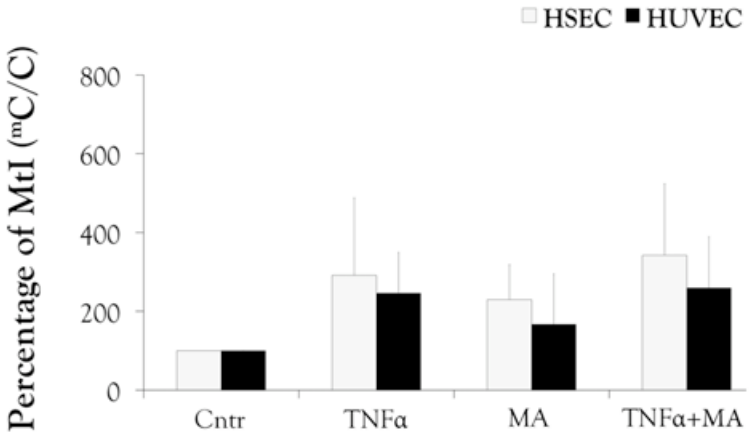

Figure 4.14 Methylation in HSEC and HUVEC. Endothelial cells were stimulated with TNFα and methylamine (MA) as before prior to bisulfite treatment of their DNA and sequence analysis. Data represent the average percentage change in methylation index (MtI: average ratio of the ^{m}C/C) of the MAdCAM-1 promoter region after treatment compared to control level of methylation (set to 100%). Data are mean ± SEM of the percentage of MtI from n=4 HSEC and n=4 HUVEC.

4.2.7 MAdCAM-1 Is Functional In Flow Based Adhesion Assays

In recent years the development of *in vitro* methodologies mimicking *in vivo* physiological flow conditions has enabled the detailed examination of leukocyte morphological change as well as leukocyte–endothelium interactions within a shear environment modelling that seen *in vivo* (Kulkarni et al., 2004). In the current study, a flow based adhesion assay was used in order to investigate the function of the MAdCAM-1 protein that was detected in HSEC and HUVEC. JY cells which express high levels of α4β7 integrin were perfused over control or stimulated endothelial monolayers at a shear stress of 0.05Pa and adhesion was recorded. Figure 4.15 shows that the combination of TNFα and methylamine caused a significant increase in the total number of adherent cells (***P=0.002)* and that treatment with TNFα alone also increased adhesion (**P=0.02)*. In order to confirm that the binding of α4β7+ JY cells to the endothelium was due to MAdCAM-1 expression, a blocking antibody directed against MAdCAM-1 (P1) was used (Figure 4.16). This antibody significantly inhibited cell adherence *(***P=0.0006,* Figure 4.16*)*. Moreover, treatment of JY cells with ACT-1 antibody directed against the α4β7 integrin caused also a decrease in the percentage of adherent cells (**P=0.04,* Figure 4.16). Confirmation of the specificity of the inhibitory effect of these antibodies is shown by lack of effect of isotype–matched control antibody IgG1 (Figure 4.17). Similar adhesion responses were noted in HUVEC (Figure 4.18), but less adhesion was observed to these cells after treatment when compared to HSEC (number of adherent cells binding under TNFα stimulation: 78.57±26.8 in HSEC and 55.7±9.73 in HUVEC and under TNFα plus methylamine stimulation: 100.2±24.9 and 73.1±25.8 in HSEC and HUVEC respectively).

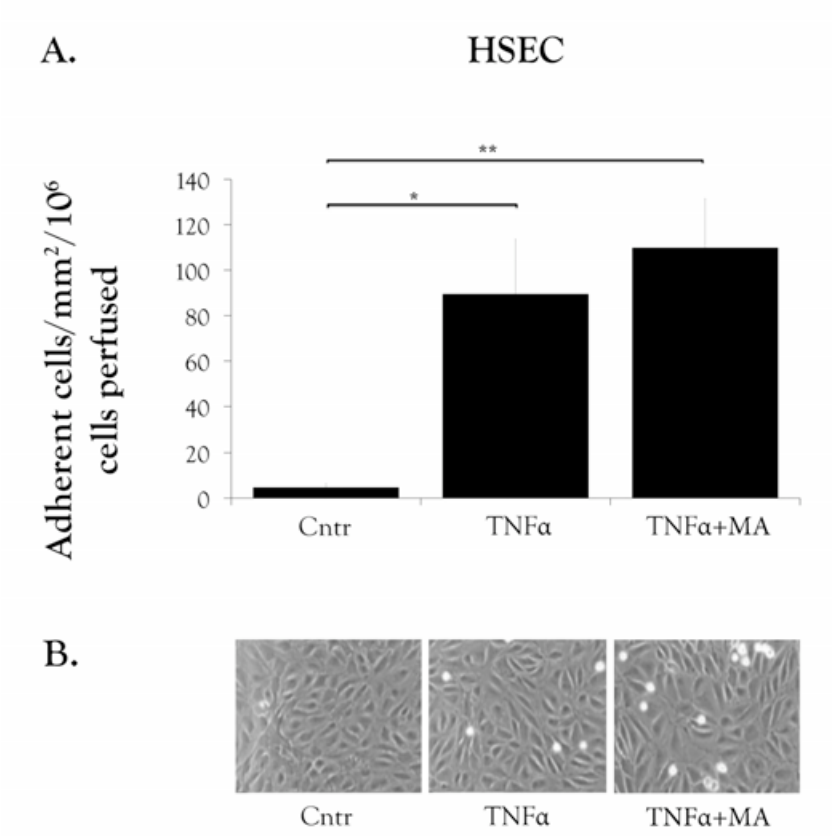

Figure 4.15 MAdCAM-1 expression supports JY cell adhesion in a flow-based adhesion assay to HSEC. Hepatic sinusoidal endothelial cells were treated with TNFα (20ng/ml) and methylamine (MA; 50μM) for 2 hours and JY cells were perfused over the monolayer at a shear stress of 0.05Pa. Adherent cells per field were counted and converted to adherent cells/$mm^2/10^6$ perfused. (A) Total adhesion of JY cells in presence of TNFα and methylamine. Data represent mean ± SEM from 7 different experiments. (B) Representative images captured from experimental videos. Statistical analysis performed by Student's t-test (*$P=0.02$, **$P=0.002$).

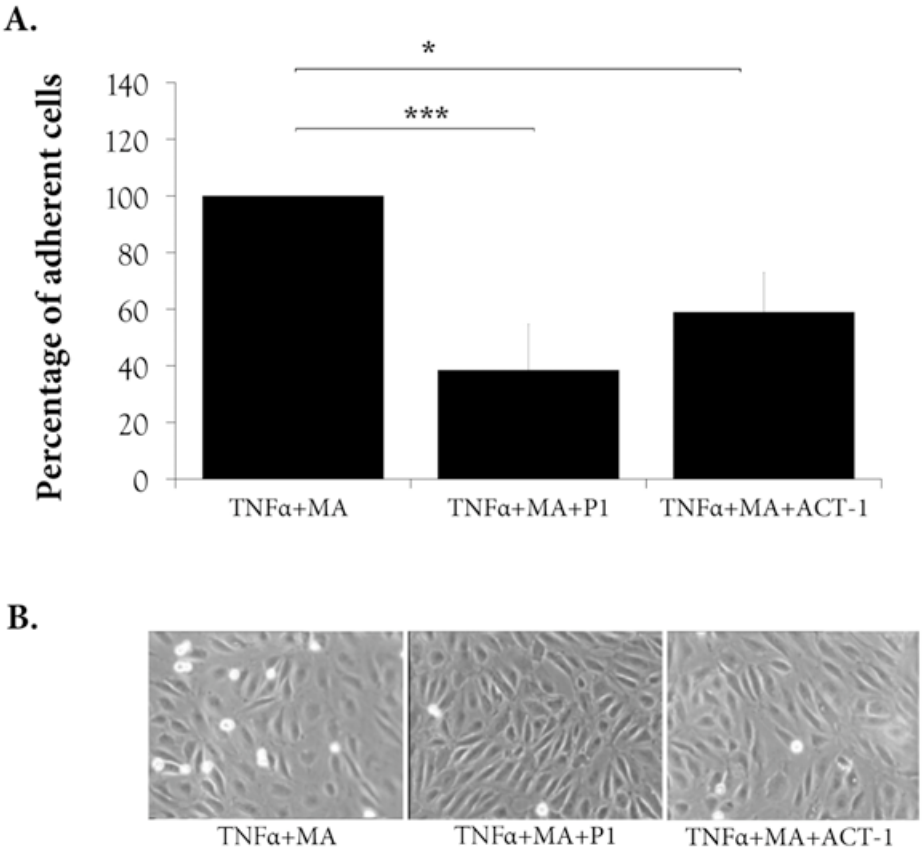

Figure 4.16 Adhesion of JY cells to stimulated endothelium is α4β7-dependent. (A) Total adhesion data for binding of JY cells to HSEC stimulated with both TNFα and methylamine for 2 hours. Where indicated, HSEC were treated with MAdCAM-1 function-blocking antibody (P1, 10ng/ml) or JY cells were treated with anti-α4β7 ACT-1 antibody (50ng/ml, Millenium) for 30 min prior to experiment. Data represent mean adhesion ± SEM in 5 different experiments. (B) Representative images captured from experimental videos. Statistical analysis performed by one–way ANOVA analysis (*$P=0.04$. ***$P=0.0006$).

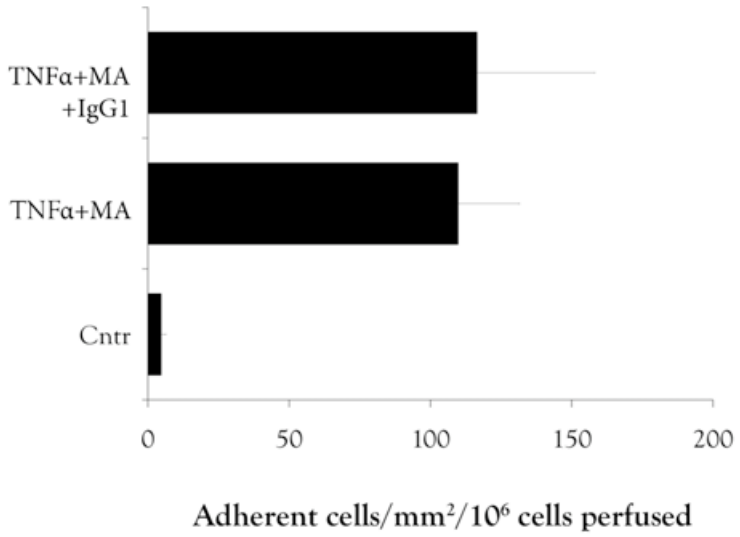

Figure 4.17 Isotype control antibodies have no effect on adhesion. HSEC were stimulated as before prior to treatment with control antibody IgG1 (5µg/ml, for 30min) and perfusion of JY cells at a shear stress of 0.05Pa. Data represent mean total number of adherent cells/mm^2/10^6 perfused ± SEM in 5 different experiments.

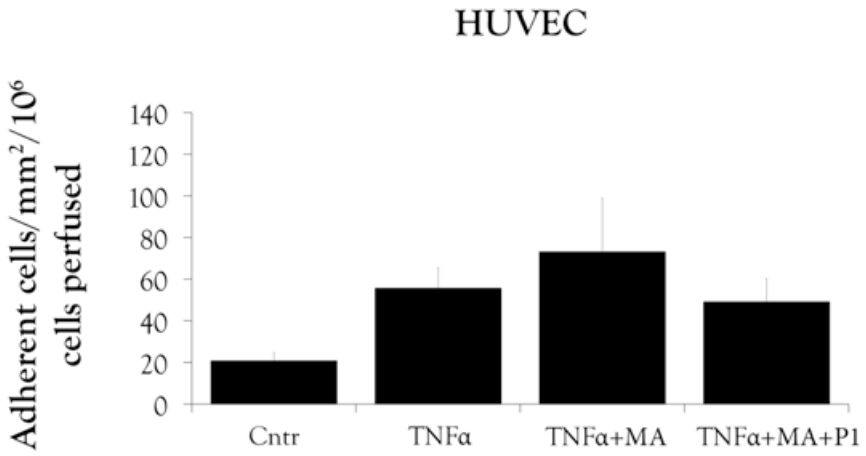

Figure 4.18 MAdCAM-1 expression supports JY cell adhesion to HUVEC. Human umbilical vein ECs were stimulated with TNFα (20ng/ml) and methylamine (MA; 50μM) for 2 hours and JY cells were perfused over the monolayer at a shear stress of 0.05Pa. Where indicated HUVEC were pretreated with anti-MAdCAM-1 P1 Ab (5μg/ml). Data represent mean total number of adherent cells/$mm^2/10^6$ perfused ± SEM in 3 different experiments.

4.3 DISCUSSION

The fact that MAdCAM-1 is expressed in human liver endothelium in liver diseases associated with IBD, led us to investigate the factors responsible for this ectopic expression. This is important for disease pathogenesis because hepatic MAdCAM-1 has been shown to support the adhesion of α4β7+ gut associated lymphocytes (Grant et al., 2001), thus leading to sustained recruitment and chronic inflammation. In this study, we report that treatment of liver endothelial cells with the pro–inflammatory cytokine TNFα in combination with other stimulants can induce expression of functionally active MAdCAM-1.

For the first time, our study shows constitutive MAdCAM-1 mRNA and protein expression in hepatic endothelial cells and umbilical vein endothelial cells cultured *in vitro*. A basal level of MAdCAM-1 mRNA was detected in both HSEC and HUVEC, which in the case of HSEC was significantly increased by TNFα (*$P=0.02$) and TNFα plus methylamine (*$P=0.01$) stimulation. An obvious difference in MAdCAM-1 mRNA levels induced by TNFα alone and TNFα plus methylamine was apparent, however although it did not reach statistical significance, suggests that methylamine may have an additive effect to that of TNFα in MAdCAM-1 up–regulation. The role of TNFα in inducing MAdCAM-1 expression in human hepatic endothelial cells has not been reported previously, however Ando T. *et al.* have demonstrated that TNFα can stimulate MAdCAM-1 in a dose– and time–dependent manner in a murine hepatic endothelial cell line (Ando et al., 2007). Moreover, in primary human intestinal microvascular endothelial cells, MAdCAM-1 has been reported to be strongly induced by TNFα (Lindholm et al., 2004)(Ogawa et al., 2005) via activation of NF-κB (Oshima et al., 2001b)(Lindholm et al., 2004)(Sasaki et al., 2002)(Takeuchi and Baichwal, 1995). TNFα has been also reported to

induce MAdCAM-1 in cultured HUVEC (Lindholm et al., 2004) which is in complete accordance with our findings, where in HUVEC the response to all stimulants [TNFα (***P=0.0002), methylamine (*P=0.04) and their combination (***P=0.0001)] was more pronounced. We believe that this could be because in HUVEC there is relatively little MAdCAM-1 expression under basal conditions, and such basal expression has not been reported before.

The expression of MAdCAM-1 mRNA and protein was also supported by the promoter region DNA methylation analysis. In both HSEC and HUVEC, there was no significant differences in the methylation status between treated and non–treated endothelial cells indicating that the MAdCAM-1 gene is transcriptionally active in both states. This fits with our data showing that MAdCAM-1 protein is present in both HSEC and HUVEC even in the absence of stimulation. Interestingly, although TNFα and methylamine stimulation induced an increase in mRNA, protein levels remained the same under the different treatments as indicated by the percentage of intensity normalised to the endogenous levels of β–actin. In order to validate the presence of MAdCAM-1, the more sensitive technique of flow cytometry was used. MAdCAM-1 protein was again detected on the surface of HSEC isolated from different diseases. A variation in the expression levels between the different diseases was apparent. Specifically, in one set of HSEC from a PBC liver, the levels of membranous MAdCAM-1 were much higher than those in HSEC from a normal liver. However, this pattern was not consistent to a particular type of disease, suggesting that the background of the individuals that the livers came from might play an important role. Moreover, apart from the membrane bound protein, cytoplasmic protein was also detected. Interestingly, in accordance with our previous data, the cytometry confirmed

that the levels of cytoplasmic and membranous MAdCAM-1 protein were unchanged by treatment with TNFα or methylamine.

The western blotting studies revealed that MAdCAM-1 protein of different molecular sizes was present in different cell compartments. A 60kDa protein, which represents the glycosylated monomer of MAdCAM-1, was detected only in the cytoplasm of HSEC, whereas MAdCAM-1 protein of 120kDa and 180kDa was present in both membrane and cytoplasmic compartments. Additional studies of sub–compartmental analysis of MAdCAM-1 protein using membrane and cytoplasmic control proteins, will further enhance our current findings. Previous studies have reported that MAdCAM-1 can exist in a dimeric form (Dando et al., 2002) through an extensive interface formed by residues in the first Ig domain, which might be important for integrin recognition and binding. In support of this, higher levels of the dimeric form were detected at the membrane, consistent with a role in integrin recognition/binding at the cell surface. Dimerisation of Ig domains has been also previously observed in other proteins including human ICAM-1 (Reilly et al., 1995)(Casasnovas et al., 1998). Currently no studies report the presence of any MAdCAM-1 oligomers, however, a MAdCAM-1 protein of 180kDa was detected in our study, which we believe is a trimeric form of the glycosylated monomer. Intriguingly, it seems that the oligomerisation occurs after synthesis and post–translational modification, primarily through O–linked glycosylation on the membrane stalk extending beyond Ig domain II, and N–glycosylation within the Ig domain I (Asn61) (though the latter site has been reported as not essential for activity) (Tan et al., 1998). Both the dimeric and trimeric forms are also present in the cytoplasm. The mechanisms that regulate the oligomerisation of MAdCAM-1, the factors or signals that cause their transfer to the membrane

as well as the role of MAdCAM-1 oligomers, still remain unknown. One possible function of oligomerisation would be to confer mechanical stability upon interaction with ligands in the leukocyte recruitment process, as happens with selectins and their ligands (Alon and Rosen, 2007). It should be noted that MAdCAM-1 protein in our positive control transfected CHO cells was of different molecular size (80kDa) to the endothelial form, which is probably due to the fact that CHO cells lack the appropriate glycosyltransferases responsible for glycosylation of MAdCAM-1.

Our finding of constant levels of protein expression, despite increased mRNA levels was explained by the immunoprecipitation studies. Analysis of HSEC supernatants after stimulation, revealed the presence of a 60kDa soluble MAdCAM-1 protein, which was significantly increased after TNFα plus methylamine stimulation. This finding was in line with our previous findings (see chapter 3), where a brownish smear was apparent above all liver tissue samples.

Release of soluble protein forms upon activation and their circulation in the blood has been reported for other adhesion molecules like E–selectin (Pigott et al., 1992)(Leeuwenberg et al., 1992)(Newman et al., 1993), ICAM-1 (Seth et al., 1991)(Rothlein et al., 1991), VCAM-1 (Pigott et al., 1992)(Gearing et al., 1992), L–selectin (Schleiffenbaum et al., 1992)(Kahn et al., 1994), P–selectin (Dunlop et al., 1992)(Katayama et al., 1992) and VAP-1 (Abella et al., 2004). Generally, soluble adhesion molecules can be released either by enzymatic cleavage of the membrane–bound molecules by proteinases in a process named shedding, or can arise at the level of RNA processing by alternative splicing of mRNA resulting in a non–membrane bound

form that lacks transmembrane domain. The enzyme(s) that catalyse the cleavage of membrane–bound forms of adhesion molecules are believed to include specific matrix metalloproteinases, expressed on the cell surface, containing a potential transmembrane domain at the C–terminus, which does not exist in other metalloproteinases (MMPs) (Sato et al., 1994). In case of L–selectin it has been supported that its soluble form is a result of proteolytic cleavage near to the cell membrane by ADAM17 (TACE) and at least another "sheddase" (Smalley and Ley, 2005). Recent studies have also demonstrated that chemoattractant stimulation of neutrophils bound to E–selectin substrate, or to activated endothelium, results in ADAM17 and L–selectin redistribution and clustering to the trailing edge of cells (Schaff et al., 2008), validating the previous reports supporting that the L–selectin sheddase should be tightly associated with the membrane rather than being a secreted enzyme, since this molecule was found unable to cleave L–selectin from adjacent cells, and its function could be dictated by its precise location on the cell surface near to L–selectin (Preece et al., 1996).

The soluble forms of E–selectin (Leeuwenberg et al., 1992), VCAM-1 (Pigott et al., 1992) (Gearing et al., 1992), ICAM-1 (Tsujisaki et al., 1991), and P–selectin (Katayama et al., 1992) are produced in a similar way. Generation of circulating forms of some of the above adhesion molecules, generated at the RNA level by alternative splicing, has been demonstrated for ICAM-1 (Seth et al., 1991)(Rothlein et al., 1991), P–selectin (Johnston et al., 1990)(Dunlop et al., 1992), and for platelet endothelial cell adhesion molecule–1 (PECAM-1) (Goldberger et al., 1994).

The shedding of membrane–bound molecules might reduce their density on the membrane, thereby regulating the adhesiveness of cells carrying the relevant ligands. In addition, inhibition of adhesion could be also caused by competition between the functional soluble adhesion molecules and their membrane bound forms (Leeuwenberg et al., 1992). Regarding MAdCAM-1, it is not clear if the soluble form detected in our experiments is a truncated form of the oligomeric surface expressed protein released by shedding, or is a different splice variant that does not contain the transmembrane domain. In our study, the molecular weight of the soluble MAdCAM-1 appeared the same as the monomeric protein. Thus we believe that the sMAdCAM-1 is produced either by cleavage of the oligomeric membrane bound protein or the monomeric form is transferred via vesicles from the cytoplasm where it seems to be stored, and released through the cell membrane. An alternatively spliced variant of MAdCAM-1 has been identified that lacks exon 4 encoding the mucin domain (Leung et al., 1996) but no splice variants lacking transmembrane domain have been reported, thus the generation of sMAdCAM-1 through proteolytic cleavage of membrane bound MAdCAM-1 or release of the monomeric form from the cytoplasm, appears more likely. Moreover, it is not clear if the soluble MAdCAM-1 released is biologically active.

A possible purpose of shedding of membrane bound MAdCAM-1 could be to reduce the number of molecules expressed on the cell surface, thus decreasing the number of leukocytes recruited to the site. Another possible role for sMAdCAM-1 could be to interact with its receptor $\alpha 4\beta 7$ integrin on leukocytes competing with the membrane bound form for the same receptor, thus preventing leukocyte recruitment. In addition, an *in vivo* role for sMAdCAM-1 could be to facilitate de–adhesion of leukocytes bound to endothelium so that transendothelial

migration can occur, a role also suggested for other soluble adhesion molecules (Gamble et al., 1990)(Seth et al., 1991)(Leeuwenberg et al., 1992)(Stoddart et al., 1996). Finally, sMAdCAM-1 might result from endothelial activation and might not have any biological function. However, even in the absence of a physiological role the presence of soluble MAdCAM-1 in the serum and urine as previously reported (Leung et al., 2004), may be of value as an immunological marker for monitoring the state and progression of the inflammatory disorders in which it is involved.

The treatment of HSEC with Brefeldin A (a chemical substance which prevents the transfer of newly synthesised proteins to the membrane) prior to TNFα and methylamine stimulation resulted in 45% more MAdCAM-1 protein accumulating in the cytoplasmic compartment when compared with stimulated cells without pre–treatment with Brefeldin A. This emerging evidence supports a model where new MAdCAM-1 protein is synthesised after stimulation, a portion of which remains in the cytoplasm and a portion is transferred to the membrane, then under as yet unknown mechanisms soluble MAdCAM-1 protein is released in the circulation.

The function of MAdCAM-1 was determined using flow based adhesion assays, which revealed that MAdCAM-1 in untreated cells was non–functional as it did not support the recruitment of α4β7+ JY cells. However, when HSEC were stimulated with TNFα (*P=0.02) and its combination with methylamine (**P=0.002) there was a significant increase in the total number of adherent cells, which was inhibited by humanised anti–MAdCAM-1 monoclonal Ab (P1; ***P=0.0006). Interestingly, the decrease in adherent cells was also seen after treatment with antibodies against the α4β7 integrin on the surface of JY cells (ACT-1; *P=0.04). However, in

both cases, there was residual binding of JY cells to the endothelium indicating that other adhesion molecules were also present. Indeed the JY cell line expresses α4β1 (B. M. Chan et al., 1992) and LFA-1 (Dustin and Springer, 1988) whose ligands are VCAM-1 and ICAM-1, respectively. Up–regulation of ICAM-1 and VCAM-1 by hepatic sinusoidal endothelial cells upon TNFα stimulation has been previously demonstrated by our group (Adams et al., 1991) (Lalor et al., 2002a). Therefore, we believe that the adherence of JY cells observed under TNFα stimulation and after blocking MAdCAM-1 in the TNFα plus methylamine stimulated cells is due to ICAM-1 and VCAM-1. Similarly, in HUVEC, the number of adherent JY cells on TNFα and TNFα plus methylamine stimulated cells where MAdCAM-1 was blocked (with P1) were almost similar, also supporting that JY cells may adhere to other adhesion molecules such as ICAM-1 and VCAM-1, which are both expressed on HUVEC treated with TNFα (Zhou et al., 2007). In HUVEC as well, increased levels of adherent cells were observed under TNFα and methylamine stimulation, which however did not achieve statistical significance. Of note, unstimulated HUVEC supported higher levels of adhesion (20.8±3.8) compared to HSEC (4.6±1.9) (adherent cells/$mm^2/10^6$ cells perfused ± SEM), which might suggest differences in basal expression of adhesion molecules other than MAdCAM-1. In accordance with our findings in the previous chapter (see chapter 3), our data suggest that under non–inflamed conditions MAdCAM-1 in HSEC and HUVEC is present in a non–functional state that cannot support leukocyte recruitment.

However, under inflammatory conditions, TNFα induces MAdCAM-1 expression, which in the presence of methylamine adopts a functional conformation, possibly by mechanisms similar to integrin activation through folding alterations from a low–affinity bent form to a high–affinity

and extended form where the ligand–binding "pocket" opens, leading to leukocyte–integrin recognition and binding. Methylamine is a primary amine produced endogenously by the metabolism of adrenaline, sarcosine, creatinine and lecithin or exogenously by ingestion from food, wine and cigarette smoke (Pirisino et al., 2001). Therefore, we propose that consumption of compounds rich in methylamine would lead to increased levels entering the liver through the portal vein. Here, methylamine could be catabolised by VAP-1 triggering the conformational change of MAdCAM-1 to a functional adhesion molecule. This would also explain the prominent staining for MAdCAM-1 we observed in the endothelium of portal vessels (see chapter 3). In support of this, experimental and clinical studies highlight the importance of methylamine, as well as ammonium and other basic compounds such as neurotoxins, which are increased in liver or renal diseases or Alzheimer's disease and vascular dementia (Pirisino et al., 2004). Thus, dietary habits or changes in nutrients in portal blood as a consequence of colitis might contribute to ectopic MAdCAM-1 expression and the "entero-hepatic" recirculation of lymphocytes.

In conclusion, in this chapter we describe the constitutive presence of MAdCAM-1 in both HSEC and HUVEC. TNFα and methylamine treatment significantly increased MAdCAM-1 mRNA levels which were translated into protein, part of which were transferred into the membrane where the surface expressed protein seemed to be cleaved in order to release soluble MAdCAM-1, and part remained in the cytoplasm, where it was post–translationally modified (Figure 4.20). Interestingly, the MAdCAM-1 protein present on unstimulated endothelial cells was non–functional being unable to support the binding of α4β7+ JY cells, whereas under TNFα and methylamine stimulation elevated functional MAdCAM-1 protein levels led to an

increase in the total number of adherent cells, which was decreased after blockade of either MAdCAM-1 or its ligand α4β7 integrin.

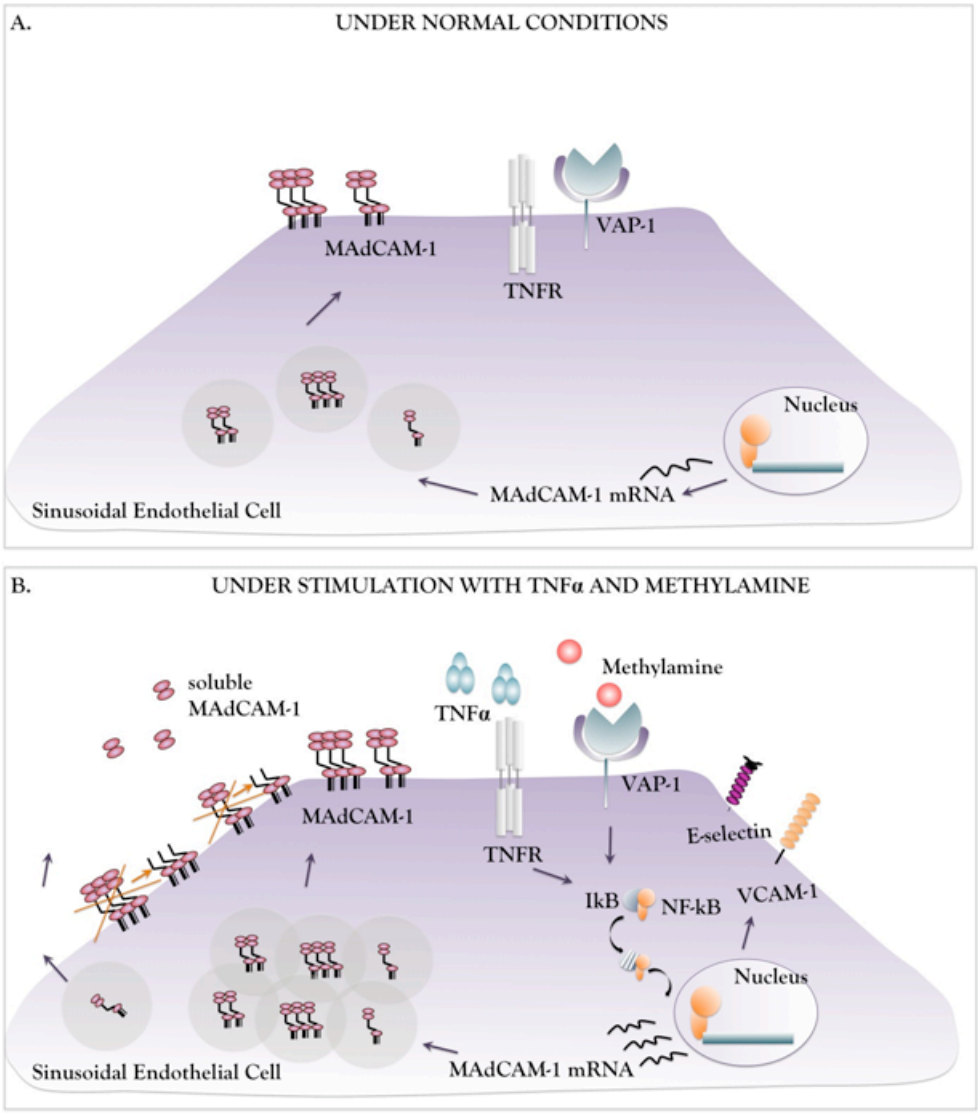

Figure 4.19 MAdCAM-1 expression in endothelial cells. Under normal conditions MAdCAM-1 mRNA and protein are present in endothelial cells. In the cytoplasmic compartment as well as in the surface, MAdCAM-1 protein of different molecular weights is present. Under stimulation with TNFα alone or in combination with methylamine, intracellular signalling pathways seem to be activated through VAP-1 and TNFR, that lead to NF-κB transcription factor activation and subsequently to the increased production of MAdCAM-1 mRNA levels. MAdCAM-1 protein of 60kDa, 120kDa and 180kDa is synthesised and part of it is transferred to the membrane where previously surface expressed protein seems to be cleaved to secrete soluble form of MAdCAM-1. Another potential pathway for sMAdCAM-1 could be the transfer of the 60kDa monomer from the cytoplasm through the cell membrane to the circulation.

CHAPTER 5

Role of VAP-1 Enzymatic Activity In MAdCAM-1 Expression In Human Hepatic Sinusoidal Endothelial Cells

5.1 INTRODUCTION

VAP-1 is a membrane bound homodimeric protein composed of two identical 90kDa subunits. It is constitutively expressed on the luminal surface of high endothelial venules of peripheral lymph nodes and tonsils, as well as within the cytoplasm of discrete venules, indicating that it is stored intracellularly (Jalkanen and Salmi, 1993). VAP-1 is also detected on hepatic sinusoidal endothelial cells and in other vascular endothelial cells particularly at sites of inflammation. Weak staining of VAP-1 has been reported in the high endothelial venules of Peyer's patches and the flat walled vessels within the lamina propria (McNab et al., 1996). VAP-1 is not restricted to endothelial cells since it is also detected in the smooth muscle cells of arteries, the bowel wall and in adipocytes, pericytes and follicular dendritic cells within germinal centres (Salmi et al., 1993)(Jaakkola et al., 1999), but VAP-1 expression has not been reported on leukocytes or epithelial cells (Salmi et al., 1993). Interestingly, under inflammatory conditions VAP-1 is rapidly up–regulated in non–lymphoid tissue such as the skin and synovium, gut and heart (Salmi et al., 1993)(Arvilommi et al., 1996)(Smith et al., 1998).

VAP-1 is an endothelial adhesion molecule that supports leukocyte rolling, firm adhesion and transmigration (Tohka et al., 2001)(Lalor et al., 2002a)(Salmi and Jalkanen, 2006). Of note, VAP-1 can operate in an L–selectin independent manner supporting the binding of both L–selectin negative and L–selectin positive lymphocytes via sialic acids present on oligosaccharides in the extracellular domain, which are important for lymphocyte binding (Salmi and Jalkanen, 1996). VAP-1 can also mediate leukocyte subtype–specific adhesion. Among mononuclear cells, the VAP-1 dependent pathway is important for binding of CD8+ T killer cells and natural killer cells but early studies suggested not for B cells or monocytes (Salmi et al., 1997). However

controversy remains concerning which particular leukocytes subsets can interact with VAP-1, and recent studies including those from our own group, have demonstrated that VAP-1 supports monocyte transendothelial migration *in vitro* and *in vivo* to sites of inflammation in models of air pouch inflammation (Merinen et al., 2005), and CD4+ Th2 helper cell adhesion in hepatic post–sinusoidal venules and sinusoids during ConA induced inflammation (Bonder et al., 2005).

What is particularly interesting about this molecule is its enzymatic activity. Cloning of VAP-1 in 1998 (Smith et al., 1998) revealed significant sequence similarity to the copper–containing amine oxidases, which are a subfamily of monoamine oxidases. Therefore, apart from being an endothelial adhesion molecule, VAP-1 is also an enzyme, or more accurately an ectoenzyme, as its extracellular domain contains its catalytic activity (Jalkanen and Salmi, 2001). VAP-1 catalyses the general reaction:

$$RCH_2NH_2 + O_2 + H_2O \longrightarrow RCHO + NH_3 + H_2O_2$$

in which a primary amine is oxidatively deaminated to the corresponding aldehyde with a simultaneous release of hydrogen peroxide and ammonia (Salmi and Jalkanen, 2001). More precisely, this reaction consists of two stages. In the reductive half reaction, the NH_2–group of the substrate (primary amine) binds to the topa–quinone cofactor located in the active site of the enzyme, leading to the formation of a covalent Schiff base between the enzyme and the substrate and the release of an aldehyde. Thereafter, in the oxidative half reaction, the enzyme is re–oxidised by the reaction with molecular oxygen resulting in the release of H_2O_2 and NH_3 (Jalkanen and Salmi, 2008).

All the end products released as a result of oxidative deamination of primary amines by VAP-1/SSAO are biologically active. The H_2O_2 end product is particularly significant, as this reactive oxygen species is toxic at higher concentrations, whereas at lower concentrations it has been recognised as a signal–transducing element (Schreck et al., 1991)(Schreck et al., 1992)(Finkel, 1998)(Kunsch and Medford, 1999)(Bogdan et al., 2000), and has been shown to be involved in up–regulation of adhesion molecules such as P–selectin and E–selectin (Jalkanen et al., 2007), and ICAM-1 (Bradley et al., 1993).

All amines can be substrates for VAP-1 but the most widely used substrate in experimental procedures is benzylamine, which is not physiological. *In vivo*, at least two endogenously formed amines, methylamine and aminoacetone, can serve as VAP-1/SSAO substrates. Methylamine is formed during endogenous degradation of sarcosine, creatinine, lecithin and adrenaline, and its oxidation results in the formation of formaldehyde (Pirisino et al., 2001). Aminoacetone is produced from the metabolism of glycine or threonine, and the corresponding aldehyde is methylglyoxal (2–oxopropanal). Both formaldehyde and methylglyoxal are potentially toxic (O'Sullivan et al., 2004).

As well as the membrane bound form of VAP-1, soluble enzymatically active VAP-1 has been also reported. sVAP-1 is found in the serum of healthy individuals and levels are increased in patients with certain inflammatory conditions particularly inflammatory liver diseases (Kurkijarvi et al., 1998). Precisely, higher levels of sVAP-1 are detected in the livers of patients with active cirrhosis due to ALD, and lower levels in patients with PBC. However, in patients with PSC, the levels of sVAP-1 have not been reported to significantly differ from those in serum of normal individuals.

On the other hand, in the inflammatory diseases of rheumatoid arthritis and inflammatory bowel diseases not elevated levels of sVAP-1 have been reported (Kurkijarvi et al., 1998).

As there is a precedent role for the metabolites of VAP-1 enzyme activity promoting adhesion molecule up–regulation, it was investigated whether the effects of methylamine on MAdCAM-1 expression observed in the previous chapter were due to VAP-1 enzymatic activity. Initially, the ability of VAP-1 expressing HSEC to up–regulate MAdCAM-1 expression after methylamine and TNFα stimulation was tested, using HSEC transduced with adenoviral constructs to ensure maximal VAP-1 expression for these experiments. Finally, the effects of the end products of methylamine deamination by VAP-1 (hydrogen peroxide, ammonia and formaldehyde) on MAdCAM-1 expression by HSEC were investigated.

5.2 RESULTS

5.2.1 Confirmation of The Enzymatic Capacities of our VAP-1 Adenoviral Constructs

The two adenoviral constructs that were used were described in section 2.14.2. In particular, the enzymatically inactive VAP-1 construct contained a single amino acid change at position 471, which changed a tyrosine residue to a phenylalanine rendering the protein enzymatically non–functional. We began by testing whether the adenoviral constructs we were supplied with, were indeed enzymatically active and inactive respectively, by using the Amplex Red assay. Here H_2O_2 released upon VAP-1 activity reacts with HRP and the Amplex Red reagent to produce a red fluorescent signal. HSEC were infected with adenoviral constructs containing wild–type hVAP-1 (hVAP-1), enzymatically dead (hVAP-1_Y471F), or constructs without any VAP-1 (LacZ). Non–infected HSEC were used as controls. When HSEC transfected with wild–type hVAP-1 were exposed to benzylamine a signal was detected over the 3 hour period (Figure 5.1A shows the first 80 minutes of the reaction), which was not observed for HSEC transfected with hVAP-1 mutant or LacZ vectors or in non–transfected cells. This signal was abolished when the endothelial cells were additionally treated with bromoethylamine (BEA), the SSAO activity inhibitor (Figure 5.1B).

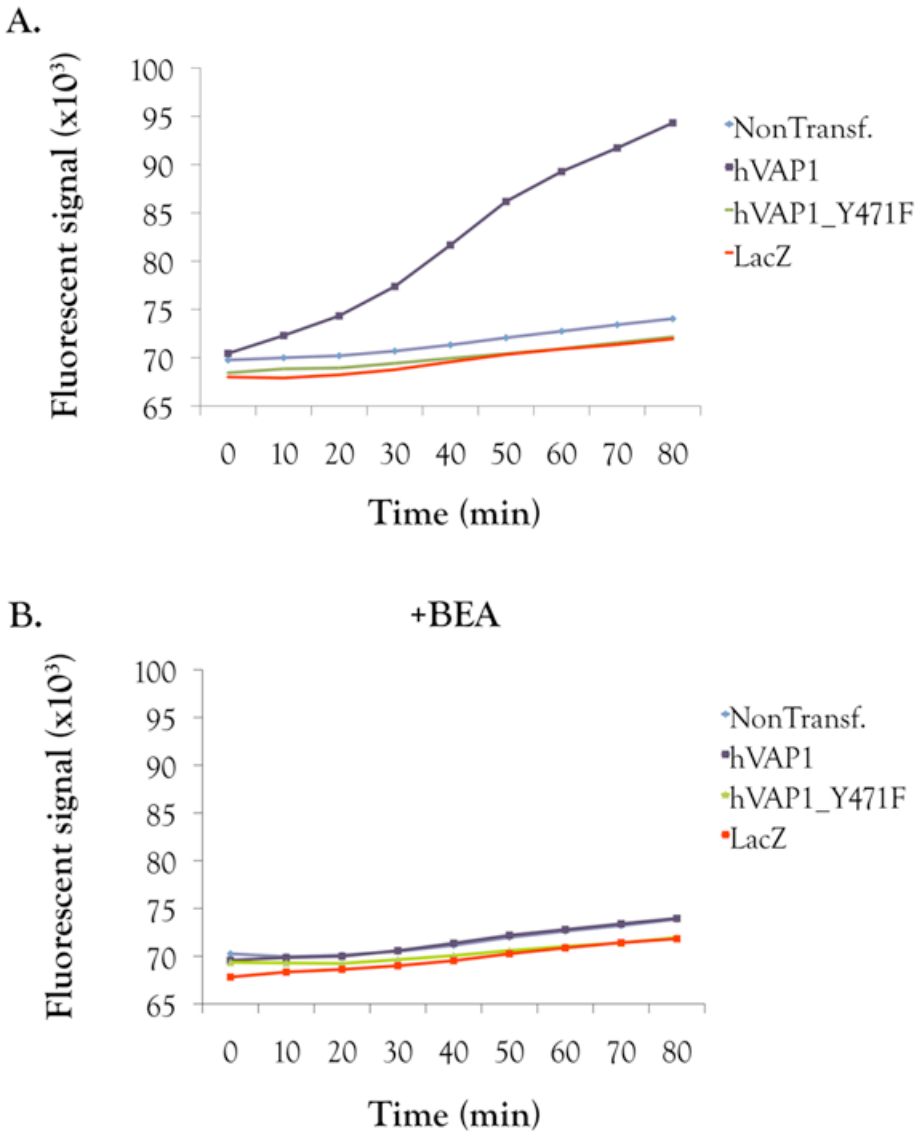

Figure 5.1 Cells transfected with wild-type VAP-1 adenoviral constructs produce enzymatically active hVAP-1. HSEC seeded on 24-well plates were transfected with adenoviral constructs containing wild-type hVAP-1, an enzymatically dead mutant of hVAP-1 (hVAP-1_Y471F) or adenoviral constructs without any hVAP-1 (only LacZ), at a plasticity of 600pfu/cell. Non-transfected HSEC were used as an additional control. (A) Cells were treated with 2mM benzylamine and (B) with benzylamine and 400μM SSAO inhibitor 5' bromoethylamine (BEA), and generation of H_2O_2 was detected using Amplex Red reagent. Data represent mean of triplicate wells for each sample in representative experiment. *y* axis shows the fluorescent signal released (signal x 10^3) over the time (x axis).

5.2.2 Role of VAP-1/SSAO Enzymatic Activity In Expression of MAdCAM-1

Hepatic sinusoidal endothelial cells were transfected with the adenoviral vectors described above and VAP-1 expression was confirmed by flow cytometry. Figure 5.2 and Table 5.1 show that greater than 95% of cells stained positively for hVAP-1 and hVAP-1_Y471F and that the median channel fluorescence (MCF) values were similar for both hVAP-1 and hVAP-1_Y471F constructs. We noted that not all endothelial cells accepted transduction with wild–type hVAP-1 adenoviral vector in the same way. In particular, a set of HSEC isolated from an AIH liver appeared apoptotic and detached from culture surface after transfection (Figure 5.3B), whereas another HSEC isolate from a PBC liver appeared normal after transduction with the same vector (Figure 5.3A).

Non–transfected HSEC, and HSEC transfected with the adenoviral constructs were treated with methylamine and TNFα either alone or in combination for 2 hours prior to analysis of MAdCAM-1 mRNA and protein expression. In non–transfected HSEC statistically significant elevated MAdCAM-1 mRNA levels were observed (*$P<0.05$)(Figure 5.4A), whereas the endothelial cells transfected with either enzymatically active or enzymatically dead hVAP-1 responded similarly after TNFα alone or TNFα plus methylamine stimulation. In both cases a 15–fold increase in MAdCAM-1 mRNA levels was observed (Figure 5.4B). Although there was no detectable difference in the effect of enzymatically active and dead mutant hVAP-1 at the transcription level, increased levels of MAdCAM-1 protein were observed in HSEC transfected with the wild–type hVAP-1 (Figure 5.5). In HSEC transduced with enzymatically active hVAP-1 there was an obvious increase in MAdCAM-1 protein levels when compared with HSEC transfected with the hVAP-1 mutant and non–transfected HSEC (Figure 5.5). Western blotting

experiments also revealed that the trimeric form of MAdCAM-1 (180kDa) was present in 4 out of the 7 cases tested (Figure 5.6, Table 5.2). The specificity of the band was confirmed by staining with an isotype–matched control antibody.

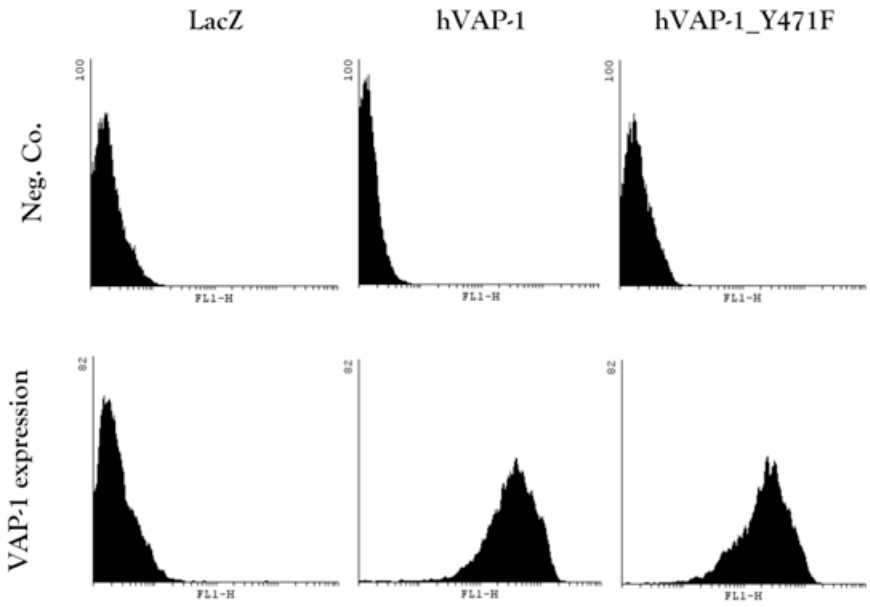

Figure 5.2 Confirmation of VAP-1 positivity of transfected cells. HSEC were transfected with adenoviral constructs containing wild-type hVAP-1 or an enzymatically inactive mutant of hVAP-1 (hVAP-1_Y471F) and stained with anti-VAP-1 or negative control mouse anti-human antibodies prior to FACs analysis. Representative data for 7 different HSEC.

HSEC+hVAP-1	% Positive Cells	MCF
Control	96.62 ± 1.38	197.58 ± 40.35
TNFα	97.11 ± 0.83	201.04 ± 47.18
MA	96.12 ± 2.09	206.60 ± 53.01
TNFα+MA	95.35 ± 2.93	212.83 ± 63.36
HSEC+hVAP-1_Y471F	**% Positive Cells**	**MCF**
Control	95.57 ± 2.06	216.75 ± 40.02
TNFα	97.18 ± 1.44	215.16 ± 39.02
MA	91.68 ± 6.85	202.17 ± 34.49
TNFα+MA	98.03 ± 0.67	199. 14 ± 22.25

Table 5.1 Expression of VAP-1 after treatment of transduced HSEC. Pooled data from n=7 different HSEC transfected with adenoviral constructs containing wild-type hVAP-1 (HSEC+hVAP-1) or enzymatically-dead mutant hVAP-1 (HSEC+hVAP-1_Y471F), showing mean values ± SEM for percentage of positive cells and median channel fluorescence (MCF) for VAP-1 staining of HSEC.

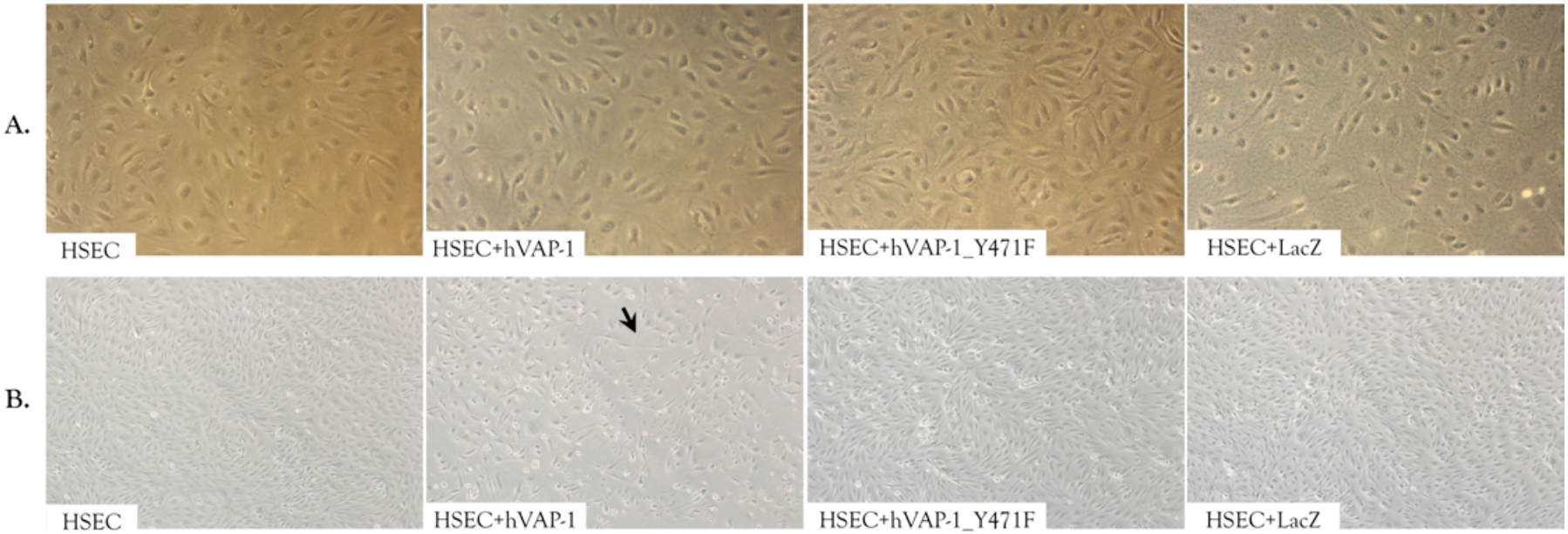

Figure 5.3 Representative images of cell morphology after adenoviral transfection. Selected images of HSEC after transfection with adenoviral constructs containing wild-type hVAP-1, enzymatically inactive hVAP-1 (hVAP-1_Y471F) or LacZ. HSEC that were not transfected were used as positive control. HSEC isolated from (A) PBC and (B) AIH liver. Pictures obtained with a 20x and 10x objectives in (A) and (B) respectively.

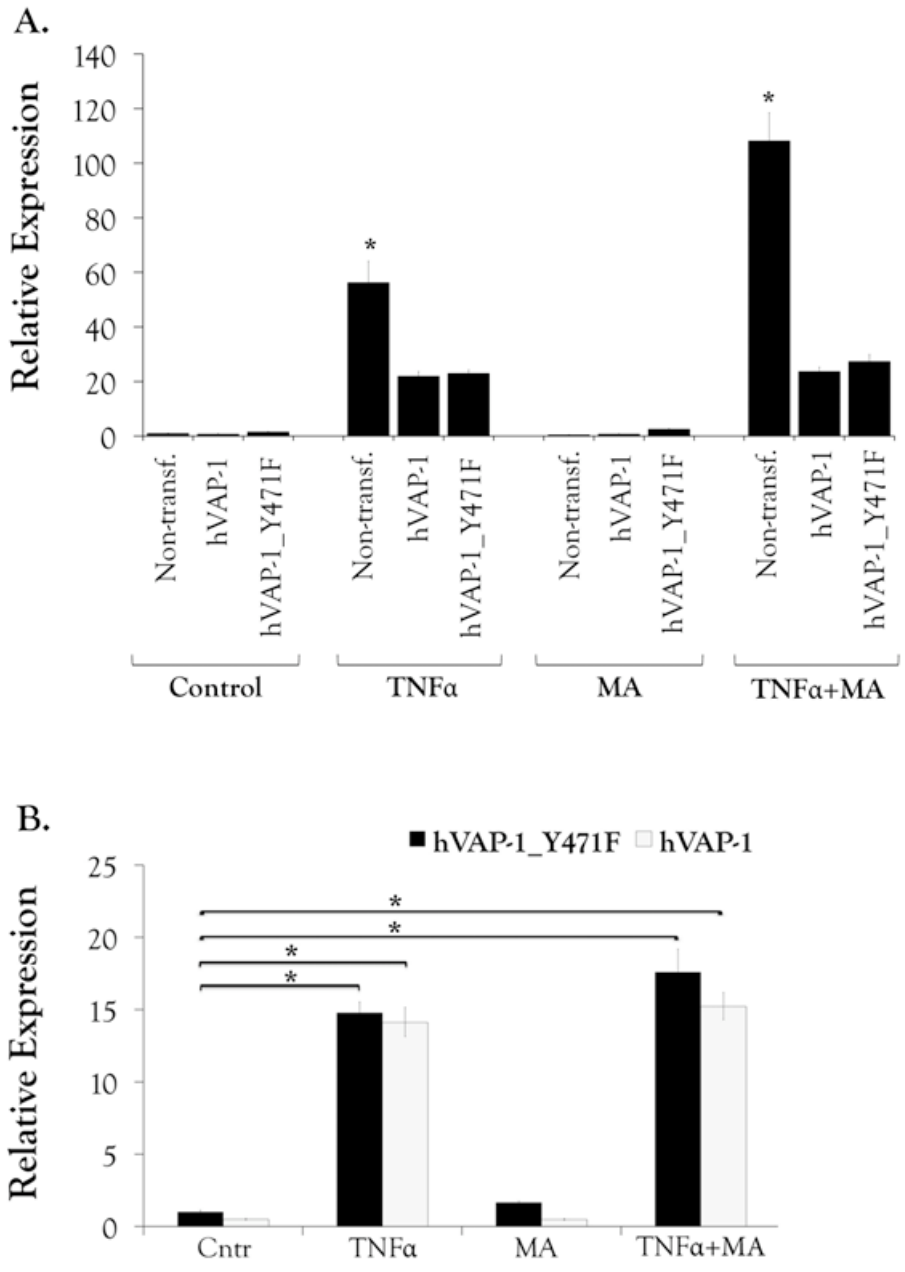

Figure 5.4 MAdCAM-1 mRNA expression in HSEC after adenoviral transfection. Non–transfected HSEC, and HSEC transfected with hVAP-1 enzymatically active or hVAP-1_Y471F, an enzymatically inactive mutant of hVAP-1, were stimulated with TNFα (20ng/ml) or methylamine (MA; 50μM) alone or in combination for 2 hours prior to RNA extraction and mRNA expression analysis using quantitative PCR. Data represent the N-fold change in MAdCAM-1 mRNA expression levels (mean ± SEM) from n=8 different HSEC (3PBC, 1AIH, 1NL, 3Resected). (A) MAdCAM-1 mRNA levels expressed relatively to non–transfected and untreated HSEC. (B) MAdCAM-1 mRNA levels expressed relatively to untreated HSEC transfected with hVAP-1_Y471F. Statistical analysis performed by Student's t-test (*$P<0.05$).

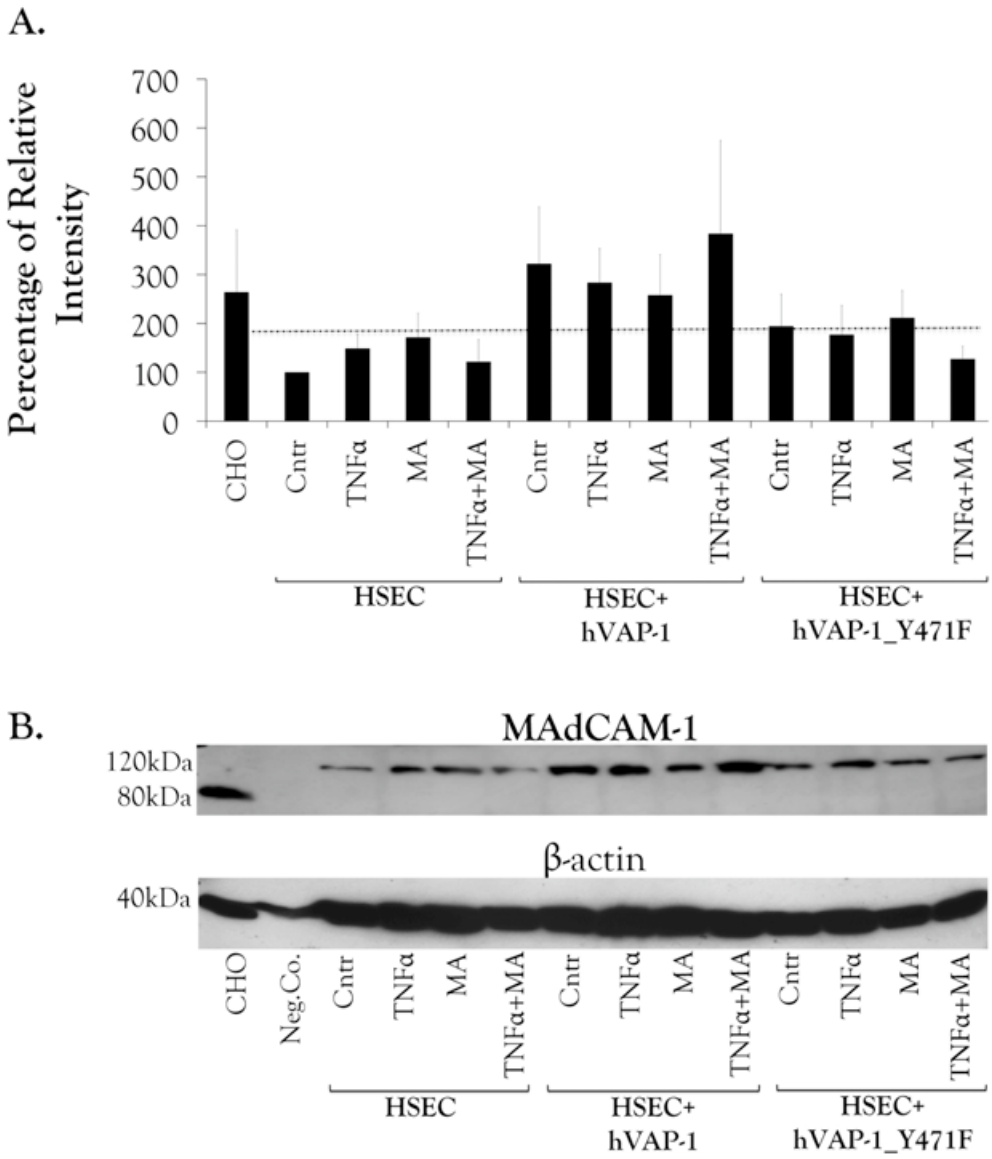

Figure 5.5 MAdCAM-1 protein expression in transfected HSEC. HSEC transfected with adenoviral constructs containing wild-type hVAP-1 or enzymatically dead hVAP-1 (hVAP-1_Y471F), as well as non-transfected HSEC, were stimulated with TNFα (20ng/ml) or methylamine (MA; 50μM) alone or in combination for 2 hours, prior to protein lysis and western blot analysis. (A) Data represent percentage of MAdCAM-1 protein expression relatively to endogenous β-actin levels, compared to expression in un–stimulated and non-transfected HSEC, (Cntr; set to 100%). Data represent mean ± SEM of percentage of relative intensity from n=7 different HSEC (3NR, 3PBC, 1AIH). (B) Representative image after western blot analysis. CHO cells were used as positive control and JY cells as negative control.

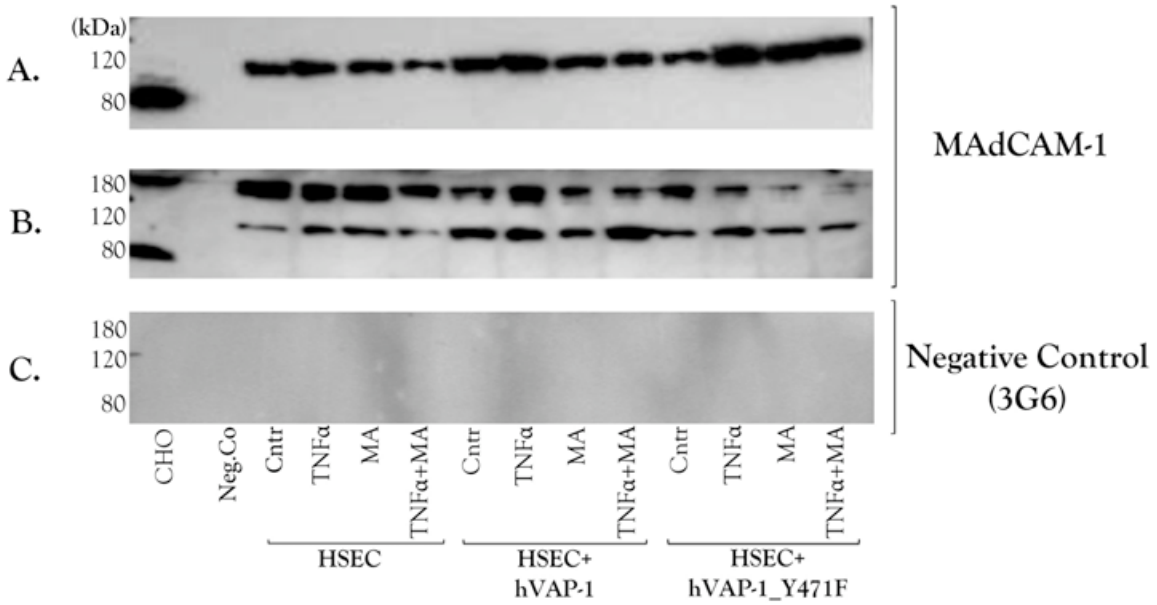

Figure 5.6 MAdCAM-1 of 180kDa molecular size is apparent in HSEC. HSEC transfected with adenoviral constructs containing wild-type hVAP-1 or enzymatically dead hVAP-1 (hVAP-1_Y471F), as well as non-transfected HSEC, were stimulated with TNFα (20ng/ml) or methylamine (MA; 50μM) alone or in combination for 2 hours, prior to protein lysis and western blot analysis. Representative images of MAdCAM-1 expression after western blot analysis from two different (A) and (B) HSEC isolates. (C) Representative image after striping and re-probing membranes with an isotype–matched control antibody (3G6). CHO cells were used as positive control and JY cells as negative control.

LIVER	MOLECULAR WEIGHT OF MADCAM-1 PROTEIN DETECTED	
	120kDa	180kDa
Resected Liver 1	+	-
Resected Liver 2	+	+
Resected Liver 3	+	+
PBC 1	+	-
PBC 2	+	+
PBC 3	+	+
AIH	+	-

Table 5.2 Expression of different MAdCAM-1 proteins in HSEC isolates. Table represents pooled data from n=7 HSEC from different liver diseases (3 Resected non-diseased, 3PBC, 1AIH) and summarises the nature of MAdCAM-1 protein species found in each isolate.

5.2.3 The End Products of VAP-1 Enzyme Activity Induce MAdCAM-1 Expression in HSEC

In order to further investigate the effects of VAP-1 enzymatic activity on MAdCAM-1 expression, the direct effects of the end products released after the oxidative deamination of methylamine by VAP-1, were studied. Non–transfected HSEC were stimulated with hydrogen peroxide (H_2O_2), formaldehyde (HCHO) and ammonia (NH_3) for 4 hours. Fresh H_2O_2 was added every 30min, in order to compensate for loss due to decomposition by endogenous cell peroxidases. The results show that the combination of all three end products used at a dose of 10μM significantly increased MAdCAM-1 expression (*P=0.04) (Figure 5.7). Interestingly, when enzymatically active sVAP-1 and methylamine were administered directly to HSEC in order to generate end products in real–time *in situ*, MAdCAM-1 expression was induced in the same pattern (Figure 5.8).

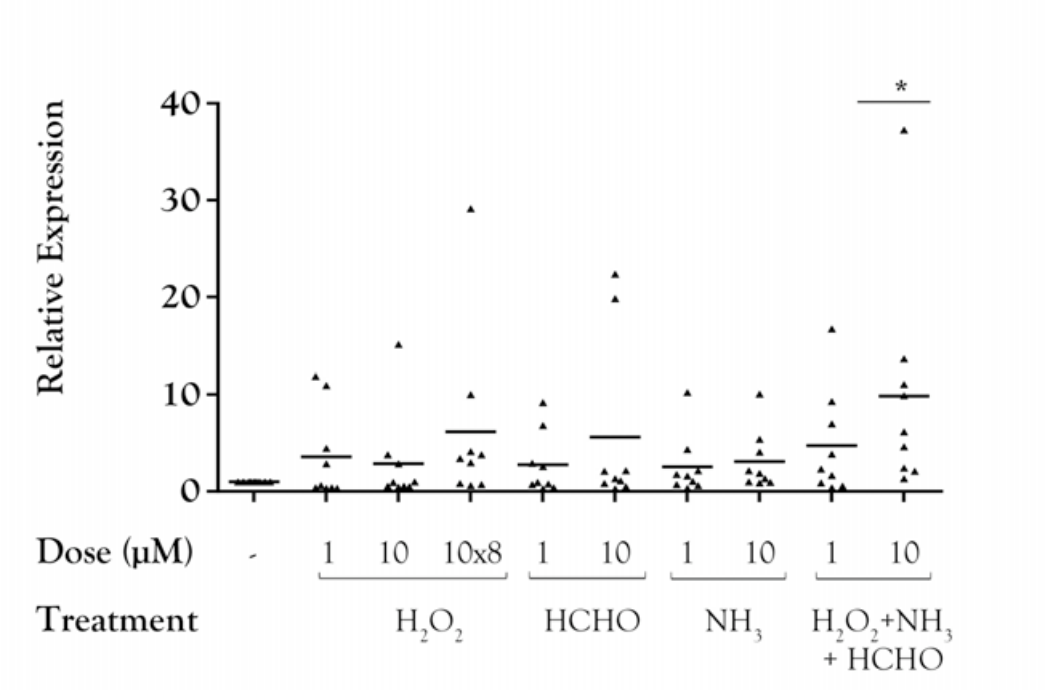

Figure 5.7 End products of VAP-1 enzyme activity induce MAdCAM-1 expression by HSEC. Non-transfected HSEC were stimulated with single doses of hydrogen peroxide (H_2O_2), formaldehyde (HCHO) and ammonia (NH_3) at 1 and 10μM for 4 hours. Where indicated, HSEC were treated repeatedly with 10μM H_2O_2 (x8 every 30min) or with the combination of all three end products (each at 1μM or 10μM, single dose, H_2O_2 repeatedly). RNA was extracted from cells and MAdCAM-1 mRNA expression was measured using real-time PCR. Data represent relative expression of treated versus non-treated HSEC [mean ± SEM from n=9 different HSEC (2NL, 3NR, 3PBC, 1AIH)]. Statistical analysis performed by Student's t-test (*P=0.04).

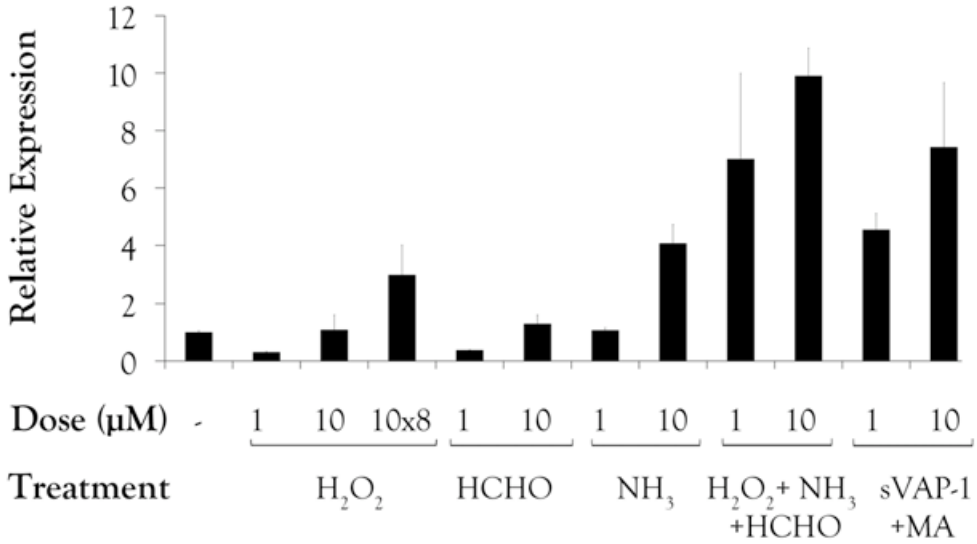

Figure 5.8 End products of methylamine deamination by VAP-1 produced locally or exogenously added, induce MAdCAM-1 expression in HSEC. Non-transfected HSEC were stimulated with single doses of hydrogen peroxide (H_2O_2), formaldehyde (HCHO) and ammonia (NH_3) at 1 and 10μM for 4 hours. Where indicated, HSEC were treated repeatedly with 10μM H_2O_2 (x8 every 30min) or with the combination of all three end products (each at 1μM or 10μM, single dose, H_2O_2 repeatedly). In separate wells, HSEC were stimulated with sVAP-1 (500ng/ml) and methylamine (MA) at 1 and 10μM for 4 hours. RNA was extracted from all cells and MAdCAM-1 mRNA expression was measured using quantitative PCR. Representative graph for one sample of HSEC showing the response of non-transfected cells to sVAP-1 and methylamine. Data represent relative expression of treated versus non-treated HSEC (mean ± SEM of a triplicate).

5.3 DISCUSSION

In this study adenoviral constructs containing human wild–type and mutant VAP-1, which were enzymatically active and inactive respectively, were used. In the mutant version a single amino acid change at position 471, changed a tyrosine residue into a phenylalanine rendering the protein enzymatically dead. The tyrosine residue is the precursor of the topa–quinone, the organic cofactor of the SSAO, which is located in the active site of the enzyme and plays a key role in the first half of the enzymatic reaction. Phenylalanine cannot be processed into topa–quinone meaning that this amino acid change (Y471F) encodes an enzymatically dead mutant, which is structurally similar to VAP-1 (Koskinen et al., 2004). The activity states of the two constructs were confirmed using the Amplex Red Assay. These viruses have previously been used by Jalkanen *et al.* in human umbilical vein endothelial cells to show the role of VAP-1/SSAO activity on P– and E– selectin expression (Jalkanen et al., 2007) and here, they were used in order to confirm the role of VAP-1 in MAdCAM-1 expression.

Interestingly, one sample of HSEC transfected with the wild–type hVAP-1 construct, showed dramatic morphological change and cell apoptosis, whilst others appeared unaffected by transfection. This may suggest as yet unidentified, disease specific changes inherent in isolated endothelial cells, which render them particularly sensitive to products of VAP-1 metabolism. However, since that effect was obvious in only 1/7 livers tested it is not feasible to draw a general conclusion regarding the role of VAP-1/SSAO in a particular liver disease. The higher molecular weight species of MAdCAM-1 protein (180kDa) was detected in 4 out of 7 samples suggesting that there may be disease–specific differences between endothelial isolates which may alter protein expression or function. It is not clear yet why some cells express the trimeric

MAdCAM-1 and some do not and the sample numbers in the current study are too small to draw disease–specific conclusions.

MAdCAM-1 mRNA levels appeared almost similar between the cells transduced with wild–type hVAP-1 and the cells transduced with the mutant hVAP-1 with no statistically significant differences among them. Statistical analysis revealed significantly elevated levels under TNFα and TNFα plus methylamine stimulation (*$P<0.05$) (Figure 5.4B) in both hVAP-1 and hVAP-1 mutant transfected cells, suggesting that the enzymatic activity of VAP-1 has little effect or no effect on MAdCAM-1 expression in HSEC. It should be noted, that the transfection of HSEC with the adenoviral constructs occurred in human serum free medium, as it is known that sVAP-1 is present in the human serum and its presence prevents transfection. Recent unpublished studies from our group (C. Weston *et al.)* demonstrate the ability of HSEC to take up sVAP-1 from circulation and present it on the endothelial cell surface where it retains its enzymatic function. Since the endothelial cells were cultured in complete endothelial medium containing human serum after transfection in order to help them recover from the shock of the procedure, it is possible that the induction of MAdCAM-1 mRNA expression seen in the presence of mutant hVAP-1 was due to the sVAP-1 from serum that was presented on the endothelial cells. Thus the magnitude of MAdCAM-1 mRNA expression in cells transduced with mutant hVAP-1 may decrease if the experiments were performed in sera depleted of sVAP-1.

In support of this hypothesis and in contrast to the relative mRNA expression data, cells that were transfected with enzymatically active hVAP-1 expressed more MAdCAM-1 protein when

compared with non–transfected cells and cells transfected with enzymatically inactive hVAP-1, suggesting that VAP-1/SSAO is involved in the translational or post–translational regulation of MAdCAM-1 expression rather than in transcriptional or post–transcriptional regulation.

Our data from non–transfected HSEC validate the role of the VAP-1/SSAO activity in MAdCAM-1 up–regulation. The combination of all the three potential end products either when added exogenously or when locally generated in real–time by sVAP-1 and methylamine, significantly induced MAdCAM-1 expression in HSEC (*P=0.04). Many studies now implicate H_2O_2 in the regulation of adhesion molecule expression. In particular, the hydrogen peroxide either alone or in combination with the other end products released by VAP-1/SSAO deamination reaction, has been shown to modulate endothelial expression of E–selectin and P–selectin (Jalkanen et al., 2007). Moreover, a variety of studies have supported the ability of the reactive oxidant H_2O_2 to induce endothelial cell expression of ICAM-1 as well as ICAM-1 dependent adhesion of polymorphonuclear cells (Lo et al., 1993)(Bradley et al., 1993)(Ichikawa et al., 1997)(Ng et al., 2002), and induction of ICAM-1 expression on human epidermal keratinocytes (Ikeda et al., 1994). The role of H_2O_2 in induction of ICAM-1 expression in human umbilical vein endothelial cells, as well as in induction of P–selectin has been also reported (Patel et al., 1991)(Lo et al., 1993). Of note, it has been demonstrated that H_2O_2 activates ICAM-1 gene transcription via AP-1 (composed of Jun and Fos protein dimers) and Ets transcription factors, but not via NF-κB (Roebuck et al., 1995). In contrast to H_2O_2, TNFα could induce ICAM-1 transcription via activation of promoter sequences containing C/EBP and NF-κB binding elements. The ability of H_2O_2 to activate the AP-1 and NF-κB transcription factors has been also reported in mouse osteoblastic cells in HeLa and Jurkat cells (Nose et al.,

1991), and in T cells H_2O_2 activates the AP-1 signal transduction pathway through tyrosine phosphorylation of kinase intermediates (K. Nakamura et al., 1993a). Although, it appears that H_2O_2 cannot induce ICAM-1 activation through NF-κB, Schreck *et al.* have reported that in some cell lines H_2O_2 activates NF-κB, possibly through post–translational modification of the NF-κB subunits themselves or by regulation of other transcriptional cofactors that influence the transcriptional activity of NF-κB (Schreck et al., 1991). These data support the presence of distinct intracellular regulatory mechanisms involving unique sequence elements within the promoter region of a gene. Interestingly, although Bradley *et al.* showed that H_2O_2 did not induce endothelial expression of E–selectin and VCAM-1, Marui *et al.* demonstrated that when using the antioxidant pyrrolidine dithiocarbamate (PDTC, an inhibitor of H_2O_2), the activation of VCAM-1 transcription and expression in HUVEC was inhibited through inhibition of NF-κB regulatory proteins (Bradley et al., 1993)(Marui et al., 1993). Studies of the human VCAM-1 promoter region have suggested that activation of VCAM-1 transcription in endothelial cells by TNFα is dependent at least in part on the activation of NF-κB (Iademarco et al., 1992)(Neish et al., 1992). Thus, although some of the above data are controversial, there is a precedent role for H_2O_2 to alter adhesion molecule expression in endothelial cells via activation of different transcription factors, and thus similar mechanisms may operate in case of MAdCAM-1 when HSEC are stimulated with hydrogen peroxide, since MAdCAM-1 promoter region contains NF-κB transcription factor sites. In support of this, recent studies from our group (Lalor et al., 2002a) show that the H_2O_2 produced during VAP-1 mediated amine oxidation induces expression of P– and E–selectin, ICAM-1 and VCAM-1 and a chemokine CXCL8 by stimulating the PI3K, MAPK and NF-κB pathways.

We believe that our study supports the hypothesis that the H_2O_2 released from the deamination reaction between VAP-1/SSAO and its substrate methylamine activates NF-κB and its binding element on the promoter region of MAdCAM-1 (Leung et al., 1997). Moreover, TNFα a classical activator of NF-κB also induced expression of MAdCAM-1, which supports NF-κB–dependent regulation of MAdCAM-1 transcription (Figure 4.19). Although it is not clear how formaldehyde and ammonia could induce MAdCAM-1 expression, other studies suggest that released aldehydes can function as direct cross–linkers between endothelial cells and lymphocytes. Ammonium ion generated by ammonia can be transported through cell membranes by special transporter proteins (Biver et al., 2008) and be processed in the liver, kidneys and skeletal muscles for conversion into urea and to glutamine.

In conclusion, in this chapter the role of methylamine in induction of MAdCAM-1 expression in hepatic endothelial cells was validated, since the use of adenoviral constructs containing enzymatically active and inactive hVAP-1 demonstrated that the end products of methylamine deamination by VAP-1 are responsible for MAdCAM-1 expression.

CHAPTER 6

MAdCAM-1 Expression In Mice

6.1 INTRODUCTION

Murine MAdCAM-1 is a 60kDa endothelial cell surface molecule, member of the Ig immunoglobulin supergene family, selectively expressed in mesenteric lymph nodes, high endothelial venules of Peyer's patches, lamina propria of the small and large intestine, in the lactating mammary gland (Shyjan et al., 1996), spleen (Kraal et al., 1995) and very weakly in pancreas (Hanninen et al., 1993) and brain (O'Neill et al., 1991).

An abundance of murine models support the contribution of MAdCAM-1 and its ligand α4β7 to lymphocyte homing to the gut (Schweighoffer et al., 1993) and chronically inflamed intestines (Arihiro et al., 2002). Interestingly, the functional significance of elevated levels of MAdCAM-1 protein in chronic inflammatory diseases is supported by several reports which show that immunoneutralisation of either MAdCAM-1 or its ligand α4β7 integrin, causes attenuation of inflammation and mucosal damage in animal models (Fong et al., 1997)(Kato et al., 2000), as well as in patients with colitis (Ghosh et al., 2003)(Feagan et al., 2005), and Crohn's disease (Guagnozzi and Caprilli, 2008)(Feagan et al., 2008).

The induction of VAP-1 in inflamed gut where MAdCAM-1 is expressed and the induction of MAdCAM-1 in chronically inflamed liver tissues where VAP-1 is normally expressed led us to investigate the role of VAP-1/SSAO activity in MAdCAM-1 expression. The results in the previous chapter show that the end products released from the enzymatic reaction of VAP-1 with its substrate methylamine induce MAdCAM-1 expression in primary cultures of human hepatic endothelial cells. In the studies described in this chapter it was investigated whether VAP-1/SSAO would have a similar role in induction of MAdCAM-1 expression *in vivo*.

6.2 RESULTS

6.2.1 VAP-1/SSAO induces MAdCAM-1 expression in PPs and MLN

To investigate the role of VAP-1/SSAO dependent methylamine deamination on MAdCAM-1 expression *in vivo*, we used mouse models available in Prof. Jalkanen's group in Turku, Finland. We used wild–type mice, VAP-1 deficient mice (VAP-1_KO) and murine VAP-1 deficient mice that expressed hVAP-1 as a transgene on endothelial cells (the cDNA for hVAP-1 was inserted under the control of the mouse Tie-1 promoter). The hVAP-1 transgene was provided as both enzymatically active and enzymatically inactive forms in different mice. We used these model systems to test whether *in vivo* VAP-1 enzymatic activity can induce MAdCAM-1 expression when supplied with methylamine (exogenously provided to the animals in drinking water for 14 days).

The expression of human VAP-1 in transgenic murine endothelial cells was confirmed by immunofluorescent staining (Figure 6.1) of several organs [Peyer's patches (PPs), liver and spleen]. We then exposed our mice to methylamine treatment and investigated the effects on MAdCAM-1 expression. Immunofluorescent staining revealed MAdCAM-1 expression in the high endothelial venules of PPs and MLN (Figure 6.2) and in the sinus–lining endothelial cells surrounding the splenic lymphoid white pulp (Figure 6.4) in all mice both before and after methylamine stimulation. Interestingly no MAdCAM-1 protein was detected in murine livers either before or after methylamine treatment (Figure 6.3). Western blotting confirmed also this pattern of protein expression. MAdCAM-1 was completely absent from the livers and kidneys of all mice studied. In PPs, MLN and spleen however high levels of MAdCAM-1 protein were

observed. Re–probing of the same membranes for actin expression, confirmed the presence of protein in the liver and kidney samples (Figure 6.5).

Relative mRNA expression analysis performed by quantitative PCR revealed significantly elevated MAdCAM-1 mRNA levels in PPs and MLN after methylamine stimulation of transgenic animals expressing enzymatically active hVAP-1, when compared with wild–type mice that were not given methylamine. In PPs a 10–fold change, and in MLN a 16–fold change in MAdCAM-1 mRNA levels were observed. Interestingly, MAdCAM-1 mRNA levels were significantly diminished in MLN of the transgenic animals expressing the enzymatically dead form of VAP-1 (compared to those with the active forms). Similarly, an obvious decrease was noted in mRNA levels in the PPs of VAP-1_EI mice but this was not statistically significant (Figure 6.6A and 6.6B). MAdCAM-1 mRNA was also significantly increased in the spleen of VAP-1_EA and VAP-1_EI mice relative to untreated WT mice. Again relative expression analysis suggested no changes in MAdCAM-1 mRNA levels in murine liver (Figure 6.6D) (Figure 6.7). This lack of inducibility of MAdCAM-1 in the liver was also observed under inflammatory conditions in mice exposed to Concavalin A induced hepatitis. Here MAdCAM-1 mRNA levels were unchanged by induction of hepatitis in either VAP-1 deficient mice or VAP-1 deficient mice expressing human VAP-1 as a transgene (Figure 6.8).

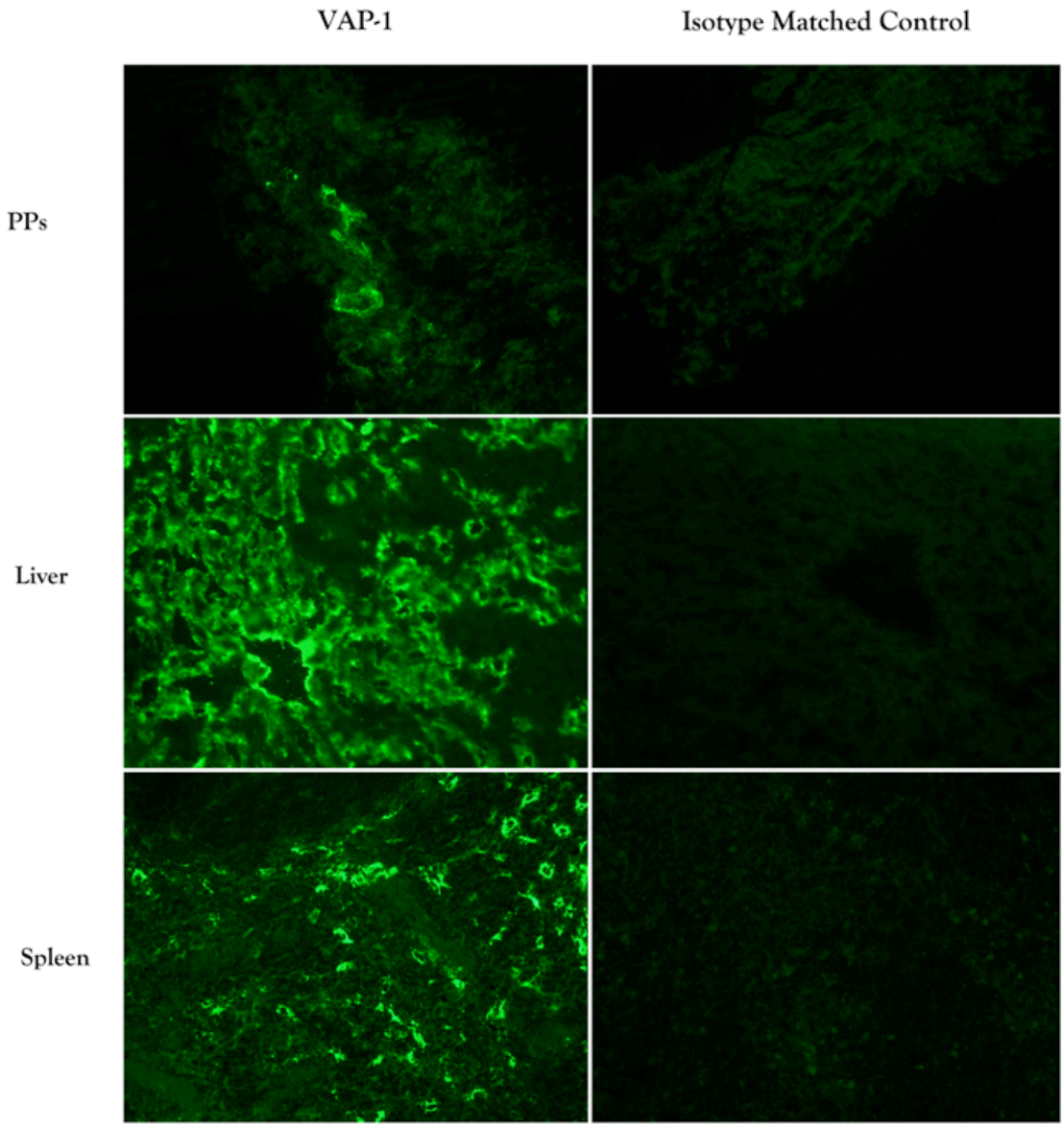

Figure 6.1 In vivo expression of hVAP-1 by transgenic mice. Representative images of immunofluorescent staining of Peyer's patches, liver and spleen of VAP-1 deficient mice that expressed hVAP-1 enzymatically active as a transgene. Murine tissues were stained with anti-human VAP-1 (left panels) or isotype-matched control antibodies (right panels), which were detected with FITC-conjugated secondary antibodies. Pictures were captured using 20x objectives.

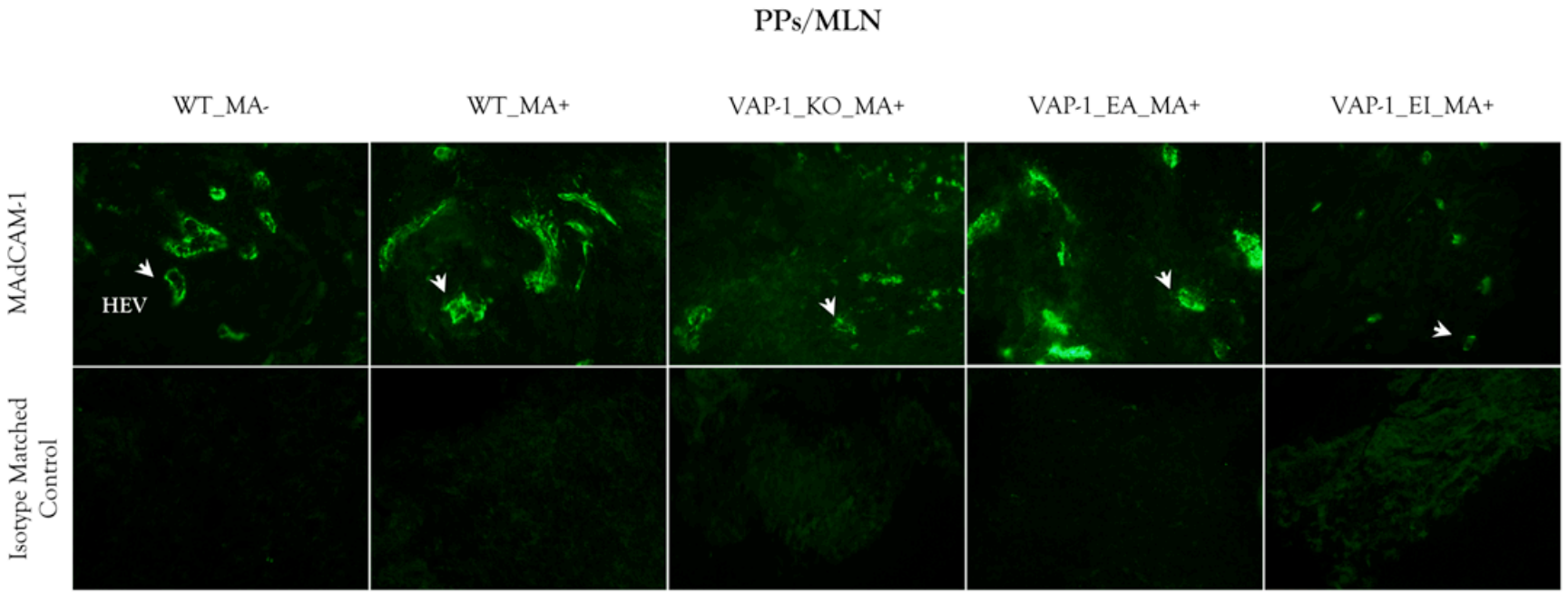

Figure 6.2 MAdCAM-1 expression in murine Peyer's patches (PPs) and mesenteric lymph nodes (MLN). Wild-type mice (WT), VAP-1 deficient mice (VAP-1_KO), VAP-1 deficient mice expressing enzymatically active human VAP-1 (VAP-1_EA), and VAP-1 deficient mice expressing enzymatically inactive human VAP-1 (VAP-1_EA) were supplied with 0.4% (w/v) methylamine (MA^+) in their drinking water for 14 days. Wild-type mice without any methylamine treatment were used as control (WT_MA^-). Images are representative of immunofluorescent staining for MAdCAM-1 or isotype-matched control. Fields were captured using 20x objectives.

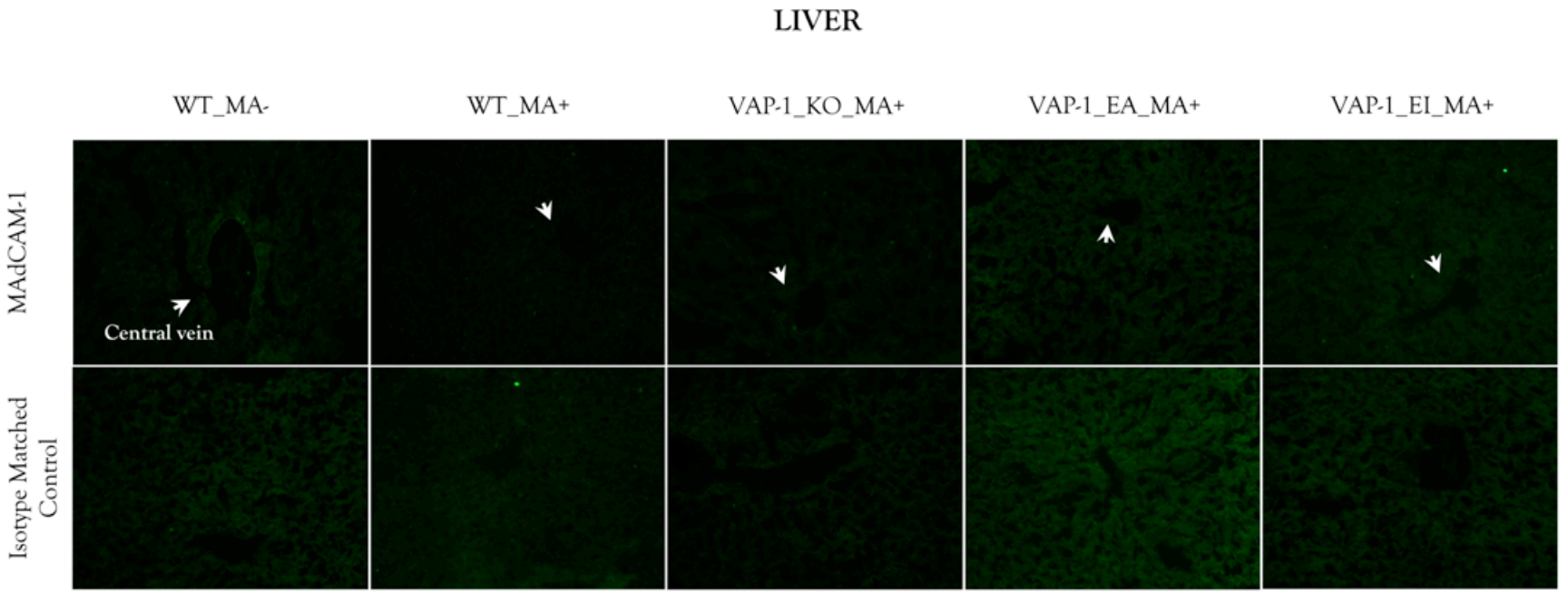

Figure 6.3 MAdCAM-1 protein is absent from mouse livers. Wild-type mice (WT), VAP-1 deficient mice (VAP-1_KO), and VAP-1 deficient mice that expressed either enzymatically active (VAP-1_EA) or enzymatically inactive (VAP-1_EI) hVAP-1 were fed with 0.4 % (w/v) methylamine for 14 days (MA^+). WT mice that were not treated with methylamine were used as control (WT_MA^-). Images are representative of immunofluorescent staining of liver for MAdCAM-1 or isotype-matched control and were captured using 20x objectives**.** White arrows point to central veins.

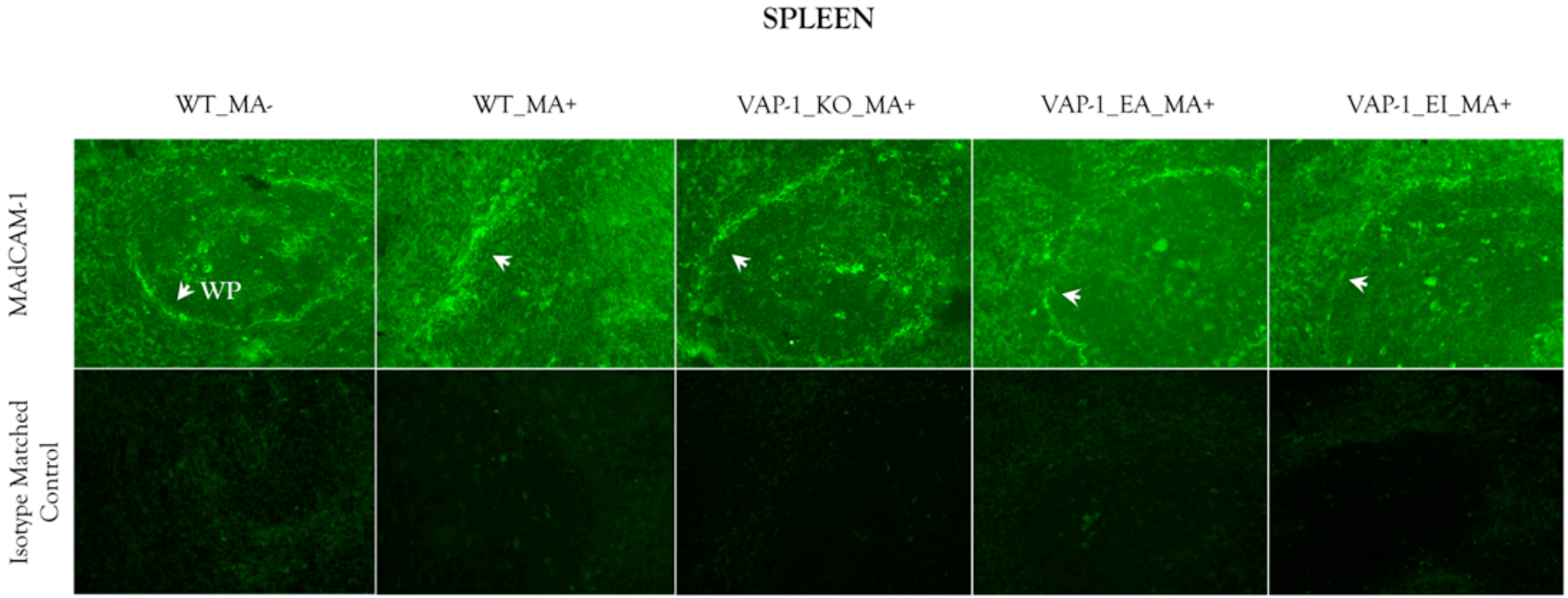

Figure 6.4 MAdCAM-1 expression in murine spleen. Wild-type mice (WT), VAP-1 deficient mice (VAP-1_KO), and VAP-1 deficient mice that expressed either enzymatically active (VAP-1_EA) or enzymatically inactive (VAP-1_EI) hVAP-1 were fed with 0.4 (w/v) methylamine for 14days. WT mice that were not treated with methylamine were used as a control (WT_MA-). Images are representative of immunofluorescent staining of spleen for MAdCAM-1 or isotype-matched control and were captured using 20x objectives. White arrows point to the sinus-lining endothelial cells of the splenic white pulp (WP).

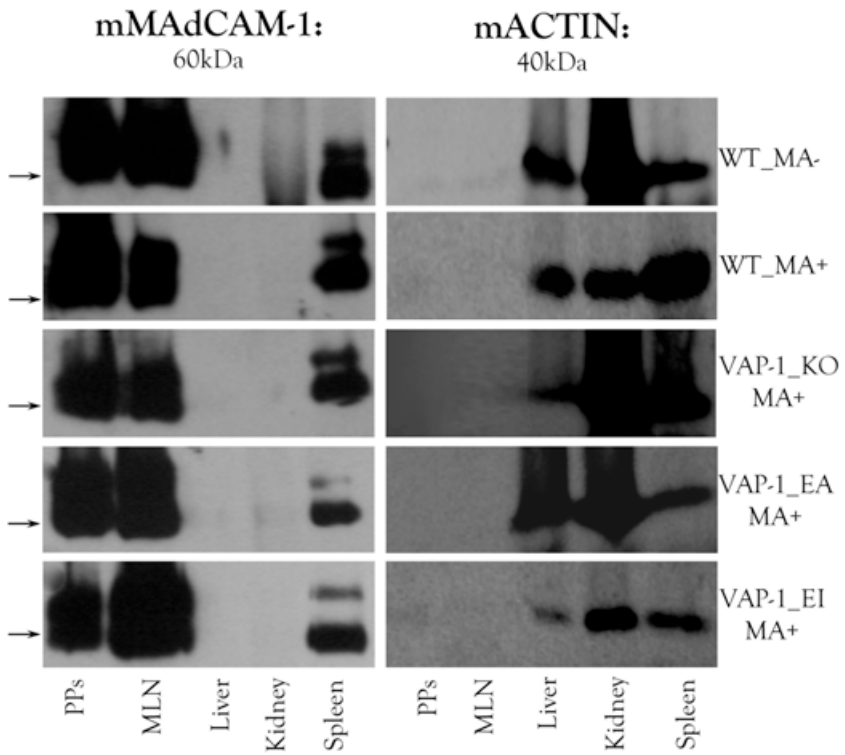

Figure 6.5 MAdCAM-1 protein is absent from murine liver and kidney. Protein lysates were prepared from PPs, MLN, liver, kidney and spleen of wild-type mice (WT), VAP-1 deficient mice (VAP-1_KO), and VAP-1 deficient mice that expressed either enzymatically active (VAP-1_EA) or enzymatically inactive (VAP-1_EI) hVAP-1 (n=3 animals in each group), after exposure to 0.4% (w/v) methylamine for 14days in their drinking water (MA^+). WT mice (n=3) without any methylamine treatment were used as control (WT_MA^-). MAdCAM-1 expression was determined by western blotting (left panels) and the same membranes were also probed for actin expression (right panels). Images are representative from single animals.

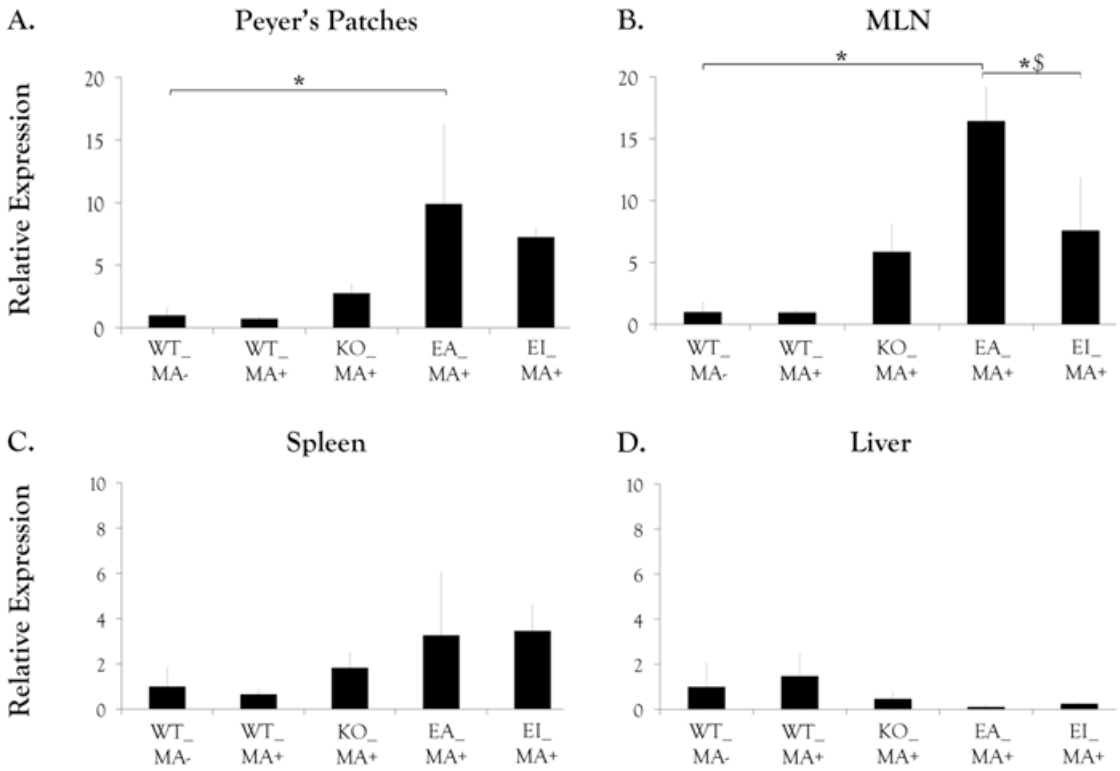

Figure 6.6 VAP-1/SSAO activity induces MAdCAM-1 mRNA expression in PPs and MLN but not in murine liver. RNA was extracted and transcribed into cDNA from PPs, MLN, liver and spleen tissues of wild-type mice (WT), VAP-1 deficient mice (VAP-1_KO), and VAP-1 deficient mice that expressed either enzymatically active (VAP-1_EA) or enzymatically inactive (VAP-1_EI) hVAP-1 after being fed with 0.4% (w/v) methylamine for 14 days in their drinking water (MA^+), and was used for MAdCAM-1 mRNA analysis using real-time PCR. RNA from WT mice that had not received any methylamine in their drinking water was used as a control (WT_MA^-). Data represent relative expression levels of MAdCAM-1 (mean ± SD) in (A) PPs, (B) MLN, (C) spleen and (D) liver from n=3 different mice in each group. Statistical analysis was performed by Student's t-test and one–way ANOVA (PPs, $^*P=0.04$; MLN, $^*P=0.04$ and $^*\$P=0.03$).

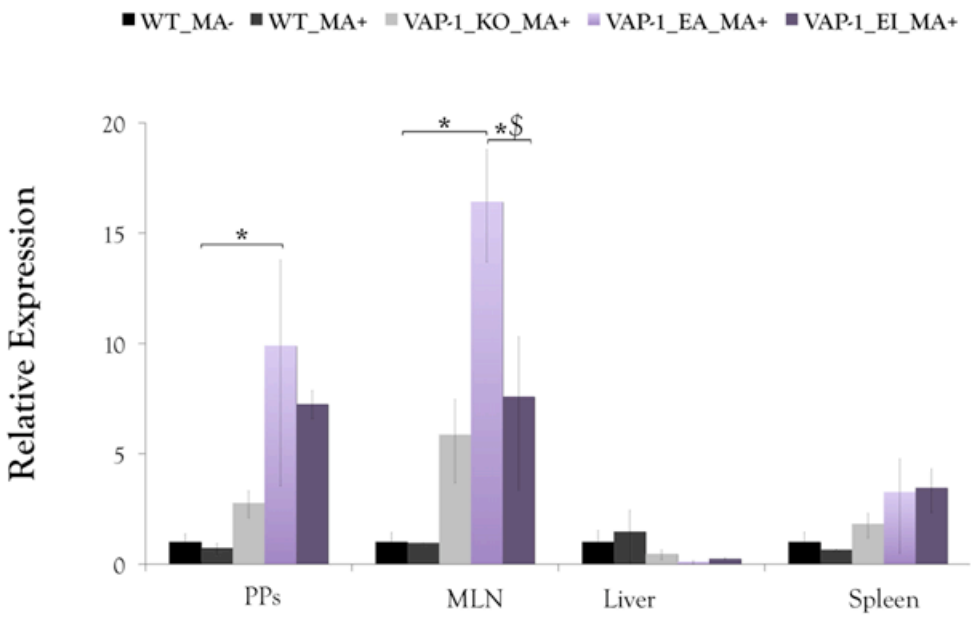

Figure 6.7 Summary of the effects of methylamine on MAdCAM-1 mRNA up-regulation. Figure shows combined data for MAdCAM-1 mRNA expression analysis in WT mice, VAP-1_KO, VAP-1_EA and VAP-1_EI after 14 days of methylamine stimulation in their drinking water. WT mice without any methylamine stimulation were used as a control. Relative expression analysis in PPs, MLN, liver and spleen compared to MAdCAM-1 levels in WT_MA-. Statistical analysis performed by Student's t-test and one–way ANOVA (PPs, *$P=0.04$; MLN, *$P=0.04$ and *$\$P=0.03$).

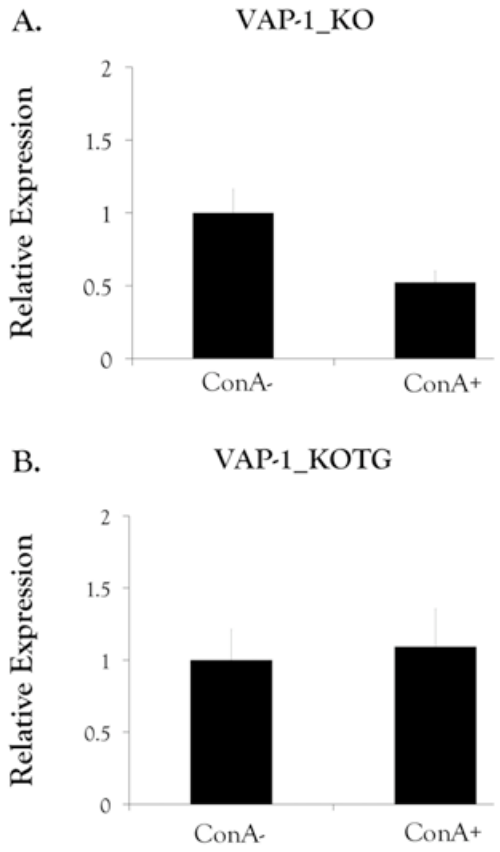

Figure 6.8 MAdCAM-1 mRNA is not induced by hepatic inflammation. RNA was extracted and transcribed into cDNA from VAP-1 deficient mice (VAP-1_KO) and VAP-1 deficient mice expressing human VAP-1 as a transgene (VAP-1_KOTG+) after induction of hepatitis in response to ConA (10mg/kg *i.v.*/4 hours) treatment, and was analysed for MAdCAM-1 mRNA expression. Relative expression levels (mean ± SD) from n=3 KO/ConA$^-$, n=4 KO/ConA$^+$, n=3 VAP-1_KOTG+/ConA$^-$ and n=4 VAP-1_KOTG+/ConA$^+$ animals.

6.3 DISCUSSION

In earlier chapters we demonstrated that the end products, released from the oxidative deamination of methylamine by VAP-1 induced the expression of MAdCAM-1. In the current chapter we extended these observations using an *in vivo* model system. Interestingly, in contrast to our human studies, where MAdCAM-1 was constitutively expressed in hepatic endothelial cells, in all the murine livers tested MAdCAM-1 was completely absent (at both mRNA and protein level). Moreover, stimulation of mice, either the VAP-1_KO or those expressing hVAP-1 as a transgene, with methylamine did not induce MAdCAM-1 expression. In addition, in mice suffering from acute Concavalin A induced hepatitis, a model which is representative of human inflammatory liver disease, MAdCAM-1 was still absent suggesting that human and mouse systems differ significantly. Our finding is consistent with other studies (Bonder et al., 2005), where MAdCAM-1 was also undetectable in the portal venules and no increase or very faint increase was observed in the postsinusoidal venules and sinusoids after ConA administration. We believe this finding is important since animal models are widely used in the development of drugs. Since the importance of MAdCAM-1 in both IBD and autoimmune hepatic complications has been well established, it is essential to know the similarities between human and animal models used for drug testing.

Western blotting revealed the expression of a 60kDa MAdCAM-1 protein in PPs, MLN and spleen. Of note, in all the above organs a second band was also apparent which we believe is a different splice variant of MAdCAM-1. The existence of an alternatively spliced mouse MAdCAM-1 mRNA transcript that lacks exon 4 containing the mucin domain and the third IgA domain has been previously reported (Sampaio et al., 1995). This truncated molecule can

still support adhesion independent of L–selectin binding and so may be functionally relevant at these sites. Further Northern blot studies have also revealed the presence of two transcripts in murine and rat tissues, formed by alternative splicing with the shorter variant lacking the exon 4 (Iizuka et al., 1998).

Although we demonstrated abundant expression of VAP-1 in our transgenic animal livers, VAP-1/SSAO enzymatic activity did not up–regulate MAdCAM-1 expression in mouse liver. In contrast, in those mice with enzymatically active hVAP-1, MAdCAM-1 expression was induced in Peyer's patches and mesenteric lymph nodes, compared with the wild–type mice. The importance of VAP-1 enzyme activity in this induction was confirmed by the comparison of MAdCAM-1 expression in mesenteric lymph nodes of transgenic mice with enzymatically inactive hVAP-1, compared to mice with the enzymatically active hVAP-1. A similar but not significant effect was also observed in PPs of transgenic mice expressing the dead mutant of hVAP-1. Interestingly, in both these organs, a slight increase in MAdCAM-1 mRNA levels was also observed in KO mice lacking VAP-1 after stimulation with methylamine, which led us to suggest that methylamine might regulate MAdCAM-1 expression in other non–VAP-1 dependent ways or in combination with other factors present in the microenvironment.

There are varied potential roles for MAdCAM-1 at extra–hepatic sites. The critical role of MAdCAM-1 in the development of the normal structure of secondary lymphoid tissues including Peyer's patches, has been demonstrated in animals that received anti–MAdCAM-1 treatment, and their PPs were much smaller containing much fewer lymphocytes (Hanninen et al., 1998). Recent studies in MAdCAM-1 knock out mice have shown that the size of PPs is

dramatically reduced when compared with that of wild–type mice (Schippers et al., 2009). This abnormal PPs phenotype is due to reduced numbers of IgM+ B cells being recruited, thus leading to the formation of small and hypocellular PPs. Of note, this important role for MAdCAM-1 in seeding the PPs with B cells and therefore for its role in normal growth of these lymphatic organs, is not observed during the embryonic development of PPs. This suggests that only the postnatal recruitment of lymphocytes into the PPs concomitant with increased antigen exposure in the gastrointestinal tract is dependent on MAdCAM-1.

Furthermore, MAdCAM-1 in the spleen might contribute to the normal marginal sinus (MS) organisation of the developing spleen endothelial cells in the postnatal period (Zindl et al., 2009), and thus to the proper trafficking of cells from the marginal zone to the white pulp, after response to a microbial challenge. MAdCAM-1 expression in the MS endothelium seems to be responsible for the maintenance of the splenic endothelial structures integrity, thereby affecting the distribution of other adhesion molecules on the MS endothelium, that lead to the recruitment of immune cells to the white pulp, since *in vivo* experiments where antibodies against α4β7 integrin were used, had no effect on the immune cell immigration into the splenic white pulp (Kraal et al., 1995).

In accordance with the studies of Kraal *et al.* and Zindl *et al.*, we also detected MAdCAM-1 in the sinus lining endothelial cells of the splenic white pulp, and we also observed increased MAdCAM-1 mRNA levels in the presence of enzymatically active hVAP-1. Of note, increased MAdCAM-1 mRNA levels were also observed in mice expressing enzymatically inactive hVAP-1 after methylamine treatment, suggesting that VAP-1/SSAO does not play a role in MAdCAM-1

induction in spleen. Knockout mice also showed an increase in MAdCAM-1 mRNA expression after methylamine treatment supporting the hypothesis that microenvironmental factors in combination with the presence of methylamine might also play a critical role in MAdCAM-1 induction, which is important for maintenance of splenic architecture.

In conclusion, our data reveal significant differences between the human and mouse system. In primary cultures of human hepatic endothelial cells and in human liver tissues MAdCAM-1 was detectable at both protein and mRNA levels. However, in mice, MAdCAM-1 was completely absent from the liver and neither the enzymatic activity of VAP-1/SSAO nor Concavalin A–induced hepatitis induced expression. However, a role for VAP-1/SSAO activity in MAdCAM-1 expression was revealed in PPs and MLN where MAdCAM-1 was significantly increased after methylamine stimulation. Importantly, this effect was significantly diminished in mice expressing the enzymatically dead mutant hVAP-1 although some induction was seen with methylamine in VAP-1 KO mice suggesting it is not completely specific for SSAO. Overall we believe that the up–regulation of VAP-1 reported *in vivo* during gut inflammation (Salmi et al., 1993) in combination with increased levels of methylamine received via dietary intake or endogenous generation might contribute to induction of MAdCAM-1 expression in Peyer's patches and mesenteric lymph nodes, therefore leading to sustained recruitment and establishment of bowel inflammation. Future *in vivo* studies, in which blocking antibodies directed against either MAdCAM-1 or its leukocyte ligand α4β7 under hVAP-1 stimulation with methylamine, might help to identify critical intermediate steps of this signalling pathway, and therefore might lead to the recognition of potential therapeutic targets.

CHAPTER 7

Transduction Of HSEC With MAdCAM-1 Enhances PBL Recruitment

7.1 INTRODUCTION

The continuous recirculation of lymphocytes between the blood, secondary lymphoid tissues and peripheral tissues, provides continuous surveillance against foreign invaders and facilitates a rapid and specific response to foreign antigens (Shetty et al., 2008). Inflammation enhances leukocyte extravasation into the inflamed areas as a result of interactions between specific adhesion molecules and chemokine receptors on circulating lymphocytes that allow them to recognise signals on endothelial cells and within inflamed tissue (Berg et al., 1989)(Salmi et al., 1998)(Butcher and Picker, 1996).

Chemokines have a fundamental role in regulating both homeostatic and inflammatory leukocyte trafficking (Rollins, 1997)(Baggiolini et al., 1997). The stimulatory signals provided by chemokines binding to specific seven transmembrane spanning receptors, result in modification of the leukocyte integrin affinity and avidity for its ligand, thereby enabling a rolling cell to firmly adhere to the vessel wall by shear–resistant adhesion and activation of motile phenotype that allows the leukocyte to migrate through the endothelium and subendothelial tissue (Cinamon et al., 2001a).

In the gut–associated lymphoid tissues, the expression of MAdCAM-1 and its critical role in physiological lymphocyte trafficking are well recognised. MAdCAM-1 can bind $\alpha4\beta7^{low}$ naïve lymphocytes through L–selectin and to $\alpha4\beta7^{high}$ cells by direct integrin binding to MAdCAM-1 (Berlin et al., 1995)(Schweighoffer et al., 1993). At these sites, the gut expresses high levels of the tissue specific chemokine CCL25, which signals through CCR9 on gut lymphocytes to activate $\alpha4\beta7$ integrin binding to MAdCAM-1 (Figure 3.1).

CCL25 is preferentially expressed in the thymus and small intestine by crypt and glandular epithelium, but not in colonic mucosa (Kunkel et al., 2003a). The only known receptor for CCL25 is CCR9, the expression of which is restricted to thymocytes and subsets of CD3+CD4+ and CD3+CD8+ gut tropic lymphocytes that express α4β7 integrin (Zaballos et al., 1999)(Kunkel et al., 2000). In addition, the majority of small intestinal lamina propria lymphocytes (LPL) and intraepithelial lymphocytes and a subset of small intestinal IgA antibody secreting plasma cells are CCR9+ (Zabel et al., 1999)(Sundstrom et al., 2008). In the colon and in peripheral blood, CCR9 is expressed at low frequencies (about 20%) on CD4 and CD8 cells (Papadakis et al., 2000), suggesting a more selective localisation of CCR9+α4β7+ cells in the small bowel, where CCL25 is predominantly expressed. In $CCR9^{-/-}$ and $CCL25^{-/-}$ deficient mice there is only a subtle decrease in T cells in both intestinal epithelium and lamina propria, suggesting that other chemokines might compensate for the CCL25 and CCR9 deficiency to promote lymphocyte recruitment into the small intestine (Wagner et al., 1996)(Wurbel et al., 2001). Inhibitors of α4β7 (MLN02 and vedolizumab) (Soler et al., 2009) and CCR9 (TRAFICET–EN, Chemocentryx) are being evaluated in patients suffering from Crohn's disease. Such clinical trials will provide proof of concept of the role of these molecules in homing to the human gut, and the use of such compounds might not only be beneficial for IBD patients but also for those suffering from the hepatic complications of IBD such as PSC and autoimmune hepatitis, because these diseases are characterised by aberrant hepatic expression of MAdCAM-1 and CCL25 associated with infiltration of α4β7+CCR9+ T cells (Eksteen et al., 2004a).

Three other chemokines, CCL28, CCL21, CXCL12, are also implicated in lymphocyte recruitment to the gut, although they are not tissue specific. CCL28 is expressed by epithelial cells within the colon and at lower levels in the small intestine as well as in salivary gland, bronchial and mammary glands and trachea (Pan et al., 2000)(W. Wang et al., 2000), and mediates its effects through binding to its receptor CCR10. This chemokine receptor is found on almost all IgA–secreting plasma cells, resident in many mucosal tissues and lymphoid organs, including tonsils, salivary gland, stomach, small and large intestine and appendix. CCR10 is also expressed in memory lymphocytes and eosinophils (Pan et al., 2000)(Kunkel et al., 2003b), and numerous studies have reported the role of CCL28 in localisation and recruitment of CCR10+ cells to both small and large intestine, as indicated by the efficacy of blocking antibodies (anti–CCL28) in inhibiting homing to both sites (Hieshima et al., 2004). Interestingly, IgA plasmablasts arising in intestinal lymphoid tissues co–express CCR10 and α4β7 and it has been proposed that these plasma cells may be able to enter CCL28 containing mucosal sites, where either MAdCAM-1 or VCAM-1 are expressed (Kunkel et al., 2003b).

CCL21 is a homeostatic chemokine expressed on high endothelial venules in areas of T cell accumulation in lymph nodes, spleen and Peyer's patches, where it plays a significant role in the recruitment of CCR7+ naïve lymphocytes (Gunn et al., 1998)(J. J. Campbell et al., 2001). The CCR7 receptor is expressed on B and T lymphocytes and on activated mature dendritic cells (Forster et al., 1999). Apart form CCL21, CCL19 is also a ligand for CCR7 and both interactions are important for T cell homing into Peyer's patches (Luther et al., 2000). On the other hand, B cell homing into Peyer's patches depends on coordinated signalling provided by CCR7 as well as CXCR4, CXCR5 and CCR6 (Okada et al., 2002). Evidence for the critical

role of the CCL21/CCR7 interaction comes from CCR7 deficient mice, where lymphocyte migration is not only affected at the level of entry to secondary lymphoid organs but also at the level of positioning these cells in their corresponding functional microenvironment (Forster et al., 1999).

The chemokine CXCL12, also called stromal (cell)–derived factor (SDF–1a), is constitutively expressed in secondary lymphoid tissues and in gut epithelium, inducing its effects via interaction with its specific receptor CXCR4, expressed at high levels on circulating B and T lymphocytes, including CD4+ and CD8+ cells, and on monocytes (Bleul et al., 1996)(Hori et al., 1998)(Terada et al., 2003). Recent studies have suggested that platelets store CXCL12 and can deposit this chemokine dynamically onto the endothelium upon activation. The presence of CXCL12 on the luminal endothelial surface is sufficient to induce increased leukocyte recruitment (Jin et al., 2006).

All of the above chemokines, CCL25, CCL21, CCL28 and CXCL12 have been reported to trigger α4β7–mediated adhesion to MAdCAM-1 in the gut (Pachynski et al., 1998)(von Andrian and Mackay, 2000), and in addition CXCL12 is capable of triggering α4β7 mediated binding of CD4+ T cells to fibronectin under conditions of shear stress (Wright et al., 2002).

The aim of the studies reported in this chapter was to investigate whether CCL25, CCL28, CCL21 and CXCL12 can trigger activation of α4β7 integrin to mediate lymphocyte arrest on hepatic endothelial cells under conditions of flow. For these experiments, HSEC were transduced to express MAdCAM-1 by transfection with adenoviral constructs. Some of the

preparatory work described in this chapter, was carried out by a previous PhD student Alice Miles, as indicated on the figures.

7.2 RESULTS

7.2.1 MAdCAM-1 Expression In Human Hepatic Endothelial Cells After Induction With Adenoviral Constructs

Hepatic endothelial cells were transfected with adenoviral constructs previously described by our group (A. Miles, PhD Thesis, University of Birmingham, 2006) (Miles et al., 2008) containing full–length (FL)–MAdCAM-1 protein at different multiplicity of infection (MOI). MAdCAM-1 protein expression was detected by western blotting, and optimal MAdCAM-1 transgene expression was achieved at a MOI of 10 (Figure 7.1). Thereafter, this viral concentration was used for the subsequent adhesion assay experiments with FL–MAdCAM-1. In addition, MAdCAM-1 expression in transfected HSEC was confirmed by fluorescence–activated cell sorter analysis (FACS) (Figure 7.2).

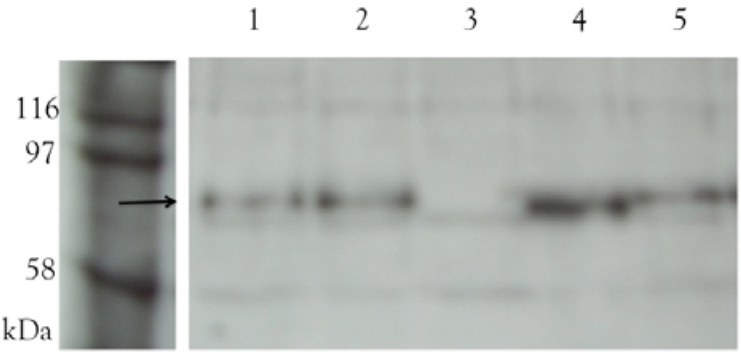

Figure 7.1 MAdCAM-1 expression in HSEC after adenoviral transfection. The expression of MAdCAM-1 was examined in protein lysates prepared from HSEC following infection with (1) FL-MAd-GFP-Ad (MOI 5), (2) FL-MAd-GFP-Ad (MOI 10), (3) GFP-Ad (MOI 50). Lysates from CHO cells transfected with (4) SV-MAdCAM-1 and (5) FL-MAdCAM-1 were included as positive controls. (Experiments performed by A. Miles).

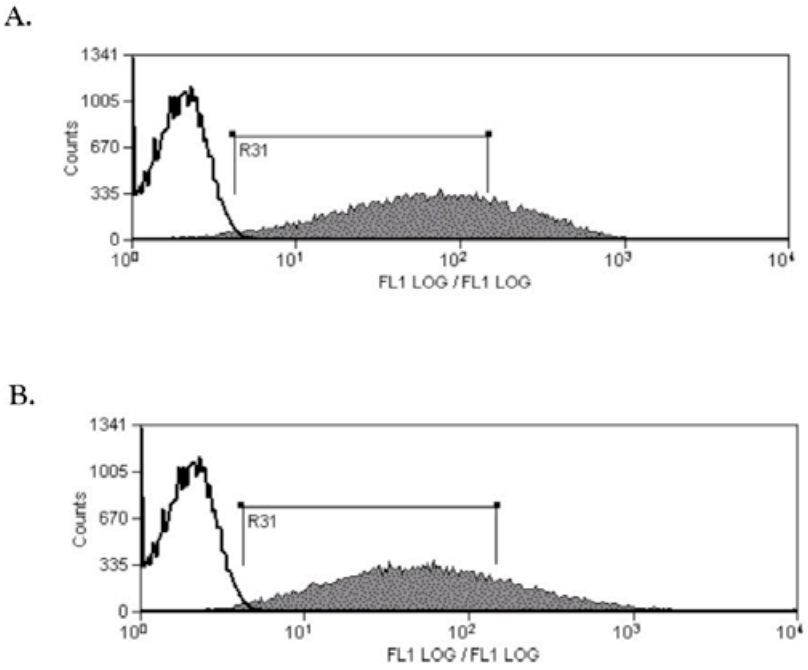

Figure 7.2 MAdCAM-1 expression in adenoviral transfected HSEC. Hepatic endothelial cells transfected with FL-MAd-GFP-Ad (at MOI 10), 24 hours post infection were analysed for GFP expression by flow cytometry. Representative histograms from two different primary isolates (A) and (B) showing MAdCAM-1 expression (filled histograms) compared with non-infected cells (un-filled histograms). (Experiments performed by A. Miles).

7.2.2 Chemokine Receptor Expression In α4β7+ PBL Populations

Prior to functional assays, the expression of α4–integrins, CCR9, CCR7, CCR10 and CXCR4, was determined on peripheral blood lymphocytes (Table 7.1). About 50% of the peripheral blood CD3+ lymphocytes expressed α4–integrin, and of those 15–20% were also positive for β7–integrin (Figure 7.3). If CD3+ T cells were subdivided into α4β7 positive and α4β7 negative populations, CXCR4 was expressed in 78% of CD3+ PBL and 74% and 75% of α4β7+ and α4β7– subpopulations, respectively. The median channel fluorescence values did not differ significantly between the different populations. CCR7 levels were reduced on α4β7– cells when compared with the whole CD3+ population and the α4β7+ population ($P<0.001$). CCR9 expression on the α4β7+ population was increased, but CCR10 expression (percentage of positive cells and median channel fluorescence) was not significantly different between the α4β7+ and α4β7–populations (Figure 7.3).

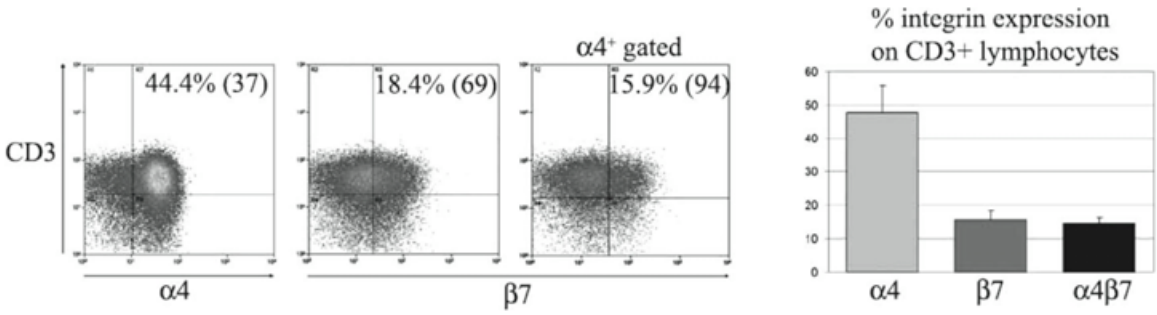

Figure 7.3 Expression of α4– and β7– integrins on T cells subpopulations. Representative dot blots showing the co expression of α4– and β7– integrins (x–axis) on CD3+ T cells (y–axis) from a single donor. Values in quadrant represent percentage of dual-positive cells and median channel fluorescence (MCF) staining intensity. Histograms on the right represent pooled data from 4 normal donors showing the percentage of CD3+ cells staining positive for α4–, β7– and α4β7– integrin. (Experiments performed by A. Miles).

	CD3 Positive Population		α4β7 negative population		α4β7 positive population	
	% positive	MCF	% positive	MCF	% positive	MCF
CXCR4	78.45±4.49	285.5±10.8	74.2±5.37	274.75±19.9	75.05±4.77	265.5±19.36
CCR7	49.42±6.41	281±4.69	9.25±1.1	161±9.6	47.37±7.37	271.75±9.7
CCR9	3.75±2.71	111.3±9.21	2.23±1.29	103.75±6.65	4.25±4.03	112.25±9.71
CCR10	1.78±2.31	59.3±8.18	1.55±1.79	55.25±9.57	1.73±2.26	51.5±9.39

Table 7.1 Expression of CXCR4, CCR7, CCR9 and CCR10 on circulating α4+ and α4β7+ T-cell populations. Pooled data from 4 normal donors showing percent of positive staining and median channel fluorescence values for chemokine receptor staining on total peripheral blood CD3+ cells. Cells were gated into α4β7 negative and α4β7 positive cells. Values are means ± SEM. (Experiments performed by A.Miles).

7.2.3 Lymphocyte Adhesion To Hepatic Endothelium Transduced To Express MAdCAM-1 Is Triggered by CCL21, CCL28, CCL25 and CXCL12

In order to determine the role of chemokine signalling in triggering binding of lymphocytes to MAdCAM-1 expressed by human hepatic endothelial cells, a flow based adhesion assay was developed in which PBL isolated either from normal individuals or from patients with IBD (which show higher levels of α4β7 integrin expression) were perfused over the adenovirally transfected endothelial monolayers at a constant shear stress of 0.05Pa. As expected, no significant adhesion of normal lymphocytes to resting endothelium was observed. However, induction of MAdCAM-1 expression permitted increased leukocyte adhesion (Figure 7.4) (***P=4.5E-08*), which was inhibited when the endothelium was treated with an antibody directed against MAdCAM-1 (P1, ***$P=0.004*). Moreover, blockade of lymphocyte α4β7 integrin also resulted in a modest reduction of adhesion (Figure 7.4). Immobilization of recombinant chemokines on transduced hepatic endothelial cells resulted in a change in the adhesive behaviour of captured lymphocytes. The total number of adherent lymphocytes from normal individuals was modestly increased by the presence of all chemokines, but no significant effects were revealed by statistical analysis (Figure 7.5A). Similarly, the presence of chemokines did not induce increased migration of normal PBL through the MAdCAM-1 transduced hepatic endothelium (Figure 7.5B). On the other hand, while the total number of adherent patient lymphocytes was almost unchanged in the presence of chemokines (Figure 7.6A), CXCL12 resulted in an increase in the number of lymphocytes migrating (**P=0.012*) (Figure 7.6B). Moreover, there was a trend for increased migration of patient lymphocytes in the presence of CCL28 and CCL25 (Figure 7.6B), which was not the case for normal lymphocytes

(Figure 7.5), and which was abolished when chemokine signalling was blocked by pertussis toxin (PTX) treatment of PBL (**$P=0.007) (Figure 7.8).

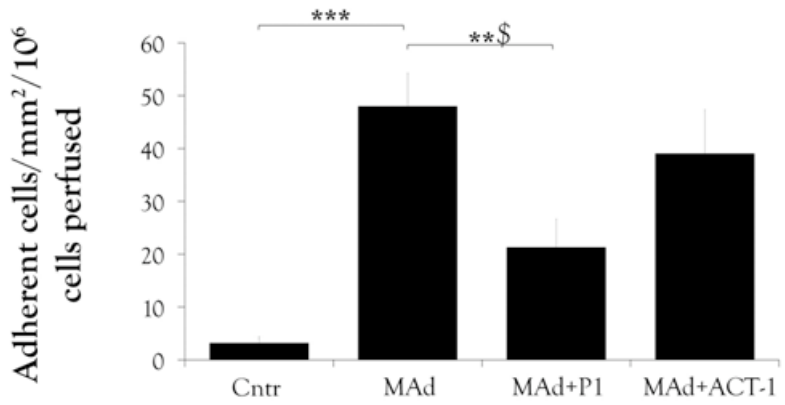

Figure 7.4 Induction of MAdCAM-1 expression in endothelial cells results in enhanced binding of lymphocytes. PBL were perfused over non-transfected HSEC (control) or cells transduced to express MAdCAM-1 (MAd) at a shear stress of 0.05Pa. Where indicated endothelial cells or lymphocytes were pre-treated with MAdCAM-1 (P1) or α4β7 integrin (ACT-1) blocking antibody, respectively. Values are means ± SE of number of adherent cells from two representative experiments. Student's t-test and one–way ANOVA analysis revealed statistically significant differences (****P=4.5E-08*, ***$P= 0.004*).

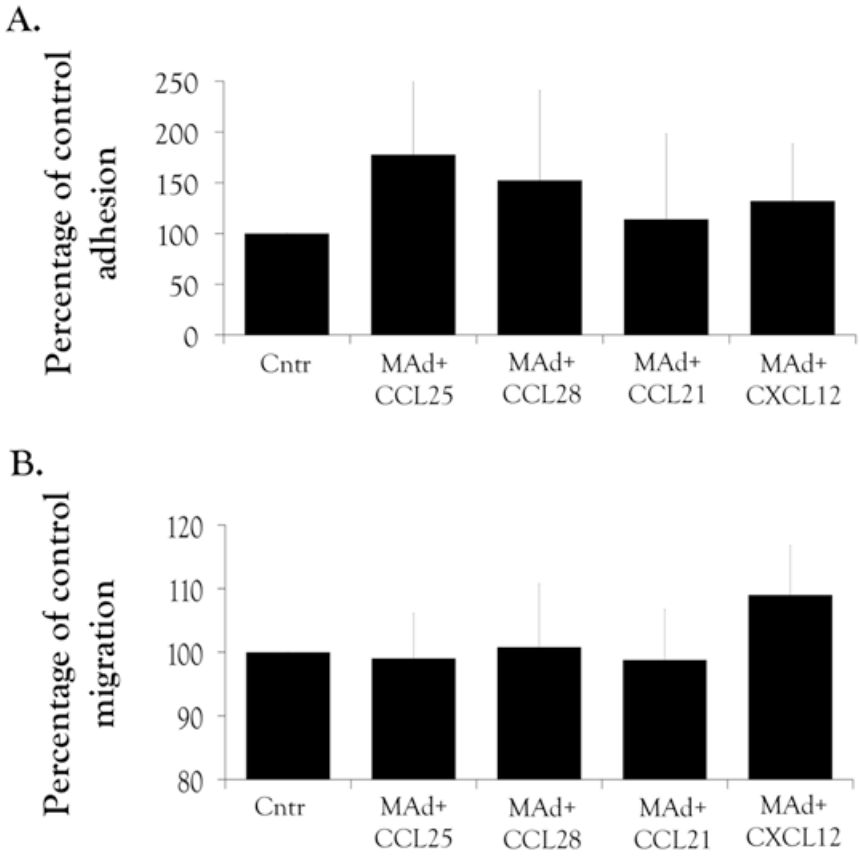

Figure 7.5 The effects of CCL25, CCL28, CCL21 and CXCL12 chemokines on normal lymphocyte adhesion to MAdCAM-1 expressing endothelial cells. PBL from normal individuals were perfused over HSEC transduced to express MAdCAM-1 at 0.05Pa. Transfected HSEC that were not pre-treated with chemokines were used as control. Where indicated HSEC were pre-incubated with recombinant chemokines (10μg/ml for 30min) prior to perfusion of PBL. Adhesion was classified as rolling, static adhesion or activation/migration, which were combined to give the total number of adherent cells/mm^2/10^6 perfused. Data represent mean ± SEM number of adherent cells in representative experiments with n=3 normal donor PBL. (A) Static adhesion is expressed as percentage of control adhesion and (B) migration is expressed as percentage of control migration.

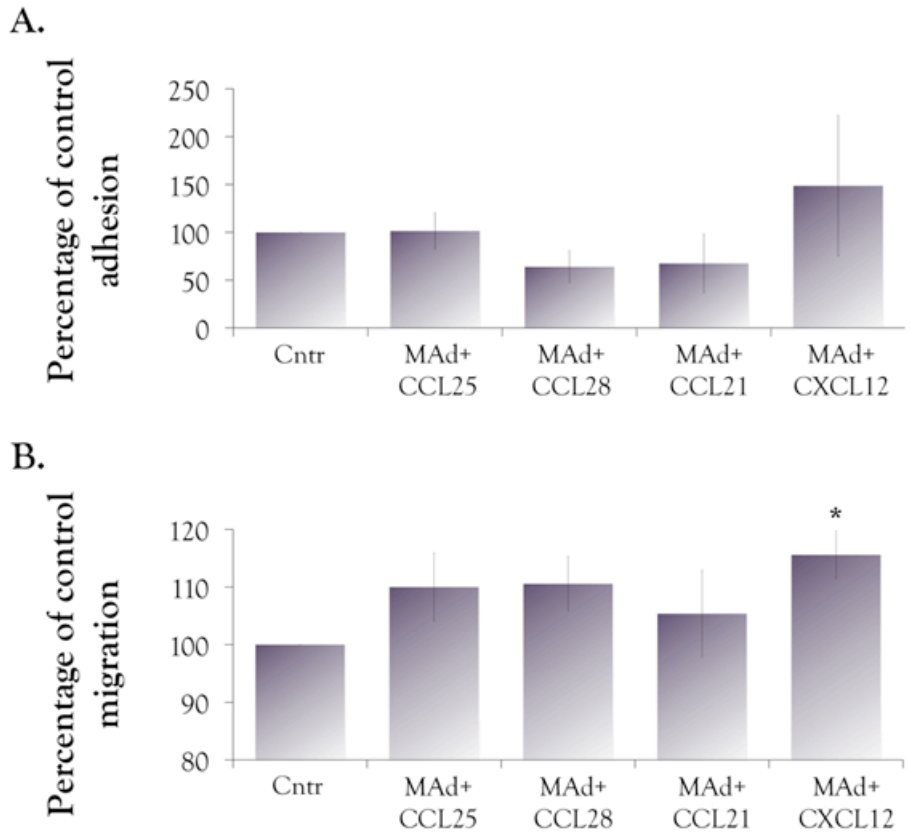

Figure 7.6 The effects of CCL25, CCL28, CCL21 and CXCL12 (SDF) chemokines on patient lymphocyte adhesion to MAdCAM-1 expressing endothelial cells. PBL from patients with IBD were perfused over HSEC transduced to express MAdCAM-1 at 0.05Pa. Transfected HSEC that were not pre-treated with chemokines were used as control. Where indicated HSEC were pre-incubated with recombinant chemokines (10μg/ml for 30min) prior to perfusion of PBL. Adhesion was classified as rolling, static adhesion or activation/migration, which were combined to give the total number of adherent cells/mm^2/10^6 perfused. Data represent mean ± SEM number of adherent cells in representative experiments with n=6 IBD patients' PBL. (A) Static adhesion is expressed as percentage of control adhesion and (B) migration is expressed as percentage of control migration. Statistical analysis was performed by Student's t-test (*P=0.012).

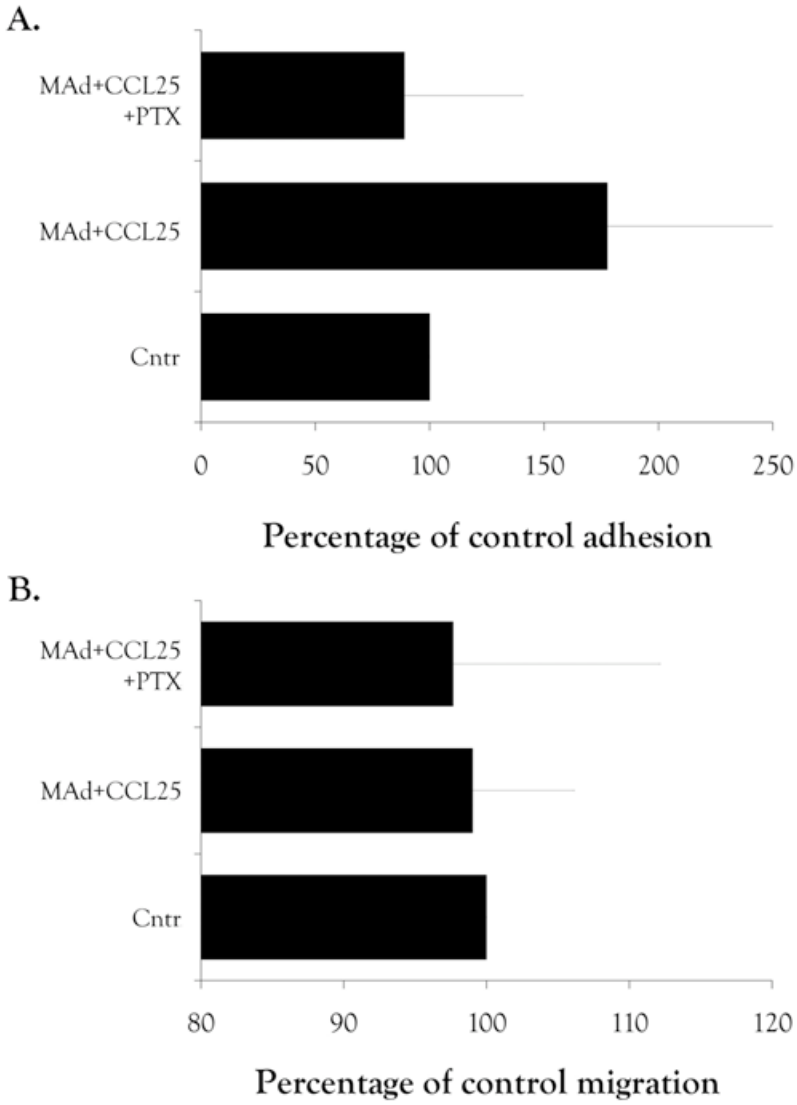

Figure 7.7 Effect of pertussis toxin (PTX) treatment on normal lymphocyte adhesion. PBL from normal patients were perfused over HSEC transduced to express MAdCAM-1 at 0.05Pa. Transfected HSEC that were not pre-treated with chemokines were used as control. Where indicated HSEC were pre-incubated with recombinant chemokines (10μg/ml for 30min at 37°C) and PBL with pertussis toxin (200ng/ml for 30min at 37°C). Data represent mean ± SEM number of adherent cells from n=3 normal PBL. (A) Static adhesion is expressed as percentage of control adhesion and (B) migration is expressed as percentage of control migration.

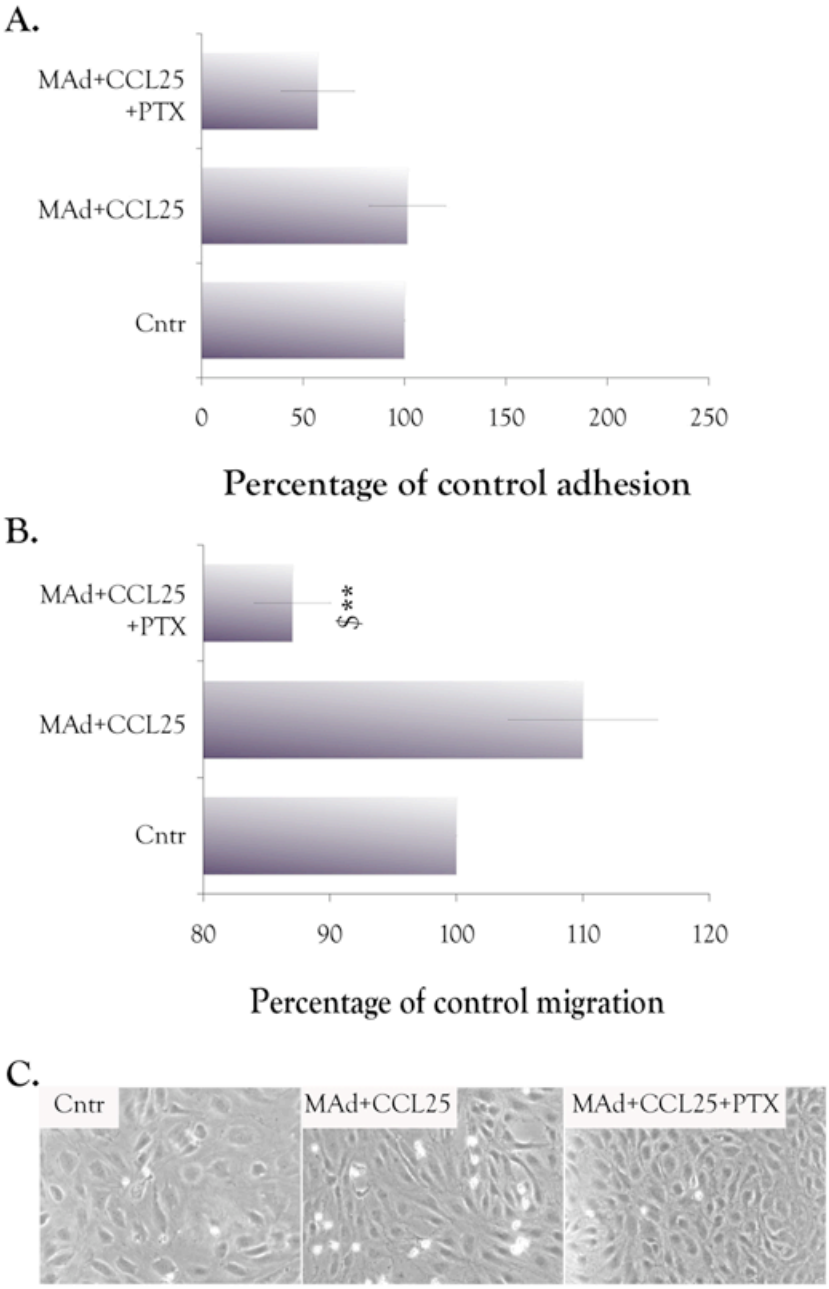

Figure 7.8 Effect of pertussis toxin (PTX) treatment on patient lymphocyte adhesion. PBL from IBD patients were perfused over HSEC transduced to express MAdCAM-1 at 0.05Pa. Transfected HSEC that were not pre-treated with chemokines were used as control. Where indicated HSEC were pre-incubated with recombinant CCL25 chemokine (10μg/ml for 30min). Data represent mean ± SEM number of adherent cells from n=6 patients PBL. (A) Static adhesion is expressed as percentage of control adhesion and (B) migration is expressed as percentage of control migration. (C) Representative video images of lymphocyte interacting with MAdCAM-1 expressing HSEC. The panels demonstrate the increased numbers of activated shape-changed lymphocytes binding to HSEC with the presence of CCL25 and how this is reduced by pre-treatment of PBL with pertussis toxin [(PTX); 200ng/ml, 30min at 37°C]. Statistical analysis was performed by one–way ANOVA (**$P=0.007).

7.3 DISCUSSION

In this study, a flow based adhesion system was developed in order to investigate the role of gut–expressed chemokines in mediating lymphocyte adhesion to MAdCAM-1 under conditions of flow. Using adenoviral constructs for FL–MAdCAM-1 we transfected hepatic endothelial cells to constitutively express MAdCAM-1 *in vitro*. The functional integrity of MAdCAM-1 protein was validated with the flow based adhesion assay where peripheral blood lymphocytes from normal individuals were perfused over the transduced endothelial monolayers at a constant shear stress of 0.05Pa, which represents the low shear environment of hepatic sinusoids. A significant increase in the total number of adherent cells was observed in cells transduced to express MAdCAM-1 (****P=4.5E-08)* when compared with the non–transfected HSEC, where adhesion was almost undetectable. When HSEC were pre–incubated with a blocking antibody directed against MAdCAM-1 (humanised P1 Ab), the total number of adherent cells was significantly diminished *(**$P=0.04)* supporting the functional role of MAdCAM-1 in the recruitment of α4β7+ PBL. Of note, when the α4β7 integrin on leukocyte surface was blocked (ACT-1 Ab) there was no statistically significant reduction of adherent cells, which we suggest is due to the ability of MAdCAM-1 to adhere to α4β1 integrin expressed on PBL.

Further studies, where HSEC transduced to express MAdCAM-1 were pre–treated with recombinant chemokines CCL21, CCL25, CCL28 and CXCL12, prior to perfusion of PBL isolated either from normal individuals or from patients suffering from IBD, were carried out to investigate the role of these chemokines in lymphocyte binding to MAdCAM-1. When normal PBL were perfused over the transduced endothelial monolayers all the chemokines had

a tendency to increase the levels of total adhesion when compared with control transfected HSEC that were not pre–treated with chemokines, although these differences were not significant. Amongst all chemokines, only CXCL12 activated transendothelial migration. The ability of CXCL12 to mediate transendothelial migration, has been previously reported by Schreiber *et al.* who demonstrated that apical presentation CXCL12 could promote locomotion on endothelium and diapedesis through endothelial cell junctions, under shear conditions (Schreiber et al., 2007). Moreover, our finding was completely in line with previous studies from our group (complementary data published by Miles *et al.,* 2008) where CXCL12 and CCL21 not only triggered arrest of rolling lymphocytes on MAdCAM-1 but also induced high integrin avidity changes via cytoskeletal rearrangements, fluidity in the plasma membrane and subsequent clustering. This resulted in stronger adhesive interactions between endothelium and leukocytes (Miles et al., 2008), thus leading the latter to adopt a flattened and extended morphology, indicative of migratory behaviour (J. R. Chan et al., 2003). Previous studies have also reported the ability of CXCL12 and CCL21 to trigger α4β7 mediated binding to MAdCAM-1 under shear stress (Pachynski et al., 1998)(Wright et al., 2002).

Of note, when PBL from patients suffering from IBD were perfused over the MAdCAM-1 transduced endothelial monolayers, the presence of CXCL12 increased the total number of adherent cells (by about 48%), and the percentage of migrating cells (*$P=0.012$). However, it should be noted that our chemokine–induced transmigration system was suboptimal, since studies have shown that chemokines (with the exception of CXCL12) should be placed below the endothelial monolayer in order to induce maximal migration. Therefore, additional flow–based adhesion assays using luminally and abluminally located chemokines might prove more

useful in determining the effects of the different chemokines in inducing migration through MAdCAM-1 expressing hepatic endothelial cells. However, using the current system, in the presence of CCL28, there was also a trend for increased migration. Previous studies have reported the ability of CCL28 to activate α4β7–mediated adhesion to MAdCAM-1 under flow (Pachynski et al., 1998). In inflamed colonic tissues from patients with ulcerative colitis elevated levels of CCL28 have been detected, which together with similarly increased levels of MAdCAM-1 in these tissues, provide further evidence for the role of this chemokine in the persistent leukocyte recruitment observed in patients with IBD (Ogawa et al., 2004). Elevated CCL28 levels have been also observed on portal vascular endothelium and biliary epithelium in livers from patients suffering from chronic inflammatory liver diseases including PSC, PBC and ALD, where it could support α4β7– and α4β1– integrin mediated adhesion of liver infiltrating lymphocytes to MAdCAM-1 and VCAM-1, respectively. In this study the CCL28 chemokine receptor CCR10 was found on almost 17% of liver infiltrating CD3+ T cells in inflamed liver but only in 6% of T cells in livers of healthy individuals (Eksteen et al., 2006). These data combined with our new evidence showing triggering of α4β7 integrin mediated binding to MAdCAM-1 in HSEC by CCL28 strengthens the role of CCL28 in continuous leukocyte recruitment to MAdCAM-1 both in IBD and its extra–intestinal complications in the liver inflammation.

CXCL12 is expressed in many tissues including lymphoid organs and normal and inflamed liver, particularly on bile ducts in portal tracts (Goddard et al., 2001)(Terada et al., 2003). Increased levels of CXCL12 are detected in PBC and PSC livers (Terada et al., 2003)(Eksteen et al., 2004a) as well as in AIH, CHC (chronic hepatitis C) and liver allograft rejection (Goddard

et al., 2001)(Terada et al., 2003)(Wald et al., 2004). We have now confirmed that this chemokine can also trigger lymphocyte interactions with MAdCAM-1 expressing hepatic endothelium. This observation may be explained by the expression of particularly high levels of CXCR4 on the α4β7+ subset and the α4+ population overall. Therefore, we suggest that the up–regulation of CXCL12 in the liver under inflammatory conditions, in combination with expression of other chemokines might be critical in regulating continuous and un–controlled leukocyte recruitment in chronic liver disease.

CCL25 is believed to be the major chemokine responsible for activation of α4β7 in the gut (Kunkel et al., 2003a). In our study, CCL25 had a tendency to increase the proportion of adherent cells undergoing transendothelial migration in patients with IBD, an effect that was abolished when chemokine signalling was blocked by pertussis toxin (**$*P*=0.007). However, the effect was not dissimilar to that induced by CCL28 which may suggest that the hierarchy of triggering signals varies from site to site. Moreover, we cannot assume that CCL25 and CCL28 were immobilised to the same extent on the endothelial monolayers without precise quantification and thus it is difficult to define the efficacy of one chemokine over another in this system. Nevertheless our CCL25 responses were in line with our previous model, where purified MAdCAM-1 protein was immobilised on a glass microslide and the co–immobilization of CCL25 also triggered arrest of rolling lymphocytes on MAdCAM-1 under conditions of physiological flow (Miles et al, 2008). However, in this system we saw no lymphocyte shape change. Therefore, we believe that the presence of an additional signal from the endothelial (HSEC) microenvironment might be needed to promote migration through the endothelial monolayer and this may come from an additional chemokine.

In conclusion, we have shown for the first time that CXCL12, CCL21, CCL28 and CCL25 chemokines were able to trigger arrest of rolling lymphocytes on HSEC–expressed MAdCAM-1, with CXCL12 being the most potent activator of both high affinity and avidity changes in α4β7 integrin. Overall, we believe that there are distinct functions, which are performed by the different chemokines and that cooperative interactions between different chemokines might be required for efficient recruitment in MAdCAM-1 expressing hepatic endothelial cells. Therefore, further investigation of the chemokine signals important during gut inflammation as well as during the extra–intestinal hepatic manifestations of IBD, may identify potential therapeutic targets.

CHAPTER 8

CONCLUSIONS & FUTURE WORK

8.1 OVERVIEW

The well established role of MAdCAM-1 in chronic inflammation of the gut, particularly in inflammatory bowel disease (IBD), and the demonstration of extra–intestinal expression in the liver of PSC (primary sclerosing cholangitis) and AIH (autoimmune hepatitis) patients, have highlighted the importance of this molecule in inflammatory gut and liver disease. Pharmaceutical companies have already begun to develop drugs targeting the specific interaction between MAdCAM-1 and its ligand α4β7 integrin [Natalizumab; anti–α4–integrin humanised antibody (Stefanelli et al., 2008), MLN02 (Behm and Bickston, 2009); anti–α4β7, Vedolizumab (Soler et al., 2009); advanced form of MLN02], which is a key player in sustained lymphocyte recruitment to the gut and liver and possibly also in pancreas and brain, where MAdCAM-1 is induced during inflammation. Recently, a study regarding the first humanised MAdCAM-1 blocking antibody has been published (Pullen et al., 2009); however, although the attention of clinicians and drug companies is focused on blocking this crucial interaction, the question as to why MAdCAM-1 is ectopically expressed in the liver under particular conditions still remains unanswered. The aim of this study was to investigate the presence of MAdCAM-1 in a variety of liver diseases and examine the role of different factors in its functional expression both *in vitro* and *in vivo*.

8.2 MADCAM-1 EXPRESSION IN HUMAN LIVER

In this study, we investigated the presence of MAdCAM-1 in human liver tissues at both protein and mRNA level. In accordance with previous studies (Hillan et al., 1999)(Grant et al., 2001), we detected MAdCAM-1 in a variety of liver diseases associated with IBD (PSC, AIH) as well as in non–IBD associated liver diseases (PBC, ALD) at comparable levels on the

endothelial cell lining of central veins and small vessels. Although, in normal livers MAdCAM-1 was mainly undetectable by immunostaining, further immunoprecipitation experiments revealed the presence of MAdCAM-1 protein even in normal livers. Since this contrasted with earlier data from our group, which did not detect any MAdCAM-1 expression in normal liver tissues by immunostaining (Grant et al, 2001), the presence of MAdCAM-1 mRNA was further investigated and was found to be present in normal samples with significantly elevated levels in PSC and AIH diseased livers. In addition, sequencing analysis of message from a normal liver revealed complete alignment with the MAdCAM-1 gene sequence, thus validating the presence of MAdCAM-1 (see section 3.2). Moreover, in the *in vitro* studies where primary cultures of hepatic endothelial cells were used, MAdCAM-1 was also constitutively expressed even in cells isolated from normal livers under basal conditions (see discussion 4.2). Surprisingly, constitutive MAdCAM-1 expression was also detected in primary cultures of human umbilical vein endothelial cells, at both mRNA and protein level although at much lower levels than in HSEC.

Our further experiments regarding the role of the pro–inflammatory cytokine TNFα and the amine substrate of SSAO, methylamine, revealed that TNFα either alone or in combination with methylamine significantly increased MAdCAM-1 mRNA levels in both HSEC and HUVEC. This was in accordance with previous studies that have supported the role of TNFα in inducing MAdCAM-1 expression in murine hepatic endothelial cells (Ando et al., 2007), human microvascular endothelial cells (Ogawa et al., 2005), and HUVEC (Lindholm et al., 2004). Surprisingly, despite increased MAdCAM-1 mRNA levels, protein levels under the same stimulatory conditions remained unchanged (section 4.2.1), and these data were further verified

by the fluorescence–activated cell sorter (FACS) analysis, where MAdCAM-1 was detected not only on the surface but also in the cytoplasm in both normal and diseased livers (section 4.2.3). Of note, additional western blotting studies revealed that MAdCAM-1 of different molecular sizes existed in different cell compartments (see section 4.2.4). The MAdCAM-1 monomer (60kDa) was detected only in the cytoplasmic compartment, whereas the dimeric form and a putative trimeric form were present in both membrane and cytoplasm cell fractions. Previous studies have reported the existence of a dimeric form of MAdCAM-1 (Dando et al., 2002), which is suggested to be more functional than the monomeric form, because point mutations to the residue (Arg70) responsible for formation and stability of the dimer, inhibit the binding of MAdCAM-1 to its integrin ligand (Green et al., 1999)(Dando et al., 2002). In support of this, we detected higher levels of the dimeric form at the membrane consistent with a critical role in integrin recognition and binding. Since, both the dimeric and trimeric forms of MAdCAM-1 were also present in the cytoplasm, it seems likely that the cell contains a pool of ready made MAdCAM-1 protein, available for transfer to the surface whenever required (Figure 4.19). It is not yet known where these molecules are stored; it could be in intracellular granules in the endothelial cells similar to those in which VAP-1 is stored (Salmi et al., 2001b) distinct from the Weibel–Palade bodies, where P–selectin is stored (Dunlop et al., 1992). Of note, no current studies report the presence of MAdCAM-1 trimer, thus further investigation needs to be performed in order to verify whether the 180kDa protein being detected is a MAdCAM-1 oligomer or a complex of MAdCAM-1 with other proteins. Moreover, the investigation of whether this trimeric form is functionally active, able to recruit $\alpha 4\beta 7^+$ lymphocytes and whether this oligomerisation serves to confer mechanical stability upon interaction with the ligands, thus leading to stronger adhesion and recruitment, might be of great importance.

In addition to the expression of MAdCAM-1 on vascular endothelium, MAdCAM-1 was also detected in defined structures inside the hepatocyte cytoplasm and in immune cells with the morphology of dendritic cells. More extensive experiments need to be carried out in order to verify the presence of MAdCAM-1 in these locations, using double–staining techniques and higher number of tissue samples, in order to draw further conclusions regarding the role of MAdCAM-1 in those cells. Epithelial expression of MAdCAM-1 has previously been reported in the choroid plexus epithelium during experimental autoimmune encephalomyelitis (EAE) where supported lymphocyte adhesion (Steffen et al., 1996). Thus our observation of hepatocyte MAdCAM-1 might serve a similar role. Alternatively, hepatocytes have the ability to take up molecules by pinocytosis and endocytosis and can engulf other cell types, so MAdCAM-1 within the hepatocyte might reflect uptake and degradation of protein produced in other cells. Expression of MAdCAM-1 has been reported on follicular dendritic cells of murine normal Peyer's patches, chronically inflamed spleen (Szabo et al., 1997), dendritic processes within human Peyer's patches (M. Briskin et al., 1997), and on dendritic cells in several liver diseases (Grant et al., 2001). Such hepatic expression of MAdCAM-1 could serve as a signal for retention of α4β7+ gut derived lymphocytes in the liver. Liver dendritic cells are poor at imprinting gut tropism (α4β7+CCR9+) (Eksteen et al., 2009) hence, α4β7+CCR9+ liver infiltrating lymphocytes are likely to have been primed in the gut before recruitment to the liver. Moreover, isolated follicular dendritic cells have been reported to express VCAM-1 (Freedman et al., 1990) and ICAM-1 (Koopman et al., 1991) and could present an antigen through clustering with α4β1 and LFA-1 expressing B cells, leading to affinity maturation and differentiation of B cells into memory cells. Thus, MAdCAM-1 expressed on hepatic DCs might

have a similar function. However, further studies would be necessary to validate the presence and the role of MAdCAM-1 in such structures.

8.2.1 Secretion of Soluble MAdCAM-1

Our *in vitro* experiments with primary cultured cells revealed increased MAdCAM-1 mRNA levels upon stimulation but no change in either extracellular or intracellular protein. Based on the immunostaining studies in human liver tissues, where a brownish smear within all liver tissues was detected (section 3.2), consistent with sMAdCAM-1 in tissue and reports from others that have revealed circulating human MAdCAM-1 in the serum and urine (Leung et al., 2004), we investigated whether MAdCAM-1 is secreted as a soluble form in our *in vitro* experiments. A 60kDa soluble MAdCAM-1 protein was detected in the supernatant of stimulated hepatic endothelial cells with statistically significant elevated levels after TNFα and methylamine treatment (section 4.2.5). It is not clear yet if this sMAdCAM-1 is a truncated form released by shedding of the dimeric or trimeric membrane bound forms, or whether the monomeric form stored in the cytoplasm is released through the cell membrane to the circulation or if sMAdCAM-1 is an alternatively spliced variant. Since no splice variants have been reported that lack the transmembrane domain (Leung et al., 1996), and since the sMAdCAM-1 detected was the same as the monomer protein, release from the cytoplasm seems more likely. As we discussed in section 4.3 it is not known if the soluble form of MAdCAM-1 is biologically active or not, or whether its secretion provides a protective mechanism to reduce the number of MAdCAM-1 molecules expressed on the endothelial surface or if sMAdCAM-1 competes with the membrane bound form for the same receptor, thus leading to decreased lymphocyte recruitment to the site. If this is the case, soluble MAdCAM-1 could possibly

provide an essential therapy for the treatment of IBD and its extra–intestinal complications. In a contrary scenario, the release of sMAdCAM-1 could act as a destructive mechanism facilitating the de–adhesion of bound lymphocytes and thus promote their transendothelial migration, as has been reported for other soluble adhesion molecules (Gamble et al., 1990)(Stoddart et al., 1996). It has been reported that VAP-1–dependent signalling induces production of soluble E–selectin, which can activate neutrophil β2 integrin, and induction of ICAM-1 and VCAM-1, resulting in enhanced lymphocyte adhesion (Lo et al., 1991)(Jalkanen et al., 2007)(Lalor et al., 2007). Knowing the already described role of MAdCAM-1 in chronic inflammation characterised by destructive leukocyte influx, we believe that the latter assumptions are more likely. However, the release of soluble MAdCAM-1 able to bind to its counterligand α4β7 integrin on the lymphocyte surface could provide an important therapy for the treatment of IBD and its extra–intestinal complications, therefore further studies investigating the factors that regulate the shedding or release of MAdCAM-1 protein and its role in leukocyte recruitment in normal and diseased livers would be of great importance in understanding the role of this molecule in disease.

8.2.2 Structural Characteristics of MAdCAM-1 In Normal Versus Diseased Liver

The contradictory observations that MAdCAM-1 is only faintly detected in normal liver tissues during immunostaining [in accordance with previously published studies from our group (Grant et al., 2001)] and the western blotting data where normal MAdCAM-1 levels were comparable to those in diseased livers, led us to suggest that MAdCAM-1 may exist in a different structural conformation under normal conditions that is not recognised by the monoclonal antibody. Indeed, western blotting of the unbound protein in the supernatant

from immunoprecipitated tissue samples with the polyclonal anti–MAdCAM-1 Ab, revealed the presence of high levels of MAdCAM-1 protein, which were not detected when the same samples were probed with the monoclonal Ab. This confirms that MAdCAM-1 protein present in normal liver tissues might have a different structural conformation not recognisable by the monoclonal antibody (see discussion 3.3).

In support of this, in the flow based adhesion assays no MAdCAM-1–dependent lymphocyte binding under basal conditions was observed, whereas under TNFα and TNFα plus methylamine treatment significantly increased numbers of adherent lymphocytes were detected (section 4.2.6). Therefore, we believe that MAdCAM-1 is present in normal human liver in a non–functional folded state that cannot support lymphocyte recruitment, whereas in inflammatory conditions the local release of TNFα induces further expression of MAdCAM-1 and in the presence of another stimulant such as methylamine, the already expressed MAdCAM-1 acquires a functional conformation, thus being able to lead to leukocyte–integrin recognition and binding. Additional X–ray crystallography and protein nuclear magnetic resonance spectroscopy (NMR) experiments will provide useful information regarding the topology and folding of the ligand–binding domains of MAdCAM-1 protein in basal and inflammatory conditions.

8.3 The Role of VAP-1/SSAO Activity In MAdCAM-1 Expression *in vitro* And *in vivo*.

In order to investigate whether methylamine had additional effects on MAdCAM-1 expression due to VAP-1 enzymatic activity, adenoviral constructs expressing enzymatically active or inactive hVAP-1 were used to transduce hepatic endothelial cells, ensuring maximal VAP-1

expression. The cells transfected with enzymatically active hVAP-1, when exposed to TNFα or methylamine expressed significantly higher levels of MAdCAM-1 protein when compared with the non–transfected cells and cells transfected with enzymatically inactive hVAP-1 (section 5.2), suggesting that VAP-1/SSAO has an effect on MAdCAM-1 expression by hepatic endothelial cells.

This role of VAP-1/SSAO activity was further validated using non–transfected HSEC, which were stimulated with the end products released from the methylamine deamination by VAP-1, hydrogen peroxide, ammonia and formaldehyde, either when added exogenously or locally generated by treatment with enzymatically active sVAP-1 and methylamine. The combination of all three end products significantly induced MAdCAM-1 expression. In support of this, previously reported studies from our group have also demonstrated that the H_2O_2 produced during VAP-1 mediated amine oxidation could induce expression of other adhesion molecules, such as P– and E–selectin, ICAM-1 and VCAM-1 and CXCL8 chemokine on HSEC by stimulating the PI3K, MAPK and NF-κB pathways (Lalor et al., 2002a). In addition, studies in human umbilical vein endothelial cells, have shown that provision of an amine substrate for VAP-1 could also induce expression of P– and E–selectin *in vitro* (Jalkanen et al., 2007).

In vivo models with wild–type mice, animals deficient for VAP-1, and animals deficient for mouse VAP-1 transduced to express enzymatically active or inactive human VAP-1 as a transgene, were used in order to test whether VAP-1 enzyme had the ability to induce MAdCAM-1 expression *in vivo.* We supplied exogenous substrate in the form of methylamine in drinking water, and we found that VAP-1 enzyme activity significantly induced MAdCAM-1

expression in Peyer's patches and mesenteric lymph nodes, which was confirmed by the comparison of MAdCAM-1 expression levels in transgenic mice with enzymatically inactive hVAP-1 (section 6.2). These findings were in line with *in vivo* studies of Jalkanen *et al.* that also demonstrated the ability of VAP-1/SSAO enzymatic activity to induce functionally active P–selectin expression in small vessels of several organs including heart and intestine of animal models stimulated with methylamine (Jalkanen et al., 2007). However, in contrast to the human data where MAdCAM-1 was found to be constitutively present in the liver, in all mouse models that were used MAdCAM-1 was completely absent from murine livers at both mRNA and protein level. Of note, neither methylamine stimulation nor hepatic inflammation induced by Concavalin A treatment up–regulated MAdCAM-1 expression, highlighting an important difference between the murine and human systems.

8.4 Role of Chemokines In Lymphocyte Adhesion To MAdCAM-1

The expression of MAdCAM-1 in the liver, paralleled observations relating to the chemokine CCL25 whose expression has also been considered to be restricted to the small intestine and thymus (Kunkel et al., 2000)(Kunkel et al., 2003a). The recruitment of lymphocytes to the gut requires not only MAdCAM-1/α4β7 integrin interaction but also a chemotactic signal provided by CCL25 and its receptor CCR9. CCR9 is co–expressed with α4β7 integrin on gut–homing lymphocytes, thus binding of CCL25 to CCR9 leads to adhesion via MAdCAM-1. Previous studies from our group have reported the expression of CCL25 in PSC patients, as well as the expression of its receptor CCR9 to be strongly associated with co–expression of the gut integrin α4β7, in approximately 20% of liver infiltrating lymphocytes (LILs) in PSC. More interestingly, in static adhesion assays, the CCR9 on LILs could be triggered by CCL25 to bind to ectopically

expressed MAdCAM-1 in PSC via α4β7, supporting the hypothesis that long–lived memory cells of mucosal origin activated in the gut are able to circulate between the liver and gut providing surveillance against gut derived antigens that have entered the liver via the hepatic portal vein (Eksteen et al., 2004a). Although, in this study, CCL25 was undetectable in other chronic inflammatory diseases, unpublished data from our group using new and better antibodies has revealed the presence of CCL25 in a variety of liver diseased tissues (ALD, PBC, PSC, AIH) as well as in normal livers (unpublished data from C. Weston, Centre for Liver Research). In the current study, MAdCAM-1 was detected in the same livers as CCL25 had been previously detected, supporting the relationship between these two molecules and their role in sustained recruitment of α4β7+CCR9+ lymphocytes both in the gut and extra–intestinal sites. Although both MAdCAM-1 and CCL25 are both expressed in the liver of patients with extra–intestinal complications of IBD, and other liver diseases, their functional role in non–IBD–related diseases is unknown. Therefore, the study of CCR9 expression in LILs from patients with different liver diseases and their ability to adhere to MAdCAM-1 expressed on the hepatic endothelium, might prove useful in determining the role of MAdCAM-1/α4β7 and CCL25/CCR9 in the pathogenesis of liver diseases.

Using the flow based adhesion assay it was further investigated whether the chemokines CCL28, CCL21 and CXCL12, also implicated in lymphocyte recruitment to the gut via α4β7–mediated adhesion to MAdCAM-1 (Pachynski et al., 1998)(von Andrian and Mackay, 2000), are able to mediate lymphocyte arrest in hepatic endothelial cells transduced to express MAdCAM-1. Interestingly, CXCL12 chemokine was the most potent activator of α4β7 integrin mediated adhesion to HSEC through MAdCAM-1. Although CXCL12 is mainly expressed in

secondary lymphoid organs, under normal conditions is also expressed on the bile ducts of hepatic portal tracts, with increased levels in diseased livers (PSC, PBC, AIH, CHC and liver allograft rejection) (Goddard et al., 2001)(Terada et al., 2003)(Eksteen et al., 2004a)(Wald et al., 2004). In the flow based adhesion assay system, co–immobilisation of CXCL12 with either primary hepatic endothelial cells transduced to express MAdCAM-1 or with purified MAdCAM-1 protein immobilised on glass microslides (Miles et al., 2008), led to enhanced α4β7–integrin–dependent transendothelial migration. In addition, CCL28 seemed to have a tendency to increase the number of migratory cells on hepatic endothelium that expressed MAdCAM-1, although the conditions in our system were suboptimal. Notably, increased levels of CCL28 have been reported in inflamed colonic tissues from UC patients (Ogawa et al., 2004), which in line with the elevated levels of MAdCAM-1 enhances the evidence that this chemokine is also important for triggering α4β7 integrin activation and lymphocyte arrest on MAdCAM-1. Furthermore, elevated levels of CCL28 have been reported in portal vascular and biliary epithelium in PSC, PBC and ALD, where it could also support α4β7–and α4β1–integrin mediated adhesion of liver infiltrating lymphocytes (LILs) to MAdCAM-1 or VCAM-1. Of note, the CCL28 receptor CCR10 was found on almost 17% of LILs in inflamed liver (Eksteen et al., 2006), thus suggesting a potential role of this chemokine to mediate lymphocyte activation and continuous recruitment through α4β7/MAdCAM-1 both in gut and liver.

Overall, it is apparent that MAdCAM-1 is constitutively expressed in human liver, where it becomes functionally active under specific stimulatory conditions. Cooperative interactions between the chemokines, which are induced in the same places as MAdCAM-1, might be

required for efficient recruitment and retention of lymphocytes and thus establishment of chronic liver inflammation.

8.5 Role Of MAdCAM-1 In Gut And Liver Inflammation

The first association between colonic ulceration and liver disease was made by Thomas C.H. in 1874, when he described the case of a young man who died of a "much enlarged, fatty liver in the presence of ulceration of the colon" (Saich and Chapman, 2008). Thereafter, the association between inflammatory bowel disease and various hepatic complications has been well established.

The etiopathogenesis of IBD still remains elusive, however many genetic and environmental factors have been associated with IBD and experimental evidence suggests that it develops in susceptible individuals as an aberrant immune response to normal gut flora. Despite the different clinicopathological features, genetic susceptibility or triggering factors between ulcerative colitis and Crohn's disease, they are both characterised by uncontrolled and destructive leukocyte accumulation in the bowel (Eksteen et al., 2008). During gut inflammation, the increased release of pro–inflammatory cytokines leads to enhanced expression of vascular adhesion molecules, hence sustaining the immuno–inflammatory process (S. Nakamura et al., 1993b). Of note, among the up–regulated adhesion molecules in IBD, MAdCAM-1 has been recognised as probably the most important receptor in the development of chronic inflammation (M. Briskin et al., 1997). Moreover, several reports have demonstrated the ability of antibodies directed against either MAdCAM-1 or its ligand $\alpha 4\beta 7$ integrin to attenuate inflammation in a variety of animal models as well as in patients with colitis

(Guagnozzi and Caprilli, 2008)(Hamann et al., 1994)(Feagan et al., 2005) and Crohn's disease (Feagan et al., 2008)(Guagnozzi and Caprilli, 2008)(Hamann et al., 1994) although with better results when combined with antibodies targeting other adhesion molecules, such as VCAM-1 (Burns et al., 2001), suggesting that a combination of adhesion molecules/integrin ligands interactions take part in the destructive inflammatory influx that characterises IBD.

TNFα is probably the most important cytokine in the initiation and progression of IBD, as demonstrated by the efficacy of anti–TNFα antibody therapy, which successfully reduces both colonic injury and expression of adhesion molecules (Behm and Bickston, 2008). In our experiments, we also found that VAP-1/SSAO enzymatic activity could induce MAdCAM-1 expression in Peyer's patches and mesenteric lymph nodes *in vivo* after methylamine stimulation, an effect that was significantly diminished in mice expressing enzymatically inactive VAP-1. This finding in combination with reports describing the induction of VAP-1 during gut inflammation (Salmi et al., 1993), led us to suggest that increased levels of methylamine caused either by enhanced absorption (food, wine or cigarette smoke) or by increased *de novo* synthesis (metabolism of adrenaline, sarcosine, creatinine and lecithin) (McEwen and Harrison, 1965)(Pirisino et al., 2001), acting through VAP-1 could lead to induction of MAdCAM-1 in gut mucosa, and thereafter to uncontrolled lymphocyte recruitment. Moreover, since the factors that regulate the induction of VAP-1 in gut mucosa are not known, it seems possible that production of VAP-1 could act as a protective feedback loop in order to metabolize excessive methylamine. Thereafter, increased levels of metabolic products released by the catalytic activity of VAP-1 could up–regulate expression of adhesion molecules, including of MAdCAM-1, and together with the adhesion–molecule like properties of VAP-1 to promote leukocyte

recruitment in the gut during inflammation and the destructive influx during IBD. Thus, we believe that increased levels of methylamine might be an early factor predisposing to gut inflammation in genetically susceptible individuals and maybe also to further liver inflammation.

The fact that liver complications, can occur in a course independent of IBD, led Grant *et al.* to suggest that long–lived memory cells initially activated in the gut during active episodes of IBD are able to be recruited in the liver via interactions with MAdCAM-1 or VAP-1 on hepatic endothelium upon encountering of an appropriate insult (Grant et al, 2001). Since methylamine is present in the portal vein that supplies the liver, it could directly contribute to hepatic inflammation. In support of this, increased levels of methylamine have been reported in liver diseases according to experimental and clinical studies (Pirisino et al., 2004).

Although hepatic MAdCAM-1 was previously detected mainly in PSC and AIH, the hepatic complications of IBD (Hillan et al, 1999) (Grant et al, 2001), we have subsequently detected MAdCAM-1 in a variety of liver diseases including PBC and ALD and in normal liver. In addition, constitutively expressed MAdCAM-1 under normal conditions seems to exist in a non–functional conformation state, with altered antibody–binding epitopes, which may possibly explain the low expression levels seen in normal tissue samples in previous studies (Grant et al, 2001). However, the presence of methylamine catabolised by VAP-1 was able to induce *in vitro* expression of functionally active MAdCAM-1 on hepatic endothelium. Therefore, we believe that circulation of methylamine through the hepatic portal vein and catabolism by VAP-1 in the liver may activate constitutive MAdCAM-1 protein in hepatic

endothelium in combination with TNFα under inflammatory conditions. Further studies investigating the structural conformation of MAdCAM-1 in normal and diseased livers using site directed mutagenesis of the residues responsible for integrin recognition and binding might help to develop therapies specifically targeting the functionally active MAdCAM-1 thereby diminishing side effects caused when widely used pathways are blocked.

It is clear that hepatic MAdCAM-1 is not only associated with the extra–intestinal complications of IBD. Up to 70–85% of PSC patients will develop inflammatory bowel disease, whereas only 2.4–7.5% of people with ulcerative colitis will develop PSC. Additionally, PSC is associated mainly with UC (90% of cases) whilst only 10% of patients with CrD will go on to develop PSC (Adams and Eksteen, 2006). This suggests that there is a missing mechanistic link relating to the liver microenvironment, which predisposes to bowel inflammation. Notably, CrD is suggested to be a Th1–mediated disease, in which Th1 cells are distinguished from other effector lineages by the expression of CCR1, CCR5 and CXCR3 whose chemokine ligands, CCL3, –4, –5, and CXCL9, –10 and –11, respectively are also found in the liver. In addition, MAdCAM-1 is more prominently expressed in CrD rather than in UC (Arihiro et al., 2002). Our belief that methylamine is an environmental candidate responsible for the endothelial induction of MAdCAM-1 in the gut is further supported by findings which demonstrate that cigarette smoking (and hence methylamine exposure) is associated with less frequent exacerbations of UC but on the contrary, with enhanced exacerbations in CrD (Baumgart and Carding, 2007). The lesser role of MAdCAM-1 in UC might also be due to the non–expression of CCL25 and lower levels of CCR9+ T cells (Papadakis et al., 2000)(Kunkel et al., 2003a). However, the purpose of the constitutive expression of MAdCAM-1 in hepatic endothelium

under normal conditions, as well as its role in the non–IBD associated liver diseases still remains to be studied.

Chronic inflammatory liver diseases, including PSC and PBC, are characterised by the development of new hepatic tertiary lymphoid tissue, a process named lymphoid neogenesis. These inflammatory lymphoid follicles provide a microenvironment for the recruitment and retention of lymphocytes at sites of inflammation (Grant et al., 2002a). Of note, CCL21 a chemokine particularly expressed in secondary lymphoid organs has also been detected in stromal tissues surrounding portal vessels and on the endothelium of CD34+ MAdCAM-1+ vessels with the morphology of HEV in lymphoid aggregates in chronic inflammatory liver diseases (Grant et al., 2001). In a complementary study, CCL21 was also able to drive α4β7–mediated migration towards MAdCAM-1 in *in vitro* flow based adhesion assays (Miles et al., 2008). Thus, we believe that in these hepatic tertiary lymphoid tissues, as in lymph nodes, in the presence of an appropriate antigenic stimulus, antigen presenting cells will activate leukocytes and in combination with the cooperative interactions between the different chemokines such as CCL21, will result in increased recruitment to highly expressed MAdCAM-1 in HEV like vessels, retention and final liver chronic inflammation.

8.6 Future Work

The well accepted dogma of science is that more questions than answers are generated during research. This is certainly true of the current study where additional work would shed light on the role of MAdCAM-1 in human liver and may lead to identification of possible therapeutic targets. Further studies should involve:

Determination of MAdCAM-1 expression sites and of factors that regulate its expression:

- Extensive investigation of MAdCAM-1 expression in human normal and diseased liver tissues, using double staining techniques in order to verify whether it is expressed on hepatocytes and liver dendritic cells, and thus understand the role of MAdCAM-1 in the liver.
- A recent report (Kamada et al., 2009) has demonstrated that lamina propria CD14+ macrophages in both normal and Crohn's disease individuals can induce the expression of β7 integrin on naïve CD4+ T cells in a retinoic–acid (RA) dependent manner. Since hepatic stellate cells serve as storage containers for retinoic acid (Friedman et al., 1992), it would be useful to determine whether the α4β7+ cells recruited to MAdCAM-1 in the liver can be produced by resident liver macrophages.
- The liver is exposed to microbial products synthesized by commensal intestinal flora that are transported via the hepatic portal vein to the liver (John and Crispe, 2005). It is well accepted that IBD develops due to a non-specific response to commensal microorganisms and that it is also associated with extra–intestinal complications in the liver. Thus we suggest that TLRs expressed on hepatic sinusoidal endothelial cells, which recognise structural motifs on pathogens and commensal microorganisms, might also regulate MAdCAM-1 expression in the liver. TLR signaling pathways culminate in activation of NF-κB, which is known to activate MAdCAM-1. Further studies investigating the possible role of TLRs in MAdCAM-1 expression might prove useful in developing therapeutic targets for both gut and liver inflammatory conditions.

Determination of the role of MAdCAM-1 in lymphocyte recruitment in the liver:

- Study the presence of α4β7+ integrin expression in liver infiltrating lymphocytes derived from PBC, ALD, AIH and normal patients and their ability to adhere to MAdCAM-1 under static adhesion assays (in tissues).
- Use the adenoviral constructs expressing enzymatically active and inactive hVAP-1 in order to determine the functionality of MAdCAM-1 in the presence of methylamine under flow based adhesion assays.
- Study the ability of CCL21, CCL28, CCL25 and CXCL12 chemokines to cause recruitment of LILs (isolated from different liver diseases) to liver tissue sections under static adhesion assays.

Structural characteristics of MAdCAM-1:

- Investigate the conformational status of MAdCAM-1 in normal and diseased livers. Use adhesion assays to observe the ability of liver– and gut– derived lymphocytes to bind to MAdCAM1 under normal or inflammatory conditions.
- Study the role of methylamine in changing the conformational status of MAdCAM-1 expressed in normal liver tissues to a functional folding state able to recruit α4β7+ lymphocytes.
- Mutational analysis targeting the residues responsible for the leukocyte integrin recognition and binding, treatment with methylamine and thus validation of its role in functional unfolding. This would be eventually useful in developing new drugs targeting the active sites of MAdCAM-1, thus inhibiting only its ability to recruit leukocytes, minimizing any side effects caused after blocking widely used pathways.

- Validate the presence of the trimeric form of MAdCAM-1 with spectophotometry and further investigate its role in the leukocyte recruitment cascade.
- Study the mechanisms that cause shedding of MAdCAM-1 and the biological role of the soluble form.
- Investigate the presence and levels of sMAdCAM-1 in the serum of patients with different liver inflammatory diseases.
- Identify the natural cleavage site of MAdCAM-1, for designing sequence specific inhibitors in order to determine the biological consequences of interfering with this process.

Intracellular pathways responsible for MAdCAM-1 expression:

- Determine whether TNFα and VAP-1 stimulate induction of MAdCAM-1 through the NF-κB transcription factors.

LIST OF REFERENCES

Abella, A., Garcia-Vicente, S., Viguerie, N., Ros-Baro, A., Camps, M., Palacin, M., Zorzano, A. and Marti, L. (2004) Adipocytes release a soluble form of VAP-1/SSAO by a metalloprotease-dependent process and in a regulated manner. **Diabetologia**, 47: (3): 429-438.

Adams, D.H., Hubscher, S.G., Shaw, J., Johnson, G.D., Babbs, C., Rothlein, R. and Neuberger, J.M. (1991) Increased expression of intercellular adhesion molecule 1 on bile ducts in primary biliary cirrhosis and primary sclerosing cholangitis. **Hepatology**, 14: (3): 426-431.

Adams, D.H., Burra, P., Hubscher, S.G., Elias, E. and Newman, W. (1994) Endothelial activation and circulating vascular adhesion molecules in alcoholic liver disease. **Hepatology**, 19: (3): 588-594.

Adams, D.H. and Shaw, S. (1994) Leucocyte-endothelial interactions and regulation of leucocyte migration. **Lancet**, 343: (8901): 831-836.

Adams, D.H., Hubscher, S.G., Fisher, N.C., Williams, A. and Robinson, M. (1996) Expression of E-selectin and E-selectin ligands in human liver inflammation. **Hepatology**, 24: (3): 533-538.

Adams, D.H. and Lloyd, A.R. (1997) Chemokines: leucocyte recruitment and activation cytokines. **Lancet**, 349: (9050): 490-495.

Adams, D.H. and Eksteen, B. (2006) Aberrant homing of mucosal T cells and extra-intestinal manifestations of inflammatory bowel disease. **Nat Rev Immunol**, 6: (3): 244-251.

Adams, D.H., Eksteen, B. and Curbishley, S.M. (2008) Immunology of the gut and liver: a love/hate relationship. **Gut**, 57: (6): 838-848.

Alberts, B., Johnson, A., Lewis, J., Raff, M., Roberts, K., Walter, P. (2002) "**Molecular Biology of Cell**". Fourth Edition.

Alon, R., Hammer, D.A. and Springer, T.A. (1995a) Lifetime of the P-selectin-carbohydrate bond and its response to tensile force in hydrodynamic flow. **Nature**, 374: (6522): 539-542.

Alon, R., Kassner, P.D., Carr, M.W., Finger, E.B., Hemler, M.E. and Springer, T.A. (1995b) The integrin VLA-4 supports tethering and rolling in flow on VCAM-1. **J Cell Biol**, 128: (6): 1243-1253.

Alon, R. and Rosen, S. (2007) Rolling on N-linked glycans: a new way to present L-selectin binding sites. **Nat Immunol**, 8: (4): 339-341.

Alon, R. and Ley, K. (2008) Cells on the run: shear-regulated integrin activation in leukocyte rolling and arrest on endothelial cells. **Curr Opin Cell Biol**, 20: (5): 525-532.

Andersen, M.H., Sorensen, R.B., Brimnes, M.K., Svane, I.M., Becker, J.C. and thor Straten, P. (2009) Identification of heme oxygenase-1-specific regulatory CD8+ T cells in cancer patients. **J Clin Invest**, 119: (8): 2245-2256.

Ando, T., Langley, R.R., Wang, Y., Jordan, P.A., Minagar, A., Alexander, J.S. and Jennings, M.H. (2007) Inflammatory cytokines induce MAdCAM-1 in murine hepatic endothelial cells and mediate alpha-4 beta-7 integrin dependent lymphocyte endothelial adhesion in vitro. **BMC Physiol**, 7: 10.

Arihiro, S., Ohtani, H., Suzuki, M., Murata, M., Ejima, C., Oki, M., Kinouchi, Y., Fukushima, K., Sasaki, I., Nakamura, S., Matsumoto, T., Torii, A., Toda, G. and Nagura, H. (2002) Differential expression of mucosal addressin cell adhesion molecule-1 (MAdCAM-1) in ulcerative colitis and Crohn's disease. **Pathol Int**, 52: (5-6): 367-374.

Arnaout, M.A., Mahalingam, B. and Xiong, J.P. (2005) Integrin structure, allostery, and bidirectional signaling. **Annu Rev Cell Dev Biol**, 21: 381-410.

Arvilommi, A.M., Salmi, M., Kalimo, K. and Jalkanen, S. (1996) Lymphocyte binding to vascular endothelium in inflamed skin revisited: a central role for vascular adhesion protein-1 (VAP-1). **Eur J Immunol**, 26: (4): 825-833.

Atkinson, M.A. and Maclaren, N.K. (1994) The pathogenesis of insulin-dependent diabetes mellitus. **N Engl J Med**, 331: (21): 1428-1436.

Ayabe, T., Satchell, D.P., Wilson, C.L., Parks, W.C., Selsted, M.E. and Ouellette, A.J. (2000) Secretion of microbicidal alpha-defensins by intestinal Paneth cells in response to bacteria. **Nat Immunol**, 1: (2): 113-118.

Baggiolini, M., Dewald, B. and Moser, B. (1997) Human chemokines: an update. **Annu Rev Immunol**, 15: 675-705.

Baltus, T., Weber, K.S., Johnson, Z., Proudfoot, A.E. and Weber, C. (2003) Oligomerization of RANTES is required for CCR1-mediated arrest but not CCR5-mediated transmigration of leukocytes on inflamed endothelium. **Blood**, 102: (6): 1985-1988.

Banchereau, J. and Steinman, R.M. (1998) Dendritic cells and the control of immunity. **Nature**, 392: (6673): 245-252.

Barreiro, O., Yanez-Mo, M., Serrador, J.M., Montoya, M.C., Vicente-Manzanares, M., Tejedor, R., Furthmayr, H. and Sanchez-Madrid, F. (2002) Dynamic interaction of VCAM-1 and ICAM-1 with moesin and ezrin in a novel endothelial docking structure for adherent leukocytes. **J Cell Biol**, 157: (7): 1233-1245.

Baumgart, D.C. and Carding, S.R. (2007) Inflammatory bowel disease: cause and immunobiology. **Lancet**, 369: (9573): 1627-1640.

Bazan, J.F., Bacon, K.B., Hardiman, G., Wang, W., Soo, K., Rossi, D., Greaves, D.R., Zlotnik, A. and Schall, T.J. (1997) A new class of membrane-bound chemokine with a CX3C motif. **Nature**, 385: (6617): 640-644.

Behm, B.W. and Bickston, S.J. (2008) Tumor necrosis factor-alpha antibody for maintenance of remission in Crohn's disease. **Cochrane Database Syst Rev**, (1): CD006893.

Behm, B.W. and Bickston, S.J. (2009) Humanized antibody to the alpha4beta7 integrin for induction of remission in ulcerative colitis. **Cochrane Database Syst Rev**, (1): CD007571.

Berg, E.L., Goldstein, L.A., Jutila, M.A., Nakache, M., Picker, L.J., Streeter, P.R., Wu, N.W., Zhou, D. and Butcher, E.C. (1989) Homing receptors and vascular addressins: cell adhesion molecules that direct lymphocyte traffic. **Immunol Rev**, 108: 5-18.

Berg, E.L., McEvoy, L.M., Berlin, C., Bargatze, R.F. and Butcher, E.C. (1993) L-selectin-mediated lymphocyte rolling on MAdCAM-1. **Nature**, 366: (6456): 695-698.

Berlin, C., Berg, E.L., Briskin, M.J., Andrew, D.P., Kilshaw, P.J., Holzmann, B., Weissman, I.L., Hamann, A. and Butcher, E.C. (1993) Alpha 4 beta 7 integrin mediates lymphocyte binding to the mucosal vascular addressin MAdCAM-1. **Cell**, 74: (1): 185-195.

Berlin, C., Bargatze, R.F., Campbell, J.J., von Andrian, U.H., Szabo, M.C., Hasslen, S.R., Nelson, R.D., Berg, E.L., Erlandsen, S.L. and Butcher, E.C. (1995) alpha 4 integrins mediate lymphocyte attachment and rolling under physiologic flow. **Cell**, 80: (3): 413-422.

Bettelli, E., Korn, T., Oukka, M. and Kuchroo, V.K. (2008) Induction and effector functions of T(H)17 cells. **Nature**, 453: (7198): 1051-1057.

Bevilacqua, M.P. and Nelson, R.M. (1993) Selectins. **J Clin Invest**, 91: (2): 379-387.

Biver, S., Belge, H., Bourgeois, S., Van Vooren, P., Nowik, M., Scohy, S., Houillier, P., Szpirer, J., Szpirer, C., Wagner, C.A., Devuyst, O. and Marini, A.M. (2008) A role for Rhesus factor Rhcg in renal ammonium excretion and male fertility. **Nature**, 456: (7220): 339-343.

Bleul, C.C., Farzan, M., Choe, H., Parolin, C., Clark-Lewis, I., Sodroski, J. and Springer, T.A. (1996) The lymphocyte chemoattractant SDF-1 is a ligand for LESTR/fusin and blocks HIV-1 entry. **Nature**, 382: (6594): 829-833.

Bluestone, J.A. and Abbas, A.K. (2003) Natural versus adaptive regulatory T cells. **Nat Rev Immunol**, 3: (3): 253-257.

Bogdan, C., Rollinghoff, M. and Diefenbach, A. (2000) Reactive oxygen and reactive nitrogen intermediates in innate and specific immunity. **Curr Opin Immunol**, 12: (1): 64-76.

Bonder, C.S., Norman, M.U., Swain, M.G., Zbytnuik, L.D., Yamanouchi, J., Santamaria, P., Ajuebor, M., Salmi, M., Jalkanen, S. and Kubes, P. (2005) Rules of recruitment for Th1 and Th2 lymphocytes in inflamed liver: a role for alpha-4 integrin and vascular adhesion protein-1. **Immunity**, 23: (2): 153-163.

Borders, C.L., Jr., Broadwater, J.A., Bekeny, P.A., Salmon, J.E., Lee, A.S., Eldridge, A.M. and Pett, V.B. (1994) A structural role for arginine in proteins: multiple hydrogen bonds to backbone carbonyl oxygens. **Protein Sci**, 3: (4): 541-548.

Bradley, J.R., Johnson, D.R. and Pober, J.S. (1993) Endothelial activation by hydrogen peroxide. Selective increases of intercellular adhesion molecule-1 and major histocompatibility complex class I. **Am J Pathol**, 142: (5): 1598-1609.

Braet, F. and Wisse, E. (2002) Structural and functional aspects of liver sinusoidal endothelial cell fenestrae: a review. **Comp Hepatol**, 1: (1): 1.

Briskin, M.J., McEvoy, L.M. and Butcher, E.C. (1993) MAdCAM-1 has homology to immunoglobulin and mucin-like adhesion receptors and to IgA1. **Nature**, 363: (6428): 461-464.

Briskin, M.J., Rott, L. and Butcher, E.C. (1996) Structural requirements for mucosal vascular addressin binding to its lymphocyte receptor alpha 4 beta 7. Common themes among integrin-Ig family interactions. **J Immunol**, 156: (2): 719-726.

Briskin, M., Winsor-Hines, D., Shyjan, A., Cochran, N., Bloom, S., Wilson, J., McEvoy, L.M., Butcher, E.C., Kassam, N., Mackay, C.R., Newman, W. and Ringler, D.J. (1997) Human mucosal addressin cell adhesion molecule-1 is preferentially expressed in intestinal tract and associated lymphoid tissue. **Am J Pathol**, 151: (1): 97-110.

Buckley, C.D., Ross, E.A., McGettrick, H.M., Osborne, C.E., Haworth, O., Schmutz, C., Stone, P.C., Salmon, M., Matharu, N.M., Vohra, R.K., Nash, G.B. and Rainger, G.E. (2006) Identification of a phenotypically and functionally distinct population of long-lived neutrophils in a model of reverse endothelial migration. **J Leukoc Biol**, 79: (2): 303-311.

Burns, R.C., Rivera-Nieves, J., Moskaluk, C.A., Matsumoto, S., Cominelli, F. and Ley, K. (2001) Antibody blockade of ICAM-1 and VCAM-1 ameliorates inflammation in the SAMP-1/Yit adoptive transfer model of Crohn's disease in mice. **Gastroenterology**, 121: (6): 1428-1436.

Butcher, E.C. and Picker, L.J. (1996) Lymphocyte homing and homeostasis. **Science**, 272: (5258): 60-66.

Butcher, E.C., Williams, M., Youngman, K., Rott, L. and Briskin, M. (1999) Lymphocyte trafficking and regional immunity. **Adv Immunol**, 72: 209-253.

Campbell, D.J. and Butcher, E.C. (2002) Rapid acquisition of tissue-specific homing phenotypes by CD4(+) T cells activated in cutaneous or mucosal lymphoid tissues. **J Exp Med**, 195: (1): 135-141.

Campbell, J.J., Murphy, K.E., Kunkel, E.J., Brightling, C.E., Soler, D., Shen, Z., Boisvert, J., Greenberg, H.B., Vierra, M.A., Goodman, S.B., Genovese, M.C., Wardlaw, A.J., Butcher, E.C. and Wu, L. (2001) CCR7 expression and memory T cell diversity in humans. **J Immunol**, 166: (2): 877-884.

Cannella, B., Cross, A.H. and Raine, C.S. (1991) Relapsing autoimmune demyelination: a role for vascular addressins. **J Neuroimmunol**, 35: (1-3): 295-300.

Carman, C.V. and Springer, T.A. (2003) Integrin avidity regulation: are changes in affinity and conformation underemphasized? **Curr Opin Cell Biol**, 15: (5): 547-556.

Carman, C.V. and Springer, T.A. (2004) A transmigratory cup in leukocyte diapedesis both through individual vascular endothelial cells and between them. **J Cell Biol**, 167: (2): 377-388.

Casasnovas, J.M., Stehle, T., Liu, J.H., Wang, J.H. and Springer, T.A. (1998) A dimeric crystal structure for the N-terminal two domains of intercellular adhesion molecule-1. **Proc Natl Acad Sci U S A**, 95: (8): 4134-4139.

Cepek, K.L., Shaw, S.K., Parker, C.M., Russell, G.J., Morrow, J.S., Rimm, D.L. and Brenner, M.B. (1994) Adhesion between epithelial cells and T lymphocytes mediated by E-cadherin and the alpha E beta 7 integrin. **Nature**, 372: (6502): 190-193.

Chan, B.M., Elices, M.J., Murphy, E. and Hemler, M.E. (1992) Adhesion to vascular cell adhesion molecule 1 and fibronectin. Comparison of alpha 4 beta 1 (VLA-4) and alpha 4 beta 7 on the human B cell line JY. **J Biol Chem**, 267: (12): 8366-8370.

Chan, J.R., Hyduk, S.J. and Cybulsky, M.I. (2003) Detecting rapid and transient upregulation of leukocyte integrin affinity induced by chemokines and chemoattractants. **J Immunol Methods**, 273: (1-2): 43-52.

Chen, S. and Springer, T.A. (1999) An automatic braking system that stabilizes leukocyte rolling by an increase in selectin bond number with shear. **J Cell Biol**, 144: (1): 185-200.

Cinamon, G., Grabovsky, V., Winter, E., Franitza, S., Feigelson, S., Shamri, R., Dwir, O. and Alon, R. (2001a) Novel chemokine functions in lymphocyte migration through vascular endothelium under shear flow. **J Leukoc Biol**, 69: (6): 860-866.

Cinamon, G., Shinder, V. and Alon, R. (2001b) Shear forces promote lymphocyte migration across vascular endothelium bearing apical chemokines. **Nat Immunol**, 2: (6): 515-522.

Cinamon, G., Shinder, V., Shamri, R. and Alon, R. (2004) Chemoattractant signals and beta 2 integrin occupancy at apical endothelial contacts combine with shear stress signals to promote transendothelial neutrophil migration. **J Immunol**, 173: (12): 7282-7291.

Connor, E.M., Eppihimer, M.J., Morise, Z., Granger, D.N. and Grisham, M.B. (1999) Expression of mucosal addressin cell adhesion molecule-1 (MAdCAM-1) in acute and chronic inflammation. **J Leukoc Biol**, 65: (3): 349-355.

Curbishley, S.M., Eksteen, B., Gladue, R.P., Lalor, P. and Adams, D.H. (2005) CXCR 3 activation promotes lymphocyte transendothelial migration across human hepatic endothelium under fluid flow. **Am J Pathol**, 167: (3): 887-899.

Cyster, J.G. (1999) Chemokines and cell migration in secondary lymphoid organs. **Science**, 286: (5447): 2098-2102.

Dando, J., Wilkinson, K.W., Ortlepp, S., King, D.J. and Brady, R.L. (2002) A reassessment of the MAdCAM-1 structure and its role in integrin recognition. **Acta Crystallogr D Biol Crystallogr**, 58: (Pt 2): 233-241.

Danese, S. and Fiocchi, C. (2006) Etiopathogenesis of inflammatory bowel diseases. **World J Gastroenterol**, 12: (30): 4807-4812.

Dardalhon, V., Awasthi, A., Kwon, H., Galileos, G., Gao, W., Sobel, R.A., Mitsdoerffer, M., Strom, T.B., Elyaman, W., Ho, I.C., Khoury, S., Oukka, M. and Kuchroo, V.K. (2008) IL-4 inhibits TGF-beta-induced Foxp3+ T cells and, together with TGF-beta, generates IL-9+ IL-10+ Foxp3(-) effector T cells. **Nat Immunol**, 9: (12): 1347-1355.

Di Nunzio, S., Cecconi, M., Passerini, L., McMurchy, A.N., Baron, U., Turbachova, I., Vignola, S., Valencic, E., Tommasini, A., Junker, A., Cazzola, G., Olek, S., Levings, M.K., Perroni, L., Roncarolo, M.G. and Bacchetta, R. (2009) Wild-type FOXP3 is selectively active in CD4+CD25hi regulatory T cells of healthy female carriers of different FOXP3 mutations. **Blood**, 114: (19): 4138-4141.

Diamond, M.S., Staunton, D.E., de Fougerolles, A.R., Stacker, S.A., Garcia-Aguilar, J., Hibbs, M.L. and Springer, T.A. (1990) ICAM-1 (CD54): a counter-receptor for Mac-1 (CD11b/CD18). **J Cell Biol**, 111: (6 Pt 2): 3129-3139.

Doherty, D.G. and O'Farrelly, C. (2000) Innate and adaptive lymphoid cells in the human liver. **Immunol Rev**, 174: 5-20.

Dunlop, L.C., Skinner, M.P., Bendall, L.J., Favaloro, E.J., Castaldi, P.A., Gorman, J.J., Gamble, J.R., Vadas, M.A. and Berndt, M.C. (1992) Characterization of GMP-140 (P-selectin) as a circulating plasma protein. **J Exp Med**, 175: (4): 1147-1150.

Dunne, J.L., Ballantyne, C.M., Beaudet, A.L. and Ley, K. (2002) Control of leukocyte rolling velocity in TNF-alpha-induced inflammation by LFA-1 and Mac-1. **Blood**, 99: (1): 336-341.

Durieu-Trautmann, O., Chaverot, N., Cazaubon, S., Strosberg, A.D. and Couraud, P.O. (1994) Intercellular adhesion molecule 1 activation induces tyrosine phosphorylation of the cytoskeleton-associated protein cortactin in brain microvessel endothelial cells. **J Biol Chem**, 269: (17): 12536-12540.

Dustin, M.L. and Springer, T.A. (1988) Lymphocyte function-associated antigen-1 (LFA-1) interaction with intercellular adhesion molecule-1 (ICAM-1) is one of at least three mechanisms for lymphocyte adhesion to cultured endothelial cells. **J Cell Biol**, 107: (1): 321-331.

Edwards, S., Lalor, P.F., Nash, G.B., Rainger, G.E. and Adams, D.H. (2005) Lymphocyte traffic through sinusoidal endothelial cells is regulated by hepatocytes. **Hepatology**, 41: (3): 451-459.

Eksteen, B., Grant, A.J., Miles, A., Curbishley, S.M., Lalor, P.F., Hubscher, S.G., Briskin, M., Salmon, M. and Adams, D.H. (2004a) Hepatic endothelial CCL25 mediates the recruitment of CCR9+ gut-homing lymphocytes to the liver in primary sclerosing cholangitis. **J Exp Med**, 200: (11): 1511-1517.

Eksteen, B., Miles, A.E., Grant, A.J. and Adams, D.H. (2004b) Lymphocyte homing in the pathogenesis of extra-intestinal manifestations of inflammatory bowel disease. **Clin Med**, 4: (2): 173-180.

Eksteen, B., Miles, A., Curbishley, S.M., Tselepis, C., Grant, A.J., Walker, L.S. and Adams, D.H. (2006) Epithelial inflammation is associated with CCL28 production and the recruitment of regulatory T cells expressing CCR10. **J Immunol**, 177: (1): 593-603.

Eksteen, B., Liaskou, E. and Adams, D.H. (2008) Lymphocyte homing and its role in the pathogenesis of IBD. **Inflamm Bowel Dis**, 14: (9): 1298-1312.

Eksteen, B., Mora, J.R., Haughton, E.L., Henderson, N.C., Lee-Turner, L., Villablanca, E.J., Curbishley, S.M., Aspinall, A.I., von Andrian, U.H. and Adams, D.H. (2009) Gut homing receptors on CD8 T cells are retinoic acid dependent and not maintained by liver dendritic or stellate cells. **Gastroenterology**, 137: (1): 320-329.

Emoto, M., Miyamoto, M., Namba, K., Schmits, R., Van Rooijen, N., Kita, E. and Kaufmann, S.H. (2000) Participation of leukocyte function-associated antigen-1 and NK cells in the homing of thymic CD8+NKT cells to the liver. **Eur J Immunol**, 30: (10): 3049-3056.

Engelhardt, B. and Wolburg, H. (2004) Mini-review: Transendothelial migration of leukocytes: through the front door or around the side of the house? **Eur J Immunol**, 34: (11): 2955-2963.

Enomoto, K., Nishikawa, Y., Omori, Y., Tokairin, T., Yoshida, M., Ohi, N., Nishimura, T., Yamamoto, Y. and Li, Q. (2004) Cell biology and pathology of liver sinusoidal endothelial cells. **Med Electron Microsc**, 37: (4): 208-215.

Ericsson, A., Svensson, M., Arya, A. and Agace, W.W. (2004) CCL25/CCR9 promotes the induction and function of CD103 on intestinal intraepithelial lymphocytes. **Eur J Immunol**, 34: (10): 2720-2729.

Erlandsen, S.L., Hasslen, S.R. and Nelson, R.D. (1993) Detection and spatial distribution of the beta 2 integrin (Mac-1) and L-selectin (LECAM-1) adherence receptors on human neutrophils by high-resolution field emission SEM. **J Histochem Cytochem**, 41: (3): 327-333.

Faveeuw, C., Gagnerault, M.C. and Lepault, F. (1994) Expression of homing and adhesion molecules in infiltrated islets of Langerhans and salivary glands of nonobese diabetic mice. **J Immunol**, 152: (12): 5969-5978.

Feagan, B.G., Greenberg, G.R., Wild, G., Fedorak, R.N., Pare, P., McDonald, J.W., Dube, R., Cohen, A., Steinhart, A.H., Landau, S., Aguzzi, R.A., Fox, I.H. and Vandervoort, M.K. (2005) Treatment of ulcerative colitis with a humanized antibody to the alpha4beta7 integrin. **N Engl J Med**, 352: (24): 2499-2507.

Feagan, B.G., Greenberg, G.R., Wild, G., Fedorak, R.N., Pare, P., McDonald, J.W., Cohen, A., Bitton, A., Baker, J., Dube, R., Landau, S.B., Vandervoort, M.K. and Parikh, A. (2008) Treatment of active Crohn's disease with MLN0002, a humanized antibody to the alpha4beta7 integrin. **Clin Gastroenterol Hepatol**, 6: (12): 1370-1377.

Feng, D., Nagy, J.A., Pyne, K., Dvorak, H.F. and Dvorak, A.M. (1998) Neutrophils emigrate from venules by a transendothelial cell pathway in response to FMLP. **J Exp Med**, 187: (6): 903-915.

Feng, N., Jaimes, M.C., Lazarus, N.H., Monak, D., Zhang, C., Butcher, E.C. and Greenberg, H.B. (2006) Redundant role of chemokines CCL25/TECK and CCL28/MEC in IgA+ plasmablast recruitment to the intestinal lamina propria after rotavirus infection. **J Immunol**, 176: (10): 5749-5759.

Finkel, T. (1998) Oxygen radicals and signaling. **Curr Opin Cell Biol**, 10: (2): 248-253.

Fong, S., Jones, S., Renz, M.E., Chiu, H.H., Ryan, A.M., Presta, L.G. and Jackson, D. (1997) Mucosal addressin cell adhesion molecule-1 (MAdCAM-1). Its binding motif for alpha 4 beta 7 and role in experimental colitis. **Immunol Res**, 16: (3): 299-311.

Forster, R., Schubel, A., Breitfeld, D., Kremmer, E., Renner-Muller, I., Wolf, E. and Lipp, M. (1999) CCR7 coordinates the primary immune response by establishing functional microenvironments in secondary lymphoid organs. **Cell**, 99: (1): 23-33.

Fraga, M.F., Rodriguez, R. and Canal, M.J. (2000) Rapid quantification of DNA methylation by high performance capillary electrophoresis. **Electrophoresis**, 21: (14): 2990-2994.

Freedman, A.S., Munro, J.M., Rice, G.E., Bevilacqua, M.P., Morimoto, C., McIntyre, B.W., Rhynhart, K., Pober, J.S. and Nadler, L.M. (1990) Adhesion of human B cells to germinal centers in vitro involves VLA-4 and INCAM-110. **Science**, 249: (4972): 1030-1033.

Friedman, S.L., Rockey, D.C., McGuire, R.F., Maher, J.J., Boyles, J.K. and Yamasaki, G. (1992) Isolated hepatic lipocytes and Kupffer cells from normal human liver: morphological and functional characteristics in primary culture. **Hepatology**, 15: (2): 234-243.

Frommer, W., Archer, L., Boon, B., Brunius, G., Collins, C.H., Crooy, P., Donikian, R., Economidis, I., Frontali, C., Gaal, T. and et al. (1992) Safe biotechnology (4). Recommendations for safety levels for biotechnological operations with microorganisms that cause diseases in plants. **Appl Microbiol Biotechnol**, 38: (2): 139-140.

Fujiyama, Y., Hokari, R., Miura, S., Watanabe, C., Komoto, S., Oyama, T., Kurihara, C., Nagata, H. and Hibi, T. (2007) Butter feeding enhances TNF-alpha production from macrophages and lymphocyte adherence in murine small intestinal microvessels. **J Gastroenterol Hepatol**, 22: (11): 1838-1845.

Gallatin, W.M., Weissman, I.L. and Butcher, E.C. (1983) A cell-surface molecule involved in organ-specific homing of lymphocytes. **Nature**, 304: (5921): 30-34.

Gamble, J.R., Skinner, M.P., Berndt, M.C. and Vadas, M.A. (1990) Prevention of activated neutrophil adhesion to endothelium by soluble adhesion protein GMP140. **Science**, 249: (4967): 414-417.

Gao, B., Jeong, W.I. and Tian, Z. (2008) Liver: An organ with predominant innate immunity. **Hepatology**, 47: (2): 729-736.

Gearing, A.J., Hemingway, I., Pigott, R., Hughes, J., Rees, A.J. and Cashman, S.J. (1992) Soluble forms of vascular adhesion molecules, E-selectin, ICAM-1, and VCAM-1: pathological significance. **Ann N Y Acad Sci**, 667: 324-331.

Gearing, A.J. and Newman, W. (1993) Circulating adhesion molecules in disease. **Immunol Today**, 14: (10): 506-512.

Ghosh, S., Goldin, E., Gordon, F.H., Malchow, H.A., Rask-Madsen, J., Rutgeerts, P., Vyhnalek, P., Zadorova, Z., Palmer, T. and Donoghue, S. (2003) Natalizumab for active Crohn's disease. **N Engl J Med**, 348: (1): 24-32.

Giagulli, C., Ottoboni, L., Caveggion, E., Rossi, B., Lowell, C., Constantin, G., Laudanna, C. and Berton, G. (2006) The Src family kinases Hck and Fgr are dispensable for inside-out, chemoattractant-induced signaling regulating beta 2 integrin affinity and valency in neutrophils, but are required for beta 2 integrin-mediated outside-in signaling involved in sustained adhesion. **J Immunol**, 177: (1): 604-611.

Girard, J.P. and Springer, T.A. (1995) High endothelial venules (HEVs): specialized endothelium for lymphocyte migration. **Immunol Today**, 16: (9): 449-457.

Gocke, A.R., Cravens, P.D., Ben, L.H., Hussain, R.Z., Northrop, S.C., Racke, M.K. and Lovett-Racke, A.E. (2007) T-bet regulates the fate of Th1 and Th17 lymphocytes in autoimmunity. **J Immunol**, 178: (3): 1341-1348.

Goddard, S., Williams, A., Morland, C., Qin, S., Gladue, R., Hubscher, S.G. and Adams, D.H. (2001) Differential expression of chemokines and chemokine receptors shapes the inflammatory response in rejecting human liver transplants. **Transplantation**, 72: (12): 1957-1967.

Godfrey, D.I. and Kronenberg, M. (2004) Going both ways: immune regulation via CD1d-dependent NKT cells. **J Clin Invest**, 114: (10): 1379-1388.

Godfrey, D.I., MacDonald, H.R., Kronenberg, M., Smyth, M.J. and Van Kaer, L. (2004) NKT cells: what's in a name? **Nat Rev Immunol**, 4: (3): 231-237.

Goldberger, A., Middleton, K.A., Oliver, J.A., Paddock, C., Yan, H.C., DeLisser, H.M., Albelda, S.M. and Newman, P.J. (1994) Biosynthesis and processing of the cell adhesion molecule PECAM-1 includes production of a soluble form. **J Biol Chem**, 269: (25): 17183-17191.

Goldsby, R.A., Kindt, T.J., Osborne, B.A., Kuby, J. (2002) "**Immunology**". Fifth Edition.

Gonzalgo, M.L. and Jones, P.A. (1997) Rapid quantitation of methylation differences at specific sites using methylation-sensitive single nucleotide primer extension (Ms-SNuPE). **Nucleic Acids Res**, 25: (12): 2529-2531.

Goto, A., Arimura, Y., Shinomura, Y., Imai, K. and Hinoda, Y. (2006) Antisense therapy of MAdCAM-1 for trinitrobenzenesulfonic acid-induced murine colitis. **Inflamm Bowel Dis**, 12: (8): 758-765.

Grant, A.J., Lalor, P.F., Hubscher, S.G., Briskin, M. and Adams, D.H. (2001) MAdCAM-1 expressed in chronic inflammatory liver disease supports mucosal lymphocyte adhesion to hepatic endothelium (MAdCAM-1 in chronic inflammatory liver disease). **Hepatology**, 33: (5): 1065-1072.

Grant, A.J., Goddard, S., Ahmed-Choudhury, J., Reynolds, G., Jackson, D.G., Briskin, M., Wu, L., Hubscher, S.G. and Adams, D.H. (2002a) Hepatic expression of secondary lymphoid chemokine (CCL21) promotes the development of portal-associated lymphoid tissue in chronic inflammatory liver disease. **Am J Pathol**, 160: (4): 1445-1455.

Grant, A.J., Lalor, P.F., Salmi, M., Jalkanen, S. and Adams, D.H. (2002b) Homing of mucosal lymphocytes to the liver in the pathogenesis of hepatic complications of inflammatory bowel disease. **Lancet**, 359: (9301): 150-157.

Green, N., Rosebrook, J., Cochran, N., Tan, K., Wang, J.H., Springer, T.A. and Briskin, M.J. (1999) Mutational analysis of MAdCAM-1/alpha4beta7 interactions reveals significant binding determinants in both the first and second immunuglobulin domains. **Cell Adhes Commun**, 7: (3): 167-181.

Grimwood, J., Gordon, L.A., Olsen, A., Terry, A., Schmutz, J., Lamerdin, J., Hellsten, U., Goodstein, D., Couronne, O., Tran-Gyamfi, M., Aerts, A., Altherr, M., Ashworth, L., Bajorek, E., Black, S., Branscomb, E., Caenepeel, S., Carrano, A., Caoile, C., Chan, Y.M., Christensen, M., Cleland, C.A., Copeland, A., Dalin, E., Dehal, P., Denys, M., Detter, J.C., Escobar, J., Flowers, D., Fotopulos, D., Garcia, C., Georgescu, A.M., Glavina, T., Gomez, M., Gonzales, E., Groza, M., Hammon, N., Hawkins, T., Haydu, L., Ho, I., Huang, W., Israni, S., Jett, J., Kadner, K., Kimball, H., Kobayashi, A., Larionov, V., Leem, S.H., Lopez, F., Lou, Y., Lowry, S., Malfatti, S., Martinez, D., McCready, P., Medina, C., Morgan, J., Nelson, K., Nolan, M., Ovcharenko, I., Pitluck, S., Pollard, M., Popkie, A.P., Predki, P., Quan, G., Ramirez, L., Rash, S., Retterer, J., Rodriguez, A., Rogers, S., Salamov, A., Salazar, A., She, X., Smith, D., Slezak, T., Solovyev, V., Thayer, N., Tice, H., Tsai, M., Ustaszewska, A., Vo, N., Wagner, M., Wheeler, J., Wu, K., Xie, G., Yang, J., Dubchak, I., Furey, T.S., DeJong, P., Dickson, M., Gordon, D., Eichler, E.E., Pennacchio, L.A., Richardson, P., Stubbs, L., Rokhsar, D.S., Myers, R.M., Rubin, E.M. and Lucas, S.M. (2004) The DNA sequence and biology of human chromosome 19. **Nature**, 428: (6982): 529-535.

Guagnozzi, D. and Caprilli, R. (2008) Natalizumab in the treatment of Crohn's disease. **Biologics**, 2: (2): 275-284.

Gunn, M.D., Tangemann, K., Tam, C., Cyster, J.G., Rosen, S.D. and Williams, L.T. (1998) A chemokine expressed in lymphoid high endothelial venules promotes the adhesion and chemotaxis of naive T lymphocytes. **Proc Natl Acad Sci U S A**, 95: (1): 258-263.

Gunn, M.D., Kyuwa, S., Tam, C., Kakiuchi, T., Matsuzawa, A., Williams, L.T. and Nakano, H. (1999) Mice lacking expression of secondary lymphoid organ chemokine have defects in lymphocyte homing and dendritic cell localization. **J Exp Med**, 189: (3): 451-460.

Hamann, A., Andrew, D.P., Jablonski-Westrich, D., Holzmann, B. and Butcher, E.C. (1994) Role of alpha 4-integrins in lymphocyte homing to mucosal tissues in vivo. **J Immunol**, 152: (7): 3282-3293.

Hammer, D.A. and Apte, S.M. (1992) Simulation of cell rolling and adhesion on surfaces in shear flow: general results and analysis of selectin-mediated neutrophil adhesion. **Biophys J**, 63: (1): 35-57.

Hanninen, A., Taylor, C., Streeter, P.R., Stark, L.S., Sarte, J.M., Shizuru, J.A., Simell, O. and Michie, S.A. (1993) Vascular addressins are induced on islet vessels during insulitis in nonobese diabetic mice and are involved in lymphoid cell binding to islet endothelium. **J Clin Invest**, 92: (5): 2509-2515.

Hanninen, A., Jaakkola, I. and Jalkanen, S. (1998) Mucosal addressin is required for the development of diabetes in nonobese diabetic mice. **J Immunol**, 160: (12): 6018-6025.

Hendriks, J., Gravestein, L.A., Tesselaar, K., van Lier, R.A., Schumacher, T.N. and Borst, J. (2000) CD27 is required for generation and long-term maintenance of T cell immunity. **Nat Immunol**, 1: (5): 433-440.

Heydtmann, M. and Adams, D.H. (2009) Chemokines in the immunopathogenesis of hepatitis C infection. **Hepatology**, 49: (2): 676-688.

Hidalgo, A., Peired, A.J., Wild, M.K., Vestweber, D. and Frenette, P.S. (2007) Complete identification of E-selectin ligands on neutrophils reveals distinct functions of PSGL-1, ESL-1, and CD44. **Immunity**, 26: (4): 477-489.

Hieshima, K., Kawasaki, Y., Hanamoto, H., Nakayama, T., Nagakubo, D., Kanamaru, A. and Yoshie, O. (2004) CC chemokine ligands 25 and 28 play essential roles in intestinal extravasation of IgA antibody-secreting cells. **J Immunol**, 173: (6): 3668-3675.

Hillan, K.J., Hagler, K.E., MacSween, R.N., Ryan, A.M., Renz, M.E., Chiu, H.H., Ferrier, R.K., Bird, G.L., Dhillon, A.P., Ferrell, L.D. and Fong, S. (1999) Expression of the mucosal vascular addressin, MAdCAM-1, in inflammatory liver disease. **Liver**, 19: (6): 509-518.

Hirschi, K.K. and D'Amore, P.A. (1996) Pericytes in the microvasculature. **Cardiovasc Res**, 32: (4): 687-698.

Hooper, L.V. and Gordon, J.I. (2001) Commensal host-bacterial relationships in the gut. **Science**, 292: (5519): 1115-1118.

Hori, T., Sakaida, H., Sato, A., Nakajima, T., Shida, H., Yoshie, O. and Uchiyama, T. (1998) Detection and delineation of CXCR-4 (fusin) as an entry and fusion cofactor for T-tropic [correction of T cell-tropic] HIV-1 by three different monoclonal antibodies. **J Immunol**, 160: (1): 180-188.

Hsu-Lin, S., Berman, C.L., Furie, B.C., August, D. and Furie, B. (1984) A platelet membrane protein expressed during platelet activation and secretion. Studies using a monoclonal antibody specific for thrombin-activated platelets. **J Biol Chem**, 259: (14): 9121-9126.

Huang, A.J., Manning, J.E., Bandak, T.M., Ratau, M.C., Hanser, K.R. and Silverstein, S.C. (1993) Endothelial cell cytosolic free calcium regulates neutrophil migration across monolayers of endothelial cells. **J Cell Biol**, 120: (6): 1371-1380.

Hynes, R.O. (2002) Integrins: bidirectional, allosteric signaling machines. **Cell**, 110: (6): 673-687.

Iademarco, M.F., McQuillan, J.J., Rosen, G.D. and Dean, D.C. (1992) Characterization of the promoter for vascular cell adhesion molecule-1 (VCAM-1). **J Biol Chem**, 267: (23): 16323-16329.

Ichikawa, H., Flores, S., Kvietys, P.R., Wolf, R.E., Yoshikawa, T., Granger, D.N. and Aw, T.Y. (1997) Molecular mechanisms of anoxia/reoxygenation-induced neutrophil adherence to cultured endothelial cells. **Circ Res**, 81: (6): 922-931.

Iigo, Y., Suematsu, M., Higashida, T., Oheda, J., Matsumoto, K., Wakabayashi, Y., Ishimura, Y., Miyasaka, M. and Takashi, T. (1997) Constitutive expression of ICAM-1 in rat microvascular systems analyzed by laser confocal microscopy. **Am J Physiol**, 273: (1 Pt 2): H138-147.

Iizuka, T., Koike, R., Miyasaka, N., Miyasaka, M. and Watanabe, T. (1998) Cloning and characterization of the rat MAdCAM-1 cDNA and gene. **Biochim Biophys Acta**, 1395: (3): 266-270.

Ikeda, M., Schroeder, K.K., Mosher, L.B., Woods, C.W. and Akeson, A.L. (1994) Suppressive effect of antioxidants on intercellular adhesion molecule-1 (ICAM-1) expression in human epidermal keratinocytes. **J Invest Dermatol**, 103: (6): 791-796.

Itoh, Y., Morita, A., Nishioji, K., Fujii, H., Nakamura, H., Kirishima, T., Toyama, T., Yamauchi, N., Nagao, Y., Narumi, S. and Okanoue, T. (2001) Time course profile and cell-type-specific production of monokine induced by interferon-gamma in Concanavalin A-induced hepatic injury in mice: comparative study with interferon-inducible protein-10. **Scand J Gastroenterol**, 36: (12): 1344-1351.

Iwasaki, A. and Medzhitov, R. (2004) Toll-like receptor control of the adaptive immune responses. **Nat Immunol**, 5: (10): 987-995.

Jaakkola, K., Kaunismaki, K., Tohka, S., Yegutkin, G., Vanttinen, E., Havia, T., Pelliniemi, L.J., Virolainen, M., Jalkanen, S. and Salmi, M. (1999) Human vascular adhesion protein-1 in smooth muscle cells. **Am J Pathol**, 155: (6): 1953-1965.

Jabri, B. and Ebert, E. (2007) Human CD8+ intraepithelial lymphocytes: a unique model to study the regulation of effector cytotoxic T lymphocytes in tissue. **Immunol Rev**, 215: 202-214.

Jaffe, E.A., Nachman, R.L., Becker, C.G. and Minick, C.R. (1973) Culture of human endothelial cells derived from umbilical veins. Identification by morphologic and immunologic criteria. **J Clin Invest**, 52: (11): 2745-2756.

Jalkanen, S. and Salmi, M. (1993) A novel endothelial cell molecule mediating lymphocyte binding in humans. **Behring Inst Mitt**, (92): 36-43.

Jalkanen, S. and Salmi, M. (2001) Cell surface monoamine oxidases: enzymes in search of a function. **EMBO J**, 20: (15): 3893-3901.

Jalkanen, S., Karikoski, M., Mercier, N., Koskinen, K., Henttinen, T., Elima, K., Salmivirta, K. and Salmi, M. (2007) The oxidase activity of vascular adhesion protein-1 (VAP-1) induces endothelial E- and P-selectins and leukocyte binding. **Blood**, 110: (6): 1864-1870.

Jalkanen, S. and Salmi, M. (2008) VAP-1 and CD73, endothelial cell surface enzymes in leukocyte extravasation. **Arterioscler Thromb Vasc Biol**, 28: (1): 18-26.

Jentoft, N. (1990) Why are proteins O-glycosylated? **Trends Biochem Sci**, 15: (8): 291-294.

Jin, D.K., Shido, K., Kopp, H.G., Petit, I., Shmelkov, S.V., Young, L.M., Hooper, A.T., Amano, H., Avecilla, S.T., Heissig, B., Hattori, K., Zhang, F., Hicklin, D.J., Wu, Y., Zhu, Z., Dunn, A., Salari, H., Werb, Z., Hackett, N.R., Crystal, R.G., Lyden, D. and Rafii, S. (2006) Cytokine-mediated deployment of SDF-1 induces revascularization through recruitment of CXCR4+ hemangiocytes. **Nat Med**, 12: (5): 557-567.

John, B. and Crispe, I.N. (2005) TLR-4 regulates CD8+ T cell trapping in the liver. **J Immunol**, 175: (3): 1643-1650.

Johnston, G.I., Bliss, G.A., Newman, P.J. and McEver, R.P. (1990) Structure of the human gene encoding granule membrane protein-140, a member of the selectin family of adhesion receptors for leukocytes. **J Biol Chem**, 265: (34): 21381-21385.

Jones, E.Y., Harlos, K., Bottomley, M.J., Robinson, R.C., Driscoll, P.C., Edwards, R.M., Clements, J.M., Dudgeon, T.J. and Stuart, D.I. (1995) Crystal structure of an integrin-binding fragment of vascular cell adhesion molecule-1 at 1.8 A resolution. **Nature**, 373: (6514): 539-544.

Jonuleit, H. and Schmitt, E. (2003) The regulatory T cell family: distinct subsets and their interrelations. **J Immunol**, 171: (12): 6323-6327.

Jung, M.Y., Park, S.Y. and Kim, I.S. (2007) Stabilin-2 is involved in lymphocyte adhesion to the hepatic sinusoidal endothelium via the interaction with alphaMbeta2 integrin. **J Leukoc Biol**, 82: (5): 1156-1165.

Jung, S. and Littman, D.R. (1999) Chemokine receptors in lymphoid organ homeostasis. **Curr Opin Immunol**, 11: (3): 319-325.

Kahn, J., Ingraham, R.H., Shirley, F., Migaki, G.I. and Kishimoto, T.K. (1994) Membrane proximal cleavage of L-selectin: identification of the cleavage site and a 6-kD transmembrane peptide fragment of L-selectin. **J Cell Biol**, 125: (2): 461-470.

Kamada, N., Hisamatsu, T., Honda, H., Kobayashi, T., Chinen, H., Kitazume, M.T., Takayama, T., Okamoto, S., Koganei, K., Sugita, A., Kanai, T. and Hibi, T. (2009) Human CD14+ macrophages in intestinal lamina propria exhibit potent antigen-presenting ability. **J Immunol**, 183: (3): 1724-1731.

Kansas, G.S. (1996) Selectins and their ligands: current concepts and controversies. **Blood**, 88: (9): 3259-3287.

Kanwar, J.R., Kanwar, R.K., Wang, D. and Krissansen, G.W. (2000) Prevention of a chronic progressive form of experimental autoimmune encephalomyelitis by an antibody against mucosal addressin cell adhesion molecule-1, given early in the course of disease progression. **Immunol Cell Biol**, 78: (6): 641-645.

Katayama, M., Handa, M., Ambo, H., Araki, Y., Hirai, S., Kato, I., Kawai, Y., Watanabe, K. and Ikeda, Y. (1992) A monoclonal antibody-based enzyme immunoassay for human GMP-140/P-selectin. **J Immunol Methods**, 153: (1-2): 41-48.

Kato, S., Hokari, R., Matsuzaki, K., Iwai, A., Kawaguchi, A., Nagao, S., Miyahara, T., Itoh, K., Ishii, H. and Miura, S. (2000) Amelioration of murine experimental colitis by inhibition of mucosal addressin cell adhesion molecule-1. **J Pharmacol Exp Ther**, 295: (1): 183-189.

Kelner, G.S., Kennedy, J., Bacon, K.B., Kleyensteuber, S., Largaespada, D.A., Jenkins, N.A., Copeland, N.G., Bazan, J.F., Moore, K.W., Schall, T.J. and et al. (1994) Lymphotactin: a cytokine that represents a new class of chemokine. **Science**, 266: (5189): 1395-1399.

Kennedy, J., Kelner, G.S., Kleyensteuber, S., Schall, T.J., Weiss, M.C., Yssel, H., Schneider, P.V., Cocks, B.G., Bacon, K.B. and Zlotnik, A. (1995) Molecular cloning and functional characterization of human lymphotactin. **J Immunol**, 155: (1): 203-209.

Kim, C.H. and Broxmeyer, H.E. (1999) Chemokines: signal lamps for trafficking of T and B cells for development and effector function. **J Leukoc Biol**, 65: (1): 6-15.

Kinashi, T. (2005) Intracellular signalling controlling integrin activation in lymphocytes. **Nat Rev Immunol**, 5: (7): 546-559.

Kivisakk, P., Mahad, D.J., Callahan, M.K., Trebst, C., Tucky, B., Wei, T., Wu, L., Baekkevold, E.S., Lassmann, H., Staugaitis, S.M., Campbell, J.J. and Ransohoff, R.M. (2003) Human cerebrospinal fluid central memory CD4+ T cells: evidence for trafficking through choroid plexus and meninges via P-selectin. **Proc Natl Acad Sci U S A**, 100: (14): 8389-8394.

Knolle, P.A., Schmitt, E., Jin, S., Germann, T., Duchmann, R., Hegenbarth, S., Gerken, G. and Lohse, A.W. (1999) Induction of cytokine production in naive CD4(+) T cells by antigen-presenting murine liver sinusoidal endothelial cells but failure to induce differentiation toward Th1 cells. **Gastroenterology**, 116: (6): 1428-1440.

Knolle, P.A. and Gerken, G. (2000) Local control of the immune response in the liver. **Immunol Rev**, 174: 21-34.

Knolle, P.A. and Limmer, A. (2003) Control of immune responses by savenger liver endothelial cells. **Swiss Med Wkly**, 133: (37-38): 501-506.

Kobayashi, T., Okamoto, S., Iwakami, Y., Nakazawa, A., Hisamatsu, T., Chinen, H., Kamada, N., Imai, T., Goto, H. and Hibi, T. (2007) Exclusive increase of CX3CR1+CD28-CD4+ T cells in inflammatory bowel disease and their recruitment as intraepithelial lymphocytes. **Inflamm Bowel Dis**, 13: (7): 837-846.

Koch, A.E., Polverini, P.J., Kunkel, S.L., Harlow, L.A., DiPietro, L.A., Elner, V.M., Elner, S.G. and Strieter, R.M. (1992) Interleukin-8 as a macrophage-derived mediator of angiogenesis. **Science**, 258: (5089): 1798-1801.

Koizumi, M., King, N., Lobb, R., Benjamin, C. and Podolsky, D.K. (1992) Expression of vascular adhesion molecules in inflammatory bowel disease. **Gastroenterology**, 103: (3): 840-847.

Koopman, G., Parmentier, H.K., Schuurman, H.J., Newman, W., Meijer, C.J. and Pals, S.T. (1991) Adhesion of human B cells to follicular dendritic cells involves both the lymphocyte function-associated antigen 1/intercellular adhesion molecule 1 and very late antigen 4/vascular cell adhesion molecule 1 pathways. **J Exp Med**, 173: (6): 1297-1304.

Kosiewicz, M.M., Nast, C.C., Krishnan, A., Rivera-Nieves, J., Moskaluk, C.A., Matsumoto, S., Kozaiwa, K. and Cominelli, F. (2001) Th1-type responses mediate spontaneous ileitis in a novel murine model of Crohn's disease. **J Clin Invest**, 107: (6): 695-702.

Koskinen, K., Vainio, P.J., Smith, D.J., Pihlavisto, M., Yla-Herttuala, S., Jalkanen, S. and Salmi, M. (2004) Granulocyte transmigration through the endothelium is regulated by the oxidase activity of vascular adhesion protein-1 (VAP-1). **Blood**, 103: (9): 3388-3395.

Kraal, G., Schornagel, K., Streeter, P.R., Holzmann, B. and Butcher, E.C. (1995) Expression of the mucosal vascular addressin, MAdCAM-1, on sinus-lining cells in the spleen. **Am J Pathol**, 147: (3): 763-771.

Kronenberg, M. and Gapin, L. (2002) The unconventional lifestyle of NKT cells. **Nat Rev Immunol**, 2: (8): 557-568.

Kulkarni, S., Nesbitt, W.S., Dopheide, S.M., Hughan, S.C., Harper, I.S. and Jackson, S.P. (2004) Techniques to examine platelet adhesive interactions under flow. **Methods Mol Biol**, 272: 165-186.

Kummer, C. and Ginsberg, M.H. (2006) New approaches to blockade of alpha4-integrins, proven therapeutic targets in chronic inflammation. **Biochem Pharmacol**, 72: (11): 1460-1468.

Kunkel, E.J., Campbell, J.J., Haraldsen, G., Pan, J., Boisvert, J., Roberts, A.I., Ebert, E.C., Vierra, M.A., Goodman, S.B., Genovese, M.C., Wardlaw, A.J., Greenberg, H.B., Parker, C.M., Butcher, E.C., Andrew, D.P. and Agace, W.W. (2000) Lymphocyte CC chemokine receptor 9 and epithelial thymus-expressed chemokine (TECK) expression distinguish the small intestinal immune compartment: Epithelial expression of tissue-specific chemokines as an organizing principle in regional immunity. **J Exp Med**, 192: (5): 761-768.

Kunkel, E.J. and Butcher, E.C. (2003) Plasma-cell homing. **Nat Rev Immunol**, 3: (10): 822-829.

Kunkel, E.J., Campbell, D.J. and Butcher, E.C. (2003a) Chemokines in lymphocyte trafficking and intestinal immunity. **Microcirculation**, 10: (3-4): 313-323.

Kunkel, E.J., Kim, C.H., Lazarus, N.H., Vierra, M.A., Soler, D., Bowman, E.P. and Butcher, E.C. (2003b) CCR10 expression is a common feature of circulating and mucosal epithelial tissue IgA Ab-secreting cells. **J Clin Invest**, 111: (7): 1001-1010.

Kunsch, C. and Medford, R.M. (1999) Oxidative stress as a regulator of gene expression in the vasculature. **Circ Res**, 85: (8): 753-766.

Kurkijarvi, R., Adams, D.H., Leino, R., Mottonen, T., Jalkanen, S. and Salmi, M. (1998) Circulating form of human vascular adhesion protein-1 (VAP-1): increased serum levels in inflammatory liver diseases. **J Immunol**, 161: (3): 1549-1557.

Lalor, P.F., Clements, J.M., Pigott, R., Humphries, M.J., Spragg, J.H. and Nash, G.B. (1997) Association between receptor density, cellular activation, and transformation of adhesive behavior of flowing lymphocytes binding to VCAM-1. **Eur J Immunol**, 27: (6): 1422-1426.

Lalor, P.F. and Adams, D.H. (1999) Adhesion of lymphocytes to hepatic endothelium. **Mol Pathol**, 52: (4): 214-219.

Lalor, P.F. and Adams, D.H. (2002) The liver: a model of organ-specific lymphocyte recruitment. **Expert Rev Mol Med**, 4: (2): 1-16.

Lalor, P.F., Edwards, S., McNab, G., Salmi, M., Jalkanen, S. and Adams, D.H. (2002a) Vascular adhesion protein-1 mediates adhesion and transmigration of lymphocytes on human hepatic endothelial cells. **J Immunol**, 169: (2): 983-992.

Lalor, P.F., Shields, P., Grant, A. and Adams, D.H. (2002b) Recruitment of lymphocytes to the human liver. **Immunol Cell Biol**, 80: (1): 52-64.

Lalor, P.F., Lai, W.K., Curbishley, S.M., Shetty, S. and Adams, D.H. (2006) Human hepatic sinusoidal endothelial cells can be distinguished by expression of phenotypic markers related to their specialised functions in vivo. **World J Gastroenterol**, 12: (34): 5429-5439.

Lalor, P.F., Sun, P.J., Weston, C.J., Martin-Santos, A., Wakelam, M.J. and Adams, D.H. (2007) Activation of vascular adhesion protein-1 on liver endothelium results in an NF-kappaB-dependent increase in lymphocyte adhesion. **Hepatology**, 45: (2): 465-474.

Lambolez, F., Kronenberg, M. and Cheroutre, H. (2007) Thymic differentiation of TCR alpha beta(+) CD8 alpha alpha(+) IELs. **Immunol Rev**, 215: 178-188.

Lasky, L.A. (1992) Selectins: interpreters of cell-specific carbohydrate information during inflammation. **Science**, 258: (5084): 964-969.

Lawrence, M.B. and Springer, T.A. (1991) Leukocytes roll on a selectin at physiologic flow rates: distinction from and prerequisite for adhesion through integrins. **Cell**, 65: (5): 859-873.

Leeuwenberg, J.F., Smeets, E.F., Neefjes, J.J., Shaffer, M.A., Cinek, T., Jeunhomme, T.M., Ahern, T.J. and Buurman, W.A. (1992) E-selectin and intercellular adhesion molecule-1 are released by activated human endothelial cells in vitro. **Immunology**, 77: (4): 543-549.

Leung, E., Greene, J., Ni, J., Raymond, L.G., Lehnert, K., Langley, R. and Krissansen, G.W. (1996) Cloning of the mucosal addressin MAdCAM-1 from human brain: identification of novel alternatively spliced transcripts. **Immunol Cell Biol**, 74: (6): 490-496.

Leung, E., Berg, R.W., Langley, R., Greene, J., Raymond, L.A., Augustus, M., Ni, J., Carter, K.C., Spurr, N., Choo, K.H. and Krissansen, G.W. (1997) Genomic organization, chromosomal mapping, and analysis of the 5' promoter region of the human MAdCAM-1 gene. **Immunogenetics**, 46: (2): 111-119.

Leung, E., Kanwar, R.K., Kanwar, J.R. and Krissansen, G.W. (2003) Mucosal vascular addressin cell adhesion molecule-1 is expressed outside the endothelial lineage on fibroblasts and melanoma cells. **Immunol Cell Biol**, 81: (4): 320-327.

Leung, E., Lehnert, K.B., Kanwar, J.R., Yang, Y., Mon, Y., McNeil, H.P. and Krissansen, G.W. (2004) Bioassay detects soluble MAdCAM-1 in body fluids. **Immunol Cell Biol**, 82: (4): 400-409.

Ley, K. (2003) The role of selectins in inflammation and disease. **Trends Mol Med**, 9: (6): 263-268.

Ley, K. and Kansas, G.S. (2004) Selectins in T-cell recruitment to non-lymphoid tissues and sites of inflammation. **Nat Rev Immunol**, 4: (5): 325-335.

Ley, K., Laudanna, C., Cybulsky, M.I. and Nourshargh, S. (2007) Getting to the site of inflammation: the leukocyte adhesion cascade updated. **Nat Rev Immunol**, 7: (9): 678-689.

Limmer, A., Ohl, J., Kurts, C., Ljunggren, H.G., Reiss, Y., Groettrup, M., Momburg, F., Arnold, B. and Knolle, P.A. (2000) Efficient presentation of exogenous antigen by liver endothelial cells to CD8+ T cells results in antigen-specific T-cell tolerance. **Nat Med**, 6: (12): 1348-1354.

Lindholm, C., Naylor, A., Johansson, E.L. and Quiding-Jarbrink, M. (2004) Mucosal vaccination increases endothelial expression of mucosal addressin cell adhesion molecule 1 in the human gastrointestinal tract. **Infect Immun**, 72: (2): 1004-1009.

Liver Cirrhosis Case Study (2008) [online]. http://nursingcrib.com/case-study/liver-cirrhosis-case-study/ [Accessed

Lo, S.K., Lee, S., Ramos, R.A., Lobb, R., Rosa, M., Chi-Rosso, G. and Wright, S.D. (1991) Endothelial-leukocyte adhesion molecule 1 stimulates the adhesive activity of leukocyte integrin CR3 (CD11b/CD18, Mac-1, alpha m beta 2) on human neutrophils. **J Exp Med**, 173: (6): 1493-1500.

Lo, S.K., Janakidevi, K., Lai, L. and Malik, A.B. (1993) Hydrogen peroxide-induced increase in endothelial adhesiveness is dependent on ICAM-1 activation. **Am J Physiol**, 264: (4 Pt 1): L406-412.

Lukacs, N.W., Strieter, R.M., Evanoff, H.L., Burdick, M.D. and Kunkel, S.L. (1994) VCAM-1 influences lymphocyte proliferation and cytokine production during mixed lymphocyte responses. **Cell Immunol**, 154: (1): 88-98.

Luster, A.D. (1998) Chemokines--chemotactic cytokines that mediate inflammation. **N Engl J Med**, 338: (7): 436-445.

Luther, S.A., Tang, H.L., Hyman, P.L., Farr, A.G. and Cyster, J.G. (2000) Coexpression of the chemokines ELC and SLC by T zone stromal cells and deletion of the ELC gene in the plt/plt mouse. **Proc Natl Acad Sci U S A**, 97: (23): 12694-12699.

MacDonald, H.R. (1995) NK1.1+ T cell receptor-alpha/beta+ cells: new clues to their origin, specificity, and function. **J Exp Med**, 182: (3): 633-638.

Macdonald, T.T. and Monteleone, G. (2005) Immunity, inflammation, and allergy in the gut. **Science**, 307: (5717): 1920-1925.

Mackay, C.R., Marston, W.L. and Dudler, L. (1990) Naive and memory T cells show distinct pathways of lymphocyte recirculation. **J Exp Med**, 171: (3): 801-817.

Mackay, C.R. (1993) Homing of naive, memory and effector lymphocytes. **Curr Opin Immunol**, 5: (3): 423-427.

Macpherson, A.J., Gatto, D., Sainsbury, E., Harriman, G.R., Hengartner, H. and Zinkernagel, R.M. (2000) A primitive T cell-independent mechanism of intestinal mucosal IgA responses to commensal bacteria. **Science**, 288: (5474): 2222-2226.

Macpherson, A.J. and Harris, N.L. (2004) Interactions between commensal intestinal bacteria and the immune system. **Nat Rev Immunol**, 4: (6): 478-485.

Macpherson, A.J., McCoy, K.D., Johansen, F.E. and Brandtzaeg, P. (2008) The immune geography of IgA induction and function. **Mucosal Immunol**, 1: (1): 11-22.

Madara, J.L. (1998) Regulation of the movement of solutes across tight junctions. **Annu Rev Physiol**, 60: 143-159.

Makgoba, M.W., Sanders, M.E., Ginther Luce, G.E., Dustin, M.L., Springer, T.A., Clark, E.A., Mannoni, P. and Shaw, S. (1988) ICAM-1 a ligand for LFA-1-dependent adhesion of B, T and myeloid cells. **Nature**, 331: (6151): 86-88.

Malarkey, D.E., Johnson, K., Ryan, L., Boorman, G. and Maronpot, R.R. (2005) New insights into functional aspects of liver morphology. **Toxicol Pathol**, 33: (1): 27-34.

Marshall, B.T., Long, M., Piper, J.W., Yago, T., McEver, R.P. and Zhu, C. (2003) Direct observation of catch bonds involving cell-adhesion molecules. **Nature**, 423: (6936): 190-193.

Marui, N., Offermann, M.K., Swerlick, R., Kunsch, C., Rosen, C.A., Ahmad, M., Alexander, R.W. and Medford, R.M. (1993) Vascular cell adhesion molecule-1 (VCAM-1) gene transcription and expression are regulated through an antioxidant-sensitive mechanism in human vascular endothelial cells. **J Clin Invest**, 92: (4): 1866-1874.

Masopust, D., Vezys, V., Marzo, A.L. and Lefrancois, L. (2001) Preferential localization of effector memory cells in nonlymphoid tissue. **Science**, 291: (5512): 2413-2417.

Matsuzaki, K., Tsuzuki, Y., Matsunaga, H., Inoue, T., Miyazaki, J., Hokari, R., Okada, Y., Kawaguchi, A., Nagao, S., Itoh, K., Matsumoto, S. and Miura, S. (2005) In vivo demonstration of T lymphocyte migration and amelioration of ileitis in intestinal mucosa of SAMP1/Yit mice by the inhibition of MAdCAM-1. **Clin Exp Immunol**, 140: (1): 22-31.

Maynard, C.L. and Weaver, C.T. (2009) Intestinal effector T cells in health and disease. **Immunity**, 31: (3): 389-400.

McCaldon, P. and Argos, P. (1988) Oligopeptide biases in protein sequences and their use in predicting protein coding regions in nucleotide sequences. **Proteins**, 4: (2): 99-122.

McCracken, V.J. and Lorenz, R.G. (2001) The gastrointestinal ecosystem: a precarious alliance among epithelium, immunity and microbiota. **Cell Microbiol**, 3: (1): 1-11.

McEver, R.P., Beckstead, J.H., Moore, K.L., Marshall-Carlson, L. and Bainton, D.F. (1989) GMP-140, a platelet alpha-granule membrane protein, is also synthesized by vascular endothelial cells and is localized in Weibel-Palade bodies. **J Clin Invest**, 84: (1): 92-99.

McEver, R.P. (2001) Adhesive interactions of leukocytes, platelets, and the vessel wall during hemostasis and inflammation. **Thromb Haemost**, 86: (3): 746-756.

McEver, R.P. (2002) Selectins: lectins that initiate cell adhesion under flow. **Curr Opin Cell Biol**, 14: (5): 581-586.

McEwen, C.M., Jr. and Harrison, D.C. (1965) Abnormalities of Serum Monoamine Oxidase in Chronic Congestive Heart Failure. **J Lab Clin Med**, 65: 546-559.

McNab, G., Reeves, J.L., Salmi, M., Hubscher, S., Jalkanen, S. and Adams, D.H. (1996) Vascular adhesion protein 1 mediates binding of T cells to human hepatic endothelium. **Gastroenterology**, 110: (2): 522-528.

Mebius, R.E., Streeter, P.R., Michie, S., Butcher, E.C. and Weissman, I.L. (1996) A developmental switch in lymphocyte homing receptor and endothelial vascular addressin expression regulates lymphocyte homing and permits CD4+ CD3- cells to colonize lymph nodes. **Proc Natl Acad Sci U S A**, 93: (20): 11019-11024.

Merinen, M., Irjala, H., Salmi, M., Jaakkola, I., Hanninen, A. and Jalkanen, S. (2005) Vascular adhesion protein-1 is involved in both acute and chronic inflammation in the mouse. **Am J Pathol**, 166: (3): 793-800.

Miles, A., Liaskou, E., Eksteen, B., Lalor, P.F. and Adams, D.H. (2008) CCL25 and CCL28 promote alpha4 beta7-integrin-dependent adhesion of lymphocytes to MAdCAM-1 under shear flow. **Am J Physiol Gastrointest Liver Physiol**, 294: (5): G1257-1267.

Miyara, M. and Sakaguchi, S. (2007) Natural regulatory T cells: mechanisms of suppression. **Trends Mol Med**, 13: (3): 108-116.

Moore, K.L. (1998) Structure and function of P-selectin glycoprotein ligand-1. **Leuk Lymphoma**, 29: (1-2): 1-15.

Mori, N., Horie, Y., Gerritsen, M.E., Anderson, D.C. and Granger, D.N. (1999) Anti-inflammatory drugs and endothelial cell adhesion molecule expression in murine vascular beds. **Gut**, 44: (2): 186-195.

Muller, W.A. (2003) Leukocyte-endothelial-cell interactions in leukocyte transmigration and the inflammatory response. **Trends Immunol**, 24: (6): 327-334.

Muller, W.A. (2009) Mechanisms of transendothelial migration of leukocytes. **Circ Res**, 105: (3): 223-230.

Nagira, M., Imai, T., Hieshima, K., Kusuda, J., Ridanpaa, M., Takagi, S., Nishimura, M., Kakizaki, M., Nomiyama, H. and Yoshie, O. (1997) Molecular cloning of a novel human CC chemokine secondary lymphoid-tissue chemokine that is a potent chemoattractant for lymphocytes and mapped to chromosome 9p13. **J Biol Chem**, 272: (31): 19518-19524.

Nakache, M., Berg, E.L., Streeter, P.R. and Butcher, E.C. (1989) The mucosal vascular addressin is a tissue-specific endothelial cell adhesion molecule for circulating lymphocytes. **Nature**, 337: (6203): 179-181.

Nakamura, K., Hori, T., Sato, N., Sugie, K., Kawakami, T. and Yodoi, J. (1993a) Redox regulation of a src family protein tyrosine kinase p56lck in T cells. **Oncogene**, 8: (11): 3133-3139.

Nakamura, S., Ohtani, H., Watanabe, Y., Fukushima, K., Matsumoto, T., Kitano, A., Kobayashi, K. and Nagura, H. (1993b) In situ expression of the cell adhesion molecules in

inflammatory bowel disease. Evidence of immunologic activation of vascular endothelial cells. **Lab Invest**, 69: (1): 77-85.

Nathan, C. (2002) Points of control in inflammation. **Nature**, 420: (6917): 846-852.

Neish, A.S., Williams, A.J., Palmer, H.J., Whitley, M.Z. and Collins, T. (1992) Functional analysis of the human vascular cell adhesion molecule 1 promoter. **J Exp Med**, 176: (6): 1583-1593.

Nemeth, E., Baird, A.W. and O'Farrelly, C. (2009) Microanatomy of the liver immune system. **Semin Immunopathol**, 31: (3): 333-343.

Neutra, M.R., Mantis, N.J. and Kraehenbuhl, J.P. (2001) Collaboration of epithelial cells with organized mucosal lymphoid tissues. **Nat Immunol**, 2: (11): 1004-1009.

Newman, W., Beall, L.D., Carson, C.W., Hunder, G.G., Graben, N., Randhawa, Z.I., Gopal, T.V., Wiener-Kronish, J. and Matthay, M.A. (1993) Soluble E-selectin is found in supernatants of activated endothelial cells and is elevated in the serum of patients with septic shock. **J Immunol**, 150: (2): 644-654.

Ng, C.K., Deshpande, S.S., Irani, K. and Alevriadou, B.R. (2002) Adhesion of flowing monocytes to hypoxia-reoxygenation-exposed endothelial cells: role of Rac1, ROS, and VCAM-1. **Am J Physiol Cell Physiol**, 283: (1): C93-102.

Niess, J.H. and Reinecker, H.C. (2006) Dendritic cells in the recognition of intestinal microbiota. **Cell Microbiol**, 8: (4): 558-564.

Nishimura, T. (2003) Expression of potential lymphocyte trafficking mediator molecules in the mammary gland. **Vet Res**, 34: (1): 3-10.

Nose, K., Shibanuma, M., Kikuchi, K., Kageyama, H., Sakiyama, S. and Kuroki, T. (1991) Transcriptional activation of early-response genes by hydrogen peroxide in a mouse osteoblastic cell line. **Eur J Biochem**, 201: (1): 99-106.

Notas, G., Kisseleva, T. and Brenner, D. (2009) NK and NKT cells in liver injury and fibrosis. **Clin Immunol**, 130: (1): 16-26.

Nourshargh, S., Krombach, F. and Dejana, E. (2006) The role of JAM-A and PECAM-1 in modulating leukocyte infiltration in inflamed and ischemic tissues. **J Leukoc Biol**, 80: (4): 714-718.

Nummer, D., Suri-Payer, E., Schmitz-Winnenthal, H., Bonertz, A., Galindo, L., Antolovich, D., Koch, M., Buchler, M., Weitz, J., Schirrmacher, V. and Beckhove, P. (2007) Role of tumor endothelium in CD4+ CD25+ regulatory T cell infiltration of human pancreatic carcinoma. **J Natl Cancer Inst**, 99: (15): 1188-1199.

Nurieva, R.I., Chung, Y., Hwang, D., Yang, X.O., Kang, H.S., Ma, L., Wang, Y.H., Watowich, S.S., Jetten, A.M., Tian, Q. and Dong, C. (2008) Generation of T follicular helper cells is

mediated by interleukin-21 but independent of T helper 1, 2, or 17 cell lineages. **Immunity**, 29: (1): 138-149.

O'Neill, J.K., Butter, C., Baker, D., Gschmeissner, S.E., Kraal, G., Butcher, E.C. and Turk, J.L. (1991) Expression of vascular addressins and ICAM-1 by endothelial cells in the spinal cord during chronic relapsing experimental allergic encephalomyelitis in the Biozzi AB/H mouse. **Immunology**, 72: (4): 520-525.

O'Sullivan, J., Unzeta, M., Healy, J., O'Sullivan, M.I., Davey, G. and Tipton, K.F. (2004) Semicarbazide-sensitive amine oxidases: enzymes with quite a lot to do. **Neurotoxicology**, 25: (1-2): 303-315.

Ogawa, H., Iimura, M., Eckmann, L. and Kagnoff, M.F. (2004) Regulated production of the chemokine CCL28 in human colon epithelium. **Am J Physiol Gastrointest Liver Physiol**, 287: (5): G1062-1069.

Ogawa, H., Binion, D.G., Heidemann, J., Theriot, M., Fisher, P.J., Johnson, N.A., Otterson, M.F. and Rafiee, P. (2005) Mechanisms of MAdCAM-1 gene expression in human intestinal microvascular endothelial cells. **Am J Physiol Cell Physiol**, 288: (2): C272-281.

Ohara, H., Isomoto, H., Wen, C.Y., Ejima, C., Murata, M., Miyazaki, M., Takeshima, F., Mizuta, Y., Murata, I., Koji, T., Nagura, H. and Kohno, S. (2003) Expression of mucosal addressin cell adhesion molecule 1 on vascular endothelium of gastric mucosa in patients with nodular gastritis. **World J Gastroenterol**, 9: (12): 2701-2705.

Okada, T., Ngo, V.N., Ekland, E.H., Forster, R., Lipp, M., Littman, D.R. and Cyster, J.G. (2002) Chemokine requirements for B cell entry to lymph nodes and Peyer's patches. **J Exp Med**, 196: (1): 65-75.

Olson, T.S. and Ley, K. (2002) Chemokines and chemokine receptors in leukocyte trafficking. **Am J Physiol Regul Integr Comp Physiol**, 283: (1): R7-28.

Oo, Y.H. and Adams, D.H. (2009) The role of chemokines in the recruitment of lymphocytes to the liver. **J Autoimmun**, 34: (1): 45-54.

Osborn, L., Vassallo, C. and Benjamin, C.D. (1992) Activated endothelium binds lymphocytes through a novel binding site in the alternately spliced domain of vascular cell adhesion molecule-1. **J Exp Med**, 176: (1): 99-107.

Oshima, T., Jordan, P., Grisham, M.B., Alexander, J.S., Jennings, M., Sasaki, M. and Manas, K. (2001a) TNF-alpha induced endothelial MAdCAM-1 expression is regulated by exogenous, not endogenous nitric oxide. **BMC Gastroenterol**, 1: 5.

Oshima, T., Pavlick, K.P., Laroux, F.S., Verma, S.K., Jordan, P., Grisham, M.B., Williams, L. and Alexander, J.S. (2001b) Regulation and distribution of MAdCAM-1 in endothelial cells in vitro. **Am J Physiol Cell Physiol**, 281: (4): C1096-1105.

Oyama, T., Miura, S., Watanabe, C., Hokari, R., Fujiyama, Y., Komoto, S., Tsuzuki, Y., Hosoe, N., Nagata, H. and Hibi, T. (2007) CXCL12 and CCL20 play a significant role in mucosal T-lymphocyte adherence to intestinal microvessels in mice. **Microcirculation**, 14: (7): 753-766.

Pabst, O., Ohl, L., Wendland, M., Wurbel, M.A., Kremmer, E., Malissen, B. and Forster, R. (2004) Chemokine receptor CCR9 contributes to the localization of plasma cells to the small intestine. **J Exp Med**, 199: (3): 411-416.

Pachynski, R.K., Wu, S.W., Gunn, M.D. and Erle, D.J. (1998) Secondary lymphoid-tissue chemokine (SLC) stimulates integrin alpha 4 beta 7-mediated adhesion of lymphocytes to mucosal addressin cell adhesion molecule-1 (MAdCAM-1) under flow. **J Immunol**, 161: (2): 952-956.

Pan, J., Kunkel, E.J., Gosslar, U., Lazarus, N., Langdon, P., Broadwell, K., Vierra, M.A., Genovese, M.C., Butcher, E.C. and Soler, D. (2000) A novel chemokine ligand for CCR10 and CCR3 expressed by epithelial cells in mucosal tissues. **J Immunol**, 165: (6): 2943-2949.

Papadakis, K.A., Prehn, J., Nelson, V., Cheng, L., Binder, S.W., Ponath, P.D., Andrew, D.P. and Targan, S.R. (2000) The role of thymus-expressed chemokine and its receptor CCR9 on lymphocytes in the regional specialization of the mucosal immune system. **J Immunol**, 165: (9): 5069-5076.

Papadakis, K.A. (2004) Chemokines in inflammatory bowel disease. **Curr Allergy Asthma Rep**, 4: (1): 83-89.

Patel, K.D., Zimmerman, G.A., Prescott, S.M., McEver, R.P. and McIntyre, T.M. (1991) Oxygen radicals induce human endothelial cells to express GMP-140 and bind neutrophils. **J Cell Biol**, 112: (4): 749-759.

Pearson, M.W. and Roberts, C.J. (1984) Drug induction of hepatic enzymes in the elderly. **Age Ageing**, 13: (5): 313-316.

Pepinsky, B., Hession, C., Chen, L.L., Moy, P., Burkly, L., Jakubowski, A., Chow, E.P., Benjamin, C., Chi-Rosso, G., Luhowskyj, S. and et al. (1992) Structure/function studies on vascular cell adhesion molecule-1. **J Biol Chem**, 267: (25): 17820-17826.

Phillipson, M., Heit, B., Colarusso, P., Liu, L., Ballantyne, C.M. and Kubes, P. (2006) Intraluminal crawling of neutrophils to emigration sites: a molecularly distinct process from adhesion in the recruitment cascade. **J Exp Med**, 203: (12): 2569-2575.

Picarella, D., Hurlbut, P., Rottman, J., Shi, X., Butcher, E. and Ringler, D.J. (1997) Monoclonal antibodies specific for beta 7 integrin and mucosal addressin cell adhesion molecule-1 (MAdCAM-1) reduce inflammation in the colon of scid mice reconstituted with CD45RBhigh CD4+ T cells. **J Immunol**, 158: (5): 2099-2106.

Picker, L.J. and Butcher, E.C. (1992) Physiological and molecular mechanisms of lymphocyte homing. **Annu Rev Immunol**, 10: 561-591.

Pigott, R., Dillon, L.P., Hemingway, I.H. and Gearing, A.J. (1992) Soluble forms of E-selectin, ICAM-1 and VCAM-1 are present in the supernatants of cytokine activated cultured endothelial cells. **Biochem Biophys Res Commun**, 187: (2): 584-589.

Pinzani, M. and Marra, F. (2001) Cytokine receptors and signaling in hepatic stellate cells. **Semin Liver Dis**, 21: (3): 397-416.

Pirisino, R., Ghelardini, C., Banchelli, G., Galeotti, N. and Raimondi, L. (2001) Methylamine and benzylamine induced hypophagia in mice: modulation by semicarbazide-sensitive benzylamine oxidase inhibitors and aODN towards Kv1.1 channels. **Br J Pharmacol**, 134: (4): 880-886.

Pirisino, R., Ghelardini, C., Pacini, A., Galeotti, N. and Raimondi, L. (2004) Methylamine, but not ammonia, is hypophagic in mouse by interaction with brain Kv1.6 channel subtype. **Br J Pharmacol**, 142: (2): 381-389.

Postigo, A.A., Sanchez-Mateos, P., Lazarovits, A.I., Sanchez-Madrid, F. and de Landazuri, M.O. (1993) Alpha 4 beta 7 integrin mediates B cell binding to fibronectin and vascular cell adhesion molecule-1. Expression and function of alpha 4 integrins on human B lymphocytes. **J Immunol**, 151: (5): 2471-2483.

Preece, G., Murphy, G. and Ager, A. (1996) Metalloproteinase-mediated regulation of L-selectin levels on leucocytes. **J Biol Chem**, 271: (20): 11634-11640.

Pullen, N., Molloy, E., Carter, D., Syntin, P., Clemo, F., Finco-Kent, D., Reagan, W., Zhao, S., Kawabata, T. and Sreckovic, S. (2009) Pharmacological characterization of PF-00547659, an anti-human MAdCAM monoclonal antibody. **Br J Pharmacol**, 157: (2): 281-293.

Puri, K.D., Finger, E.B., Gaudernack, G. and Springer, T.A. (1995) Sialomucin CD34 is the major L-selectin ligand in human tonsil high endothelial venules. **J Cell Biol**, 131: (1): 261-270.

Rada, C., Lorenzi, R., Powis, S.J., van den Bogaerde, J., Parham, P. and Howard, J.C. (1990) Concerted evolution of class I genes in the major histocompatibility complex of murine rodents. **Proc Natl Acad Sci U S A**, 87: (6): 2167-2171.

Reilly, P.L., Woska, J.R., Jr., Jeanfavre, D.D., McNally, E., Rothlein, R. and Bormann, B.J. (1995) The native structure of intercellular adhesion molecule-1 (ICAM-1) is a dimer. Correlation with binding to LFA-1. **J Immunol**, 155: (2): 529-532.

Reynaert, H., Thompson, M.G., Thomas, T. and Geerts, A. (2002) Hepatic stellate cells: role in microcirculation and pathophysiology of portal hypertension. **Gut**, 50: (4): 571-581.

Rivera-Nieves, J., Olson, T., Bamias, G., Bruce, A., Solga, M., Knight, R.F., Hoang, S., Cominelli, F. and Ley, K. (2005) L-selectin, alpha 4 beta 1, and alpha 4 beta 7 integrins participate in CD4+ T cell recruitment to chronically inflamed small intestine. **J Immunol**, 174: (4): 2343-2352.

Rivera-Nieves, J., Ho, J., Bamias, G., Ivashkina, N., Ley, K., Oppermann, M. and Cominelli, F. (2006) Antibody blockade of CCL25/CCR9 ameliorates early but not late chronic murine ileitis. **Gastroenterology**, 131: (5): 1518-1529.

Roebuck, K.A., Rahman, A., Lakshminarayanan, V., Janakidevi, K. and Malik, A.B. (1995) H2O2 and tumor necrosis factor-alpha activate intercellular adhesion molecule 1 (ICAM-1) gene transcription through distinct cis-regulatory elements within the ICAM-1 promoter. **J Biol Chem**, 270: (32): 18966-18974.

Rollins, B.J. (1997) Chemokines. **Blood**, 90: (3): 909-928.

Rosen, S.D. (2004) Ligands for L-selectin: homing, inflammation, and beyond. **Annu Rev Immunol**, 22: 129-156.

Rossi, D. and Zlotnik, A. (2000) The biology of chemokines and their receptors. **Annu Rev Immunol**, 18: 217-242.

Rothlein, R., Mainolfi, E.A., Czajkowski, M. and Marlin, S.D. (1991) A form of circulating ICAM-1 in human serum. **J Immunol**, 147: (11): 3788-3793.

Sackstein, R. (2005) The lymphocyte homing receptors: gatekeepers of the multistep paradigm. **Curr Opin Hematol**, 12: (6): 444-450.

Sadhu, C., Ting, H.J., Lipsky, B., Hensley, K., Garcia-Martinez, L.F., Simon, S.I. and Staunton, D.E. (2007) CD11c/CD18: novel ligands and a role in delayed-type hypersensitivity. **J Leukoc Biol**, 81: (6): 1395-1403.

Saich, R. and Chapman, R. (2008) Primary sclerosing cholangitis, autoimmune hepatitis and overlap syndromes in inflammatory bowel disease. **World J Gastroenterol**, 14: (3): 331-337.

Sallusto, F., Mackay, C.R. and Lanzavecchia, A. (2000) The role of chemokine receptors in primary, effector, and memory immune responses. **Annu Rev Immunol**, 18: 593-620.

Salmi, M., Kalimo, K. and Jalkanen, S. (1993) Induction and function of vascular adhesion protein-1 at sites of inflammation. **J Exp Med**, 178: (6): 2255-2260.

Salmi, M. and Jalkanen, S. (1996) Human vascular adhesion protein 1 (VAP-1) is a unique sialoglycoprotein that mediates carbohydrate-dependent binding of lymphocytes to endothelial cells. **J Exp Med**, 183: (2): 569-579.

Salmi, M., Tohka, S., Berg, E.L., Butcher, E.C. and Jalkanen, S. (1997) Vascular adhesion protein 1 (VAP-1) mediates lymphocyte subtype-specific, selectin-independent recognition of vascular endothelium in human lymph nodes. **J Exp Med**, 186: (4): 589-600.

Salmi, M., Adams, D. and Jalkanen, S. (1998) Cell adhesion and migration. IV. Lymphocyte trafficking in the intestine and liver. **Am J Physiol**, 274: (1 Pt 1): G1-6.

Salmi, M. and Jalkanen, S. (2001) VAP-1: an adhesin and an enzyme. **Trends Immunol**, 22: (4): 211-216.

Salmi, M., Alanen, K., Grenman, S., Briskin, M., Butcher, E.C. and Jalkanen, S. (2001a) Immune cell trafficking in uterus and early life is dominated by the mucosal addressin MAdCAM-1 in humans. **Gastroenterology**, 121: (4): 853-864.

Salmi, M., Yegutkin, G.G., Lehvonen, R., Koskinen, K., Salminen, T. and Jalkanen, S. (2001b) A cell surface amine oxidase directly controls lymphocyte migration. **Immunity**, 14: (3): 265-276.

Salmi, M., Koskinen, K., Henttinen, T., Elima, K. and Jalkanen, S. (2004) CLEVER-1 mediates lymphocyte transmigration through vascular and lymphatic endothelium. **Blood**, 104: (13): 3849-3857.

Salmi, M. and Jalkanen, S. (2006) Developmental regulation of the adhesive and enzymatic activity of vascular adhesion protein-1 (VAP-1) in humans. **Blood**, 108: (5): 1555-1561.

Sampaio, S.O., Li, X., Takeuchi, M., Mei, C., Francke, U., Butcher, E.C. and Briskin, M.J. (1995) Organization, regulatory sequences, and alternatively spliced transcripts of the mucosal addressin cell adhesion molecule-1 (MAdCAM-1) gene. **J Immunol**, 155: (5): 2477-2486.

Sanchez-Madrid, F. and del Pozo, M.A. (1999) Leukocyte polarization in cell migration and immune interactions. **EMBO J**, 18: (3): 501-511.

Sans, M., Panes, J., Ardite, E., Elizalde, J.I., Arce, Y., Elena, M., Palacin, A., Fernandez-Checa, J.C., Anderson, D.C., Lobb, R. and Pique, J.M. (1999) VCAM-1 and ICAM-1 mediate leukocyte-endothelial cell adhesion in rat experimental colitis. **Gastroenterology**, 116: (4): 874-883.

Sasaki, M., Jordan, P., Joh, T., Itoh, M., Jenkins, M., Pavlick, K., Minagar, A. and Alexander, S.J. (2002) Melatonin reduces TNF-a induced expression of MAdCAM-1 via inhibition of NF-kappaB. **BMC Gastroenterol**, 2: 9.

Sato, H., Takino, T., Okada, Y., Cao, J., Shinagawa, A., Yamamoto, E. and Seiki, M. (1994) A matrix metalloproteinase expressed on the surface of invasive tumour cells. **Nature**, 370: (6484): 61-65.

Schaff, U., Mattila, P.E., Simon, S.I. and Walcheck, B. (2008) Neutrophil adhesion to E-selectin under shear promotes the redistribution and co-clustering of ADAM17 and its proteolytic substrate L-selectin. **J Leukoc Biol**, 83: (1): 99-105.

Schippers, A., Leuker, C., Pabst, O., Kochut, A., Prochnow, B., Gruber, A.D., Leung, E., Krissansen, G.W., Wagner, N. and Muller, W. (2009) Mucosal addressin cell-adhesion molecule-1 controls plasma-cell migration and function in the small intestine of mice. **Gastroenterology**, 137: (3): 924-933.

Schleiffenbaum, B., Spertini, O. and Tedder, T.F. (1992) Soluble L-selectin is present in human plasma at high levels and retains functional activity. **J Cell Biol**, 119: (1): 229-238.

Schrage, A., Wechsung, K., Neumann, K., Schumann, M., Schulzke, J.D., Engelhardt, B., Zeitz, M., Hamann, A. and Klugewitz, K. (2008) Enhanced T cell transmigration across the murine liver sinusoidal endothelium is mediated by transcytosis and surface presentation of chemokines. **Hepatology**, 48: (4): 1262-1272.

Schreck, R., Rieber, P. and Baeuerle, P.A. (1991) Reactive oxygen intermediates as apparently widely used messengers in the activation of the NF-kappa B transcription factor and HIV-1. **EMBO J**, 10: (8): 2247-2258.

Schreck, R., Albermann, K. and Baeuerle, P.A. (1992) Nuclear factor kappa B: an oxidative stress-responsive transcription factor of eukaryotic cells (a review). **Free Radic Res Commun**, 17: (4): 221-237.

Schreiber, T.H., Shinder, V., Cain, D.W., Alon, R. and Sackstein, R. (2007) Shear flow-dependent integration of apical and subendothelial chemokines in T-cell transmigration: implications for locomotion and the multistep paradigm. **Blood**, 109: (4): 1381-1386.

Schuermann, G.M., Aber-Bishop, A.E., Facer, P., Lee, J.C., Rampton, D.S., Dore, C.J. and Polak, J.M. (1993) Altered expression of cell adhesion molecules in uninvolved gut in inflammatory bowel disease. **Clin Exp Immunol**, 94: (2): 341-347.

Schulte, A., Schulz, B., Andrzejewski, M.G., Hundhausen, C., Mletzko, S., Achilles, J., Reiss, K., Paliga, K., Weber, C., John, S.R. and Ludwig, A. (2007) Sequential processing of the transmembrane chemokines CX3CL1 and CXCL16 by alpha- and gamma-secretases. **Biochem Biophys Res Commun**, 358: (1): 233-240.

Schwartz, M.A., Schaller, M.D. and Ginsberg, M.H. (1995) Integrins: emerging paradigms of signal transduction. **Annu Rev Cell Dev Biol**, 11: 549-599.

Schweighoffer, T., Tanaka, Y., Tidswell, M., Erle, D.J., Horgan, K.J., Luce, G.E., Lazarovits, A.I., Buck, D. and Shaw, S. (1993) Selective expression of integrin alpha 4 beta 7 on a subset of human CD4+ memory T cells with Hallmarks of gut-trophism. **J Immunol**, 151: (2): 717-729.

Scoazec, J.Y. and Feldmann, G. (1994) The cell adhesion molecules of hepatic sinusoidal endothelial cells. **J Hepatol**, 20: (2): 296-300.

Senoo, H., Imai, K., Matano, Y. and Sato, M. (1998) Molecular mechanisms in the reversible regulation of morphology, proliferation and collagen metabolism in hepatic stellate cells by the three-dimensional structure of the extracellular matrix. **J Gastroenterol Hepatol**, 13 Suppl: S19-32.

Seth, R., Raymond, F.D. and Makgoba, M.W. (1991) Circulating ICAM-1 isoforms: diagnostic prospects for inflammatory and immune disorders. **Lancet**, 338: (8759): 83-84.

Shang, L., Thirunarayanan, N., Viejo-Borbolla, A., Martin, A.P., Bogunovic, M., Marchesi, F., Unkeless, J.C., Ho, Y., Furtado, G.C., Alcami, A., Merad, M., Mayer, L. and Lira, S.A. (2009) Expression of the chemokine binding protein M3 promotes marked changes in the accumulation of specific leukocytes subsets within the intestine. **Gastroenterology**, 137: (3): 1006-1018, 1018 e1001-1003.

Shattil, S.J. (2005) Integrins and Src: dynamic duo of adhesion signaling. **Trends Cell Biol**, 15: (8): 399-403.

Shetty, S., Lalor, P.F. and Adams, D.H. (2008) Lymphocyte recruitment to the liver: molecular insights into the pathogenesis of liver injury and hepatitis. **Toxicology**, 254: (3): 136-146.

Shih, D.Q., Targan, S.R. and McGovern, D. (2008) Recent advances in IBD pathogenesis: genetics and immunobiology. **Curr Gastroenterol Rep**, 10: (6): 568-575.

Shyjan, A.M., Bertagnolli, M., Kenney, C.J. and Briskin, M.J. (1996) Human mucosal addressin cell adhesion molecule-1 (MAdCAM-1) demonstrates structural and functional similarities to the alpha 4 beta 7-integrin binding domains of murine MAdCAM-1, but extreme divergence of mucin-like sequences. **J Immunol**, 156: (8): 2851-2857.

Sinha, R.K., Yang, G., Alexander, C. and Mage, R.G. (2006) De novo expression of MECA-79 glycoprotein-determinant on developing B lymphocytes in gut-associated lymphoid tissues. **Immunology**, 119: (4): 461-469.

Smalley, D.M. and Ley, K. (2005) L-selectin: mechanisms and physiological significance of ectodomain cleavage. **J Cell Mol Med**, 9: (2): 255-266.

Smedsrod, B. (2004) Clearance function of scavenger endothelial cells. **Comp Hepatol**, 3 Suppl 1: S22.

Smith, D.J., Salmi, M., Bono, P., Hellman, J., Leu, T. and Jalkanen, S. (1998) Cloning of vascular adhesion protein 1 reveals a novel multifunctional adhesion molecule. **J Exp Med**, 188: (1): 17-27.

Soler, D., Chapman, T., Yang, L.L., Wyant, T., Egan, R. and Fedyk, E.R. (2009) The binding specificity and selective antagonism of vedolizumab, an anti-alpha4beta7 integrin therapeutic antibody in development for inflammatory bowel diseases. **J Pharmacol Exp Ther**, 330: (3): 864-875.

Springer, T.A. (1995) Traffic signals on endothelium for lymphocyte recirculation and leukocyte emigration. **Annu Rev Physiol**, 57: 827-872.

Steegmaier, M., Levinovitz, A., Isenmann, S., Borges, E., Lenter, M., Kocher, H.P., Kleuser, B. and Vestweber, D. (1995) The E-selectin-ligand ESL-1 is a variant of a receptor for fibroblast growth factor. **Nature**, 373: (6515): 615-620.

Stefanelli, T., Malesci, A., De La Rue, S.A. and Danese, S. (2008) Anti-adhesion molecule therapies in inflammatory bowel disease: touch and go. **Autoimmun Rev**, 7: (5): 364-369.

Steffen, B.J., Breier, G., Butcher, E.C., Schulz, M. and Engelhardt, B. (1996) ICAM-1, VCAM-1, and MAdCAM-1 are expressed on choroid plexus epithelium but not endothelium and mediate binding of lymphocytes in vitro. **Am J Pathol**, 148: (6): 1819-1838.

Steinhoff, G., Behrend, M., Schrader, B., Duijvestijn, A.M. and Wonigeit, K. (1993) Expression patterns of leukocyte adhesion ligand molecules on human liver endothelia. Lack of ELAM-1 and CD62 inducibility on sinusoidal endothelia and distinct distribution of VCAM-1, ICAM-1, ICAM-2, and LFA-3. **Am J Pathol**, 142: (2): 481-488.

Steinhoff, U., Klemm, U., Greiner, M., Bordasch, K. and Kaufmann, S.H. (1998) Altered intestinal immune system but normal antibacterial resistance in the absence of P-selectin and ICAM-1. **J Immunol**, 160: (12): 6112-6120.

Steiniger, B., Barth, P. and Hellinger, A. (2001) The perifollicular and marginal zones of the human splenic white pulp : do fibroblasts guide lymphocyte immigration? **Am J Pathol**, 159: (2): 501-512.

Stewart, M. and Hogg, N. (1996) Regulation of leukocyte integrin function: affinity vs. avidity. **J Cell Biochem**, 61: (4): 554-561.

Stoddart, J.H., Jr., Jasuja, R.R., Sikorski, M.A., von Andrian, U.H. and Mier, J.W. (1996) Protease-resistant L-selectin mutants. Down-modulation by cross-linking but not cellular activation. **J Immunol**, 157: (12): 5653-5659.

Stolen, C.M., Marttila-Ichihara, F., Koskinen, K., Yegutkin, G.G., Turja, R., Bono, P., Skurnik, M., Hanninen, A., Jalkanen, S. and Salmi, M. (2005) Absence of the endothelial oxidase AOC3 leads to abnormal leukocyte traffic in vivo. **Immunity**, 22: (1): 105-115.

Streeter, P.R., Berg, E.L., Rouse, B.T., Bargatze, R.F. and Butcher, E.C. (1988) A tissue-specific endothelial cell molecule involved in lymphocyte homing. **Nature**, 331: (6151): 41-46.

Strober, W., Murray, P.J., Kitani, A. and Watanabe, T. (2006) Signalling pathways and molecular interactions of NOD1 and NOD2. **Nat Rev Immunol**, 6: (1): 9-20.

Sundstrom, P., Lundin, S.B., Nilsson, L.A. and Quiding-Jarbrink, M. (2008) Human IgA-secreting cells induced by intestinal, but not systemic, immunization respond to CCL25 (TECK) and CCL28 (MEC). **Eur J Immunol**, 38: (12): 3327-3338.

Swain, M.G. (2008) Hepatic NKT cells: friend or foe? **Clin Sci (Lond)**, 114: (7): 457-466.

Szabo, M.C., Butcher, E.C. and McEvoy, L.M. (1997) Specialization of mucosal follicular dendritic cells revealed by mucosal addressin-cell adhesion molecule-1 display. **J Immunol**, 158: (12): 5584-5588.

Tachedjian, M., Yu, M., Lew, A.M., Rockman, S., Boyle, J.S., Andrew, M.E. and Wang, L. (2006) Molecular cloning and characterization of pig, cow and sheep MAdCAM-1 cDNA and the demonstration of cross-reactive epitopes amongst mammalian homologues. **Tissue Antigens**, 67: (5): 419-426.

Takeda, K. and Akira, S. (2004) Microbial recognition by Toll-like receptors. **J Dermatol Sci**, 34: (2): 73-82.

Takeuchi, M. and Baichwal, V.R. (1995) Induction of the gene encoding mucosal vascular addressin cell adhesion molecule 1 by tumor necrosis factor alpha is mediated by NF-kappa B proteins. **Proc Natl Acad Sci U S A**, 92: (8): 3561-3565.

Tan, K., Casasnovas, J.M., Liu, J.H., Briskin, M.J., Springer, T.A. and Wang, J.H. (1998) The structure of immunoglobulin superfamily domains 1 and 2 of MAdCAM-1 reveals novel features important for integrin recognition. **Structure**, 6: (6): 793-801.

Tanaka, Y., Adams, D.H., Hubscher, S., Hirano, H., Siebenlist, U. and Shaw, S. (1993) T-cell adhesion induced by proteoglycan-immobilized cytokine MIP-1 beta. **Nature**, 361: (6407): 79-82.

Targan, S.R., Feagan, B.G., Fedorak, R.N., Lashner, B.A., Panaccione, R., Present, D.H., Spehlmann, M.E., Rutgeerts, P.J., Tulassay, Z., Volfova, M., Wolf, D.C., Hernandez, C., Bornstein, J. and Sandborn, W.J. (2007) Natalizumab for the treatment of active Crohn's disease: results of the ENCORE Trial. **Gastroenterology**, 132: (5): 1672-1683.

Teague, T.K., Lazarovits, A.I. and McIntyre, B.W. (1994) Integrin alpha 4 beta 7 co-stimulation of human peripheral blood T cell proliferation. **Cell Adhes Commun**, 2: (6): 539-547.

Tedder, T.F., Penta, A.C., Levine, H.B. and Freedman, A.S. (1990) Expression of the human leukocyte adhesion molecule, LAM1. Identity with the TQ1 and Leu-8 differentiation antigens. **J Immunol**, 144: (2): 532-540.

Tedder, T.F., Steeber, D.A., Chen, A. and Engel, P. (1995a) The selectins: vascular adhesion molecules. **FASEB J**, 9: (10): 866-873.

Tedder, T.F., Steeber, D.A. and Pizcueta, P. (1995b) L-selectin-deficient mice have impaired leukocyte recruitment into inflammatory sites. **J Exp Med**, 181: (6): 2259-2264.

Terada, R., Yamamoto, K., Hakoda, T., Shimada, N., Okano, N., Baba, N., Ninomiya, Y., Gershwin, M.E. and Shiratori, Y. (2003) Stromal cell-derived factor-1 from biliary epithelial cells recruits CXCR4-positive cells: implications for inflammatory liver diseases. **Lab Invest**, 83: (5): 665-672.

The Internet Encyclopedia of science, Anatomy & Physiology, Liver [online]. http://www.daviddarling.info/encyclopedia/L/liver.html [Accessed

Thomson, A.W., Drakes, M.L., Zahorchak, A.F., O'Connell, P.J., Steptoe, R.J., Qian, S. and Lu, L. (1999) Hepatic dendritic cells: immunobiology and role in liver transplantation. **J Leukoc Biol**, 66: (2): 322-330.

Timpl, R. (1996) Macromolecular organization of basement membranes. **Curr Opin Cell Biol**, 8: (5): 618-624.

Tohka, S., Laukkanen, M., Jalkanen, S. and Salmi, M. (2001) Vascular adhesion protein 1 (VAP-1) functions as a molecular brake during granulocyte rolling and mediates recruitment in vivo. **FASEB J**, 15: (2): 373-382.

Tortora, G.J. and Grabowski, S.R. (1996) "**Principles of anatomy and physiology**". Eighth Edition.

Trotta, R., Parihar, R., Yu, J., Becknell, B., Allard, J., 2nd, Wen, J., Ding, W., Mao, H., Tridandapani, S., Carson, W.E. and Caligiuri, M.A. (2005) Differential expression of SHIP1 in CD56bright and CD56dim NK cells provides a molecular basis for distinct functional responses to monokine costimulation. **Blood**, 105: (8): 3011-3018.

Tsujisaki, M., Imai, K., Hirata, H., Hanzawa, Y., Masuya, J., Nakano, T., Sugiyama, T., Matsui, M., Hinoda, Y. and Yachi, A. (1991) Detection of circulating intercellular adhesion molecule-1 antigen in malignant diseases. **Clin Exp Immunol**, 85: (1): 3-8.

Tupin, E., Kinjo, Y. and Kronenberg, M. (2007) The unique role of natural killer T cells in the response to microorganisms. **Nat Rev Microbiol**, 5: (6): 405-417.

Turowski, P., Martinelli, R., Crawford, R., Wateridge, D., Papageorgiou, A.P., Lampugnani, M.G., Gamp, A.C., Vestweber, D., Adamson, P., Dejana, E. and Greenwood, J. (2008) Phosphorylation of vascular endothelial cadherin controls lymphocyte emigration. **J Cell Sci**, 121: (Pt 1): 29-37.

Uguccioni, M., Gionchetti, P., Robbiani, D.F., Rizzello, F., Peruzzo, S., Campieri, M. and Baggiolini, M. (1999) Increased expression of IP-10, IL-8, MCP-1, and MCP-3 in ulcerative colitis. **Am J Pathol**, 155: (2): 331-336.

Van Assche, G., Van Ranst, M., Sciot, R., Dubois, B., Vermeire, S., Noman, M., Verbeeck, J., Geboes, K., Robberecht, W. and Rutgeerts, P. (2005) Progressive multifocal leukoencephalopathy after natalizumab therapy for Crohn's disease. **N Engl J Med**, 353: (4): 362-368.

Veldhoen, M., Uyttenhove, C., van Snick, J., Helmby, H., Westendorf, A., Buer, J., Martin, B., Wilhelm, C. and Stockinger, B. (2008) Transforming growth factor-beta 'reprograms' the differentiation of T helper 2 cells and promotes an interleukin 9-producing subset. **Nat Immunol**, 9: (12): 1341-1346.

Vermi, W., Lonardi, S., Bosisio, D., Uguccioni, M., Danelon, G., Pileri, S., Fletcher, C., Sozzani, S., Zorzi, F., Arrigoni, G., Doglioni, C., Ponzoni, M. and Facchetti, F. (2008) Identification of CXCL13 as a new marker for follicular dendritic cell sarcoma. **J Pathol**, 216: (3): 356-364.

Vestweber, D. and Blanks, J.E. (1999) Mechanisms that regulate the function of the selectins and their ligands. **Physiol Rev**, 79: (1): 181-213.

Vestweber, D. (2002) Regulation of endothelial cell contacts during leukocyte extravasation. **Curr Opin Cell Biol**, 14: (5): 587-593.

Viney, J.L., Jones, S., Chiu, H.H., Lagrimas, B., Renz, M.E., Presta, L.G., Jackson, D., Hillan, K.J., Lew, S. and Fong, S. (1996) Mucosal addressin cell adhesion molecule-1: a structural and functional analysis demarcates the integrin binding motif. **J Immunol**, 157: (6): 2488-2497.

Voisin, M.B., Woodfin, A. and Nourshargh, S. (2009) Monocytes and neutrophils exhibit both distinct and common mechanisms in penetrating the vascular basement membrane in vivo. **Arterioscler Thromb Vasc Biol**, 29: (8): 1193-1199.

von Andrian, U.H. and Mackay, C.R. (2000) T-cell function and migration. Two sides of the same coin. **N Engl J Med**, 343: (14): 1020-1034.

von Boehmer, H. and Hafen, K. (1993) The life span of naive alpha/beta T cells in secondary lymphoid organs. **J Exp Med**, 177: (4): 891-896.

Wagner, N., Lohler, J., Kunkel, E.J., Ley, K., Leung, E., Krissansen, G., Rajewsky, K. and Muller, W. (1996) Critical role for beta7 integrins in formation of the gut-associated lymphoid tissue. **Nature**, 382: (6589): 366-370.

Wagner, N., Lohler, J., Tedder, T.F., Rajewsky, K., Muller, W. and Steeber, D.A. (1998) L-selectin and beta7 integrin synergistically mediate lymphocyte migration to mesenteric lymph nodes. **Eur J Immunol**, 28: (11): 3832-3839.

Wald, O., Pappo, O., Safadi, R., Dagan-Berger, M., Beider, K., Wald, H., Franitza, S., Weiss, I., Avniel, S., Boaz, P., Hanna, J., Zamir, G., Eid, A., Mandelboim, O., Spengler, U., Galun, E. and Peled, A. (2004) Involvement of the CXCL12/CXCR4 pathway in the advanced liver disease that is associated with hepatitis C virus or hepatitis B virus. **Eur J Immunol**, 34: (4): 1164-1174.

Wang, S., Voisin, M.B., Larbi, K.Y., Dangerfield, J., Scheiermann, C., Tran, M., Maxwell, P.H., Sorokin, L. and Nourshargh, S. (2006) Venular basement membranes contain specific matrix protein low expression regions that act as exit points for emigrating neutrophils. **J Exp Med**, 203: (6): 1519-1532.

Wang, W., Soto, H., Oldham, E.R., Buchanan, M.E., Homey, B., Catron, D., Jenkins, N., Copeland, N.G., Gilbert, D.J., Nguyen, N., Abrams, J., Kershenovich, D., Smith, K., McClanahan, T., Vicari, A.P. and Zlotnik, A. (2000) Identification of a novel chemokine (CCL28), which binds CCR10 (GPR2). **J Biol Chem**, 275: (29): 22313-22323.

Ward, S.G., Bacon, K. and Westwick, J. (1998) Chemokines and T lymphocytes: more than an attraction. **Immunity**, 9: (1): 1-11.

Warnecke, P.M., Stirzaker, C., Melki, J.R., Millar, D.S., Paul, C.L. and Clark, S.J. (1997) Detection and measurement of PCR bias in quantitative methylation analysis of bisulphite-treated DNA. **Nucleic Acids Res**, 25: (21): 4422-4426.

Warnock, R.A., Askari, S., Butcher, E.C. and von Andrian, U.H. (1998) Molecular mechanisms of lymphocyte homing to peripheral lymph nodes. **J Exp Med**, 187: (2): 205-216.

Watanabe, C., Miura, S., Hokari, R., Teramoto, K., Ogino, T., Komoto, S., Hara, Y., Koseki, S., Tsuzuki, Y., Nagata, H., Granger, D.N. and Ishii, H. (2002) Spatial heterogeneity of TNF-alpha-induced T cell migration to colonic mucosa is mediated by MAdCAM-1 and VCAM-1. **Am J Physiol Gastrointest Liver Physiol**, 283: (6): G1379-1387.

Wegmann, F., Petri, B., Khandoga, A.G., Moser, C., Khandoga, A., Volkery, S., Li, H., Nasdala, I., Brandau, O., Fassler, R., Butz, S., Krombach, F. and Vestweber, D. (2006) ESAM supports neutrophil extravasation, activation of Rho, and VEGF-induced vascular permeability. **J Exp Med**, 203: (7): 1671-1677.

Wilson, E. and Butcher, E.C. (2004) CCL28 controls immunoglobulin (Ig)A plasma cell accumulation in the lactating mammary gland and IgA antibody transfer to the neonate. **J Exp Med**, 200: (6): 805-809.

Wisse, E., De Zanger, R.B., Charels, K., Van Der Smissen, P. and McCuskey, R.S. (1985) The liver sieve: considerations concerning the structure and function of endothelial fenestrae, the sinusoidal wall and the space of Disse. **Hepatology**, 5: (4): 683-692.

Wong, J., Johnston, B., Lee, S.S., Bullard, D.C., Smith, C.W., Beaudet, A.L. and Kubes, P. (1997) A minimal role for selectins in the recruitment of leukocytes into the inflamed liver microvasculature. **J Clin Invest**, 99: (11): 2782-2790.

Woodfin, A., Voisin, M.B. and Nourshargh, S. (2007) PECAM-1: a multi-functional molecule in inflammation and vascular biology. **Arterioscler Thromb Vasc Biol**, 27: (12): 2514-2523.

Wright, N., Hidalgo, A., Rodriguez-Frade, J.M., Soriano, S.F., Mellado, M., Parmo-Cabanas, M., Briskin, M.J. and Teixido, J. (2002) The chemokine stromal cell-derived factor-1 alpha modulates alpha 4 beta 7 integrin-mediated lymphocyte adhesion to mucosal addressin cell adhesion molecule-1 and fibronectin. **J Immunol**, 168: (10): 5268-5277.

Wurbel, M.A., Malissen, M., Guy-Grand, D., Meffre, E., Nussenzweig, M.C., Richelme, M., Carrier, A. and Malissen, B. (2001) Mice lacking the CCR9 CC-chemokine receptor show a mild impairment of early T- and B-cell development and a reduction in T-cell receptor gammadelta(+) gut intraepithelial lymphocytes. **Blood**, 98: (9): 2626-2632.

Yachida, S., Kokudo, Y., Wakabayashi, H., Maeba, T., Kaneda, K. and Maeta, H. (1998) Morphological and functional alterations to sinusoidal endothelial cells in the early phase of endotoxin-induced liver failure after partial hepatectomy in rats. **Virchows Arch**, 433: (2): 173-181.

Yago, T., Zarnitsyna, V.I., Klopocki, A.G., McEver, R.P. and Zhu, C. (2007) Transport governs flow-enhanced cell tethering through L-selectin at threshold shear. **Biophys J**, 92: (1): 330-342.

Yang, X.D., Michie, S.A., Tisch, R., Karin, N., Steinman, L. and McDevitt, H.O. (1994) A predominant role of integrin alpha 4 in the spontaneous development of autoimmune diabetes in nonobese diabetic mice. **Proc Natl Acad Sci U S A**, 91: (26): 12604-12608.

Yang, X.O., Pappu, B.P., Nurieva, R., Akimzhanov, A., Kang, H.S., Chung, Y., Ma, L., Shah, B., Panopoulos, A.D., Schluns, K.S., Watowich, S.S., Tian, Q., Jetten, A.M. and Dong, C. (2008) T helper 17 lineage differentiation is programmed by orphan nuclear receptors ROR alpha and ROR gamma. **Immunity**, 28: (1): 29-39.

Yoong, K.F., McNab, G., Hubscher, S.G. and Adams, D.H. (1998) Vascular adhesion protein-1 and ICAM-1 support the adhesion of tumor-infiltrating lymphocytes to tumor endothelium in human hepatocellular carcinoma. **J Immunol**, 160: (8): 3978-3988.

Yoshida, R., Imai, T., Hieshima, K., Kusuda, J., Baba, M., Kitaura, M., Nishimura, M., Kakizaki, M., Nomiyama, H. and Yoshie, O. (1997) Molecular cloning of a novel human CC chemokine EBI1-ligand chemokine that is a specific functional ligand for EBI1, CCR7. **J Biol Chem**, 272: (21): 13803-13809.

Yoshie, O., Imai, T. and Nomiyama, H. (2001) Chemokines in immunity. **Adv Immunol**, 78: 57-110.

Zaballos, A., Gutierrez, J., Varona, R., Ardavin, C. and Marquez, G. (1999) Cutting edge: identification of the orphan chemokine receptor GPR-9-6 as CCR9, the receptor for the chemokine TECK. **J Immunol**, 162: (10): 5671-5675.

Zabel, B.A., Agace, W.W., Campbell, J.J., Heath, H.M., Parent, D., Roberts, A.I., Ebert, E.C., Kassam, N., Qin, S., Zovko, M., LaRosa, G.J., Yang, L.L., Soler, D., Butcher, E.C., Ponath, P.D., Parker, C.M. and Andrew, D.P. (1999) Human G protein-coupled receptor GPR-9-6/CC chemokine receptor 9 is selectively expressed on intestinal homing T lymphocytes, mucosal lymphocytes, and thymocytes and is required for thymus-expressed chemokine-mediated chemotaxis. **J Exp Med**, 190: (9): 1241-1256.

Zhou, Z., Connell, M.C. and MacEwan, D.J. (2007) TNFR1-induced NF-kappaB, but not ERK, p38MAPK or JNK activation, mediates TNF-induced ICAM-1 and VCAM-1 expression on endothelial cells. **Cell Signal**, 19: (6): 1238-1248.

Zindl, C.L., Kim, T.H., Zeng, M., Archambault, A.S., Grayson, M.H., Choi, K., Schreiber, R.D. and Chaplin, D.D. (2009) The lymphotoxin LTalpha(1)beta(2) controls postnatal and adult spleen marginal sinus vascular structure and function. **Immunity**, 30: (3): 408-420.

Zlotnik, A. and Yoshie, O. (2000) Chemokines: a new classification system and their role in immunity. **Immunity**, 12: (2): 121-127.